

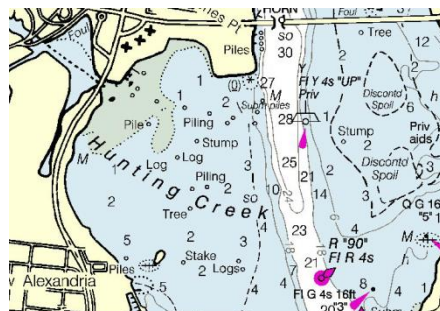
An Ecological Study of Hunting Creek



2022

FINAL REPORT

June 29, 2023



by

R. Christian Jones

Professor, Project Director

T. Reid Nelson

Assistant Professor, Co-Principal Investigator

Benoit Van Aken

Associate Professor, Co-Principal Investigator

Amy Fowler

Assistant Professor, Co-Principal Investigator

Potomac Environmental Research and Education Center

Department of Environmental Science and Policy

Department of Chemistry and Biochemistry

George Mason University

to

Alexandria Renew Enterprises

Alexandria, VA

This page intentionally blank.

Table of Contents

Table of Contents	iii
Executive Summary	v
List of Abbreviations	xii
The Aquatic Monitoring Program for the Hunting Creek Area of the Tidal Freshwater Potomac River - 2022	1
Acknowledgements	2
Introduction.....	3
Methods.....	8
A. Profiles and Plankton: Sampling Day	8
B. Profiles and Plankton: Follow up Analysis	13
C. Adult and Juvenile Fish.....	14
D. Submersed Aquatic Vegetation.....	16
E. Benthic Macroinvertebrates.....	16
F. Water Quality Mapping (Dataflow).....	17
G. Data Analysis	17
Results.....	19
A. Climate and Hydrological Factors - 2022	19
B. Physico-chemical Parameters: tidal stations – 2022	22
C. Physico-chemical Parameters: tributary stations – 2022	48
D. Phytoplankton – 2022	65
E. Zooplankton – 2022	77
F. Ichthyoplankton – 2022	83
G. Adult and Juvenile Fish – 2022	85
H. Submersed Aquatic Vegetation – 2022	98
I. Benthic Macroinvertebrates – 2022	99
Discussion.....	114
A. 2022 Synopsis	114
B. Correlation Analysis of Hunting Creek Data: 2013-2022.....	117
C. Water Quality: Comparison among Years	121
D. Phytoplankton: Comparison among Years	134
E. Zooplankton: Comparison among Years.....	149
F. Ichthyoplankton: Comparison among Years	157
G. Adult and Juvenile Fish: Comparison among Years.....	158
H. Submersed Aquatic Vegetation: Comparison among Years...	165
I. Benthic Macroinvertebrates: Comparison among Years.....	166
Literature Cited	171
 Anadromous Fish Survey Cameron Run – 2022	 173
Introduction.....	173
Methods.....	173
Results and Discussion	175
Conclusions.....	180
Literature Cited	181

Escherichia coli Abundances in Hunting Creek/Cameron Run
and Adjacent Potomac River - 2022182

 Introduction.....182

 Methods.....183

 Results and Discussion186

 Conclusions.....191

 Literature Cited191

 Appendices.....193

An Ecological Study of Hunting Creek - 2022 Executive Summary

Hunting Creek is an embayment of the tidal Potomac River located just downstream of the City of Alexandria and the I-95/I-495 Woodrow Wilson bridge. This embayment receives treated wastewater from the Alexandria Renew Enterprises wastewater treatment plant and inflow from Cameron Run which drains most of the Cities of Alexandria and Falls Church and much of eastern Fairfax County. The Hunting Creek embayment is bordered on the north by the City of Alexandria and on the west and south by the George Washington Memorial Parkway and associated park land. Due to its tidal nature and shallowness, the embayment does not seasonally stratify vertically, and its water is flushed by rainstorms and may mix readily with the adjacent tidal Potomac River mainstem.

The Chesapeake Bay, of which the tidal Potomac River is a major subestuary, is the largest and most productive coastal system in the United States. The use of the Bay as a fisheries and recreational resource has been threatened by overenrichment with nutrients which can cause nuisance algal blooms, hypoxia in stratified areas, loss of submersed aquatic vegetation, and declining fisheries. As a major discharger of treated wastewater into Hunting Creek, AlexRenew has been proactive in decreasing nutrient loading since the late 1970s. Also of concern are *E. coli* and nutrients derived from combined sewer overflows (CSOs) and nonpoint sources within the drainage basin as well as sediments derived from the watershed.

Beginning in 2013 the Potomac Environmental Research and Education Center (PEREC) in collaboration with Alexandria Renew Enterprises (AlexRenew) initiated a program to monitor water quality, biological communities, and *Escherichia coli* (*E. coli*) in the Hunting Creek area including stations in the embayment itself, its tributaries, and the adjacent river mainstem. This document presents results from 2022 and compares them with those from the previous nine years. Another year of benthic macroinvertebrate and water quality sampling on many tributaries of Cameron Run and Hunting Creek is also presented.



Hunting Creek area of the Tidal Potomac River showing water quality, plankton, and benthos sampling stations. AR2, AR3, and AR4 are embayment stations. AR11 and AR31 have been retired. Stations shown in red were new for 2020 and continued in 2021 2022. Stations in green are macroinvertebrate bioassessment stations.

Air temperature was above normal in all months. Precipitation closer to normal in 2021 than in the extremely wet year 2018. However, it was again well above normal in 2021, especially in June and August. Water temperature followed a typical seasonal pattern at all tidal stations with highest values approaching 30°C in late July and August. Specific conductance exhibited a gradual upward trend at most tidal stations except for AR1, AR24, and AR25 which were quite variable, probably due to the variable impact of the AlexRenew effluent and Cameron Run discharge. Chloride patterns closely followed those in specific conductance. Dissolved oxygen (DO) followed a seasonal decline when expressed in mg/L at all tidal stations, but DO as percent saturation was less seasonal especially at AR2 and AR3. Apparently, at these two stations active photosynthesis kept DO higher in the summer, but it rarely exceeded saturation. However, water quality mapping on July 18 indicated an area of supersaturation in the middle of the Hunting Creek embayment. Field pH measured in the semimonthly cruises showed little evidence of enhanced photosynthesis, but an area of high pH was observed on July 18 corresponding to the same area as the elevated DO, consistent with a high rate of photosynthesis. Total alkalinity was in the 60-100 range with a modest upward seasonal trend at most of the tidal river sites, but at AR1 values were generally variable and often below 60 mg/L

Light penetration was generally somewhat higher in the river than in the embayment. At all tidal main stations there was a consistent decline in Secchi disk depth and light attenuation coefficient over the year. A strong decline in light penetration was observed in early August following two moderately large runoff events in Cameron Run. Field turbidity readings also reflected these trends. Low light transparency continues to work against re-establishment of submersed aquatic vegetation (SAV) in Hunting Creek.

Ammonia nitrogen was quite variable seasonally at all stations. Generally, AR1 had the highest values being immediately below the AlexRenew outfall. However, on one occasion values at AR24 and AR25 (near AR1) spiked even higher. Nitrate showed a general pattern of decline from April into August which is probably attributable to less input and uptake by phytoplankton and other biota. Nitrite was low at all stations, but showed a clear upward seasonal trend. Organic N was showed a seasonal increase from April to July and then a steady decrease at most tidal stations. As with some other variables, AR1, AR24 and AR25 were generally higher and more variable. Total P exhibited a similar pattern. All ortho-P values were quite low, but showed little spatial or temporal patterns. N/P ratio showed a general decline consistently pointed to P limitation, with values generally in the 10-30 range being greater than 7.2 threshold in all samples. BOD was consistently below 4 mg/L at most stations. TSS values did not vary consistently at most tidal stations, but there were extreme fluctuations at AR1, AR4, A24, AR25 some of which corresponded to high flows in mid-August.

The grouping of tidal stations into Tidal Main Stations and Tidal Impact Stations did not reveal any major differences in any variables other than perhaps more variability at the Tidal CSO Impact stations. However, the timing and volume of CSO discharges was not known.

In the tributaries, seasonal temperature patterns were similar to the tidal stations with the marked drop in late June, but somewhat reduced maximum values near 25°C. In contrast to the tidal stations, specific conductance exhibited a marked seasonal decline especially at the Cameron Run Axis stations probably due to the slow flushing of road salt residuals from near surface groundwater. The patterns in chloride, a main component of road salt, backed up these trends in specific conductance. Dissolved oxygen was 60-100% saturation at the tributary stations except for AR34 which is at the lower end of the Hooffs Run Axis and influenced by the AlexRenew effluent. AR34 showed values at low as 1 mg/L or 20% saturation. Field pH was fairly constant, slightly lower than lab pH, and generally differed little among stations being 7.0-7.5. Lab pH values were even more consistent over time and stations, centered slightly below 7.5. YSI turbidity was very low at all tributary stations on all dates except for AR23, AR13, and AR34. These stations are at the lower end of their axes and near the influence of the AlexRenew effluent. Total alkalinity was quite consistent at most stations and throughout the year. Again, the exception was AR23 which often showed elevated values. Chloride declined seasonally from a high of about 120 mg/L in April to about 40 mg/L in early August.

Total phosphorus values were frequently below 0.1 mg/L except at AR23 and AR34. Ortho-P values in the Cameron Run Axis stations were generally below 0.03 mg/L and were quite variable over time at all stations, but they were correlated in their variability. Organic N at most stations was below 0.5 mg/L and did not show much seasonal change. Exceptions again were AR23 and AR34 which had substantially higher and more variable values. Ammonia N was generally very low (<0.1 mg/L) with a few exceptions at AR23 and AR34. Nitrate on the Hooffs Run Axis was definitely higher, especially at AR33, located in a residential area which was consistently higher over 2.5 mg/L. Nitrate was even higher at AR35 which has a suburban/park-like drainage area. Many stations reached a maximum in mid-August when stream flows were high suggesting sources in the watershed. Nitrite N was consistently very low, generally less than 0.03 mg/L, but underwent two peaks late in the year: mid-August and September stations in the Cameron Run Axis. TSS and VSS were consistently low (<10 mg/L) at most Cameron Run Axis tributary stations. Values were consistently higher and more variable at AR23. TSS and VSS were variable at the Hoofs Run Axis stations especially at AR34. Unexplained very high values were found at two stations in September: AR35 and AR12.

Correlation analysis was conducted among PEREC-collected water quality parameters from the regular sampling. These reflect relationships over all nine years of the study. Indicators of photosynthesis (DOPPM, DOSAT, Field pH) were highly intercorrelated. Also, measures of particles in the water column and resultant water clarity (turbidity, TSS, Secchi disk depth, and extinction coefficient) were also highly intercorrelated. Indicators of phytoplankton abundance (CHLDI, CHLSF, and VSSSF) were highly intercorrelated. A similar correlation analysis was conducted among AlexRenew/Mooney lab parameters. Among the most highly correlated variables in this dataset were TSS and VSS. Total P was positively correlated with organic N, TSS and VSS. Most phosphorus is bound to particles so these correlations make sense. TP was negatively correlated with N to P ratio and this makes sense since it is in the denominator of this ratio. Organic N

was highly correlated with TSS, VSS, and BOD. VSS and TSS were highly correlated with BOD.

Since the study began in 2013 it has been noted that certain water quality variables appear to be impacted by major rainfall and runoff events. This year we have tested the correlations between recent runoff flowing through Cameron Run and a wide array of water quality variables. This analysis revealed that many variables are strongly correlated with recent stream flow. Specific conductance, chloride, pH, and alkalinity are all significantly reduced by increased streamflow, probably due to the dilution effects of the runoff on the water already in the river. Turbidity, Secchi depth, light attenuation, and TSS are all increased by runoff because solids are either brought in or resuspended by the higher runoff resulting in poorer light penetration.

A fundamental change in the Hunting Creek ecosystem occurred in 2018 with the disappearance of SAV due to high flows that year. SAV has yet to recolonize. Water quality variables that show a clear difference between these two periods using the box plot analysis include Secchi disk depth, light attenuation coefficient, turbidity, TSS, and VSS, all variables related to water clarity.

Phytoplankton biomass as indicated by chlorophyll *a* exhibited two distinct maxima at Hunting Creek embayment stations (AR2 and AR3) in late July and late August. The late July peak occurred following a period of low rainfall and corresponded with high dissolved oxygen and high pH observed in both semimonthly cruises and data mapping indicating strong photosynthesis by phytoplankton. This peak in late July of 40 µg/L is similar to that attained in 2020 and 2022 which are among the highest values observed in the nine years of study. At the river station AR4 chlorophyll values rose seasonally to a peak of about 20 µg/L in early July. YSI sonde chlorophyll followed similar patterns as solvent-extracted chlorophyll. However, YSI sonde *in situ* chlorophyll *a* was found to underestimate extracted chlorophyll by about 3.5 times, meaning a sonde value of 10 corresponded with an extracted value of about 30 µg/L. Phytoplankton cell density at AR2 peaked in late August at the same time as the second peak in chlorophyll *a* at AR2. At this time green algae led by the colonial alga *Volvox* dominated. At AR4 phytoplankton cell density peaked on the same date led by the colonial green alga *Volvox*. Phytoplankton biovolume was generally dominated by diatoms including *Melosira* and *Biddulphia* unidentified pennate diatoms at both AR2 and AR4. Other algae such as discoid centrics, *Cryptomonas*, and *Euglena* were also dominant on some occasions.

Phytoplankton biomass as measured by chlorophyll *a* showed a clear increase at both AR2 and AR3 in the post 2018 samples as compared with the pre-2018 samples. The total phytoplankton cell count and biovolume data did not show this increase, partially due to the error associated with these counts. However, a few individual taxa have declined since the SAV disappearance including the cyanobacterium *Oscillatoria*, the diatom *Melosira*, and the cryptophyte *Cryptomonas*.

Peak rotifer abundance of 850/L in late August was much less than the 8000/L at AR2 and as was the maximum of about 800/L at AR4. As is typical, *Brachionus* was the

dominant rotifer representing over half of the individuals in any given sample. The small cladoceran *Bosmina* had a high short-lived peak in early June at AR4 of about 150/L. *Diaphanosoma* was the dominant large cladoceran and was abundant at AR2 reaching maxima in mid-June and early August, at about 1000/m³. *Leptodora* reached a modest peak of about 300/m³ in early June. *Daphnia* had a large peak in late May at AR4. Chydorids experienced two large peaks in the river. Among the copepods the immature copepod nauplii reached a strong peak of about 600/L in early June at AR2 and then showed a slow decline thereafter. *Eurytemora* as the most abundant larger copepod had a maximum of over 5000/m³ in April and a secondary peak in early June of 2500/m³ at AR4. Highest values of 1000/m³ were found in April and mid-June at AR2. *Mesocyclops* was also abundant at AR4 in early August.

Some of the zooplankton species did appear to show an effect of the ecosystem change in 2018. The rotifer *Brachionus* has been more abundant since 2018 than before. Several other taxa were depressed in 2018, but have partially recovered including copepod nauplii, the small cladoceran *Bosmina*, and a larger cladoceran *Diaphanosoma*. Others like the cyclopoid copepods *Cyclops* and *Mesocyclops* have continued to decline.

2022 marks the tenth year of our fish collections in Hunting Creek. Both trends and inter-annual variability become apparent when comparing the years of data. Total larval density is similar to 2021, but lower than previous years except for 2018 and 2020, which were poorly represented (Table 28). Although total abundance was lower, River Herring and other Clupeids remained the most abundant species similar to previous years. Interestingly, White Perch larvae was the most abundant we have seen throughout the course of this study, matching the trends in adult and juvenile fishes seen this year. Although abundances were somewhat diminished, three out of the four anadromous *Alosa* species were collected in Hunting Creek, demonstrating that this waterbody remains an important nursery habitat for these imperiled species of concern.

Trawl sampling was conducted between April and September at stations AR3 and AR4. A total of 2,829 fishes comprising of at least 20 species were collected with trawls. Collections were dominated by White Perch (72.98%). The second most abundant species was Spottail Shiner (13.04%), followed by *Alosa* sp. (6.93%), Gizzard Shad (3.04%), Bay Anchovy (1.56 %), and Blue Catfish (1.4 %). Our highest catch occurred on July 21, due to the high abundance of White Perch in that trawl sample. A notable difference among AR3 and AR4 was the collection of 40 Blue Catfish at AR4, but only one at AR3. At both stations, we collected the highest numbers of White Perch. The catches at AR3 and AR4 were both greater than last year, with almost five- and three-fold increases at AR3 and AR4 respectively, driven by White Perch collections. Similar to last year catfishes other than Blue Catfish (Brown Bullhead, Channel Catfish, and Flathead Catfish) were mostly absent in our trawl samples, only collecting 3 White Bullhead.

A total of 20 seine samples were taken (10 per station), comprising 5,748 fishes of at least 23 species. Similar to previous years, White Perch (75.87 %) was the dominant species (n = 4,361) in seine catches followed by Banded Killifish (8.94 %), *Alosa* sp. (6.33 %). and Mummichog (2.82 %). This continues the trend of greater White Perch dominance seen in recent years (2019 onward) where submerged aquatic vegetation has not been present.

As in 2018-2021, SAV was virtually absent in 2022 as verified by surveys conducted during datamapping. This is most certainly attributable to the very turbid water in 2018 and continued turbidity at critical periods in 2019, 2020, and 2021.

Similar to previous years, the macroinvertebrate community at the tidal stations was dominated by Annelids (including Oligochaetes and Leeches) across sites, with Oligochaetes contributing most to this group. Outside of the Annelids, Crustaceans (dominated by gammarid amphipods) and Turbellarians (flatworms) were the most abundant groups at AR4, while both AR2 and AR3 were dominated by Insect larvae from the Chironomidae family (midges). Each site had their own unique taxa. Insect larvae from the Leptoceridae family were only found at AR2. AR4 had the highest number of unique taxa, with nine (Turbellarians, the isopod *Cyathura polita*, three species of gastropods, including the invasive Japanese mystery snails-*Cipangopaludina japonica* and insect larvae from the families Heptageniidae, Gomphidae, Elimidae, Epheneridae). Comparing percent contributions of all non-Annelida taxa across all of the sites, months were dominated by the Crustaceans (June and July), Turbellarians (June, August, and September) or Insecta (May and August). Ordination analyses of the communities indicated a separation between communities sampled from each site across the months. This could be due to the type of habitat found at each site; while the habitat at AR2 is mostly leaves and organic debris, the habitat at both AR3 and AR4 is composed of the shells of dead Asian clams. This was also reflected in the substrate analyses, with positive relationships between percent shell composition and macroinvertebrate richness and abundance at AR4. There was also a change of the community composition throughout the months, as is common for aquatic communities experiencing changes in abiotic conditions and recruitment during the summer.

In 2016 a benthic macroinvertebrate sampling program was implemented for the flowing tributary streams starting with six stations. In 2018 two more stations were added with sampling continuing annually in November. Seventeen taxa were identified across all sites in 2021. Looking across all sites and years, the taxa that dominate are members of the Insecta family Hydropsychidae. They are the dominant group 40% of the time across all years and sites. This year, the majority of sites were dominated by Hydropsychidae. The next most abundant group across all sites and years are members of the Insecta family Chironomidae (26% across all years and sites), known as midges. All of these sites are probably influenced by differences in the types and amounts of nutrients and sediments moving from terrestrial sources, the flow of water, and anthropogenic impacts to the system. The relative importance of a variety of abiotic factors on determining benthic macroinvertebrate community structure probably varies annually, and even monthly, due to climatic events. Therefore, site-level trends may be apparent with continued annual sampling.

Anadromous fish sampling continued in Cameron Run in 2022. During the sampling period, we only collected five Alewife across two sampling days. However, this abundance of Alewife was similar to our overall Alewife abundance in previous sampling years. Although we did not intercept any adult Blueback Herring this year, we did collect larval Blueback Herring and Alewife indicating that this creek was used for spawning by both species. We positively identified 710 Alewife, and nine Blueback Herring larvae (Table 3) from our larval fish samples, collecting more total larvae than in 2021 or 2019.

The finding of river herring adults and larvae in an area above the AlexRenew outfall signifies that the water of Cameron Run is clean enough to use as spawning habitat for these species of concern.

E. coli studies indicate that virtually the entire area sampled, including the mainstem of the Potomac River (AR-4), is impaired for the bacteriological water quality criterion (*E. coli*) content under Section 9VAC25-260-170 of the Virginia Water Quality Standards. Even though over the period 2014 – 2017, both the percent exceedances and average counts suggested worsening of the water conditions, these trends are not observed for the period 2018 – 2021. Sampling additional sites in Hooffs Run/Cameron Run and the Potomac River helped to determine the potential contribution of Alex Renew CSOs to receiving waters. The 2022 data may indicate a contribution of the Cameron Run CSO and Hooffs Run CSO to the contamination of these streams by *E. coli*. Similarly, the data may indicate a contribution of the Royal St. CSO outfall to the contamination of the Potomac River. The 2022 data does not suggest a significant contribution of the Pendleton St. CSO to the contamination of mainstem Potomac River.

We recommend that:

1. The basic ecosystem monitoring should continue. A range of climatic conditions is needed to effectively establish baseline conditions in Hunting Creek. Interannual, seasonal and spatial patterns are starting to appear, but need validation with future years data. With record rainfall and runoff, 2018 provided a glimpse of the vulnerability of the system to flushing and sediment related effects which eliminated SAV from Hunting Creek. Continued monitoring will allow us to assess the resiliency of the ecosystem; i.e., how quickly will it recovery from a very wet year. With the continued absence of SAV from Hunting Creek, the system remains in a degraded state.
2. Water quality mapping should be continued. This provides much needed spatial resolution of water quality patterns as well as allowing mapping of SAV distributions.
3. Fyke nets have proven to be a useful new gear to enhance fish collections and should be continued.
4. Anadromous fish sampling is an important part of this monitoring program and has gained interest now that the stock of river herring has collapsed generally, and a moratorium on these taxa has been established in 2012. The discovery and continue presence of river herring spawning in Cameron Run increases the importance of continuing studies of anadromous fish in the study area.
5. We recommend continuing the more intensive *E. coli* sampling plan which seems to be giving better insight into the dynamics of *E. coli* in the study area.
6. We recommend that continuing macroinvertebrate studies the tributaries of Hunting Creek to further ascertain overall aquatic biota health. The tidal benthos sampling should continue and the data should be more thoroughly examined.

List of Abbreviations

BOD	Biochemical oxygen demand
cfs	cubic feet per second
DO	Dissolved oxygen
ha	hectare
l	liter
LOWESS	locally weighted sum of squares trend line
m	meter
mg	milligram
MGD	Million gallons per day
NS	not statistically significant
NTU	Nephelometric turbidity units
SAV	Submersed aquatic vegetation
SRP	Soluble reactive phosphorus
TP	Total phosphorus
TSS	Total suspended solids
um	micrometer
VSS	Volatile suspended solids
#	number



The Aquatic Monitoring Program for the Hunting Creek Area of the Tidal Freshwater Potomac River 2022

**FINAL REPORT
June 29, 2023**

by

R. Christian Jones

**Professor, Department of Environmental Science and Policy
Director, Potomac Environmental Research and Education Center
George Mason University
Project Director**

T. Reid Nelson

**Assistant Professor, Department of Environmental Science and Policy
George Mason University
Co-Principal Investigator**

Amy Fowler

**Assistant Professor, Department of Environmental Science and Policy
George Mason University
Co-Principal Investigator**

to

**Alexandria Renew Enterprises
Alexandria, VA**

ACKNOWLEDGEMENTS

The authors wish to thank the numerous individuals and organizations whose cooperation, hard work, and encouragement have made this project successful. We wish to thank the people of AlexRenew especially CEO Karen Pallansch for her vision in initiating the study and to Stephanie Lavey, Allison Deines, and Aster Tekle of AlexRenew for their advice and assistance during the study.

Without a dedicated group of field and laboratory workers this project would not have been possible. Thanks go to Laura Birsa for managing water quality/plankton/benthos field trips. We thank Rachel Kelmartin for her role in leading the majority of field efforts and for her tireless efforts in larval fish identification. Support was also provided by field/lab workers Chelsea Gray, Tabitha King, Alex Mott, David Tolentino, Sam Mohnney, Ben Stablow, Alexis Berger, and Liam Palmer, Riley Moreau, Erik Maki, Dylan Wake, Cassandra Boston, Cheyenne Hawkins, Beverly Bachman, and Kiah Gallaher. Benthic samples were analyzed with the help of Dasha Maslyukova; Liam Palmer; Katheryn Hout; Cathryn Mcvicker; Shel Johnson; Helene Pinto; Kelly Grantz. *E. coli* samples were collected and processed with the assistance of Aaron Newborn, Fanella Zamcho, Ayesah Karamat, and Alison Gomeiz. We thank two high school interns Mita Ramesh and Sarah Cho for their help this summer as part of the George Mason Aspiring Scientist Summer Internship Program (ASSIP). Dr. Saiful Islam conducted all phytoplankton counts. Claire Buchanan served as a voluntary consultant on plankton identification.

This work would not have been possible without Dr. Kim de Mutsert ensuring that a field crew and resources were in place to continue working during the Co-PI transition. We thank her for her dedication to this project from its inception and during this transitional period. We also thank Rachel Kelmartin for taking a large role in the field collection and laboratory processing of these fishes, the work would not have been completed without her. Finally, we thank Daya Hall-Stratton Breanna Hart, Sammie Alexander, and Beverly Bachman for their assistance with fish sampling and data processing throughout the project.

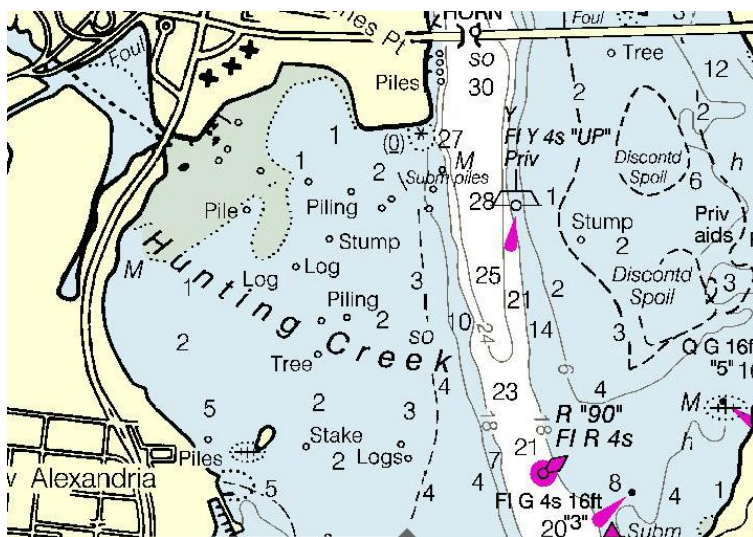
INTRODUCTION

This section reports the results of the tenth year of an aquatic monitoring program conducted for Alexandria Renew Enterprises by the Potomac Environmental Research and Education Center (PEREC) in the College of Science at George Mason University. A special feature of this year's report will be an in-depth analysis of changes during the decade of continuous and standardized research with a special focus on the changes that occurred in the ecosystem as a result of the 2018 transition from an SAV-dominated system to one without SAV. We will also be conscious of setting a baseline for completion of the on-coming River Renew project which will be completed soon and virtually eliminate combined sewer overflows (CSOs).

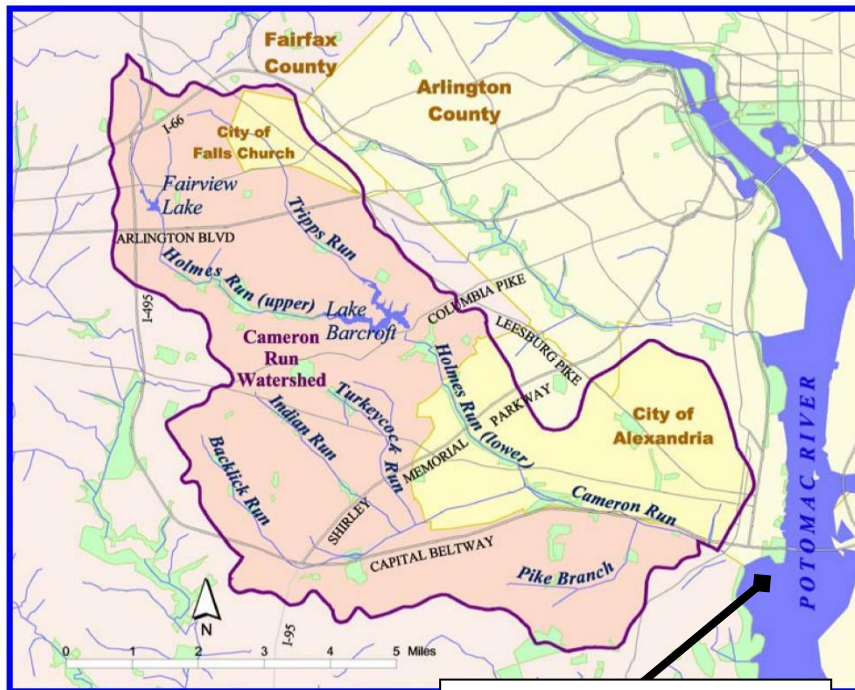
This work was in response to a request from Karen Pallansch, Chief Executive Officer of Alexandria Renew Enterprises (Alex Renew), operator of the wastewater reclamation and reuse facility (WRRF) which serves about 330,000 people in the City of Alexandria and the County of Fairfax in northern Virginia. The study is patterned on the long-running Gunston Cove Study which PEREC has been conducting in partnership with the Fairfax County Department of Public Works and Environmental Services since 1984. The goal of these projects is to provide baseline data and on-going trend analysis of the ecosystems receiving reclaimed water from wastewater treatment facilities with the objective of adaptive management of these valuable freshwater resources. This will facilitate the formulation of well-grounded management strategies for maintenance and improvement of water quality and biotic resources in the tidal Potomac. A secondary but important educational goal is to provide training for Mason graduate and undergraduate students in water quality and biological monitoring and assessment.

Setting of Hunting Creek

Hunting Creek is an embayment of the tidal Potomac River located just downstream of the City of Alexandria and the Woodrow Wilson Bridge. Waters are shallow with the entire embayment having a depth of 2 m or less at mean tide. According to the "Environmental Atlas of the Potomac Estuary" (Lippson et al. 1981), the mean depth of Hunting Creek is 1.0 m, the surface area is 2.26 km², and the volume of 2.1 x 10⁶ m³.



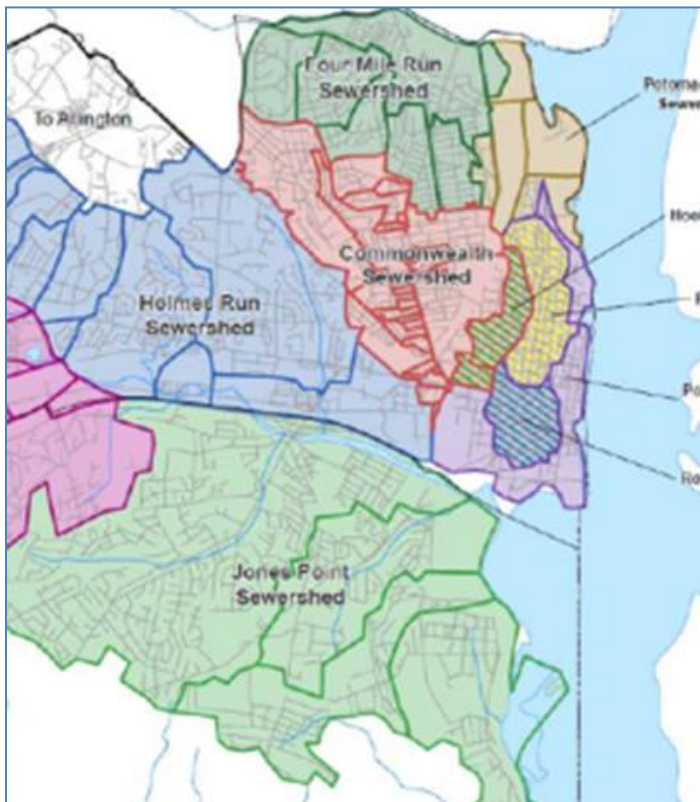
On the left is the Hunting Creek embayment. The Woodrow Wilson Bridge spans the tidal Potomac River at the top of the map. The Potomac River main channel is the whitish area running from north to south through the middle of the map. Soundings (numbers on the map) are in feet at mean low water. For the purposes of this report "Hunting Creek" will extend to the head of tide, roughly to Telegraph Rd. as the is VDEQ's definition.



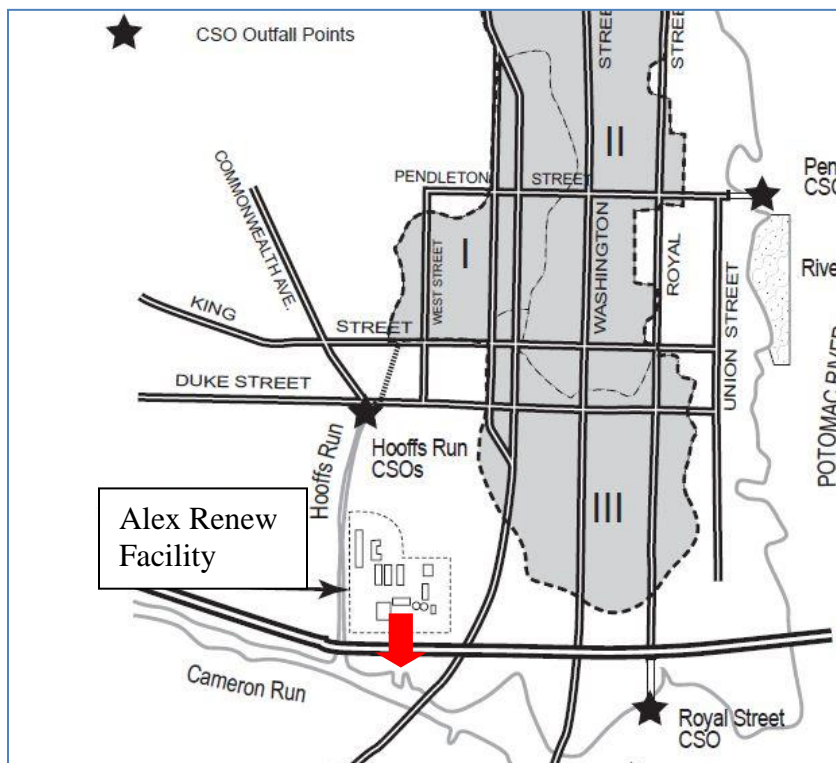
Hunting Creek embayment

On the left is a map of the Hunting Creek watershed. Cameron Run is the freshwater stream which drains the vast majority of the watershed of Hunting Creek. The watershed is predominantly suburban in nature with areas of higher density commercial and residential development. The watershed has an area of 44 square miles and drains most of the Cities of Alexandria and Falls Church and much of east central Fairfax County. A major aquatic feature of the watershed is Lake Barcroft. The suburban land uses in the watershed are a source of nonpoint pollution to Hunting Creek.

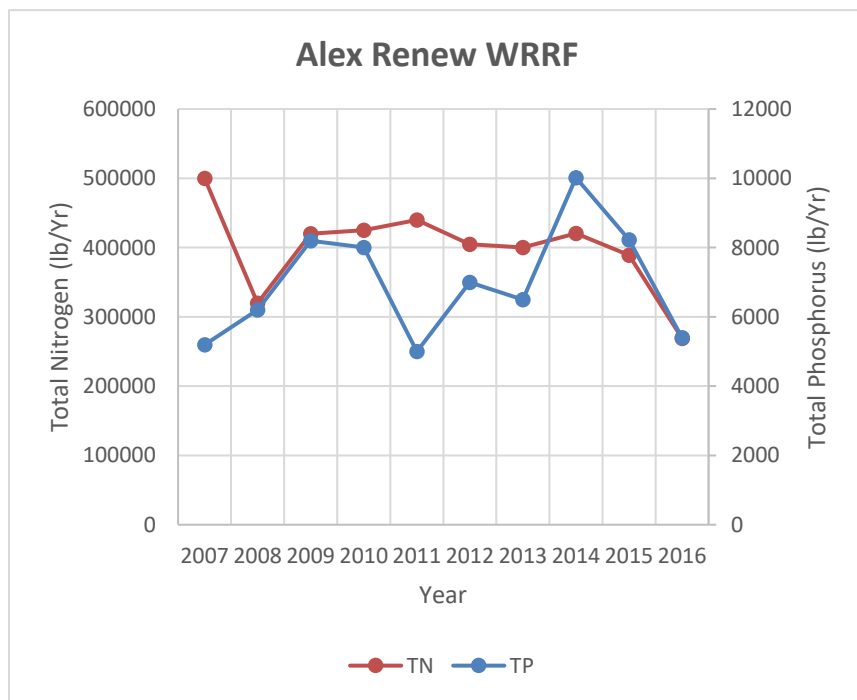
The Alex Renew WRRF serves an area similar in extent to the Cameron Run watershed with the addition of some areas along the Potomac shoreline from Four Mile Run to Dyke Marsh. The effluent of the AlexRenew plant enters the upper tidal reach of Hunting Creek under the Rt 1/I-95 interchange.



The map at the left shows the sewer sheds which contribute to the AlexRenew WRRF. Of particular note are the shaded areas within the City of Alexandria. These sewer sheds (Hooffs Run, Pendleton, and Royal St.) all contain combined sewers meaning that domestic wastewater is co-mingled with street runoff. Under most conditions, all of this water is directed to the AlexRenew WRRF for treatment. But in extreme runoff conditions (like torrential rains), some may be diverted directly into the tidal Potomac via a Combined Sewer outfalls (CSOs).



The map at the left is an enlargement of the area where the AlexRenew WRRF is found and where the discharge sites of the CSO's are located. Note the close proximity of two of the CSO's to the Alex Renew WRRF discharge (shown as red arrow).



The graph at the left shows the loading of nitrogen and phosphorus from the Alexandria Renew WRRF for seven recent years. Loadings of both nutrient elements were among the lowest in the last decade in 2016: 269,000 lb/yr for nitrogen and 5,400 lb/yr for phosphorus.

Ecology of the Freshwater Tidal Potomac

The tidal Potomac River is an integral part of the Chesapeake Bay tidal system and at its mouth the Potomac is contiguous to the bay proper. The tidal Potomac is often called a subestuary of the Chesapeake Bay and as such it is the largest subestuary of the bay in terms of size and amount of freshwater input. The mixing of freshwater with saltwater is the hallmark of an estuary. While the water elevation in an estuary is “sea level”, the water contained in an estuary is not pure sea water such as found in the open ocean. Pure ocean sea water has a salt concentration of about 35 parts per thousand by weight (ppt). Water in Chesapeake Bay ranges from about 30 ppt near its mouth to 0 ppt in the upper reaches where there is substantial freshwater inflow such as in the upper tidal Potomac River. Salinity at a given location is determined by the balance between freshwater input and salt water mixing in from the ocean. It generally varies with season being lower in spring when freshwater inflows are greater and higher in summer when there is less freshwater inflow. In the Hunting Creek study area, the salinity is essentially zero year round.

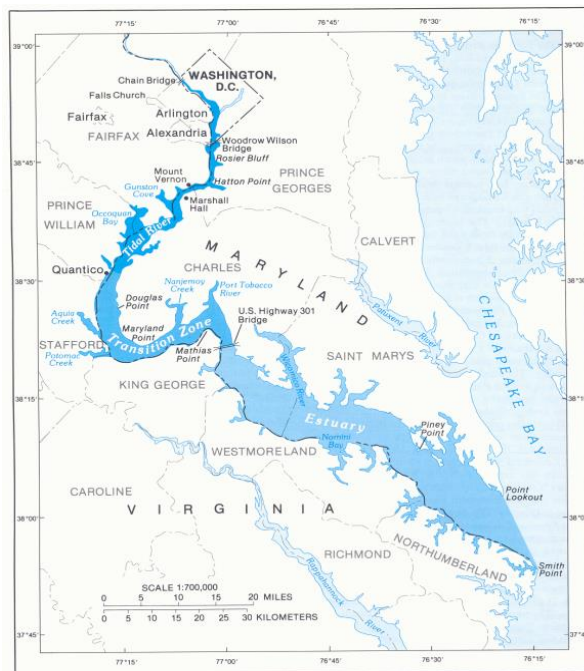


Figure 2. The tidal Potomac River and Estuary.

(map courtesy USGS)

The tidal Potomac is generally divided into three salinity zones as indicated by the map to the left:

- Estuarine or Mesohaline zone (6-14 ppt)
 - Transition or Oligohaline zone (0.5-6 ppt)
 - Tidal River or Tidal Fresh zone (<0.5 ppt)
- Hunting Creek is in the upper part of the Tidal River/Tidal Fresh zone and as such it never experiences detectable salinity

Within the tidal freshwater zone, the flora and fauna are generally characterized by the same species that would occur in a freshwater lake in this area and the food web is similar. Primary producers are freshwater species of submersed aquatic vegetation (SAV) such as native taxa *Vallisneria americana* (water celery), *Potamogeton* spp, (pondweeds), and *Ceratophyllum* (coontail) as well as introduced species such as *Hydrilla verticillata* (hydrilla) and *Myriophyllum spicatum* (water milfoil). Historical accounts indicate that most of the shallow areas of the tidal freshwater Potomac were colonized by SAV when observations were made around 1900 (Carter et al. 1985).

The other group of important primary producers are phytoplankton, a mixed assemblage

of algae and cyanobacteria which may turn over rapidly on a seasonal basis. The dominant groups of phytoplankton in the tidal freshwater Potomac are diatoms (considered a good food source for aquatic consumers) and cyanobacteria (considered a less desirable food source for aquatic consumers). For the latter part of the 20th century, the high nutrient loadings into the river favored cyanobacteria over both diatoms and SAV resulting in large production of undesirable food for consumers. In the last decade or so, as nutrient reductions have become manifest, cyanobacteria have decreased and diatoms and SAV have increased. Recently, since 2018, SAV has declined to very low levels in the Hunting Creek embayment, due apparently to high river and tributary flows in 2018 which resulted in flushing of the SAV from the embayment.

The biomass contained in the cells of phytoplankton nourishes the growth of zooplankton and benthic macroinvertebrates which provide an essential food supply for the juvenile and smaller fish. These in turn provide food for the larger fish like striped bass and largemouth bass. The species of zooplankton and benthos found in the tidal fresh zone are similar to those found in lakes in the area, but the fish fauna is augmented by species that migrate in and out from the open interface with the estuary.

Resident fish species include typical lake species such as sunfish (*Lepomis* spp.), bass (*Micropterus* spp.), and crappie (*Pomoxis* spp.) as well as estuarine species such as white perch (*Morone americana*) and killifish (*Fundulus* spp.). Species which spend part of their year in the area include striped bass (*Morone saxatilis*) and river herrings and shad (*Alosa* spp.). Non-native fish species have also become established in the tidal freshwater Potomac such as northern snakehead (*Channa argus*) and blue catfish (*Ictalurus furcatus*).

Larval fishes are transitional stages in the development of juvenile fishes. They range in development from newly hatched, embryonic fish to juvenile fish with morphological features similar to those of an adult. Many fishes such as clupeids (herring family), white perch, striped bass, and yellow perch disperse their eggs and sperm into the open water. The larvae of these species are carried with the current and termed “ichthyoplankton”. Other fish species such as sunfish and bass lay their eggs in “nests” on the bottom and their larvae are rare in the plankton.

After hatching from the egg, the larva draws nutrition from a yolk sack for a few days. When the yolk sack diminishes to nothing, the fish begins a life of feeding on other organisms. This post yolk sack larva feeds on small planktonic organisms (mostly small zooplankton) for a period of several days. It continues to be a fragile, almost transparent larva and suffers high mortality to predatory zooplankton and juvenile and adult fishes of many species, including its own. When it has fed enough, it changes into an opaque juvenile, with greatly enhanced swimming ability. It can no longer be caught with a slow-moving plankton net, but is soon susceptible to capture with the seine or trawl net.

METHODS

A. Profiles and Plankton: Sampling Day

Tidal Stations

Sampling was conducted on a semimonthly basis at stations representing both the Hunting Creek embayment and the Potomac mainstem (Figure 1a). Two stations (AR 2 & 3) were located in the Hunting Creek embayment proper. A fourth station (AR 4) was located in the river channel about 100 m upstream from Buoy 90. Dates for sampling as well as weather conditions on sampling dates and immediately preceding days are shown in Table 1. Note that certain dates had significant rainfall in days preceding sampling which may have impacted conditions in Hunting Creek due to its shallow nature and relatively large watershed contributing runoff.

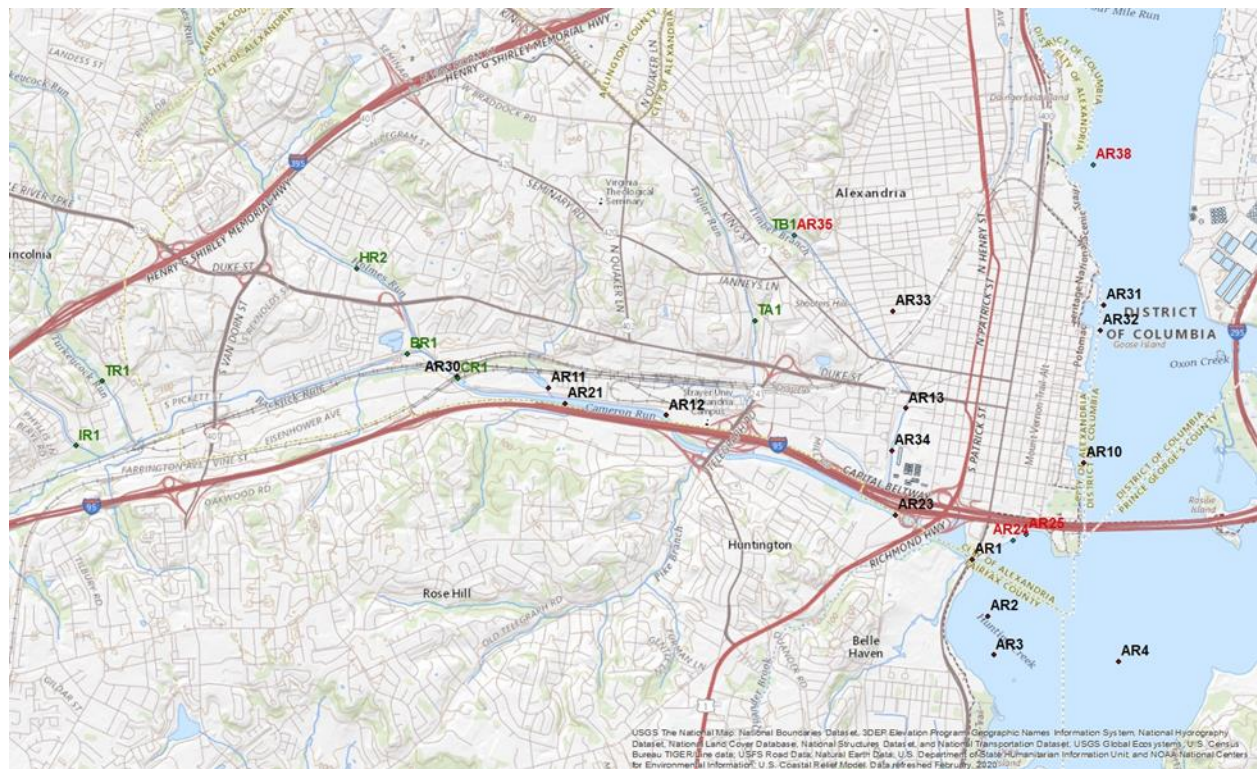


Figure 1a. Hunting Creek area of the Tidal Potomac River showing water quality, plankton, and benthos sampling stations. AR2, AR3, and AR4 are embayment stations. AR11 and AR31 have been retired. Stations shown in red were new for 2020 and continued in 2021 & 2022. Stations in green are macroinvertebrate bioassessment stations. AR1, AR3, AR10, AR23, AR31, AR32, AR33, and AR34 represent water quality only stations, AR2 and AR4 also include the phytoplankton and zooplankton and AR2, AR3, and AR4 are tidal benthos stations.

Table 1. Water quality monitoring stations.

Station ID	Access Type	Sample Type	Other Sampling	Location Description	Latitude	Longitude
AR1	Shore	Surface Grab	None	Hunting Cr at the GW Parkway Bridge	38.78992	-77.05126
AR2	Boat	Surface Bottom	Plankton Benthos	Northern portion of Hunting Cr.	38.78509	-77.04951
AR3	Boat	Surface Bottom	Benthos	Southern portion of Hunting Cr.	38.78181	-77.04890
AR4	Boat	Surface Bottom	Plankton Benthos	Potomac River Mainstem off Hunting Cr.	38.78124	-77.03529
AR10	Boat	Surface Grab	None	Potomac River North of Wilson Bridge	38.79816	-77.03907
AR12	Shore	Surface Grab	None	Last Riffle of Cameron Run near Beltway crossing	38.80218	-77.08467
AR13	Shore	Surface Grab	None	Hoff's Run upstream of CSO 003 and 004 outfalls	38.80278	-77.05848
AR21	Shore	Surface Grab	None	South side of Cameron Run downstream from Lake Cook drain	38.80318	-77.09565
AR23	Shore	Surface Grab	None	South side of upper Hunting Creek across from AlexRenew outfall	38.79372	-77.05966
AR24	Shore	Surface Grab	None	Hunting Creek north shore W. of Royal Street CSO outfall	38.79156	-77.04680
AR25	Shore	Surface Grab	None	Hunting Creek north shore E. of Royal Street CSO outfall	38.79205	-77.04538
AR30	Shore	Surface Grab	None	Cameron Run upstream near metro rail bridge	38.80545	-77.10745
AR32	Boat	Surface Grab	None	Potomac River Mainstem just S of Orinoco Bay CSO outfall	38.80940	-77.03727
AR33	Shore	Surface Grab	None	Hooffs Run at Linden St.	38.81103	-77.05993
AR34	Shore	Surface Grab	None	Hooffs Run at Alex Renew	38.79918	-77.05997
AR35	Shore	Surface Grab	None	Timber Branch at Ivy Hill Cemetery	38.8175	-77.07065
AR38	Boat	Surface Grab	None	Potomac River Mainstem near Daingerfield Island	38.82348	-77.03802

For the purpose of graphical analysis the stations were parsed into groups as follow:

Tidal Main Stations: AR1, AR2, AR3, AR4

Tidal CSO Impact Stations: AR10 (control), AR25 (Royal St CSO), AR24 (Royal St CSO), AR32 (Orinoco Bay CSO), AR38 (control)

Cameron Run Axis Tributaries: AR30, AR21, AR12, AR23

Hooffs Run Axis Tributaries: AR35, AR33, AR13, AR34

Table 2
Hunting Creek Study: Sampling Dates and Weather Data for 2022

Date	Type of Sampling						Avg Daily Temp (°C)		Precipitation (cm)	
	WP	B	D	T	S	F	1-Day	3-Day	1-Day	3-Day
April 20	X						10.0	8.5	0	2.31
April 22				(2)	(2)	(2)	17.8	13.7	0	0
May 2	X						17.8	15.4	0	0.33
May 6				(2)	(2)		16.1	17.0	2.54	3.86
May 17	X						21.7	20.9	0	1.80
May 19				(2)	(2)	(2)	21.7	20.9	0.08	0.10
June 1	X						29.4	27.4	0	0
June 2				(2)	(2)	(2)	26.7	28.0	0	0
June 13	X						26.7	23.1	0.03	0.23
June 16				(2)	(2)	(1)	26.1	26.3	0	0.10
July 7				(2)	(2)		26.1	26.9	0.08	0.30
July 14	X						26.7	26.1	0	1.12
July 18			D				27.8	26.5	0	3.53
July 21				(2)	(2)	(2)	29.4	28.7	0.20	0.20
July 28	X						28.9	27.0	0.51	0.51
August 4				(2)	(2)	(2)	28.9	28.7	2.36	2.36
August 11	X						25.6	28.0	0	1.32
August 16			D				23.3	23.3	0	0.33
August 18				(2)	(2)	(2)	23.3	23.5	0	0
August 30	X						27.2	27.8	0.36	0.36
Sept 8				(2)	(2)		22.8	23.9	0	2.13
Sept 13	X						24.4	24.4	0	2.46

Type of Sampling: WP: Water quality (samples to AlexRenew Lab), profiles and plankton, B: benthos, D: dataflow (water quality mapping), T: fish collected by trawling, S: fish collected by seining. F: fish collected by fyke net. T under Precipitation equals “trace”. Numbers in parenthesis for T, S, and F indicate the number of stations sampled for fish on each date.

Sampling was initiated about 9:00 am. Four types of measurements or samples were obtained depending on the station. At stations AR2, AR3, and AR4 (Tidal Main Stations), (1)

depth profiles of temperature, conductivity, dissolved oxygen, pH, and irradiance (photosynthetically active radiation, PAR) measured directly in the field; (2) water samples for GMU lab determination of chlorophyll *a* and phytoplankton species composition and abundance (phytoplankton at AR2 and AR4 only); (3) water samples for determination of N and P forms, BOD, COD, alkalinity, hardness, suspended solids, chloride, and pH by the Alexandria Renew Enterprises lab; (4) net sampling of zooplankton and ichthyoplankton (AR2 and AR4 only).

Profiles of temperature, conductivity, and dissolved oxygen were conducted at each Tidal Main station using a YSI 6600 datasonde with temperature, conductivity, dissolved oxygen and pH probes. Measurements were taken at 0.3 m increments from surface to bottom at the embayment stations. In the river measurements were made with the sonde at depths of 0.3 m and 2.0 m increments to the bottom. At the other three groups of stations, one sonde measurement was collected at the time of water collection. Meters were checked for calibration before and after sampling. At Tidal Main Stations (except AR1) profiles of irradiance (photosynthetically active radiation, PAR) were collected with a LI-COR underwater flat scalar PAR probe. PAR measurements were taken at 10 cm intervals to a depth of 1.0 m. Simultaneous measurements were made with a terrestrial probe in air during each profile to correct for changes in ambient light if needed. Secchi depth was also determined. The readings of at least two crew members were averaged due to variability in eye sensitivity among individuals. If the Secchi disk was still visible at the bottom or if its path was blocked by SAV while still visible, a proper reading could not be obtained.

At Tidal Main Stations (except AR2), a 1-L sample was constructed from equal volumes of water collected at each of three depths (0.3 m below the surface, middepth, and 0.3 m off of the bottom) using a submersible bilge pump. At AR2 only two depths were used. A 100-mL aliquot of the 1-L sample was preserved immediately with acid Lugol's iodine for later identification and enumeration of phytoplankton at stations AR2 and AR4. The remainder of the samples were placed in an insulated cooler with ice. A separate 1-liter surface sample was collected from 0.3 m using the submersible bilge pump and placed in the insulated cooler with ice for lab analysis of surface chlorophyll *a*.

At selected embayment and river mainstream sampling stations (AR2, AR3, and AR4), 2-liter samples were collected at each station from just below the surface (0.3 m) and near the bottom (0.3 m off bottom) at each station using the submersible pump. At other tidal and tributary stations, 2-liter samples were collected by hand from just below the surface. The 2-L samples were promptly delivered to either the Alexandria Renew Laboratory or the Prince William Mooney Laboratory for determination of nitrogen, phosphorus, BOD, TSS, VSS, pH, total alkalinity, and chloride. Surface water grab samples were collected in sterile 1-L containers at all stations for *E. coli* determination (see *E. coli* chapter). These were promptly delivered to Dr. Van Aken's lab at Potomac Science Center for analysis.

At stations AR2 and AR4, microzooplankton was collected by pumping 32 liters from each of three depths (0.3 m, middepth, and 0.3 m off the bottom) through a 44 μm mesh sieve. The sieve consisted of a 12-inch long cylinder of 6-inch diameter PVC pipe with a piece of 44 μm nitex net glued to one end. The 44 μm cloth was backed by a larger mesh cloth to protect it. The pumped water was passed through this sieve from each depth and then the collected

microzooplankton was backflushed into the sample bottle. The resulting sample was treated with about 50 mL of club soda and then preserved with formalin containing a small amount of rose bengal to a concentration of 5-10%.

At stations AR2 and AR4, macrozooplankton was collected by towing a 202 μm net (0.3 m opening, 2 m long) for 1 minute at each of three depths (near surface, middepth, and near bottom). Ichthyoplankton (larval fish) was sampled by towing a 333 μm net (0.5 m opening, 2 m long) for 2 minutes at each of the same depths at Stations AR2 and AR4. In the embayment, the boat traveled from AR2 toward AR3 during the tow while in the river the net was towed in a linear fashion along the channel. Macrozooplankton tows were about 300 m and ichthyoplankton tows about 600 m. Actual distance depended on specific wind conditions and tidal current intensity and direction, but an attempt was made to maintain a constant slow forward speed (approximately 3 miles per hour) through the water during the tow. The net was not towed directly in the wake of the engine. A General Oceanics flowmeter, fitted into the mouth of each net, was used to establish the exact towing distance. During towing the three depths were attained by playing out rope equivalent to about 1.5-2 times the desired depth. Samples which had obviously scraped bottom were discarded and the tow was repeated. Flowmeter readings taken before and after towing allowed precise determination of the distance towed and when multiplied by the area of the opening produced the total volume of water filtered.

Macrozooplankton were preserved immediately with rose bengal formalin with club soda pretreatment. Ichthyoplankton was preserved in 70% ethanol. Macrozooplankton was collected on each sampling trip; ichthyoplankton collections ended after July because larval fish were normally not found after this time.

Benthic macroinvertebrate samples were collected monthly at stations AR2, AR3, and AR4. Three samples were collected at each station using a petite ponar grab. The bottom material was first passed through a 5 mm screen to catch leaves, shells, and other large particles which might contribute to habitat for benthic fauna. The material passing through this coarse screen was then sieved through a 0.5 mm stainless steel sieve and resulting organisms were preserved in rose bengal formalin for lab analysis.

Samples for water quality determination were maintained on ice and delivered to the AlexRenew Laboratory or Prince William Mooney Lab by 2 pm on sampling day and returned to GMU by 3 pm. At GMU 10-15 mL aliquots of both depth-integrated and surface samples were filtered through 0.45 μm membrane filters (Gelman GN-6 and Millipore MF HAWP) at a vacuum of less than 10 lbs/in² for chlorophyll a and pheopigment determination. During the final phases of filtration, 0.1 mL of MgCO₃ suspension (1 g/100 mL water) was added to the filter to prevent premature acidification. Filters were stored in 20 mL plastic scintillation vials in the lab freezer for later analysis. Seston dry weight (TSS) and seston organic weight (VSS) were measured by filtering 200-400 mL of depth-integrated sample through a pretared glass fiber filter (Whatman 984AH).

Tributary Stations

At tributary stations, 2-liter samples were collected by hand from just below the surface. This water was promptly delivered to the nearby AlexRenew laboratory or Prince William Mooney Lab for determination of nitrogen, phosphorus, BOD, TSS, VSS, pH, total alkalinity, and chloride. While at the site, water temperature, specific conductance, dissolved oxygen, pH, and turbidity were taken at 0.1 m depth with a YSI ProDDS minisonde. Surface water grab samples were collected at all of these stations for *E. coli* determination (see *E. coli* chapter).

Sampling day activities were normally completed by 5:30 pm.

B. Profiles and Plankton: Follow-up Analyses

Chlorophyll *a* samples were processed using an overnight soaking procedure which has been shown to give comparable results to the traditional homogenization process. (Huntley et al. 1987). The filters had been stored in the freezer in 20 mL plastic scintillation vials. 15 mL of 90% acetone was added to each vial and the vials were shaken. They were placed in the refrigerator overnight. The next day they were mixed and assayed fluorometrically.

Chlorophyll *a* concentration in the extracts was determined fluorometrically using a Turner Designs Trilogy fluorometer configured for chlorophyll analysis as specified by the manufacturer. The instrument was calibrated using standards obtained from Turner Designs. Chlorophyll was determined and then after acidification with 2 drops of 10% HCl pheophytin was determined. Chlorophyll filters were stored in the freezer pending analysis in October.

Phytoplankton species composition and abundance was determined using the inverted microscope-settling chamber technique (Lund et al. 1958). Ten milliliters of well-mixed algal sample were added to a settling chamber and allowed to stand for several hours. The chamber was then placed on an inverted microscope and random fields were enumerated. At least two hundred cells were identified to species and enumerated on each slide. Counts were converted to number per mL by dividing number counted by the volume counted. Biovolume of individual cells of each species was determined by measuring dimensions microscopically and applying volume formulae for appropriate solid shapes.

Microzooplankton and macrozooplankton samples were rinsed by sieving a well-mixed subsample of known volume and resuspending it in tap water. This allowed subsample volume to be adjusted to obtain an appropriate number of organisms for counting and for formalin preservative to be purged to avoid fume inhalation during counting. One mL subsamples were placed in a Sedgewick-Rafter counting cell and whole slides were analyzed until at least 200 animals had been identified and enumerated. A minimum of two slides was examined for each sample. References for identification were: Ward and Whipple (1959), Pennak (1978), and Rutner-Kolisko (1974). Zooplankton counts were converted to number per liter (microzooplankton) or per cubic meter (macrozooplankton) with the following formula:

$$\text{Zooplankton (\#/L or \#/m}^3\text{)} = NV_s / (V_c V_f)$$

where N = number of individuals counted

V_s = volume of reconstituted sample, (mL)

V_c = volume of reconstituted sample counted, (mL)

V_f = volume of water sieved, (L or m^3)

Larval fish were picked from the ethanol-preserved ichthyoplankton samples with the aid of a stereo dissecting microscope. Identification of ichthyoplankton was made to family and further to genus and species where possible. If the number of animals in the sample exceeded several hundred, then the sample was split with a plankton splitter and the resulting counts were multiplied by the subsampling factor. The works Hogue et al. (1976), Jones et al. (1978), Lippson and Moran (1974), and Mansueti and Hardy (1967) were used for identification. The number of ichthyoplankton in each sample was expressed as number per $10\ m^3$ using the following formula:

$$\text{Ichthyoplankton (\#/10m}^3\text{)} = 10N/V$$

where N = number ichthyoplankton in the sample

V = volume of water filtered, (m^3)

C. Adult and Juvenile Fish

Fishes were sampled by trawling at stations AR3 and AR4, and seining at stations AR5 and AR6 (Figure 1b). For trawling, a try-net bottom trawl with a 15-foot horizontal opening, a $\frac{3}{4}$ inch square body mesh and a $\frac{1}{4}$ inch square cod end mesh was used. The otter boards were 12 inches by 24 inches. Towing speed was 2-3 miles per hour and tow length was 5 minutes. The trawls were towed upriver parallel to the channel at AR4, and following the curve away from the channel at AR3. The direction of tow should not be crucial. Dates of sampling and weather conditions are found in Table 1.

Seining was performed with a bag seine that was 50 feet long, 3 feet high, and made of knotted nylon with a $\frac{1}{4}$ inch square mesh. The bag is located in the middle of the net and measures $3\ ft^3$. The seining procedure was standardized as much as possible. The net was stretched out perpendicular to the shore with the shore end right at the water line. The net was then pulled parallel to the shore for a distance of 100 feet by a worker at each end moving at a slow walk. Actual distance was recorded if in any circumstance it was lower than 100 feet. At the end of the prescribed distance, the offshore end of the net was swung in an arc to the shore and the net pulled up on the beach to trap the fish. Dates for seine sampling were the same as those for trawl sampling (Table 1).

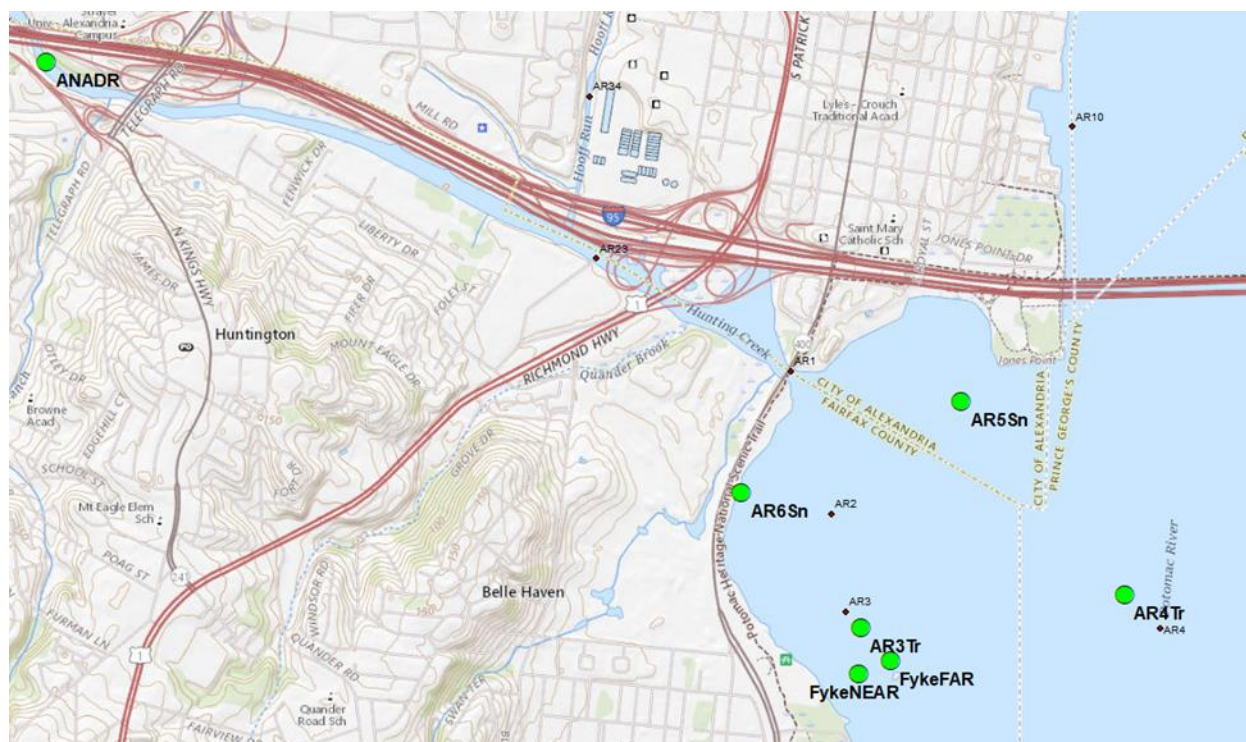


Figure 1b. Hunting Creek area of the Tidal Potomac River showing fish monitoring stations – Large Green circles. Stations with Tr in name are trawl stations; those with Sn in name are seine stations and those with Fyke in name are fyke stations. ANADR is the anadromous station. Water quality stations shown as small symbols and lettering for comparison.

Due to extensive submerged aquatic vegetation (SAV) cover in Hunting Creek, we adjusted our sampling regime in years of high SAV growth to include fyke netting. Two fyke nets were set in the area close to AR3 (Figure 1). The fyke net sampling stations are called ‘fyke near’ and ‘fyke far’ in reference to their distance from shore. These fyke nets were set within areas of former SAV to sample the fish community that uses that area as habitat. Fyke nets were set for 4 hours to passively collect fish. The fyke nets have 5 hoops, a 1/4 inch mesh size, 16 feet wings and a 32 feet lead. Fish enter the net by actively swimming and/or due to tidal motion of the water. The lead increases catch by capturing the fish swimming parallel to the wings. Fyke nets were not set in 2020 due to crew limitations under COVID. Trawling in this location (AR3) continued throughout the year in 2022 (Table 1).

After the catch from each of these three gear types was hauled in, the fishes were measured for standard length and total length to the nearest mm. Standard length is the distance from the front tip of the snout to the end of the vertebral column and base of the caudal fin. This is evident in a crease perpendicular to the axis of the body when the caudal fin is pulled to the side. Total length is the distance from the tip of the snout to the tip of the longer lobe of the caudal fin, measured by straightening the longer lobe toward the midline.

If the identification of the fish was not certain in the field, a specimen was preserved in 70% ethanol and identified later in the lab. All fishes retained for laboratory analysis or

identification were first euthanized by submerging them in an ice sludge conforming to the IACUC protocol. Identification was based on characteristics in dichotomous keys found in several books and articles, including Jenkins and Burkhead (1983), Hildebrand and Schroeder (1928), Loos et al (1972), Dahlberg (1975), Scott and Crossman (1973), Bigelow and Schroeder (1953), Eddy and Underhill (1978), Page and Burr (1998), and Douglass (1999).

The number of fykes, seines, and trawls completed each sampling day is shown below:

Date	Fyke	Seine	Trawl
2022-04-22	2	2	2
2022-05-06	0	2	2
2022-05-19	2	2	2
2022-06-02	2	2	2
2022-06-16	1	2	2
2022-07-07	0	2	2
2022-07-21	2	2	2
2022-08-04	2	2	2
2022-08-18	2	2	2
2022-09-08	0	2	2

D. Submersed Aquatic Vegetation

Data on coverage and composition of submersed aquatic vegetation (SAV) are generally obtained from the SAV webpage of the Virginia Institute of Marine Science (<http://www.vims.edu/bio/sav>). Information on this web site is obtained from aerial photographs near the time of peak SAV abundance as well as ground surveys which are used to determine species composition. We also recorded SAV relative abundance on a 0-3 scale at 4 minute intervals using visual observations and rake tow during data mapping cruises.

E. Benthic Macroinvertebrates

Benthic macroinvertebrates were sampled monthly using a petite ponar sampler at embayment stations AR2, AR3, and AR4. Triplicate samples were collected at each station monthly. Field processing of benthic samples was described earlier. In the laboratory benthic samples were rinsed with tap water through a 0.5 mm sieve to remove formalin preservative and resuspended in tap water. All organisms were picked, sorted, identified and enumerated. Debris contained in the ponar samples which was collected in the 5 mm sieve was dried and weighed in the lab.

In 2022 benthic invertebrates were also sampled at selected flowing tributary stations which possessed natural riffle-run areas. At each site one-minute kick samples were collected at one riffle and one run and composited in a single bottle. The sample was preserved with formalin

to a concentration of 5%. In the lab the sample was sieved through a 0.5 mm mesh (same as the kick net) and thoroughly washed with tap water before picking and sorting. Following sorting animals were enumerated by taxon and held in ethanol-glycerin. Sampling sites for tributary macroinvertebrate sampling are shown in Figure 1c.

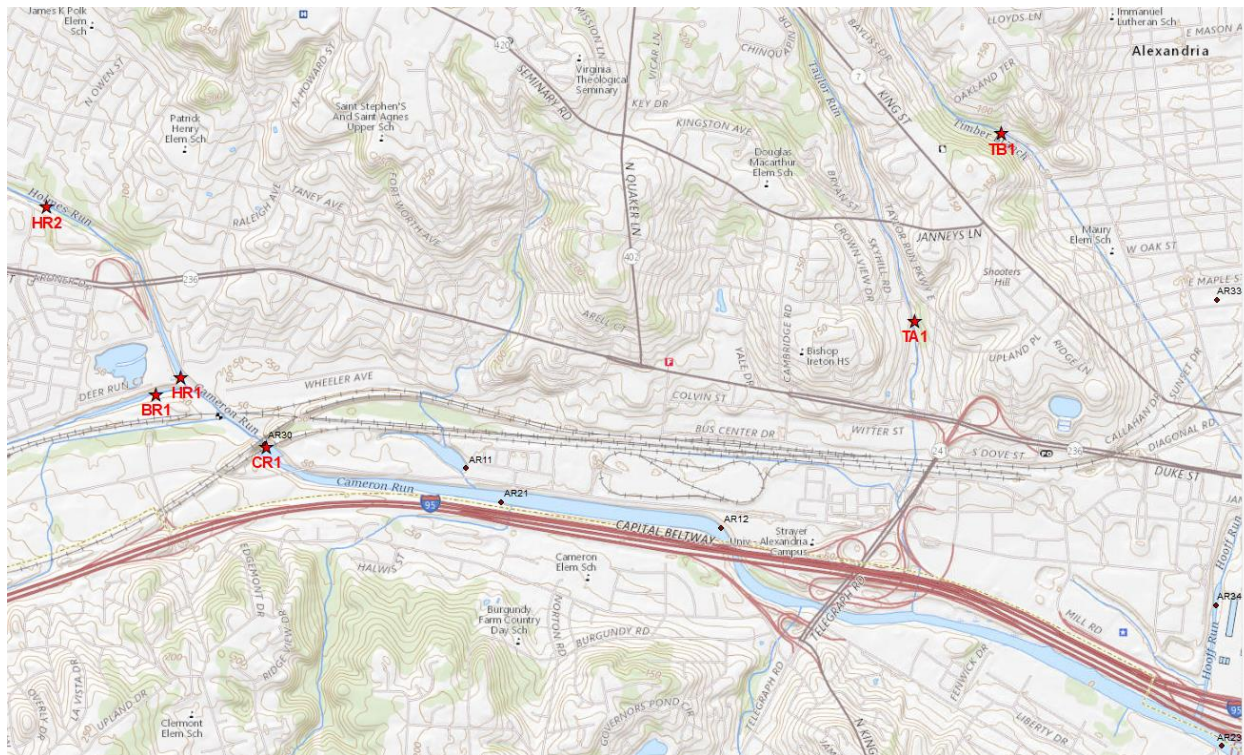


Figure 1c. Benthic sampling stations on flowing tributaries of Cameron Run. CR1: Cameron Run; HR1, HR2: Holmes Run; BR: Backlick Run; IR: Indian Run; TR: Turkeycock Run.

F. Water Quality Mapping (Dataflow)

On two additional dates in 2022 *in situ* water quality mapping was conducted by slowly transiting through much of the Hunting Creek study area as water was pumped through a chamber containing a YSI EXO sonde equipped with temperature, specific conductance, dissolved oxygen, pH, turbidity, and chlorophyll probes. Readings were recorded at 15 second intervals along with simultaneous GPS position readings. Every 4 minutes SAV relative abundance by species was recorded and every 4 minutes water samples were collected for extracted chlorophyll and TSS determination. These surveys allowed a much better understanding of spatial patterns in water quality within the Hunting Creek area which facilitated interpretation of data from the fixed stations. This approach is in wide use in the Chesapeake Bay region by both Virginia and Maryland under the name “dataflow”.

G. Data Analysis

Data for each parameter were entered into spreadsheets (Excel or SigmaPlot) for graphing of temporal and spatial patterns. SYSTAT was used for statistical calculations and to

create illustrations of the water quality mapping cruises. JMP v8.0.1 was used for fish graphs. Other data analysis approaches are explained in the text.

RESULTS

A. Climatic and Hydrologic Factors - 2022

In 2022 air temperature was above normal in all months except August (Table 3). There were 34 days with maximum temperature above 32.2°C (90°F) in 2022 which is well above the median number over the past decade. Precipitation was closer to normal in 2022 than in the extremely wet year 2018. However, it was again well above normal, especially in May and July.

Table 3. Meteorological Data for 2022. National Airport. Monthly Summary.

MONTH	Air Temp (°C)		Precipitation (cm)	
	March	10.0	(8.1)	7.0
April	13.6	(13.4)	9.7	(7.0)
May	19.6	(18.7)	16.2	(9.7)
June	24.4	(23.6)	7.5	(8.0)
July	26.8	(26.2)	19.3	(9.3)
August	26.4	(25.2)	6.2	(8.7)
September	22.4	(21.4)	5.8	(9.6)

Note: 2022 monthly averages or totals are shown accompanied by long-term monthly averages (1971-2000). Source: Local Climatological Data. National Climatic Data Center, National Oceanic and Atmospheric Administration.

Temperature followed the expected seasonal trend with July being the month with the greatest air temperatures followed closely by August (Table 3). All months exceeded the long-term average values. The differences between July and August was only 0.4°C which was less than the long term average of 1.0°C. These patterns were revealed in more detail by looking at the daily average temperatures over the period (Figure 2).

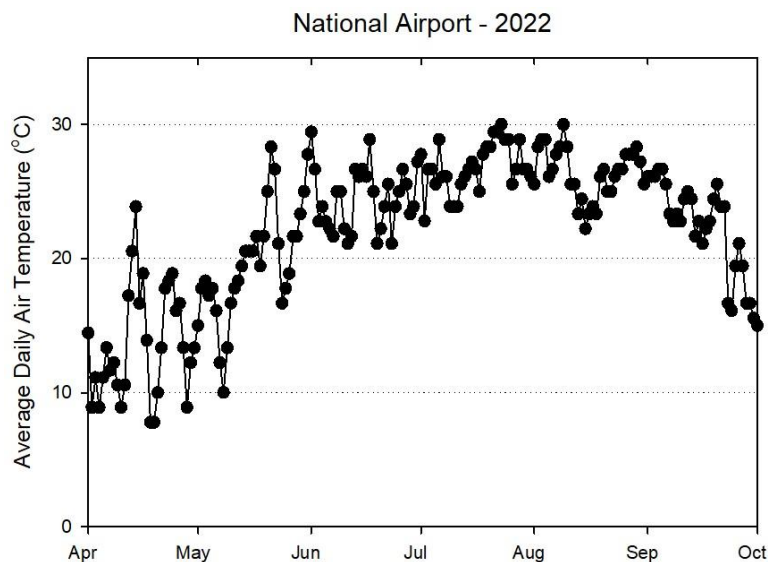


Figure 2. Mean daily air temperature over the study period.

Table 4. Monthly mean discharge at USGS Stations representing freshwater flow into the study area. (+) 2022 month > 2x Long Term Avg. (-) 2022 month < ½ Long Term Avg.

	Potomac River at Little Falls (cfs)		Cameron Run at Wheeler Ave (cfs)	
	2022	Long Term Average	2022	Long Term Average
March	9738 (-)	23600	43.2	55
April	16290	20400	63.9	42
May	23058	15000	86.4 (+)	41
June	5787	9030	48.9	38
July	3724	4820	59.3	31
August	3174	4550	26.3	28
September	3605	5040	20.6	38

River and tributary stream flow in 2022 were close to average for all months except March in the river when it was very low and May in Cameron Run and in the river when it was well above average (Table 4).

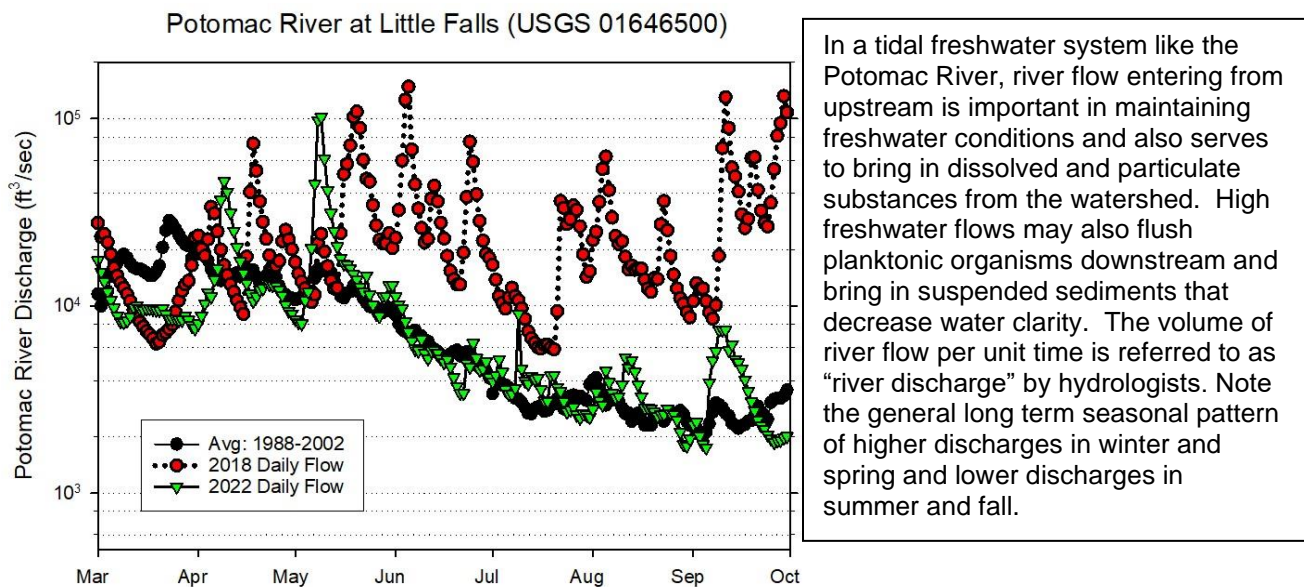
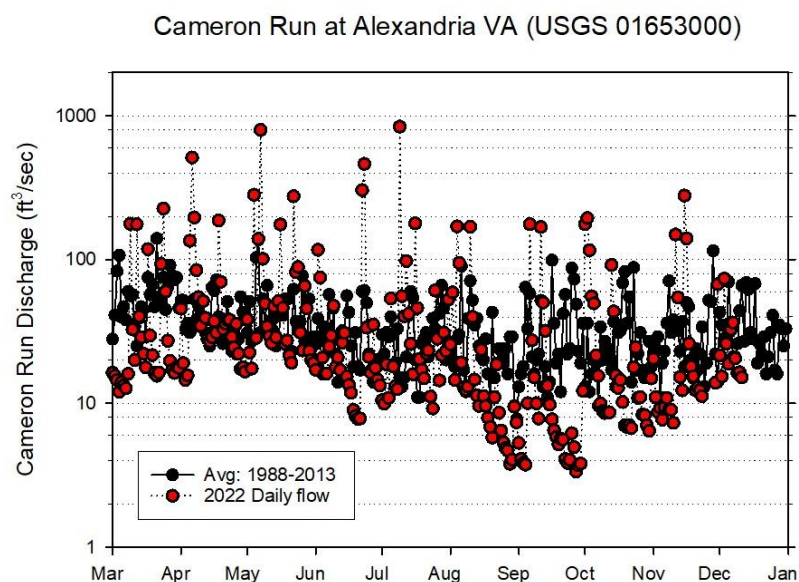


Figure 3. Mean Daily Discharge: Potomac River at Little Falls (USGS Data). Month tick is at the beginning of the month.

These same patterns were seen in the graphs of daily river flow when compared to long-term averages (Figure 3). The long-term average shows a steadily decreasing trend from March through September. In 2022 this general seasonal pattern was observed except for the notable surges in April and May which have the potential to strongly impact the early growth of SAV in Hunting Creek and plankton in Hunting Creek and the river. SAV is more vulnerable to these periods of poor growing conditions as it cannot spring back quickly from these periods of poor growing conditions.



In the Hunting Creek region of the tidal Potomac, freshwater discharge is occurring from both the major Potomac River watershed upstream (measured at Little Falls) and from immediate tributaries, principally Cameron Run which empties directly into Hunting Creek. The gauge on Cameron Run at Wheeler Avenue is located just above the head of tide and covers most area which contributes runoff directly to the Hunting Creek embayment from the watershed. The contributing area to the Wheeler Ave gauge is 33.9 sq mi. (USGS)

Figure 4. Mean Daily Discharge: Cameron Run at Alexandria (Wheeler Ave) (USGS Data).

Discharge in Cameron Run was generally at or below the long-term average, but showed frequent short-lived pulses especially from April through early July (Figure 4). There were 9 days on which daily average flow exceeded 200 cfs, 1 in March, 2 in April, 3 in May, 2 in June, and 1 in July.

B. Physico-chemical Parameters: Embayment and River Stations – 2022

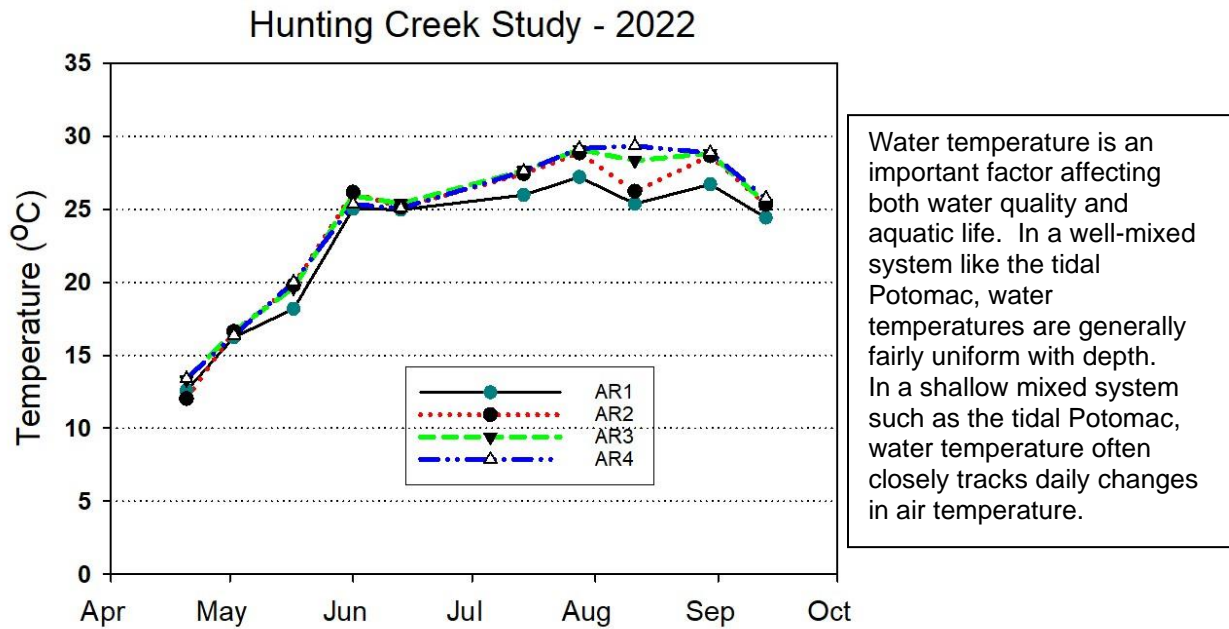
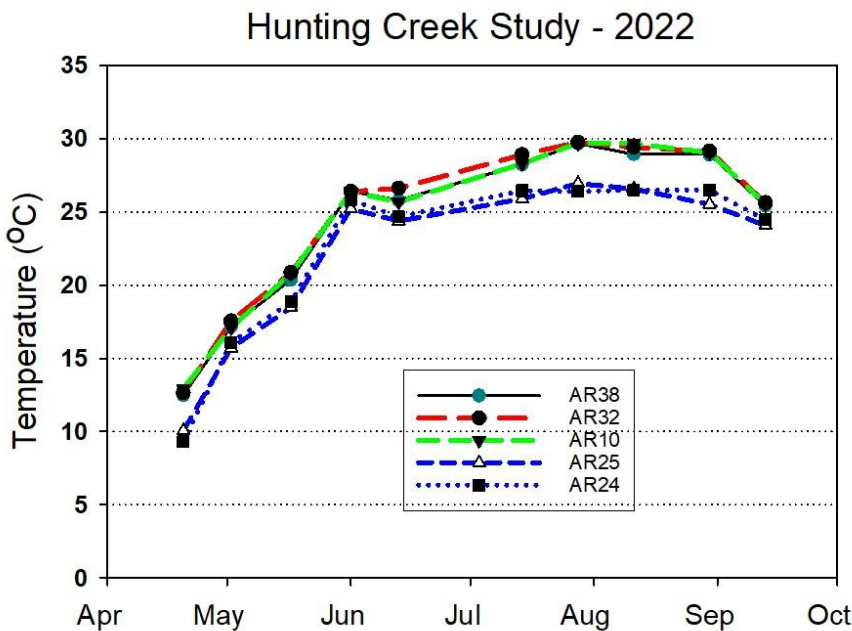


Figure 5. Water Temperature (°C). Tidal Main Stations. Month tick is at first day of month.

Water temperature followed the typical seasonal pattern at Tidal Main Stations (Figure 5). Temperatures reached 25°C by early June and in late July approached 30°C and remained high in August, dropping slightly in September. Similar patterns were observed at the Tidal CSO Impact Stations with the exception that AR24 and AR25 were consistently 2-5 degrees cooler (Figure 6). These were sampled earlier in the morning which may explain the differences.



In this section of the report, we have placed the stations into two groups: Tidal Main Stations which were sited to get general conditions in the tidal open water in Hunting Creek and the Potomac mainstem. The second group was Tidal CSO Impact Stations that were situated above and below CSO outfalls to examine their effects on tidal water quality.

Figure 6. Water Temperature (°C). Tidal CSO Impact Stations.

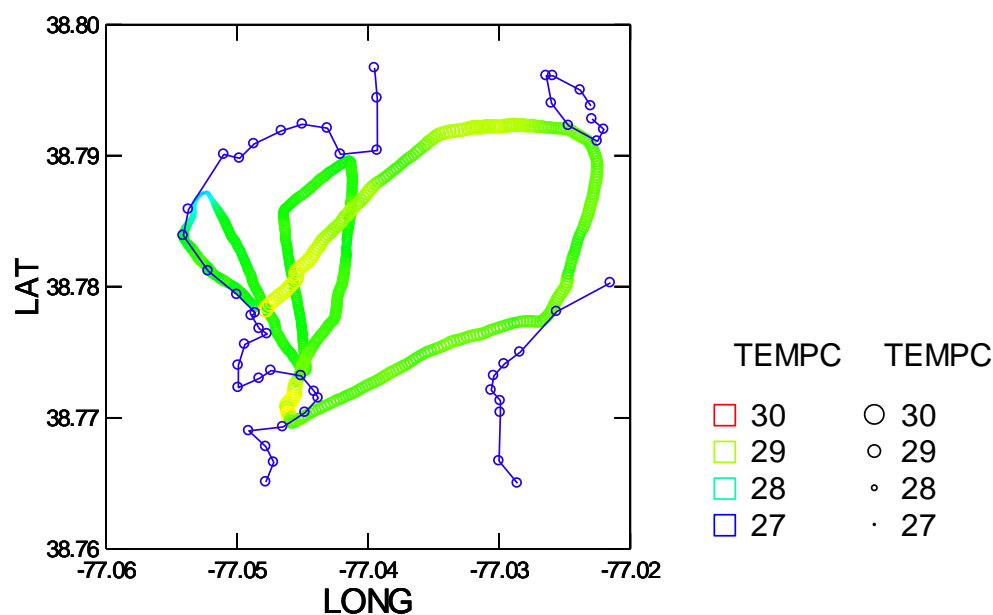


Figure 7a. Water Quality Mapping July 18, 2022. Temperature (°C).

Mapping of water temperature was conducted on July 18 and August 16, 2022. Water temperature ranged from 27°C to 30°C in July and 24°C to 28°C in August. Temperatures were pretty uniform on the July cruise with slightly higher values in the Hunting Creek embayment (Figure 7a). In August, temperatures increased steadily moving west to east across the study area, being about 26°C in the embayment increasing to 28°C in the river mainstem (Figure 7b). The three day average temperature leading up to the August sampling was 23.3°C (Table 2), much cooler than earlier in August. This cooling would have been felt much more rapidly in the shallow embayment than the deeper river. The three day average temperature for July 18 was 26.5.

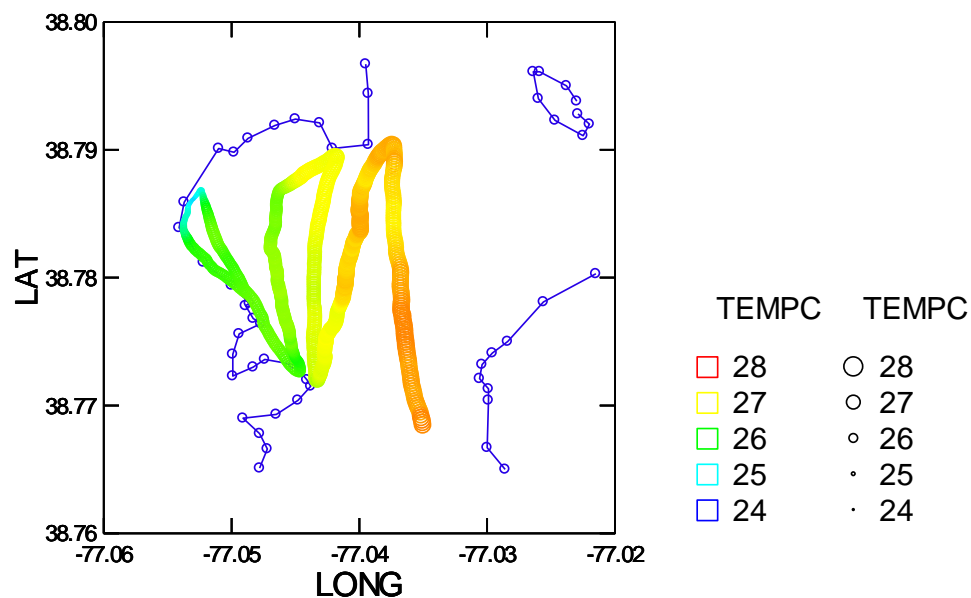
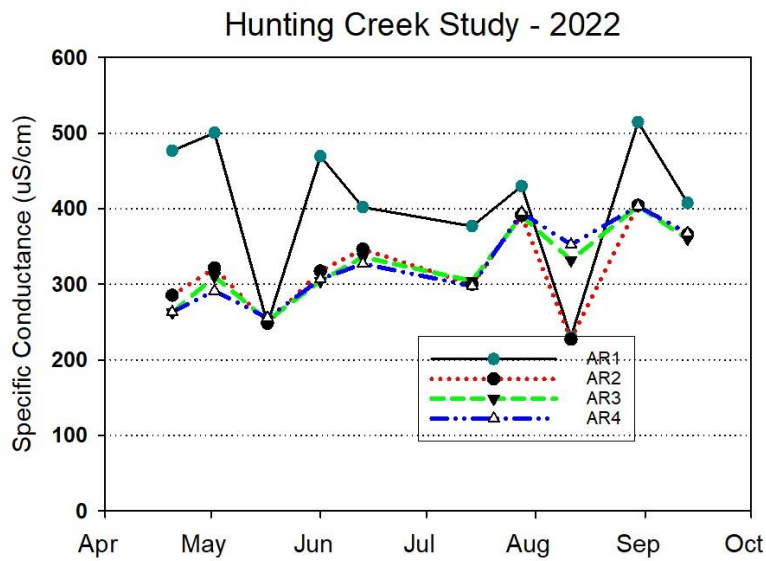


Figure 7b. Water Quality Mapping August 16, 2022. Temperature (°C).



Specific conductance measures the capacity of the water to conduct electricity standardized to 25°C. This is a measure of the concentration of dissolved ions in the water. In freshwater, conductivity is relatively low. Ion concentration generally increases slowly during periods of low freshwater inflow and decreases during periods of high freshwater inflow. Sewage treatment facilities can be a source of elevated conductivity. In winter road salts can be a major source of conductivity in urban streams.

Figure 8. Specific Conductance (µS/cm). Tidal Main Stations. Month tick is at first day of month.

Specific conductance followed a gradual increase at most Tidal Main stations through the sample period except at AR1 (Figure 8). It was much more variable at AR1, generally higher than at the other three station (Figure 8). Lowest values at AR1 were observed in late May and early August when 3 day precipitation was high presumably causing dilution by Cameron Run inflow (Table 2). On sampling dates preceded by typical lower Cameron Run inflow, higher values of conductivity resulted from elevated conductivity of Alex Renew inflows. Values at other stations AR10, AR32, and AR38 exhibited similar and slowly increasing values that were similar to most of the Tidal Main Stations. AR24 and AR25 on the north shore of Hunting Creek were generally higher and more variable perhaps due to some disturbance of the water while collecting samples.

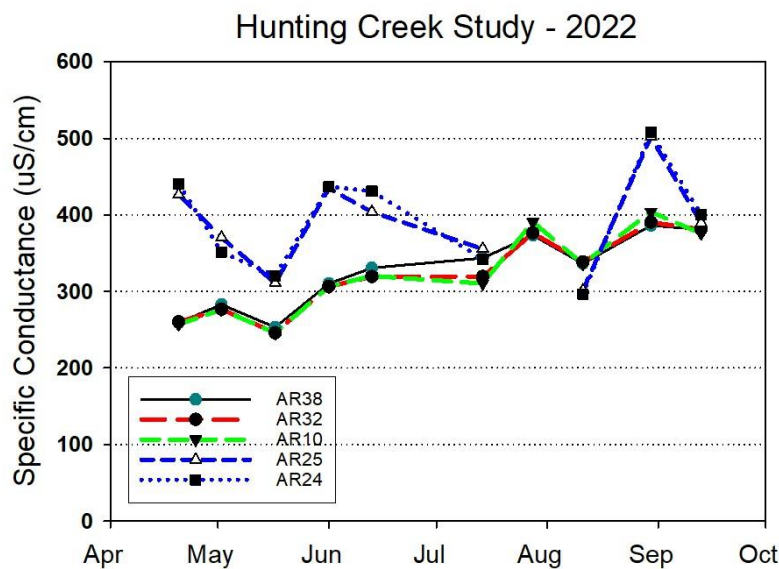
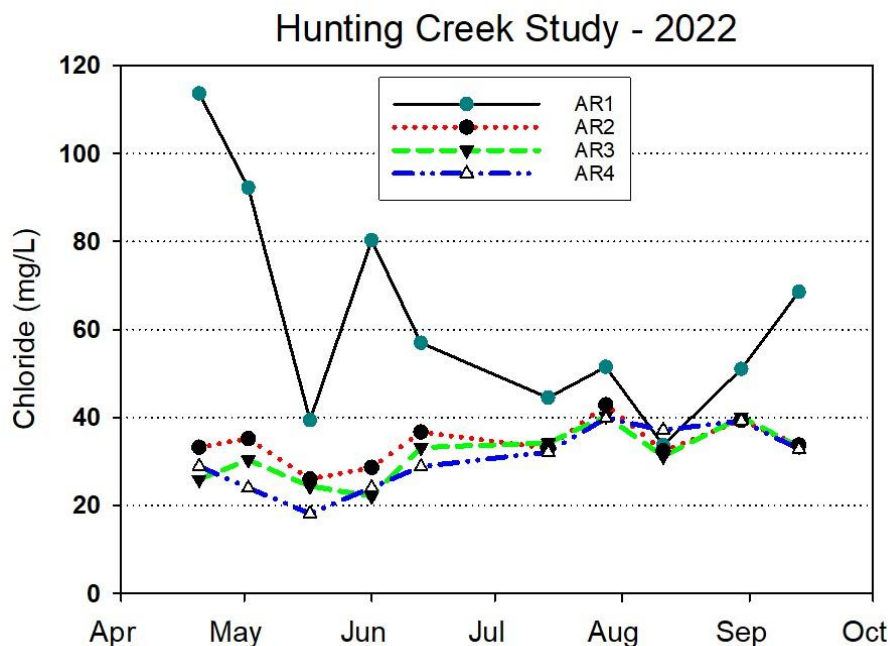


Figure 9. Specific Conductance (µS/cm). Tidal CSO Impact Stations.



Chloride ion (Cl^-) is a principal contributor to conductance. Major sources of chloride in the study area are sewage treatment plant discharges, road salt, and brackish water from the downriver portion of the tidal Potomac. Chloride concentrations observed in the Hunting Creek area are very low relative to those observed in brackish, estuarine, and coastal areas of the Mid-Atlantic region. Chloride may increase slightly in late summer or fall when brackish water from down estuary may reach the area as freshwater discharge declines.

Figure 10. Chloride (mg/L). Tidal Main Stations. Month tick is at first day of month.

Chloride exhibited a similar pattern to specific conductance at most of the tidal main stations increasing from April through August, but the increase was more modest (Figure 10). Lowest values were again observed in mid-May and mid-August periods of increased flow. AR10, AR32, and AR38, located on the mainstem of the Potomac, followed a seasonal pattern similar to most of the Tidal Main Stations whereas AR24 and AR25 were more variable with peaks in early June and early July (Figure 11).

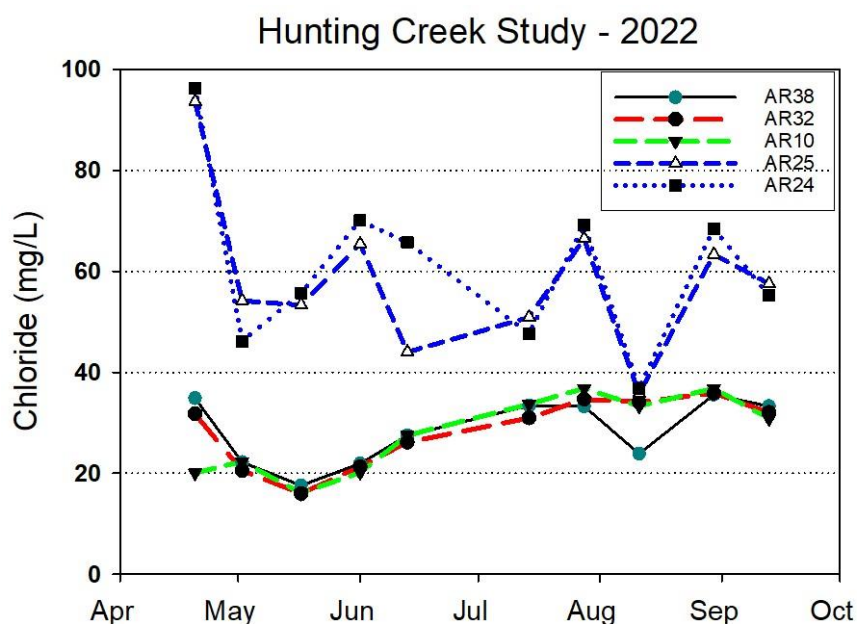


Figure 11. Chloride (mg/L). Tidal CSO Impact Stations

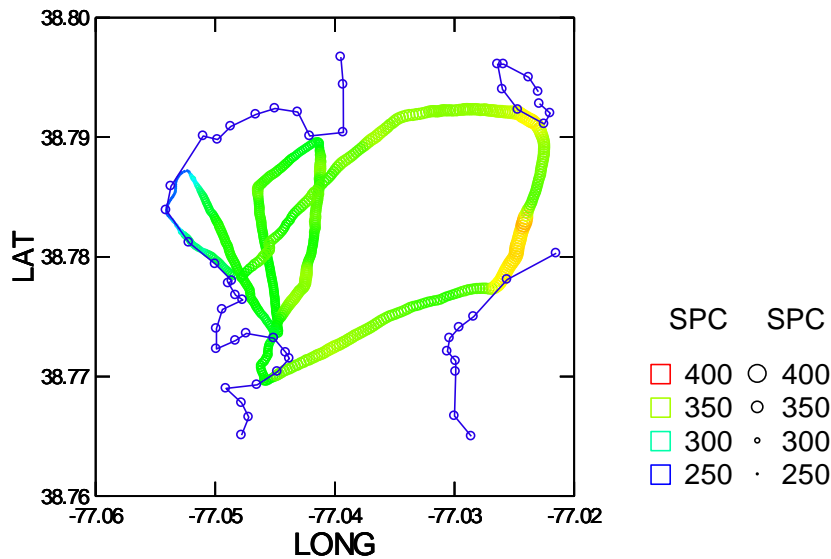


Figure 12a. Water Quality Mapping. July 18, 2022. Specific Conductance (uS/cm).

On July 18 specific conductance (SPC) was about 300-350 uS/cm in most of the Hunting Creek embayment and the Potomac mainstem. Slightly higher values were observed in the river mainstem along the Maryland shore. On August 16 SPC values of 410-430 were found over most of the study area with highest values (440-460 uS/cm) found along the northwest corner of Hunting Creek near the entrance of water to the embayment under the GW Parkway bridge. This reflects water slightly higher in ions, probably attributable to the AlexRenew effluent.

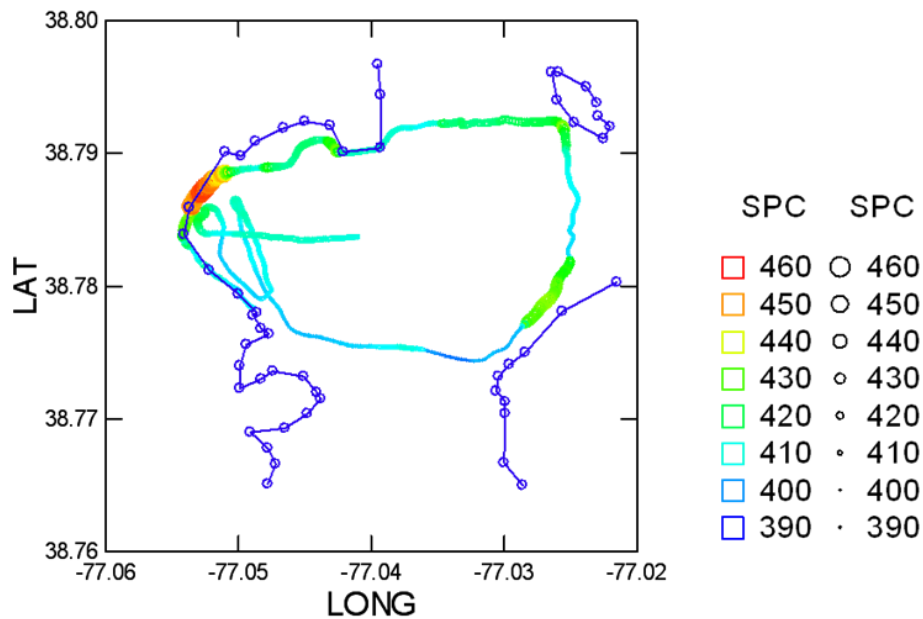
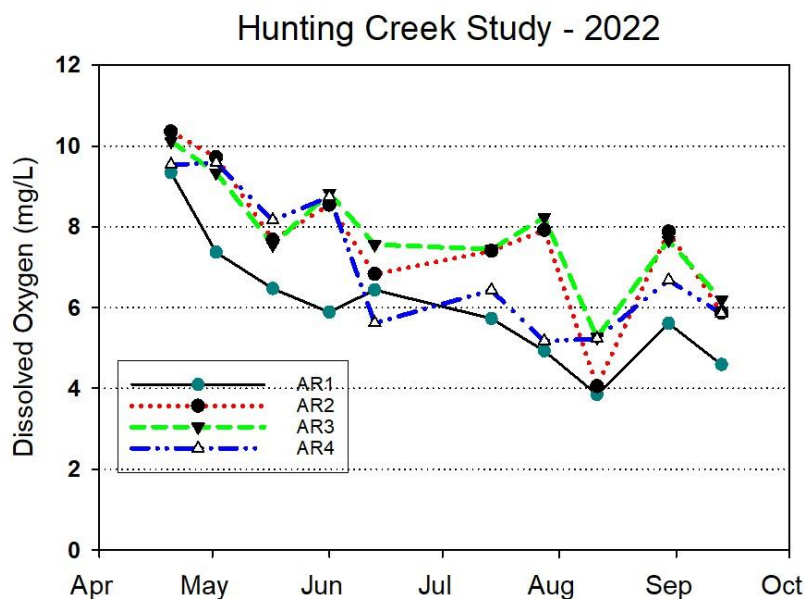


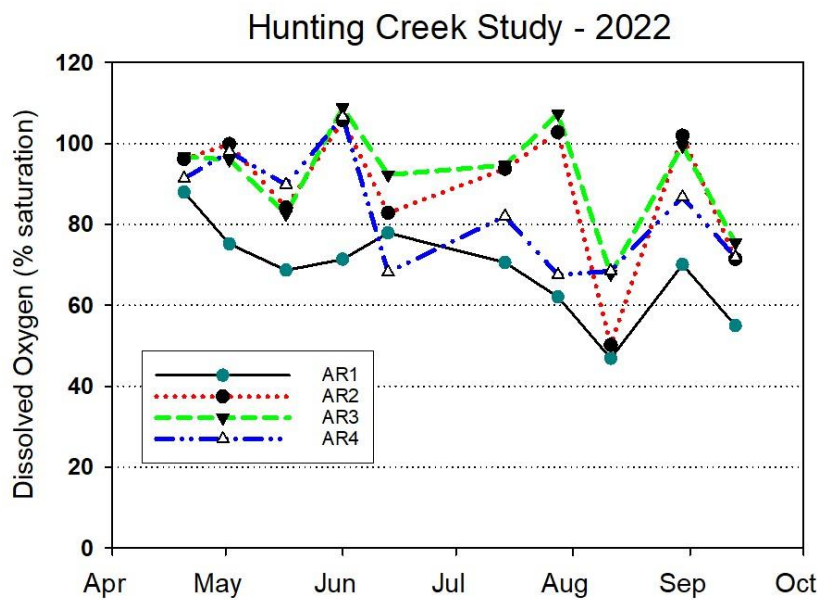
Figure 12b. Water Quality Mapping. August 16, 2022. Specific Conductance (uS/cm).



Oxygen dissolved in the water is required by freshwater animals for survival. The standard for dissolved oxygen (DO) in most surface waters is 5 mg/L. Oxygen concentrations in freshwater are in balance with oxygen in the atmosphere, but oxygen is only weakly soluble in water so water contains much less oxygen than air. This solubility is determined by temperature with oxygen more soluble at low temperatures.

Figure 13. Dissolved Oxygen (mg/L). Tidal Main Stations. Month tick is at first day of month.

The general pattern for dissolved oxygen (mg/L) at Tidal Main Stations was a gradual decline from April through September (Figure 13). AR1 and AR4 showed the most consistent decline while AR2 and AR3 leveled off in July and August except for a marked decline in mid-August. Looking at DO as percent saturation (Figure 14), values were more consistent seasonally. Peaks were observed at most stations in early June and late July at over 100% saturation. A significant decline was seen at AR1, AR2, and AR3 in early August; that date was preceded by significant rainfall which may have resulted in a decline due to decreased algal biomass due to flushing and decreased photosynthesis due to a poor light environment..



The temperature effect on oxygen concentration can be removed by calculating DO as percent saturation. This allows examination of the balance between photosynthesis and respiration both of which also impact DO. Photosynthesis adds oxygen to the water while respiration removes it. Values above 120% saturation are indicative of intense photosynthesis while values below 80% reflect a preponderance of respiration or decomposition.

Figure 14. Dissolved Oxygen (% saturation). Tidal Main Stations. Month tick is at first day.

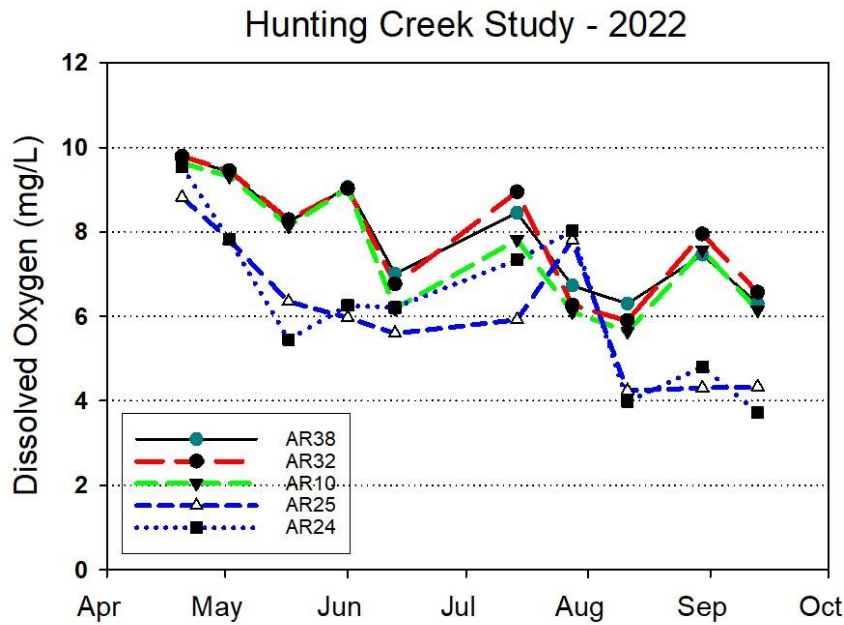


Figure 15. Dissolved oxygen (mg/L). Tidal CSO Impact Stations.

At the Tidal CSO Impact Stations there was general decline at AR10, AR32, and AR38 except in late May (Figure 15). The two stations in northern Hunting Creek bracketing the CSO outfall (AR24 and AR25) exhibited generally lower values than the other stations. DO as percent saturation at AR10, AR32, and AR38 did not show a general trend over the study period although exceeding 100% on two occasions (Figure 16). The levels at AR24 and AR25 were substantially lower for most of the year than the other stations..

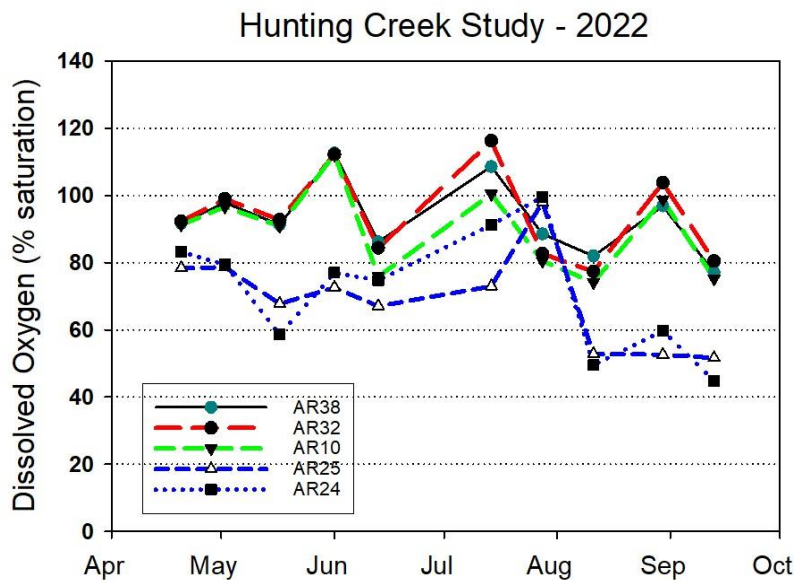


Figure 16. Dissolved oxygen (% saturation). Tidal CSO Impact Stations.

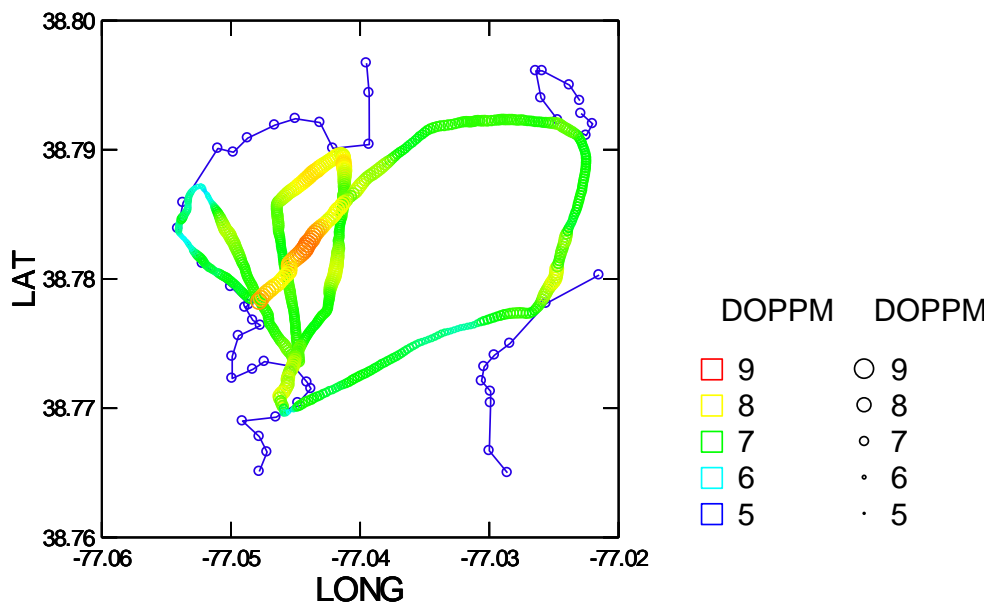


Figure 17a. Water Quality Mapping. July 18, 2022. Dissolved oxygen (mg/L).

On July 13 DO values were higher in the Hunting Creek embayment attaining 9 mg/L and 150% saturation (Figure 17a) whereas in the river mainstem values were well below saturation with values typically about 7 mg/ and 80-90% saturation (17b). this suggests active photosynthesis in the cove and more respiration in the river.

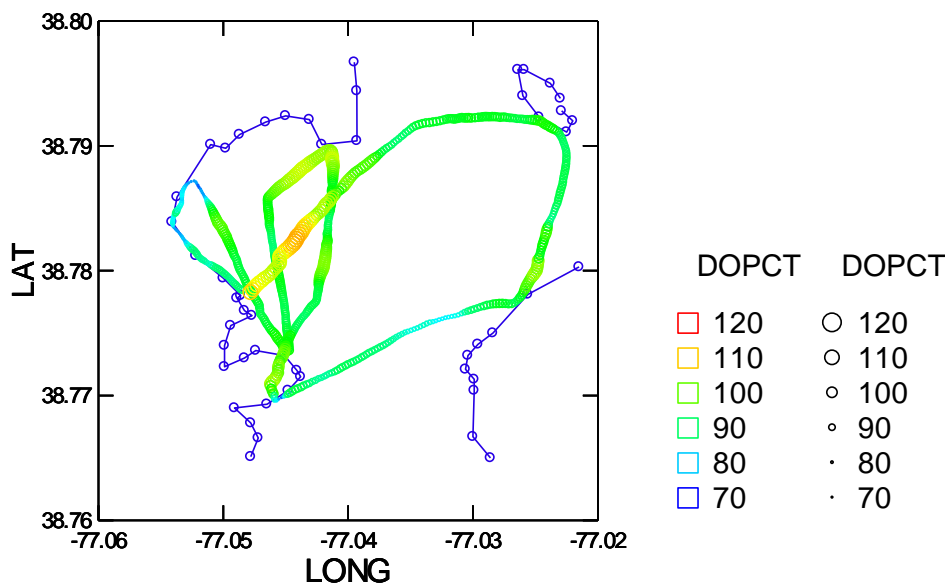


Figure 17b. Water Quality Mapping. July 18, 2022. Dissolved oxygen (percent saturation)

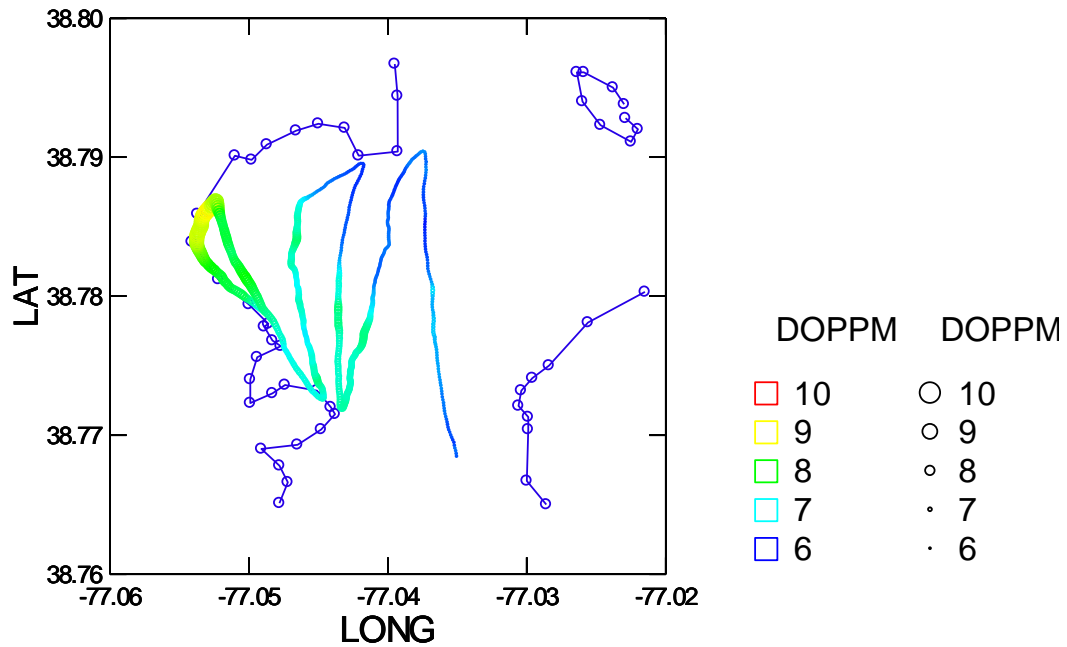


Figure 18a. Water Quality Mapping. August 16, 2022. Dissolved oxygen (mg/L).

Water quality mapping of dissolved oxygen on August 16 revealed higher values of up to 9 mg/L and 110% saturation in the Hunting Creek embayment (Figure 16a) while values of 6-7 mg/L and consistently below saturation in the Potomac mainstem (Figure 16b). This spatial pattern suggests significant photosynthetic activity by phytoplankton in Hunting Creek especially in the extreme western end.

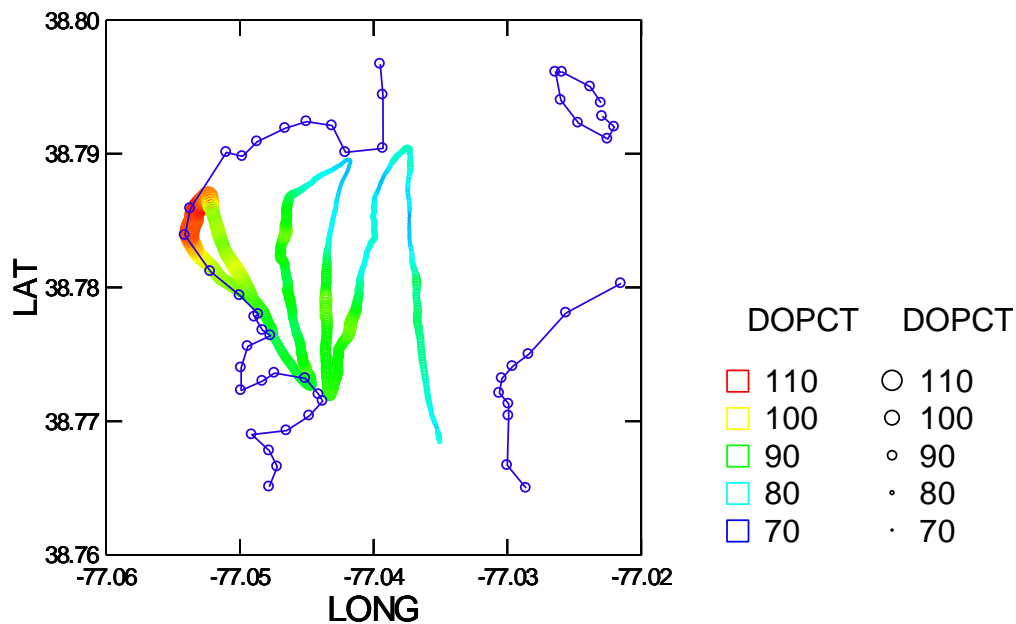


Figure 18b. Water Quality Mapping. August 16, 2022. Dissolved oxygen (percent saturation).

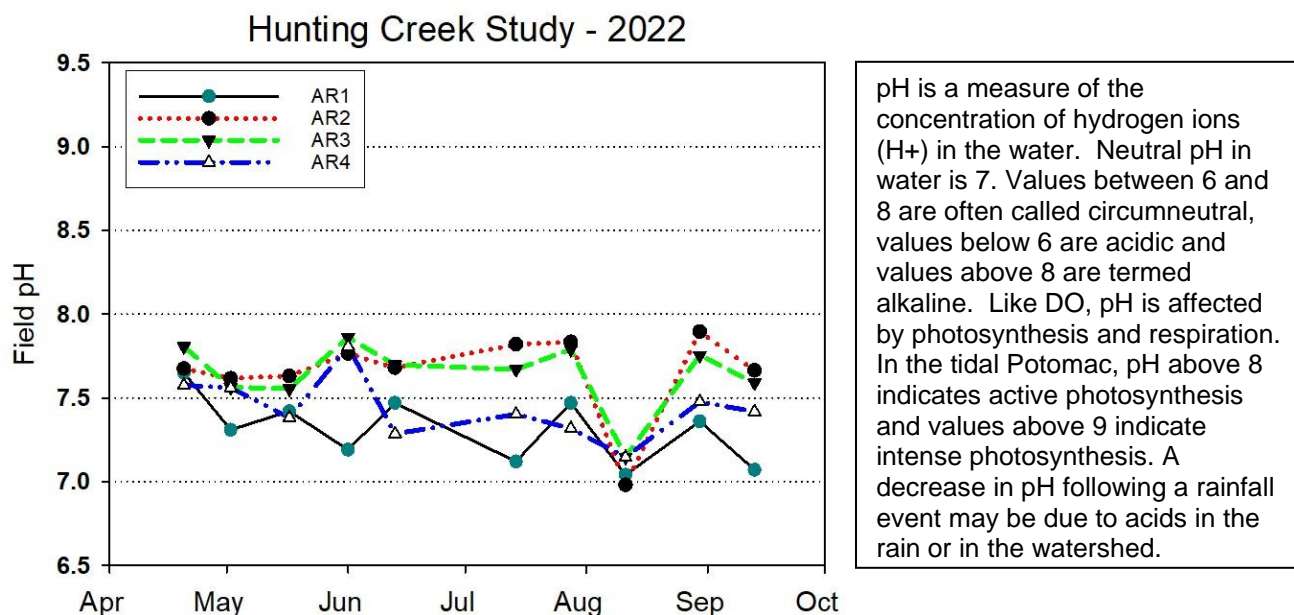


Figure 19. Field pH. Tidal Main Stations. Month tick is at first day of month.

While variable from week to week, field pH values remained in a fairly narrow range (7.2-7.8) with little seasonal pattern at the Tidal Main Stations (Figure 17). The one exception was in early August at all stations when pH was reduced to 7 at all stations in the wake of the significant rainfall-runoff event days before sampling. In the tidal CSO impact stations pH was generally 7 and 8 and was more variable at the stations on the river mainstem than at AR24 and AR25 (Figure 20).

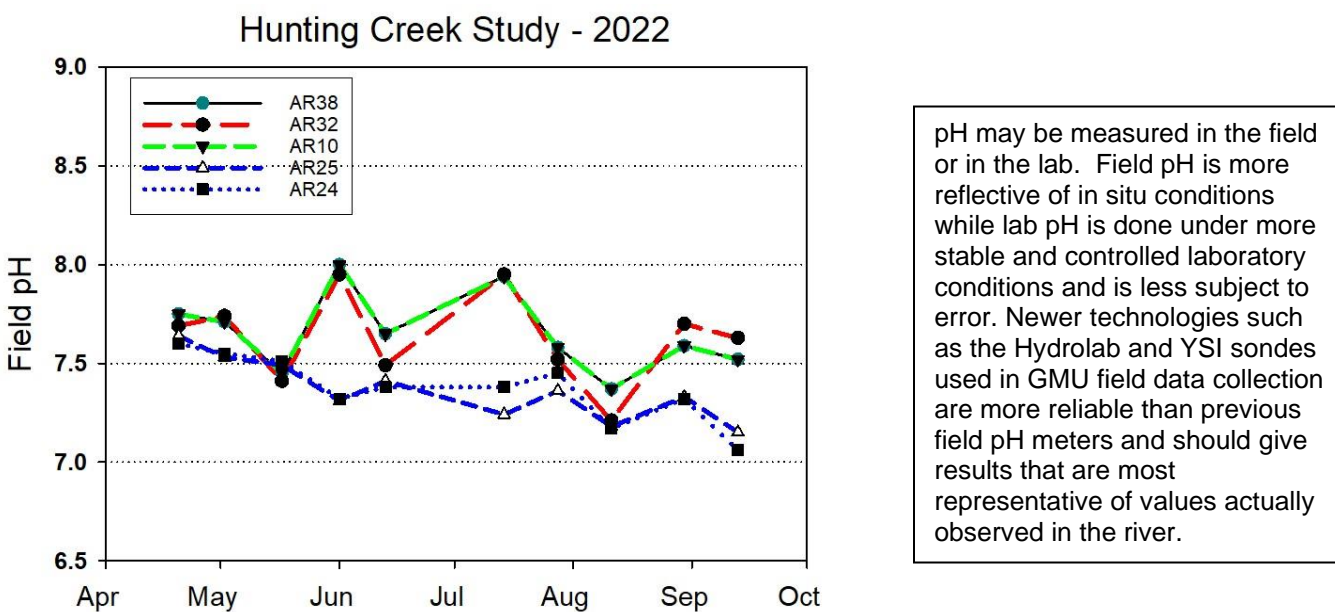


Figure 20. Field pH. Tidal CSO Impact Stations. Month tick is at first day of month.

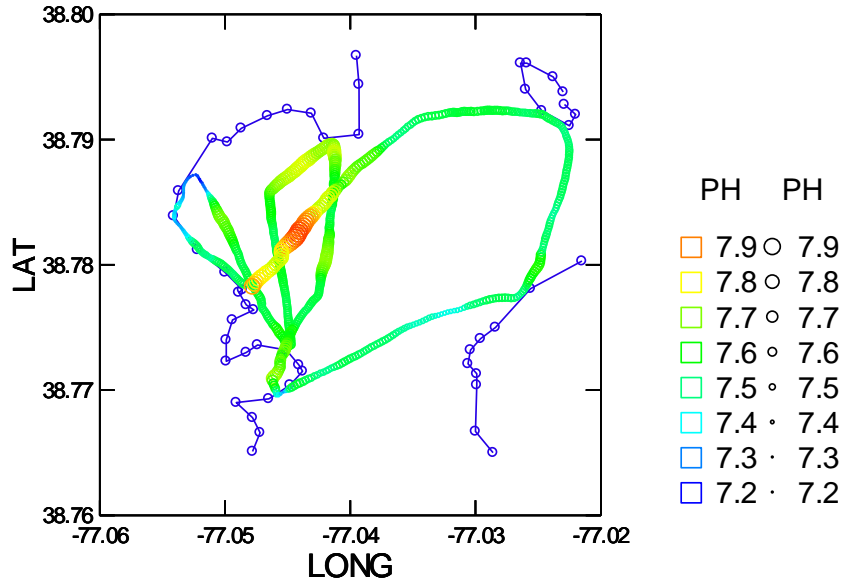


Figure 21a. Water Quality Mapping. July 18, 2022. Field pH.

Water quality mapping of pH showed a spatial pattern similar to dissolved oxygen (Figure 21a,b). Values above 7.8 were found in various parts of the Hunting Creek embayment on both dates which, like dissolved oxygen, suggests significant photosynthesis by phytoplankton.

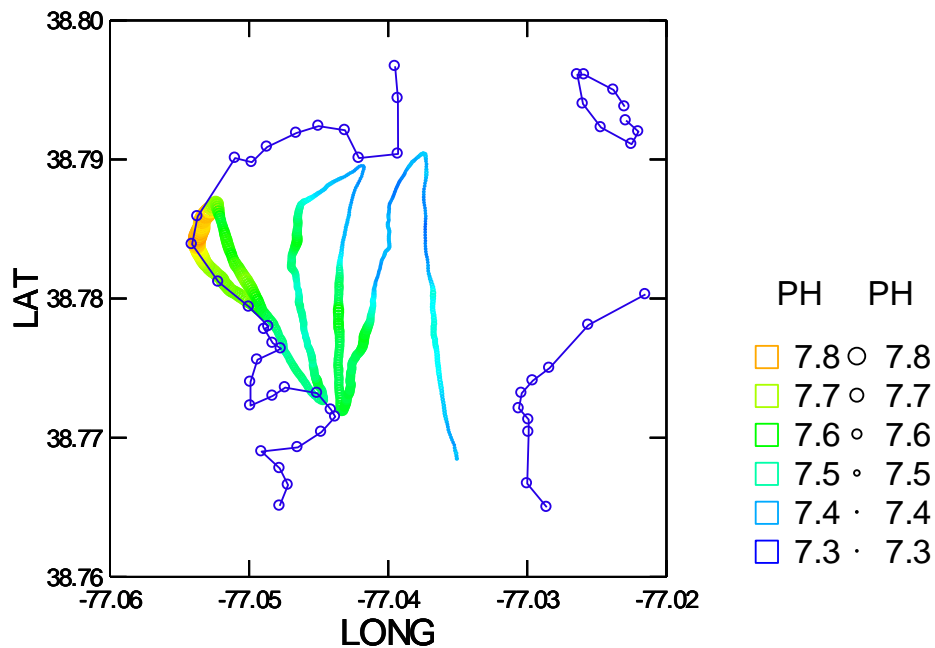


Figure 21b. Water Quality Mapping. August 16, 2022. Field pH.

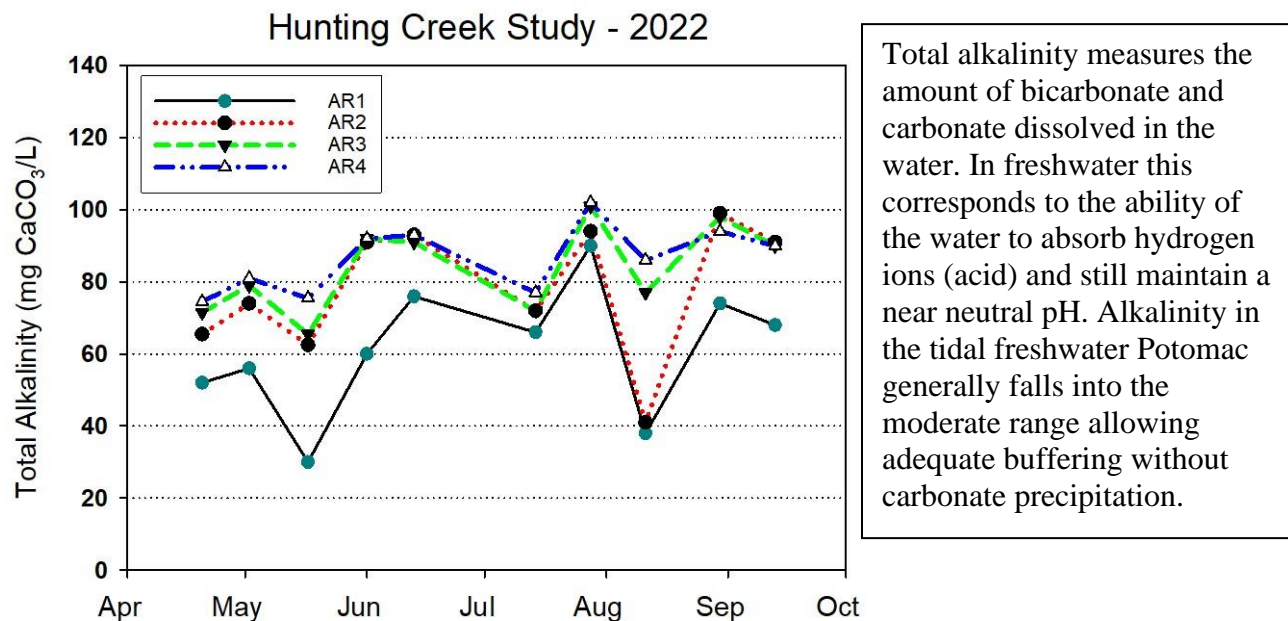


Figure 22. Total Alkalinity (mg/L as CaCO₃). Tidal Main Stations. Month tick is at first day.

Total alkalinity exhibited a gradual increase at the tidal main stations except for AR1 which was quite variable with a marked decline in early August at the time of substantial antecedent precipitation (Figure 22). AR10, AR32, and AR38 also exhibited a gradual increase while AR24 and AR25 did not exhibit a temporal trend and were consistently lower than the other stations (Figure 23).

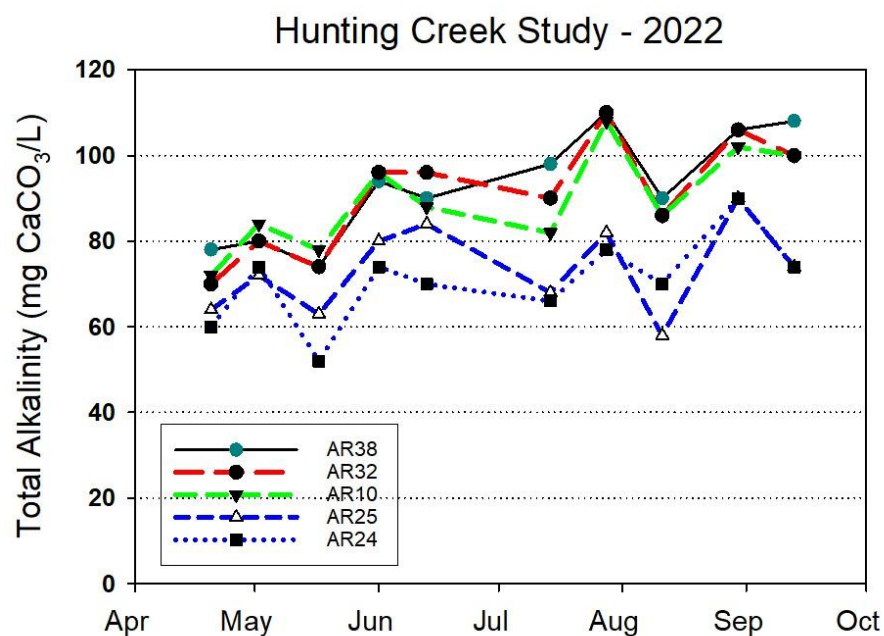


Figure 23. Total Alkalinity (mg/L as CaCO₃). Tidal CSO Impact Stations.

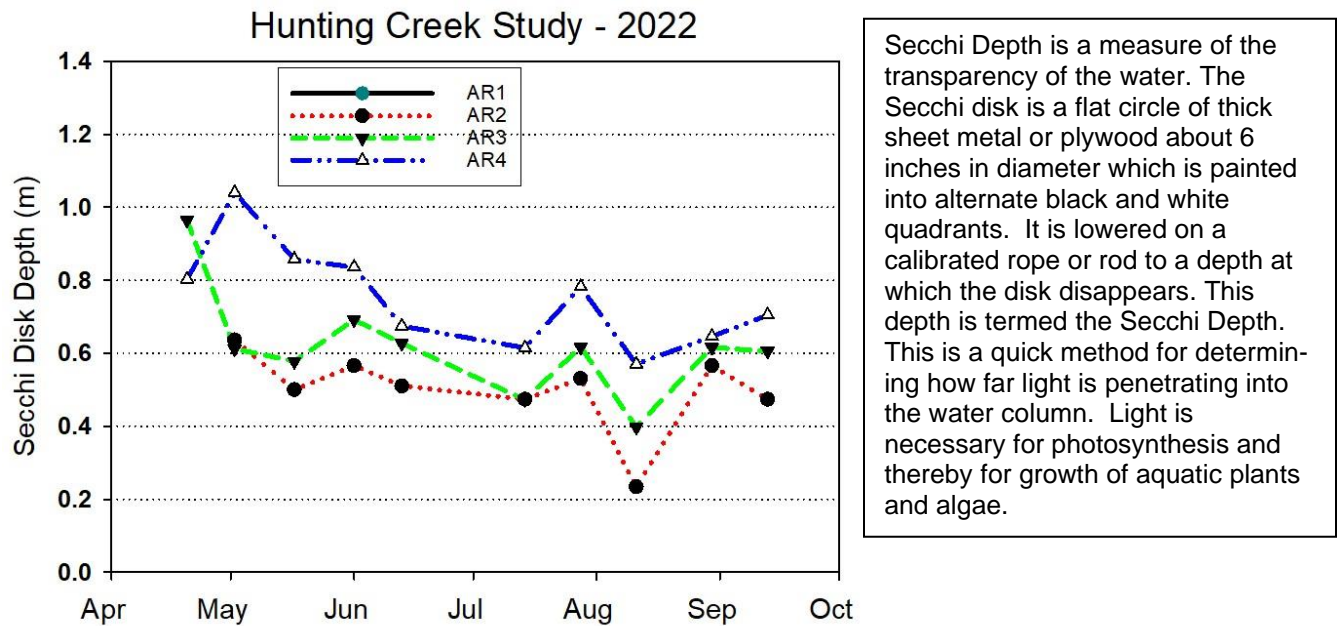


Figure 24. Secchi Disk Depth (m). Tidal Main Stations. Month tick is at first day of month.

Water clarity as reflected by Secchi disk showed a fairly consistent seasonal decline at all Tidal Main stations values declining from nearly 1 m in April to about 0.5 m in June, July, and August (Figure 24). At AR4 values were consistently somewhat greater than Ar2 and AR3, hovering at about 0.6-0.8 m for most of the year. Light attenuation (Figure 25) was somewhat less (less negative coefficient) in the river (AR4) and higher in the cove. AR2 exhibited a strong increase in light attenuation (more negative coefficient) in early August, another indication of the effect of antecedent precipitation on the light environment of Hunting Creek.

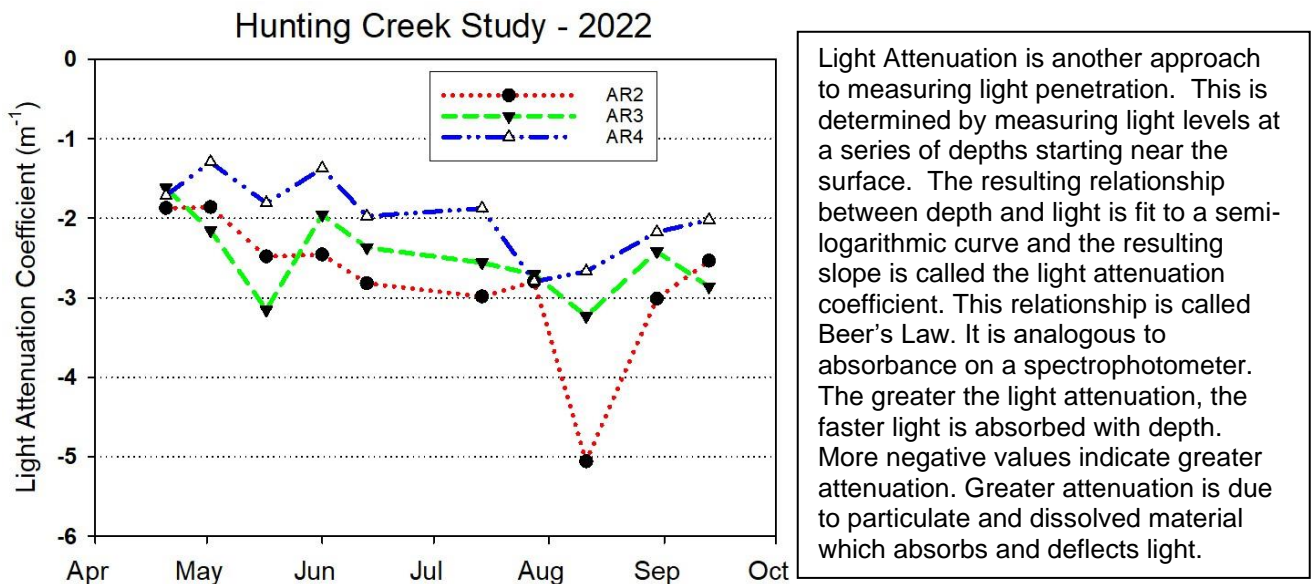


Figure 25. Light Attenuation Coefficient (m^{-1}). Tidal Main Stations. Month tick is at first day of month.

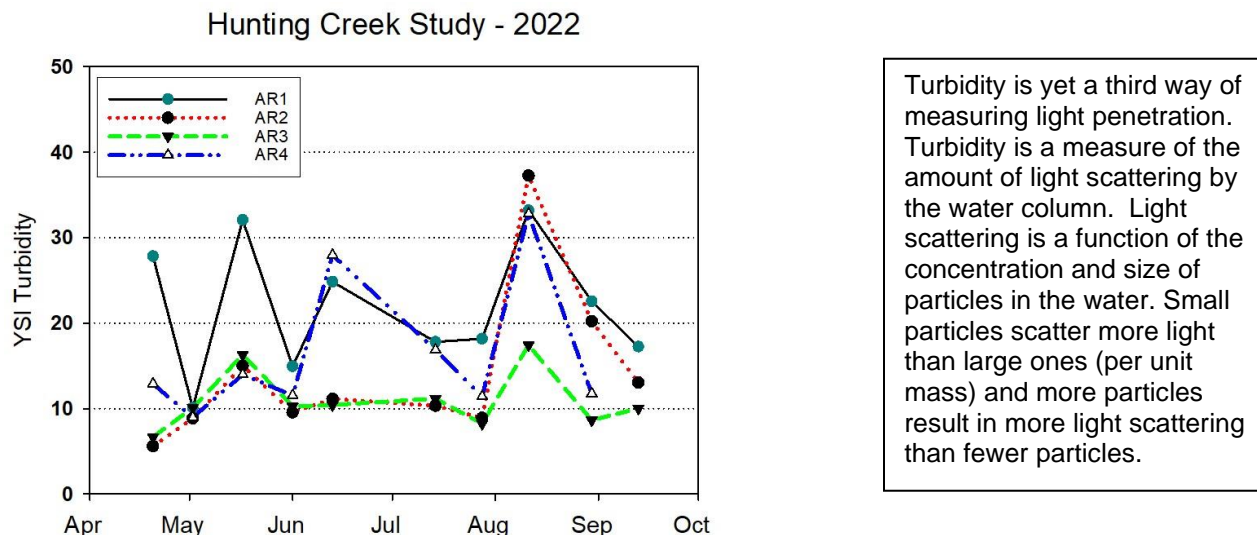


Figure 26. Turbidity (NTU). Tidal Main Stations. Month tick is at first day of month.

Turbidity values were generally low to moderate (<20 NTU) at the Tidal Main Stations (Figure 26). The exceptions were two very high values at AR2 and elevated values at AR3 in mid-August, again related to antecedent precipitation before that sampling date and corresponding with the low Secchi disk readings and high light attenuation observed earlier. Elevated values were observed frequently at AR1, attributable to smaller flow events. Levels at AR4 were also more variable, perhaps due to sediment resuspension which affected observations near the bottom of the water column and therefore the water column average. At the Tidal CSO impact stations values were generally below 20 NTU (Figure 27). Much higher values were observed on several dates at AR24 and AR25. These may have been due to disturbance of the bottom during sample collection as these two stations are accessed from shore.

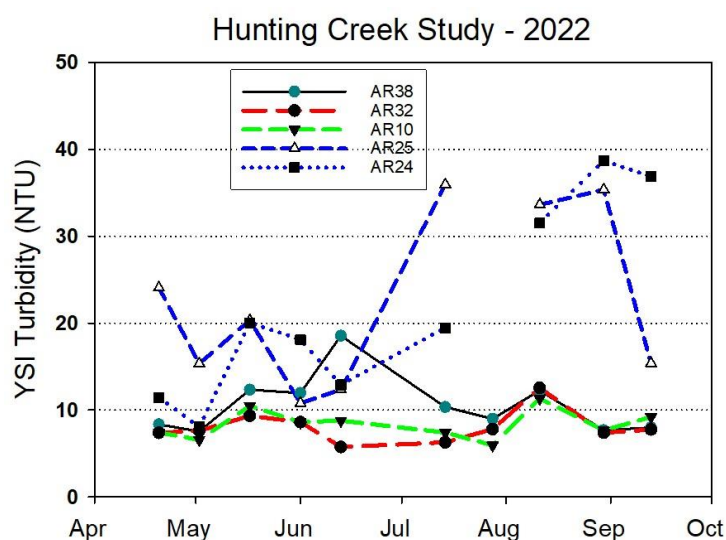


Figure 27. Turbidity (NTU). Tidal CSO Impact Stations.

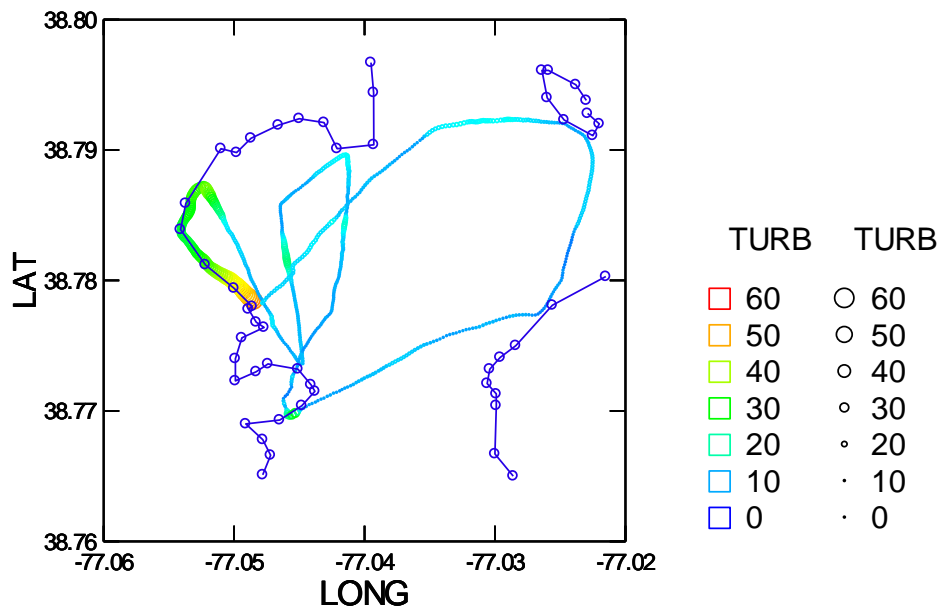


Figure 28a. Water Quality Mapping. July 18, 2022. Turbidity YSI.

Turbidity was measured during the two data mapping cruises and was generally quite low through much of the study area on both dates with values typically about 10-20 NTU (Figures 28a,b). Some higher values were found along the shoreline of the Hunting Creek embayment near areas of elevated chlorophyll and may have resulted from enhanced algal densities at these sites (Figure 28b).

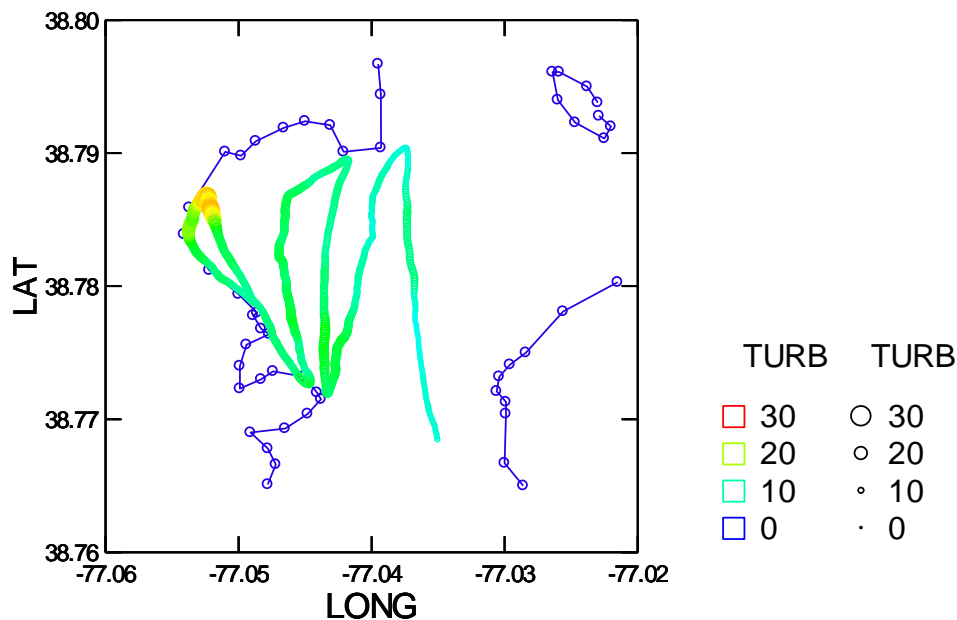


Figure 28b. Water Quality Mapping. August 16, 2022. Turbidity YSI.

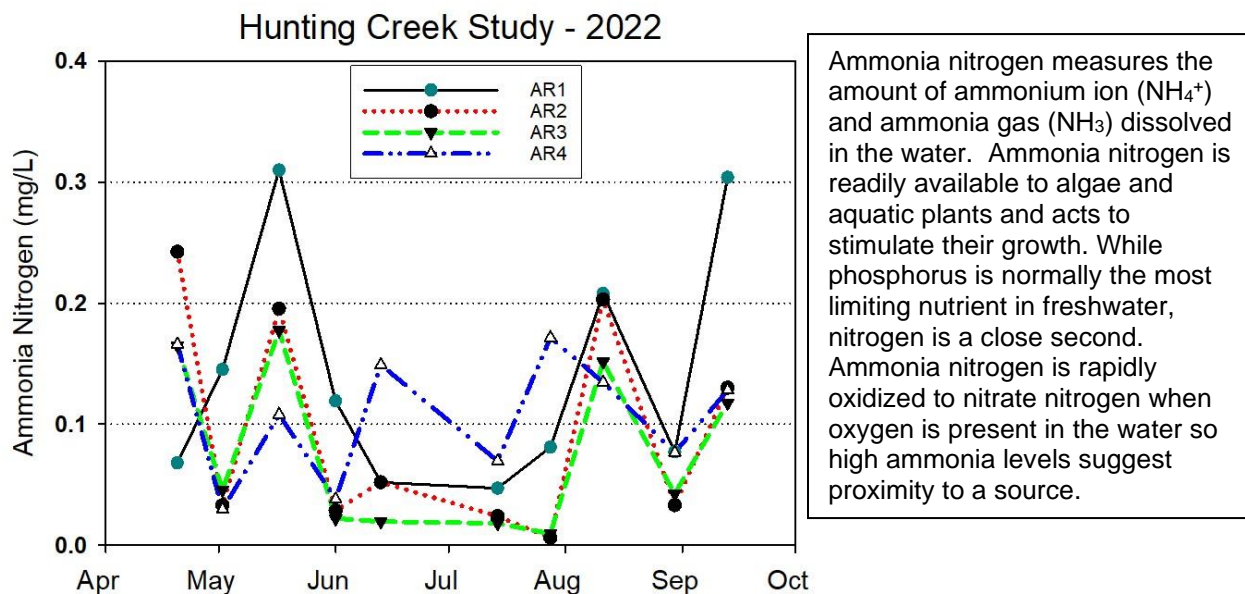


Figure 29. Ammonia Nitrogen (mg/L). Tidal Main Stations. Month tick is at first day of month.

Ammonia nitrogen was consistently low for almost the entire study period at both Tidal Main and Tidal CSO impact stations (Figure 29&30). Elevated values were observed at Hunting Creek stations AR2 and AR3 on in late May and early August, days of high antecedent flow. Values spiked strongly at AR24 and AR25 in late May.

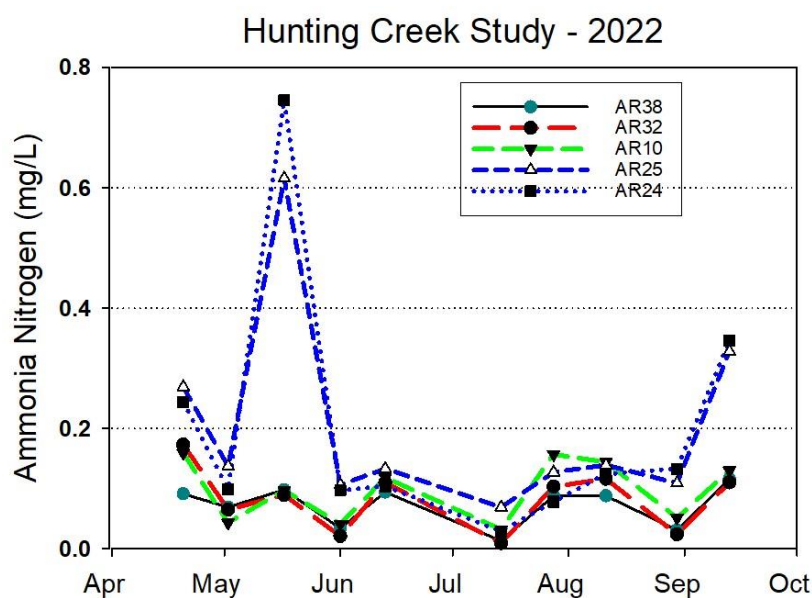


Figure 30. Ammonia Nitrogen (mg/L). Tidal CSO Impact Stations.

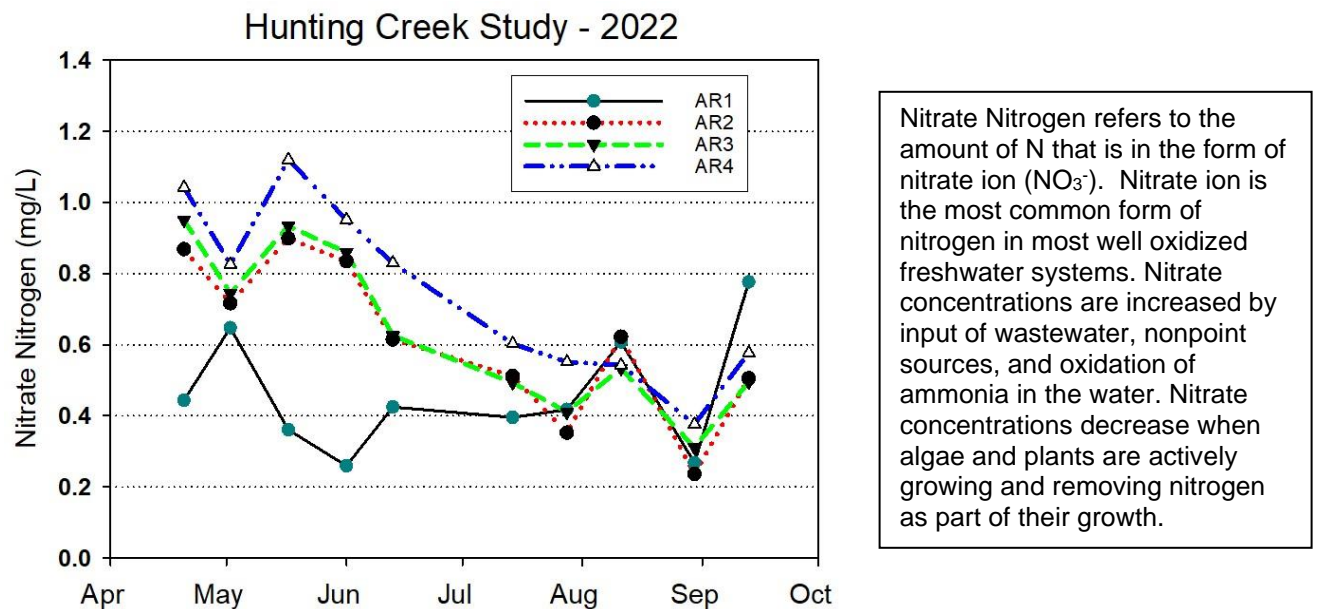


Figure 31. Nitrate Nitrogen (mg/L). Tidal Main Stations. Month tick is at first day of month.

At most of the Tidal Main stations, nitrate nitrogen levels showed a general pattern of decrease from April through early August with a slight uptick in September (Figure 31). At AR1 values did not show a seasonal pattern and were generally somewhat lower than at the other Tidal Main stations. A similar pattern was observed at the Tidal CSO Impact stations except at AR24 and AR25 which did not show a strong seasonal trend (Figure 32).

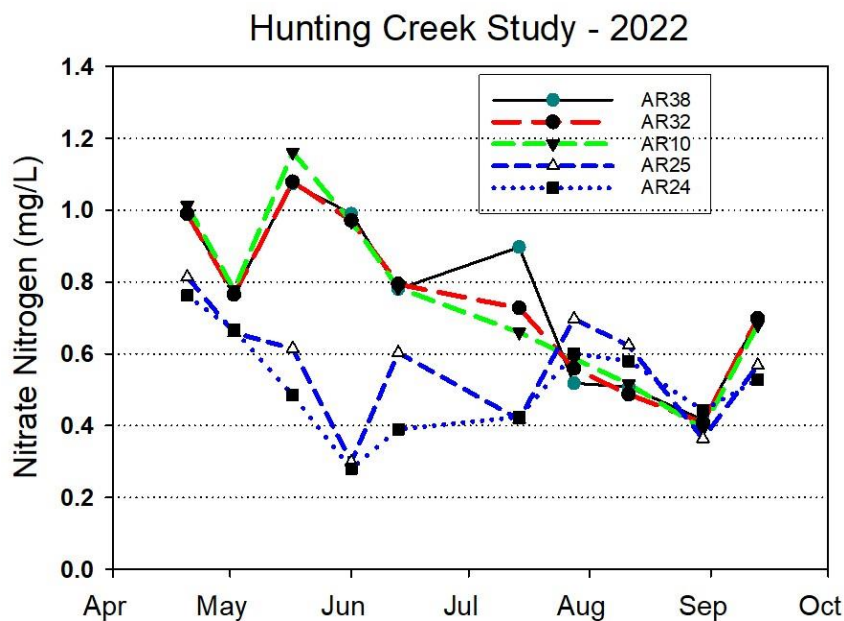


Figure 32. Nitrate Nitrogen (mg/L). Tidal CSO Impact Stations.

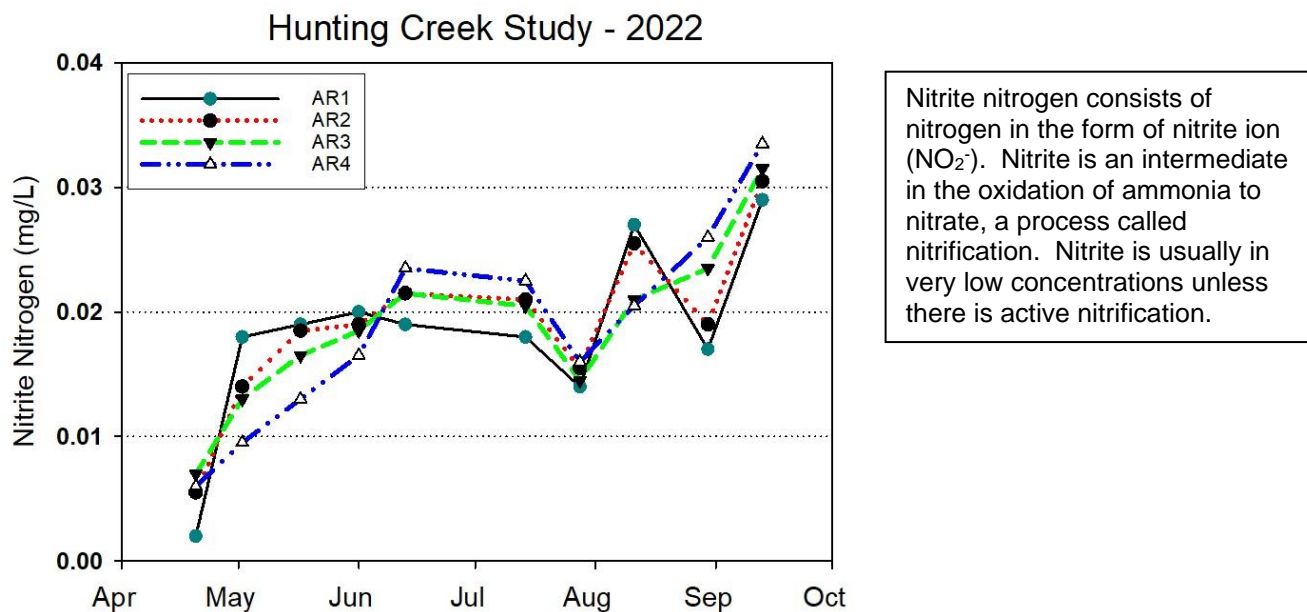


Figure 33. Nitrite Nitrogen (mg/L). Tidal Main Stations. Month tick is at first day of month.

Nitrite nitrogen was generally low (<0.04 mg/L) at all stations throughout the year (Figures 33&34). A consistent seasonal increase was observed at many stations starting with values less than 0.01 mg/L in April to a maximum of about 0.03 mg/L in September.

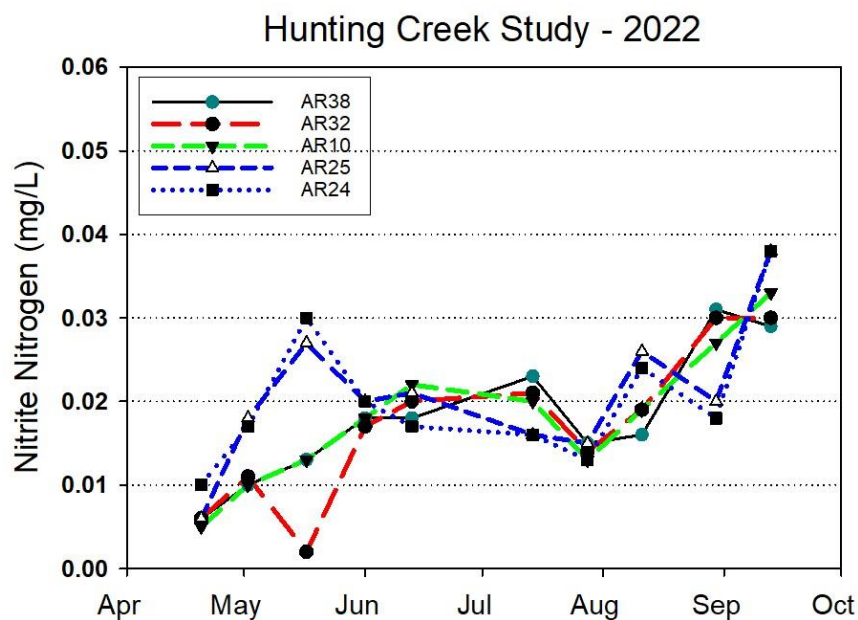


Figure 34. Nitrite Nitrogen (mg/L). Tidal CSO Impact Stations.

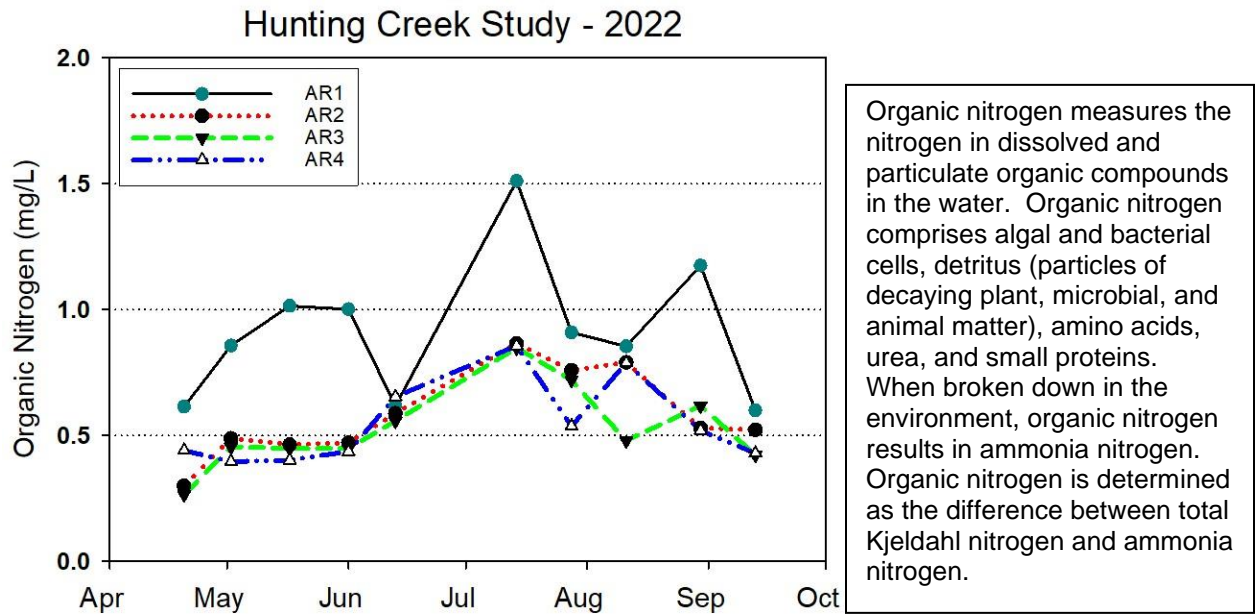


Figure 35. Organic Nitrogen (mg/L). Tidal Main Stations. Month tick is at first day of month.

Organic nitrogen values were generally in the range of 0.2-0.8 mg/L at most stations throughout the year at both Tidal Main and CSO Impact stations (Figures 35&36). AR1, AR24, and AR25 were consistently higher and more variable. There was some indication of a seasonal increase from April through July followed by a gradual decline.

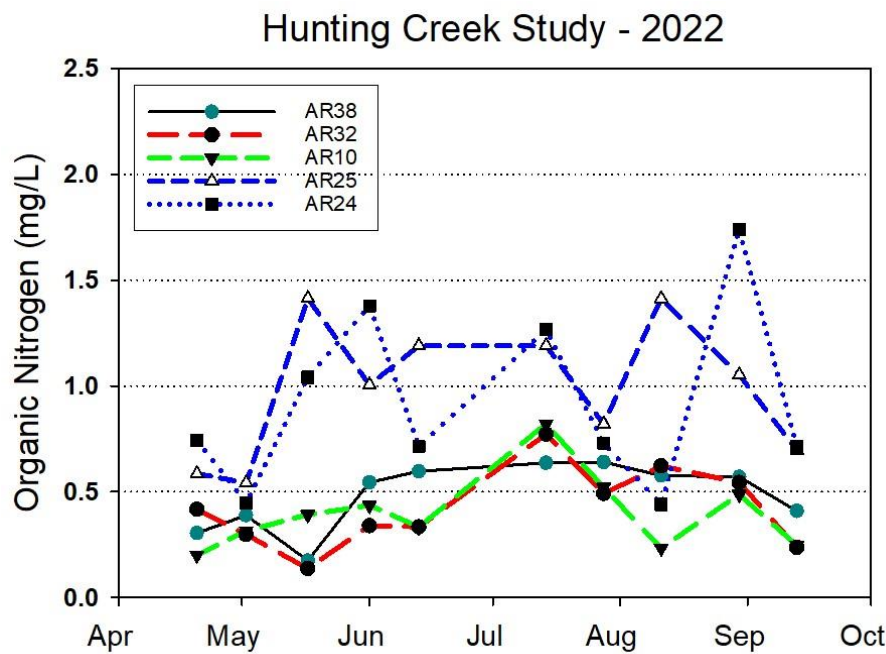


Figure 36. Organic Nitrogen (mg/L). Tidal CSO Impact Stations.

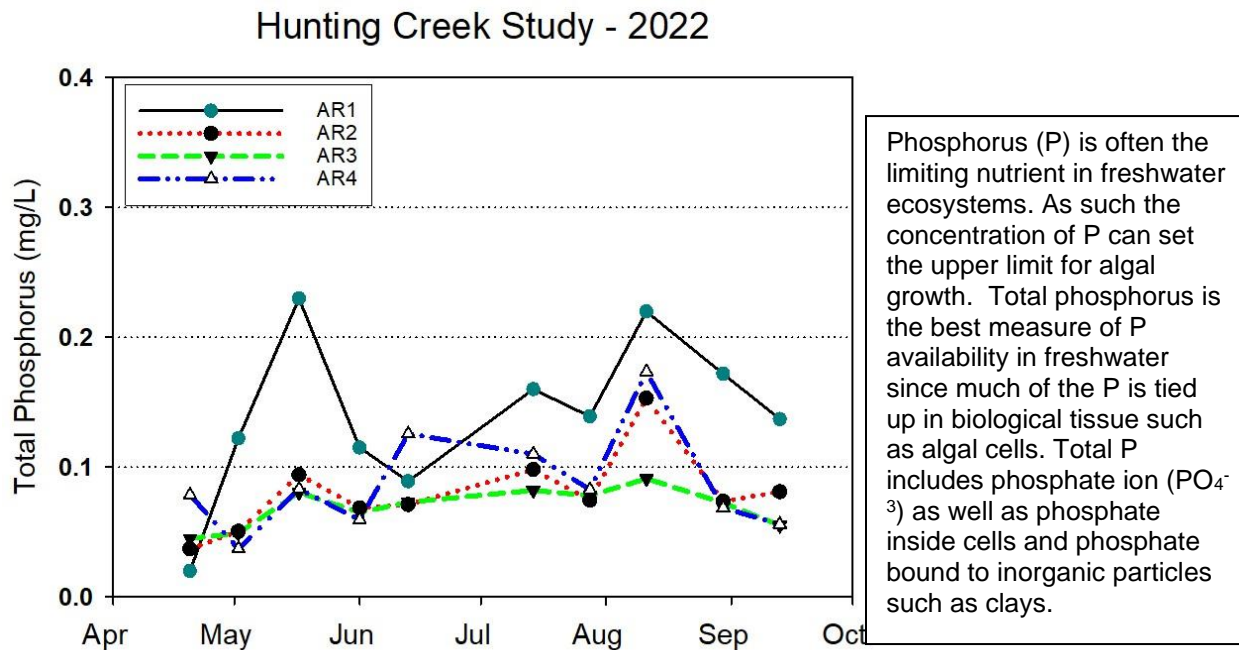


Figure 37. Total Phosphorus (mg/L). Tidal Main Stations. Month tick is at first day of month.

Total phosphorus weak seasonal trend at most stations remaining in the 0.05 to 0.10 range (Figures 37&38). Higher values and more variable values were observed at AR1, AR24, and AR25 along the northern shore of Hunting Creek similar to organic nitrogen and other variables. A minor peak was observed at AR2 and AR4 in early August.

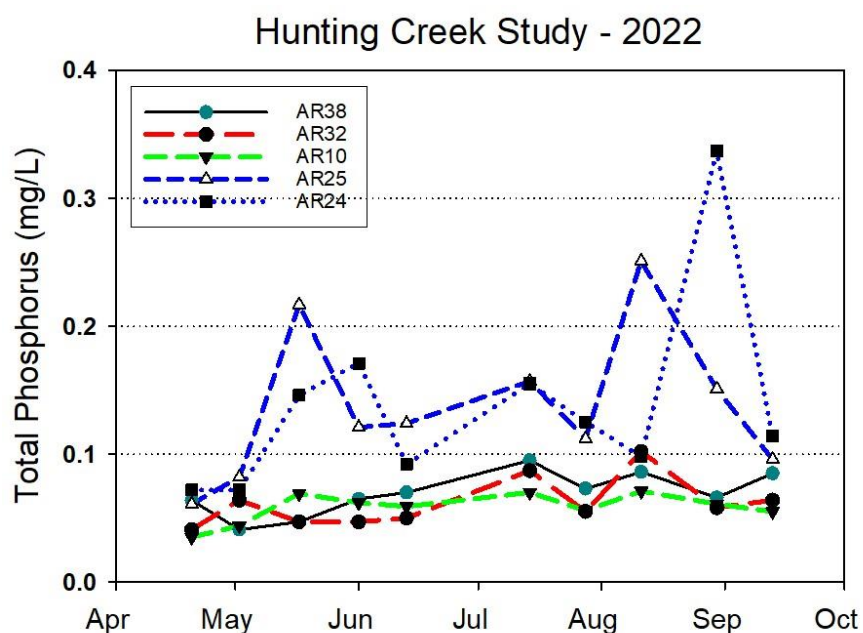


Figure 38. Total Phosphorus (mg/L). Tidal CSO Impact Stations.

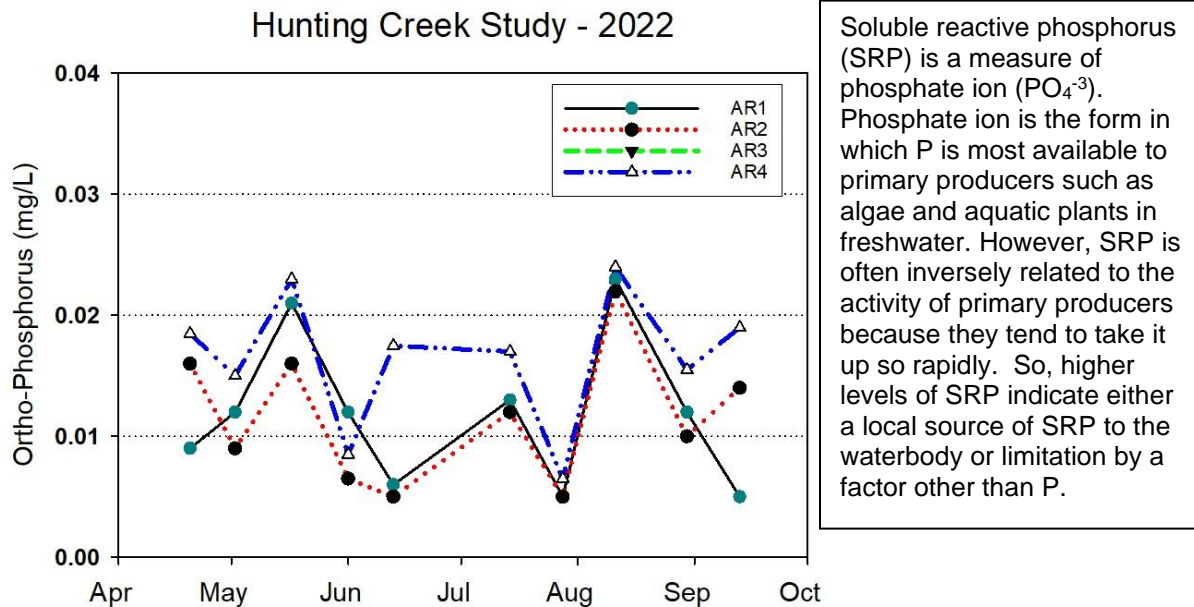


Figure 39. Ortho-Phosphorus (mg/L). Tidal Main Stations. Month tick is at first day of month.

Ortho-phosphorus values were generally very low which is typical of the tidal Potomac (Figures 39&40). There was a fair amount of variability, but this is most likely due to the levels being near the limits of detection for ortho-phosphorus. Elevated values of ortho-phosphorus, if observed, would be evidence of a nearby source of untreated sewage.

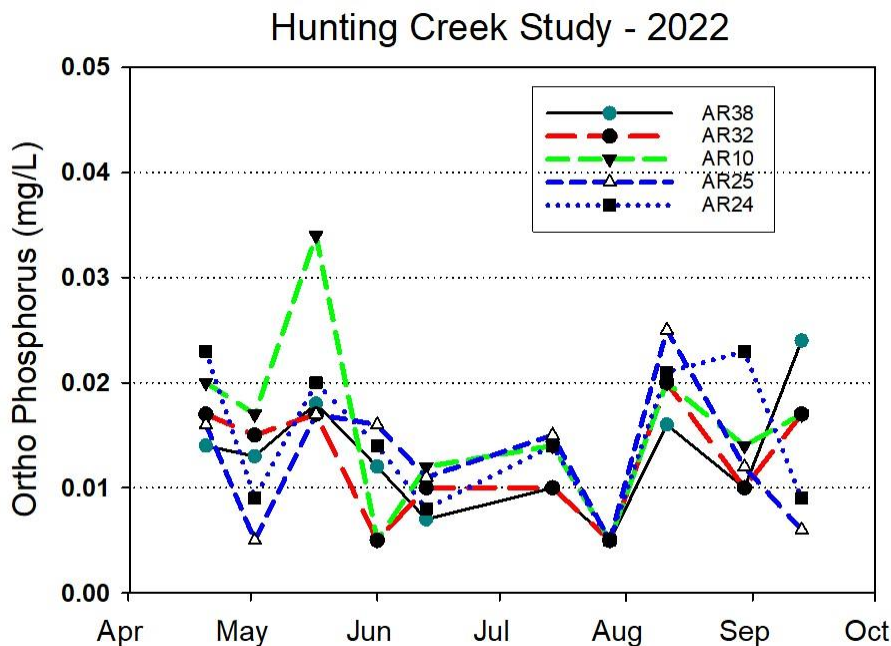


Figure 40. Ortho-Phosphorus (mg/L). Tidal CSO Impact Stations.

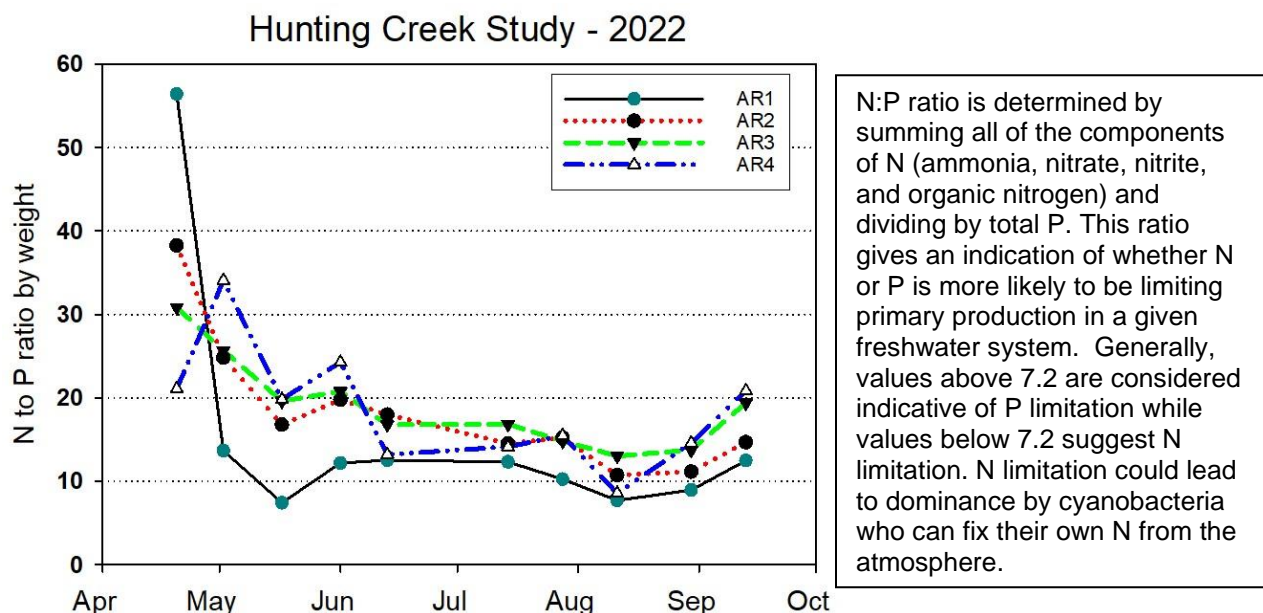


Figure 41. N/P Ratio (by mass). Tidal Main Stations. Month tick is at first day of month.

N/P ratio consistently pointed to P limitation, with values generally in the 10-30 range being greater than 7.2 threshold in all samples (Figure 41). Values at Tidal Main stations showed a general seasonal decline reaching minima in early August. At the Tidal CSO Impact stations values were again above 10 in almost all samples with a general trend for higher values in the April to June period and lower and more uniform values thereafter (Figure 42).

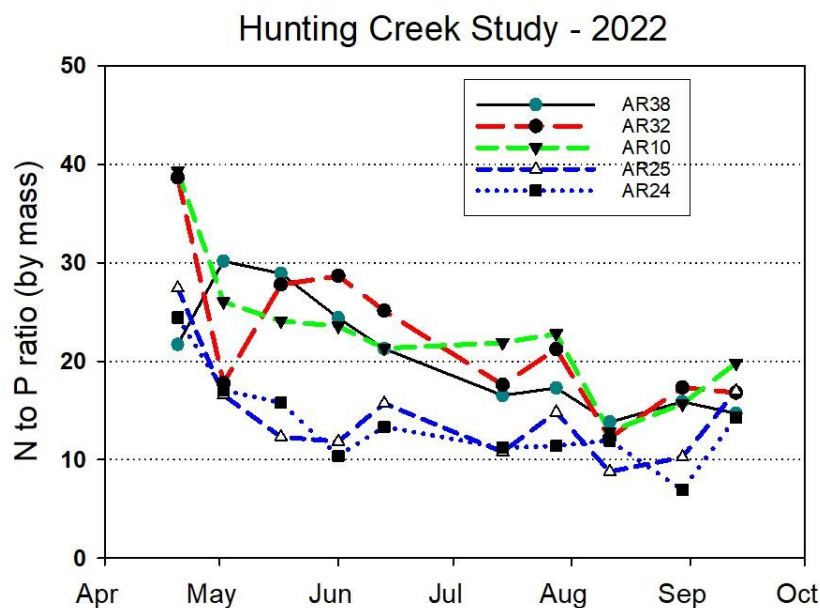


Figure 42. N/P Ratio (by mass). Tidal CSO Impact Stations.

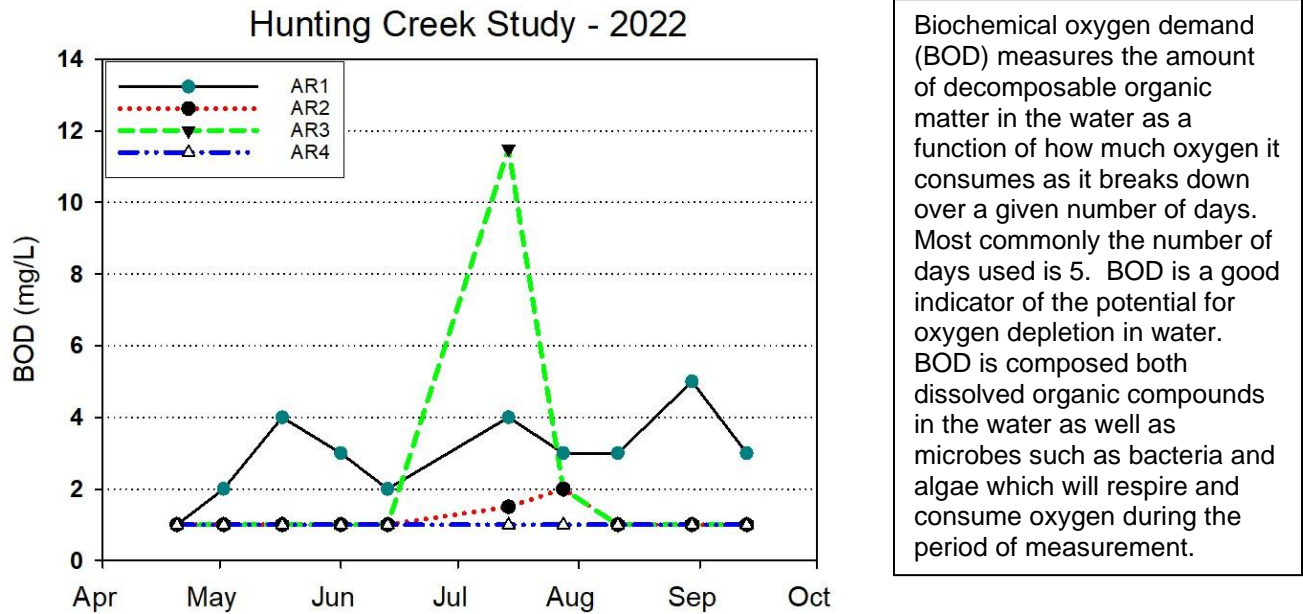


Figure 43. Biochemical Oxygen Demand (mg/L). Tidal Main Stations. Month tick is at first day of month.

BOD was consistently less than 2 mg/L at AR2, AR3, and AR4 (Figure 43). A spike at AR3 in early July was hard to explain. At AR1 values were generally higher, but remained below 4 mg/L. At the AR24 and AR25 values were often above 2, but at other Tidal CSO Impact stations values below 2 mg/L were typical (Figure 44).

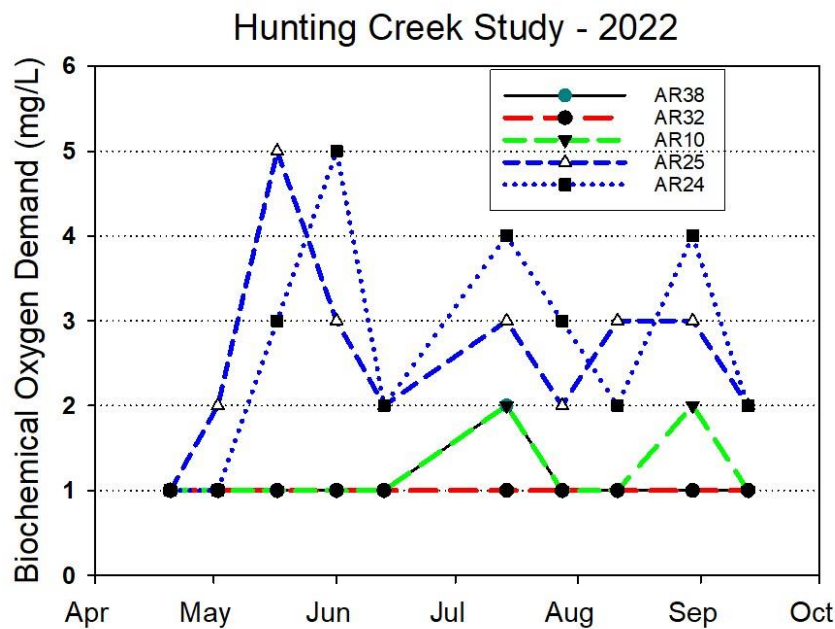


Figure 44. Biochemical Oxygen Demand (mg/L). Tidal CSO Impact Stations.

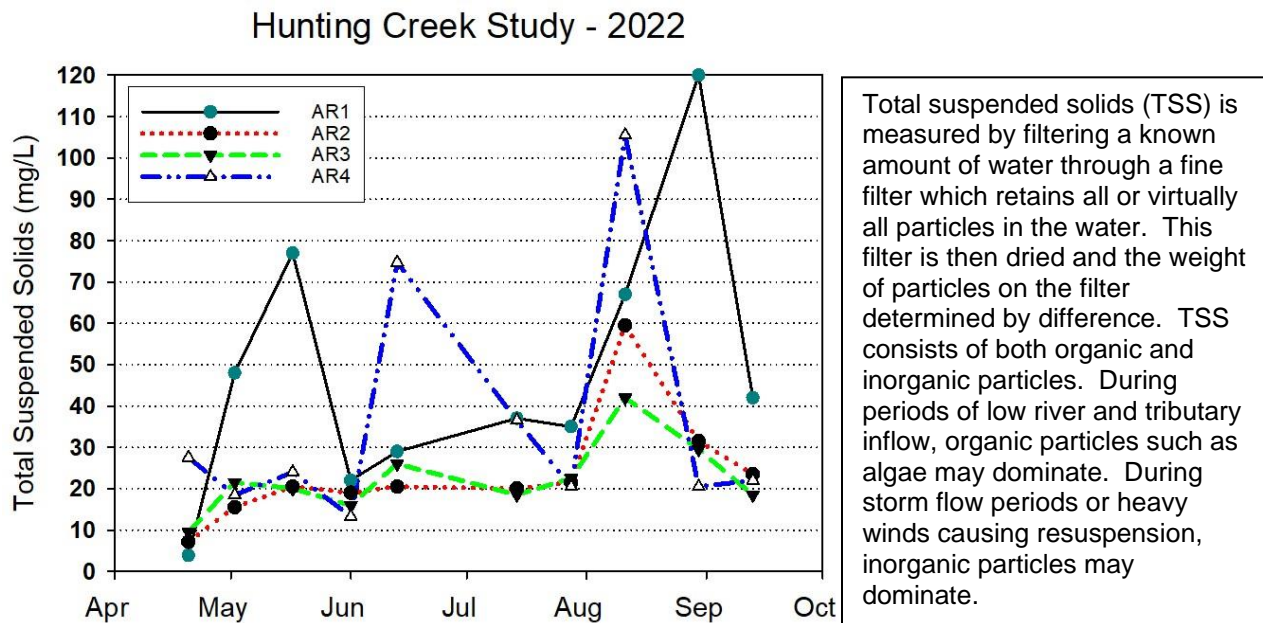


Figure 45. Total Suspended Solids (mg/L). Tidal Main Stations. Month tick is at first day of month.

Total suspended solids (TSS) was generally in the range 5-30 mg/L at the Tidal Main stations and at AR10, AR32, and AR38 (Figures 45&46). Higher values were observed episodically at AR1, AR4, AR24, and AR25 similar to organic nitrogen and total phosphorus. The elevated values at AR4 were due to much higher values in the bottom samples due apparently to sediment resuspension.

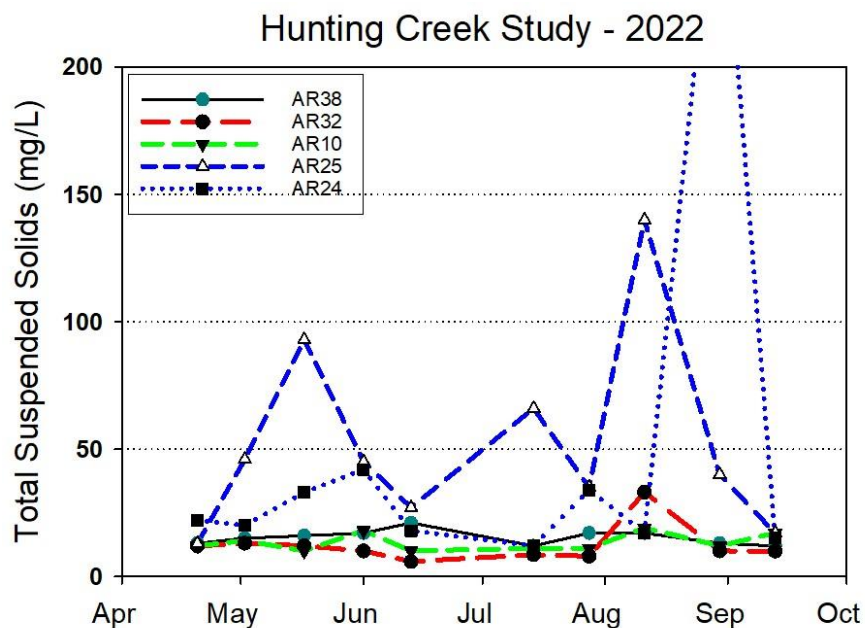


Figure 46. Total Suspended Solids. Tidal CSO Impact Stations. Month tick is at first day of month.

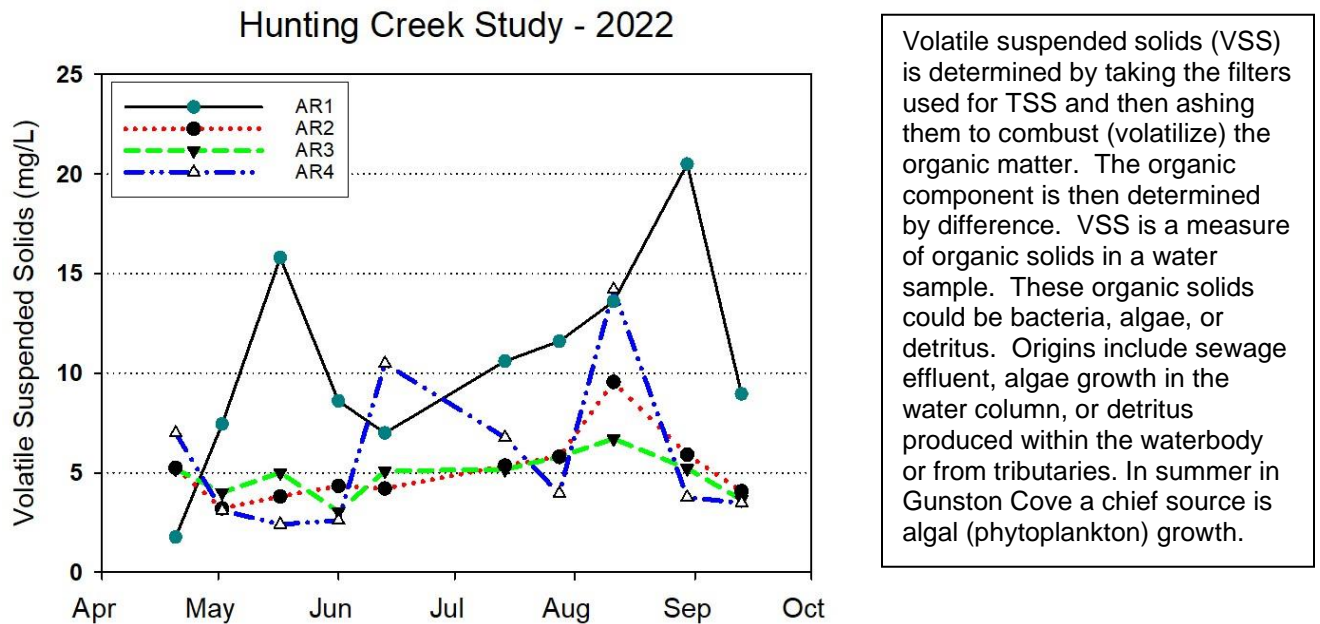


Figure 47. Volatile Suspended Solids (mg/L). Surface Tidal Main Stations. Month tick is at first day of month.

VSS values followed similar patterns but at substantially lower values, generally 10 mg/L or less. At the Tidal Main Stations and AR32 and AR38 values remained in the 2-6 mg/L range (Figures 47&48). Higher values were observed at AR1, AR4, AR24, and AR25 for the reasons described above for TSS.

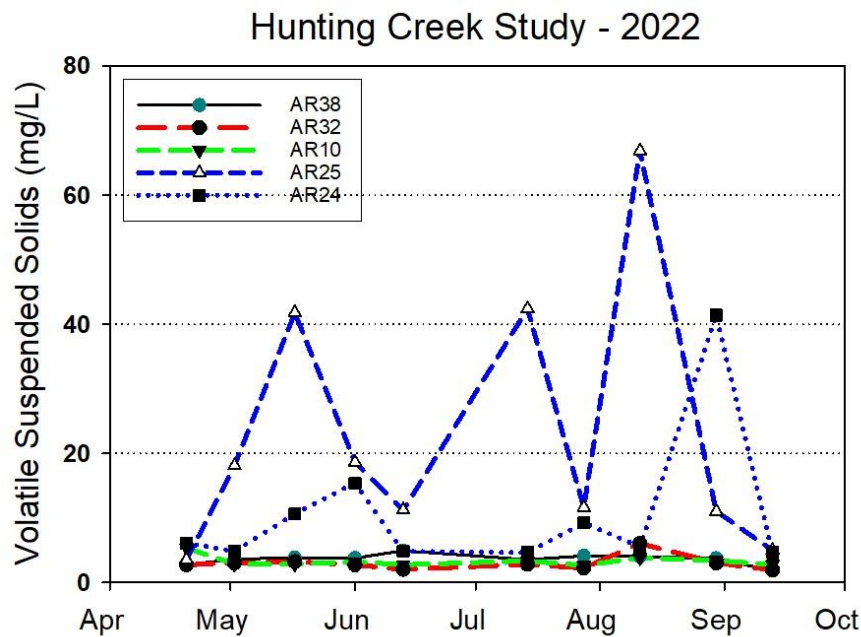


Figure 48. Volatile Suspended Solids (mg/L). Tidal CSO Impact Stations.

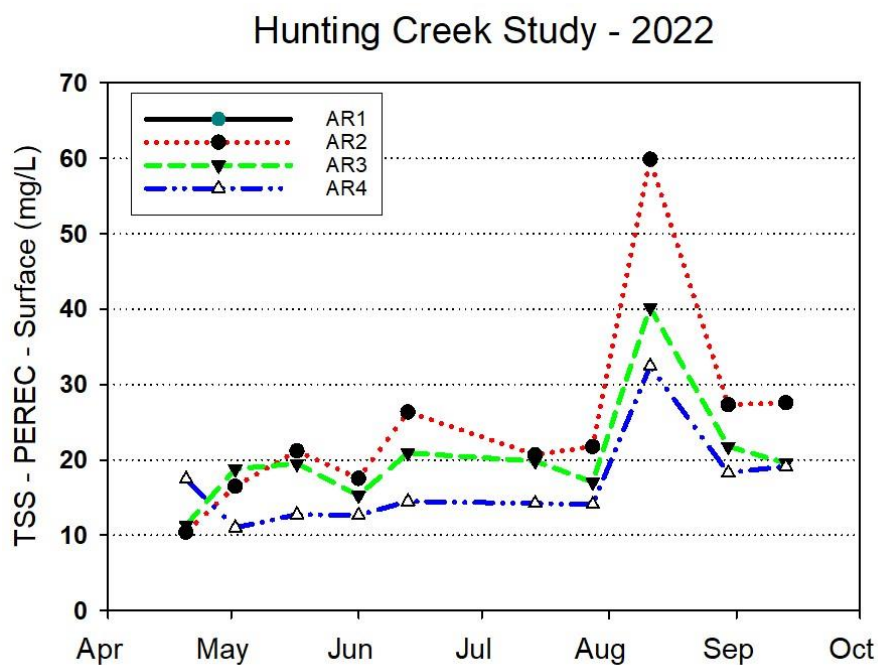


Figure 49. Total Suspended Solids. PEREC. Tidal Main Stations.

PEREC staff conducted TSS and VSS at the Tidal Main stations. Again, AR2, AR3, and AR4 were generally in the 15-30 mg/L range for TSS (Figure 49). The exception was early August when AR2, AR3, and AR4 were highly elevated at 30-60 mg/L and 6-10mg/L for VSS (Figure 50).

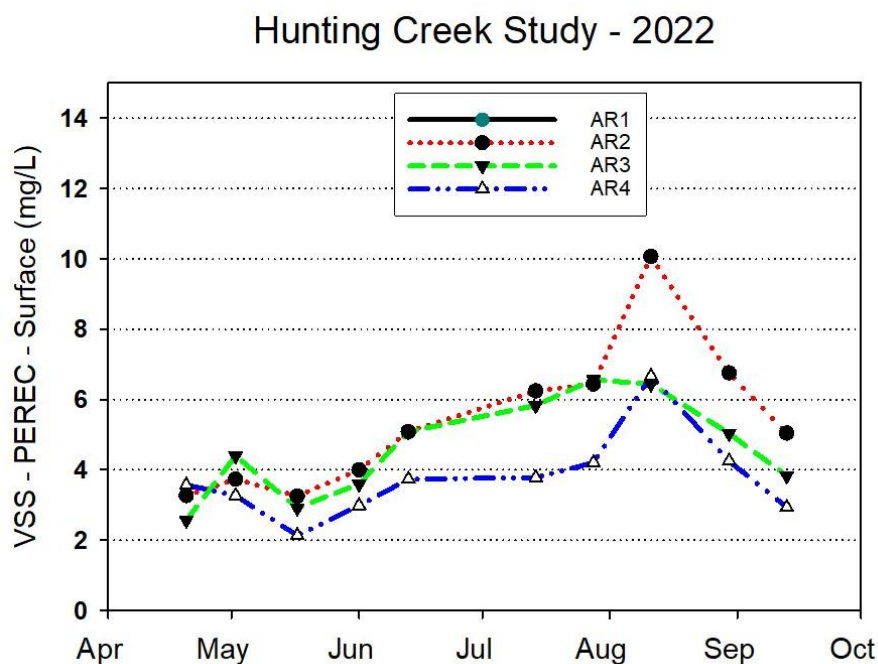


Figure 50. Volatile Suspended Solids. PEREC. Tidal CSO Impact Stations.

C. Physico-chemical Parameters: Tributary Stations – 2022

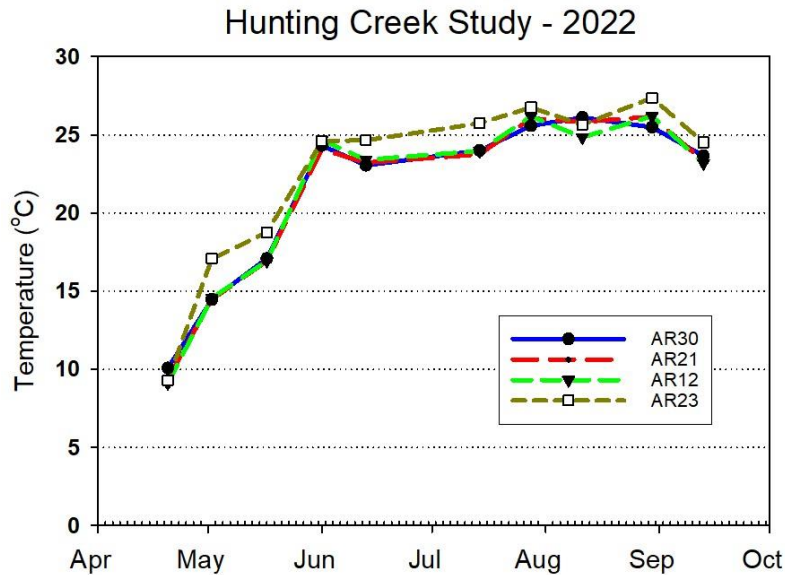


Figure 51. Water Temperature (°C). GMU Field Data. Cameron Run Axis Tributaries. Month tick is at first day of month.

Water quality data for the tributary stations was graphed in two sets for each parameter: Cameron Run Axis stations running the length of Cameron Run and Hooffs Run Axis stations along the Hooffs Run Axis. Stations are arranged in the legends from upstream to downstream. Temperatures at almost all stations closely followed air temperatures (Figure 51&52). During summer, the Cameron Run Axis stations were about 26°C while the Hooffs Run Axis stations were about 24°C.

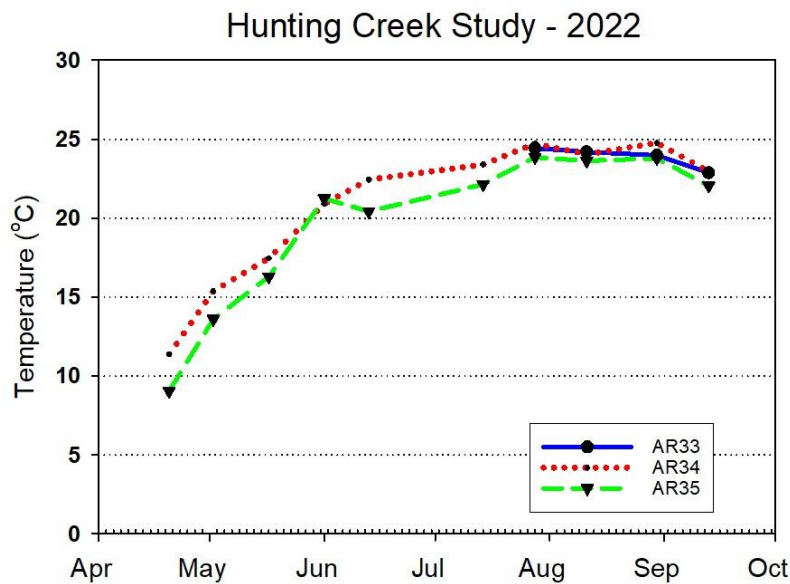


Figure 52. Water Temperature (°C). GMU Field Data. Hooffs Run Axis Tributaries. Month tick is at first day of month.

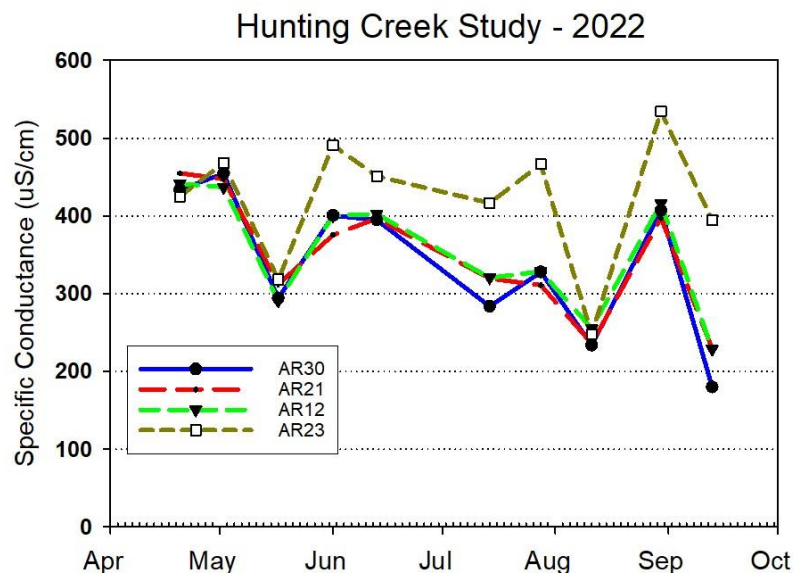


Figure 53. Specific Conductance (uS/cm). GMU Field Data. Cameron Run Axis Tributaries. Month tick is at first day of month.

Specific conductance was generally in the 200-500 uS/cm range and showed a clear decrease seasonally at the Cameron Run Axis stations (Figure 53). AR23 showed some higher values which may be explained by its proximity to the AlexRenew outfall. On the Hooffs Run Axis specific conductance showed little seasonal pattern, but values increased from upstream (AR35) to downstream (AR34) (Figure 54).

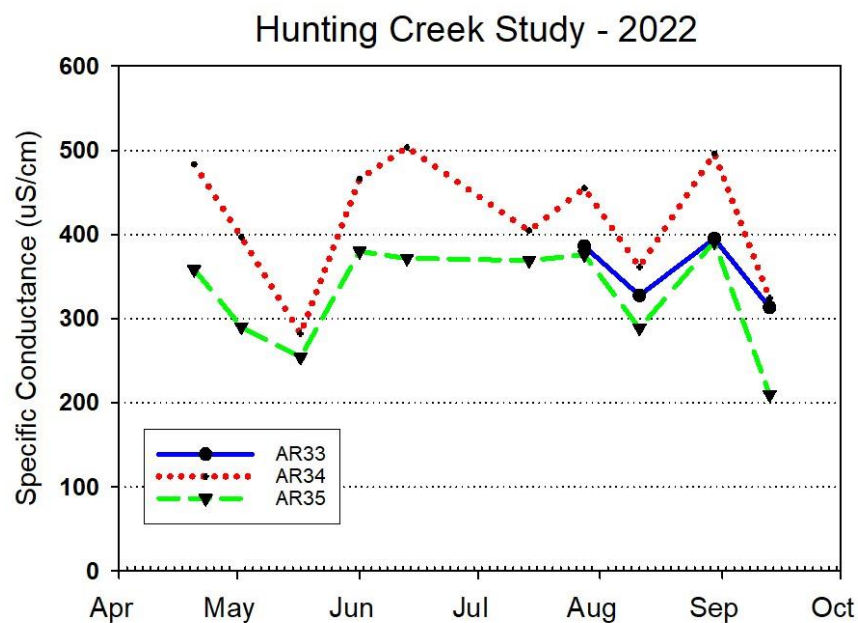


Figure 54. Specific Conductance (uS/cm). GMU Field Data. Hooffs Run Axis Tributaries. Month tick is at first day of month.

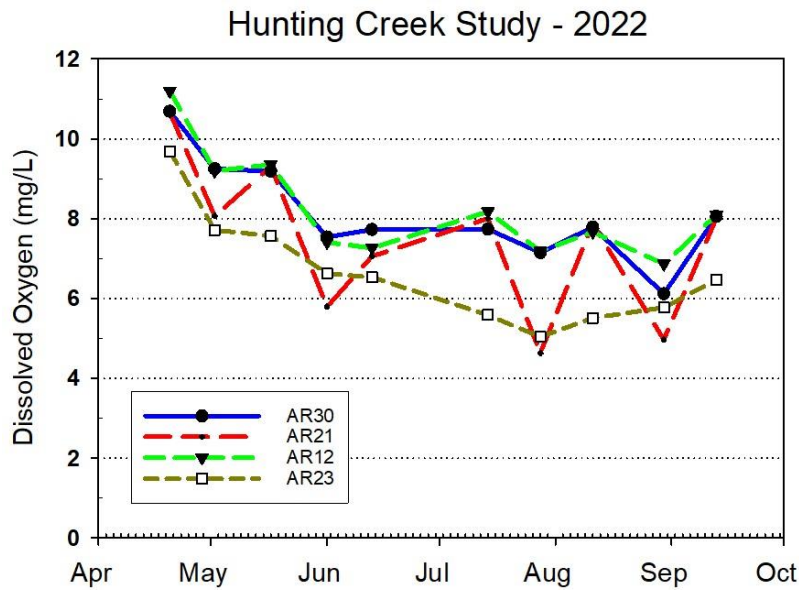


Figure 55. Dissolved Oxygen (mg/L) GMU Field Data. Cameron Run Axis stations. Month tick is at first day of month.

Dissolved oxygen (mg/L) at most of the Cameron Run Axis stations showed a seasonal pattern of declining values through the year reaching lows of 5-7 mg/L in July through September (Figure 55). Most of this trend was due to temperature effects since percent saturation values were generally in the 80-100% range with little seasonal pattern (Figure 56). And again, AR23 (near the AlexRenew outfall) showed lower values and AR21 showed more variable values.

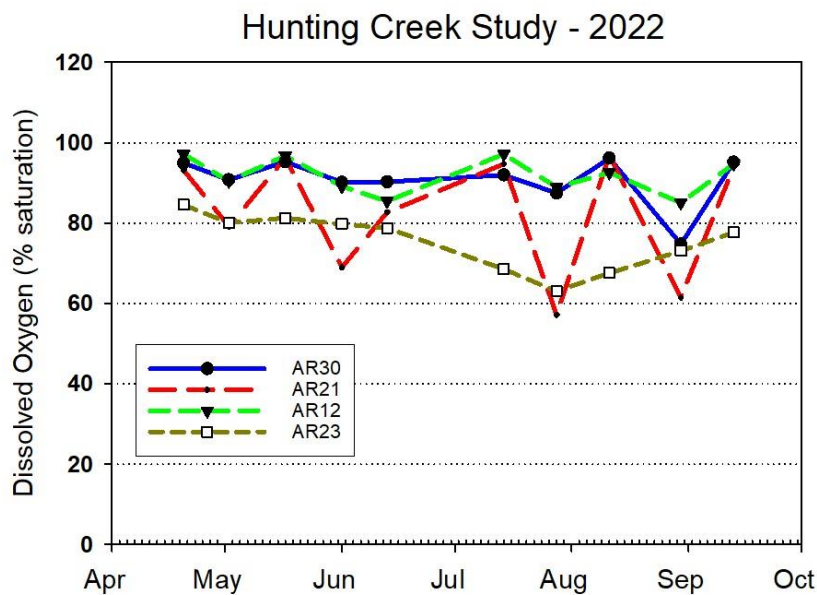


Figure 56. Dissolved Oxygen (% saturation) GMU Field Data. Cameron Run Axis stations. Month tick is at first day of month.

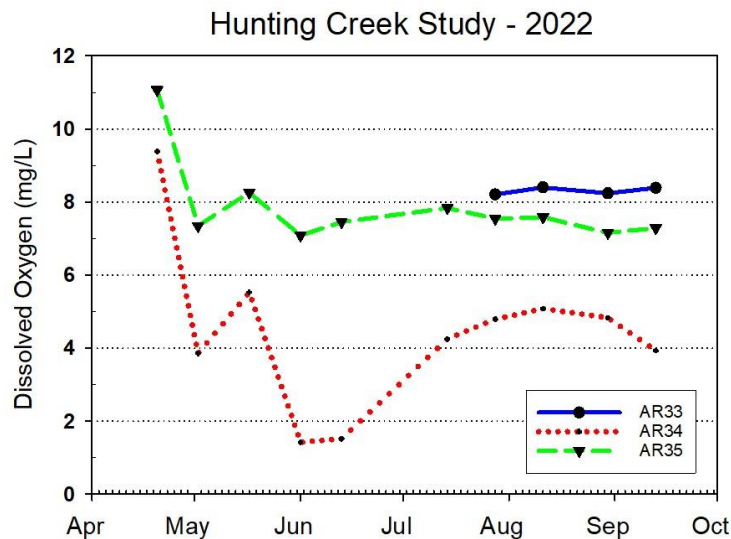


Figure 57. Dissolved Oxygen (mg/L) GMU Field Data. Hooffs Run Axis stations. Month tick is at first day of month.

In the Hooffs Run Axis stations two distinct patterns emerged (Figures 57&58). AR35, the farthest upstream station, showed very constant percent saturation values, generally between 80% and 100%. AR34 exhibited an unusual pattern with near saturation values plummeting less than 20% saturation and 2 mg/L DO in late May and early June. DO then recovered to 60% saturation and 5 mg/L by late July and August. Water at AR34 is susceptible to both runoff and tides and there may be some stagnation leading to DO depletion especially during summer,

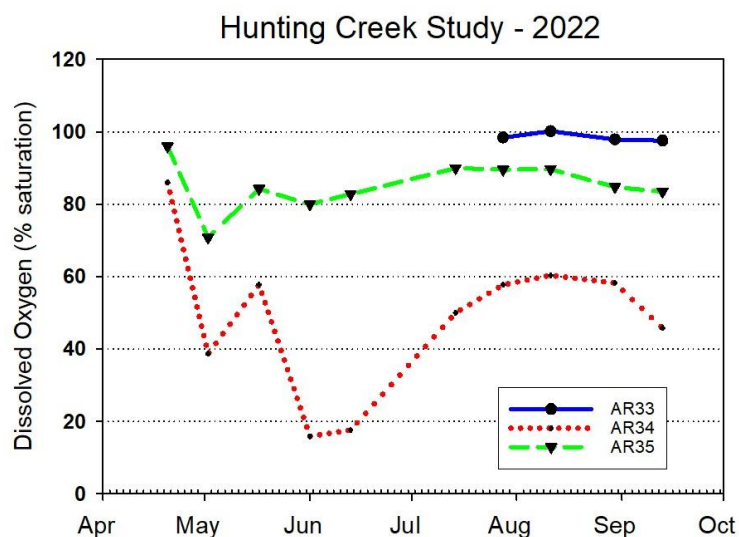


Figure 58. Dissolved Oxygen (% saturation) GMU Field Data. Hooffs Run Axis stations. Month tick is at first day of month.

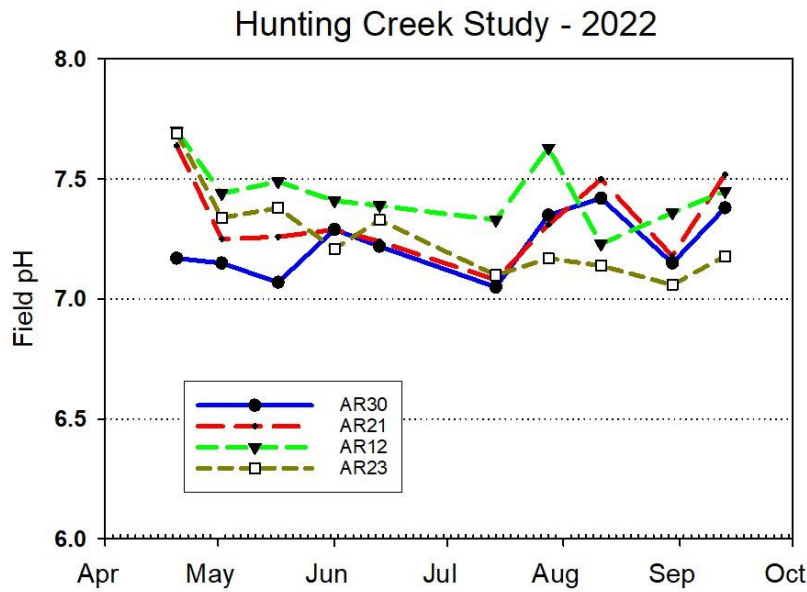


Figure 59. Field pH. GMU Field Data. Cameron Run Axis stations. Month tick is at first day of month.

Field pH followed a very similar seasonal pattern at all Cameron Run axis stations with most values between 7.0 and 7.5 (Figure 59). In the Hooffs Run Axis stations was in the same general range, but showed a slight pattern of decline (Figure 60).

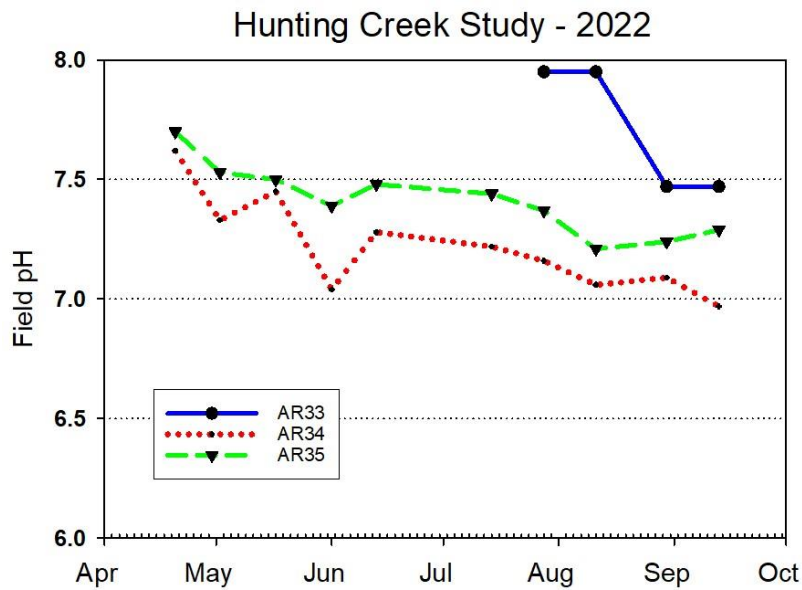


Figure 60. Field pH. GMU Field Data. Hooffs Run Axis stations. Month tick is at first day of month.

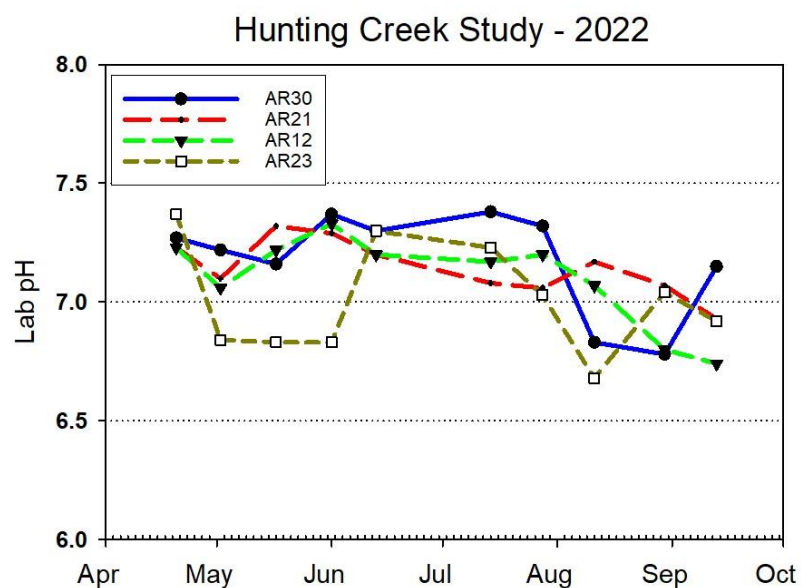


Figure 61. Lab pH. Alex Renew Lab Data. Cameron Run Axis stations. Month tick is at first day of month.

Lab pH exhibited a slight seasonal decline at Cameron Run Axis stations from about 7.2 in the spring and early summer to 6.5-7.0 in August and September (Figure 61). The Hooffs Run Axis stations exhibited a slight increase seasonally (Figure 62).

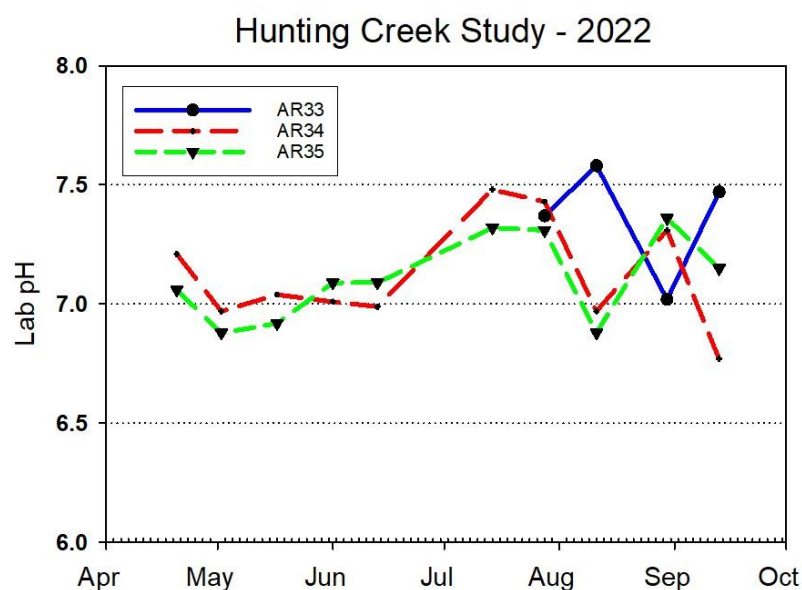


Figure 62. Lab pH. Alex Renew Lab Data. Hooffs Run Axis stations. Month tick is at first day of month.

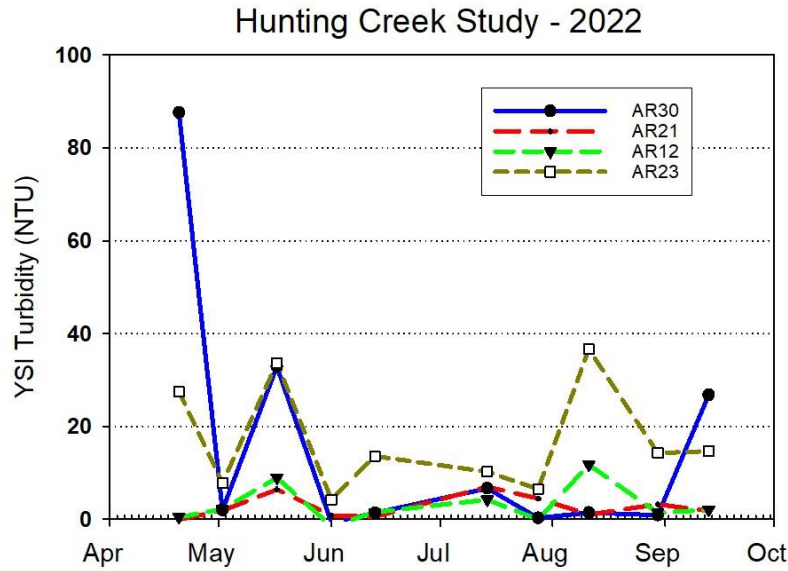


Figure 63. YSI Turbidity. GMU Field Data. Cameron Run Axis stations. Month tick is at first day of month.

YSI Turbidity was generally below 10 NTU at most stations on most dates at Cameron Run Axis stations (Figure 63). On three occasions AR30 was much higher and on one date AR23 was well above 10 NTU. On the Hooffs Run Axis AR35 was very low on most dates, while AR 34 at the terminus of Hooffs Run and impacted by both runoff and tides was higher and quite variable (Figure 64).

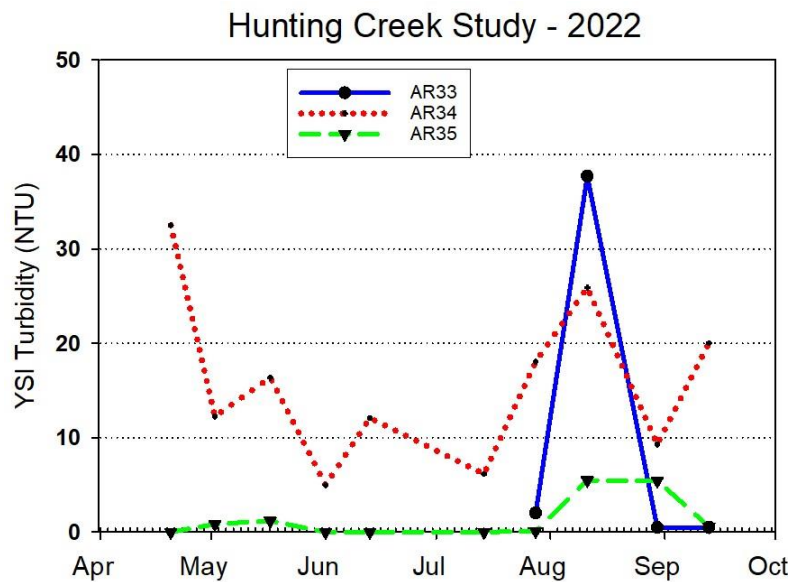


Figure 64. YSI Turbidity. GMU Field Data. Hooffs Run Axis stations. Month tick is at first day of month.

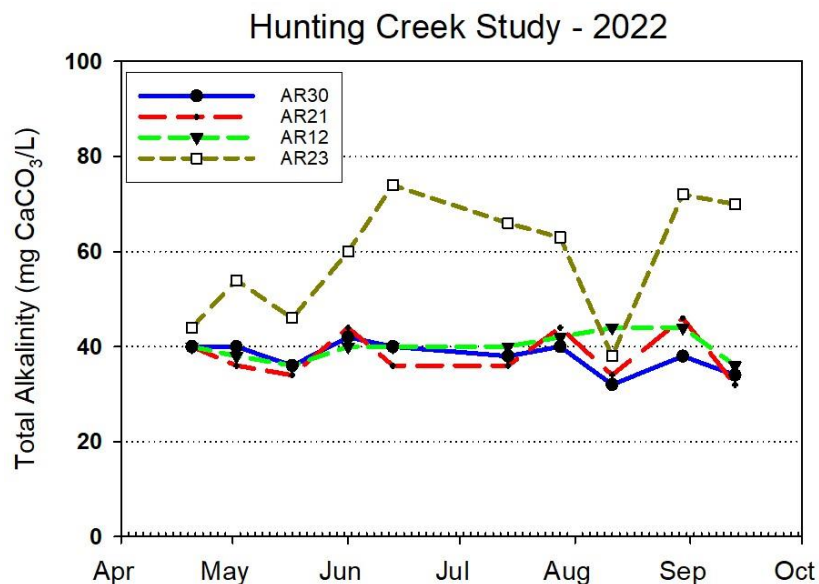


Figure 65. Total Alkalinity (mg/L as CaCO₃) AlexRenew Lab Data. Cameron Run Axis stations. Month tick is at first day of month.

Total alkalinity was generally in the 35-45 mg/L range with little seasonal change observed. (Figure 65). Clearly different was AR23 which often had much higher values. This may have been attributable to the fact that AR23 is directly across from the AlexRenew effluent discharge. AR35, the most upstream Hooffs Run station, also exhibited this constancy through time (Figure 66). However, AR35 downstream near the mouth of Hooffs Run was higher and quite variable, probably due to differential inputs from tidal and runoff sources.

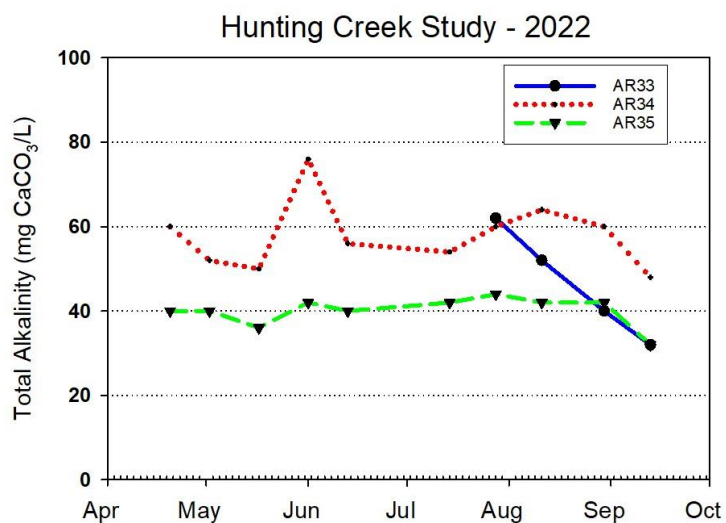


Figure 66. Total Alkalinity (mg/L as CaCO₃) AlexRenew Lab Data. Hooffs Run Axis stations. Month tick is at first day of month.

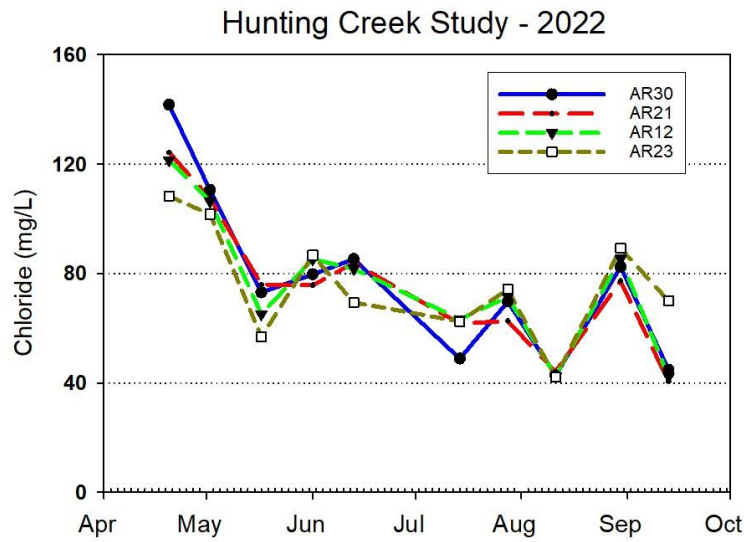


Figure 67. Chloride (mg/L) AlexRenew Lab Data. Cameron Run Axis stations. Month tick is at first day of month.

Similar to conductivity, chloride levels showed a strong pattern of decrease from April through to mid-September at Cameron Run Axis stations (Figure 65). At Hooffs Run Axis stations values were similar except one very high value at the upstream station AR35.

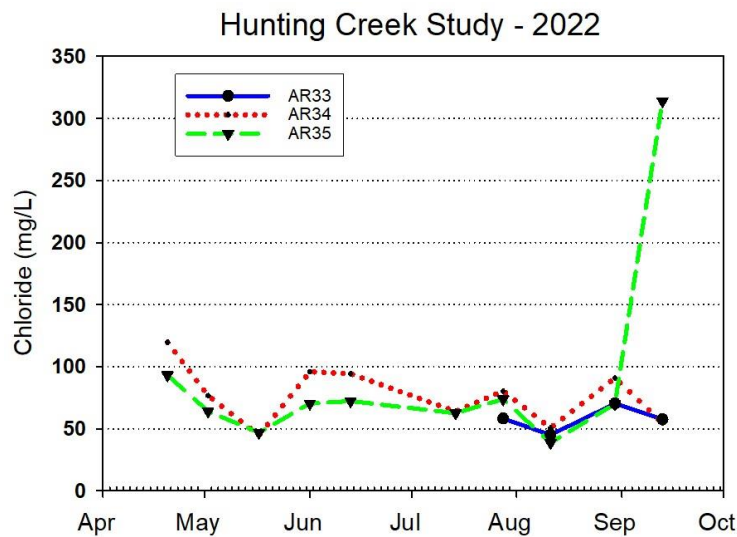


Figure 68. Chloride (mg/L) AlexRenew Lab Data. Hooffs Run Axis stations. Month tick is at first day of month.

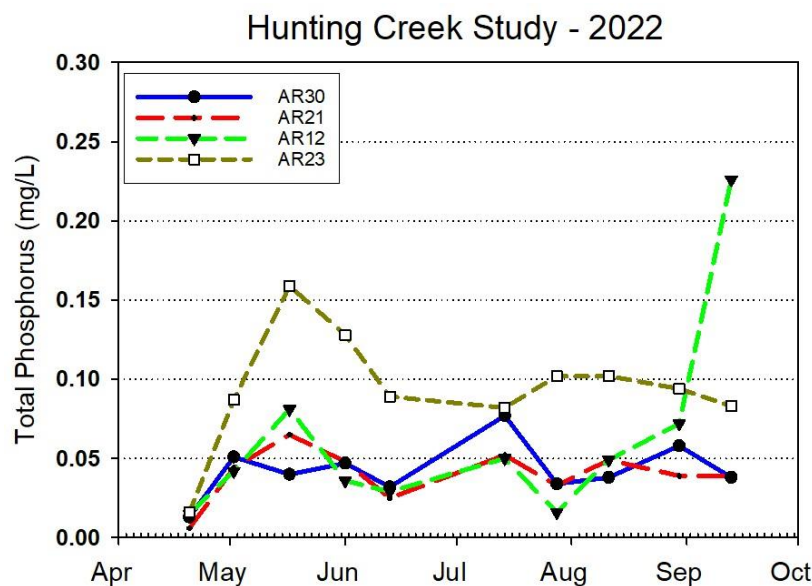


Figure 69. Total Phosphorus (mg/L) AlexRenew Lab Data. Cameron Run Axis stations. Month tick is at first day of month.

Total phosphorus at Cameron Run Axis stations was generally about 0.05 mg/L except at AR23 farthest downstream which was much higher and more variable (Figure 69). Values along the Hooffs Run axis were also generally lowest at AR35 (furthest upstream) (Figure 70). At the lower end of this axis AR34 had numerous higher values especially in spring.

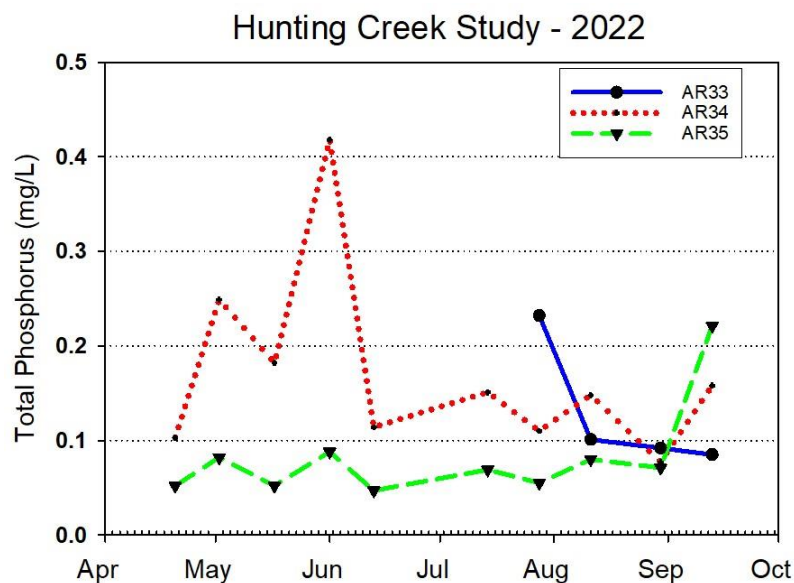


Figure 70. Total Phosphorus (mg/L) AlexRenew Lab Data. Hooffs Run Axis stations. Month tick is at first day of month.

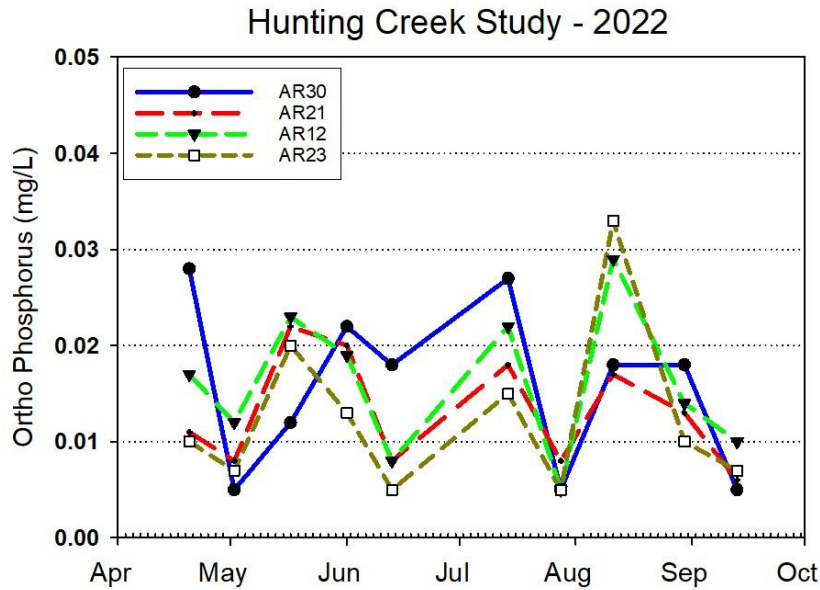


Figure 71. Ortho-Phosphorus (mg/L) AlexRenew Lab Data. Cameron Run Axis stations. Month tick is at first day of month.

Ortho phosphorus levels were very low and quite variable at Cameron Run Axis stations (Figure 71). Some slightly higher readings were observed at AR35 and AR33 (Figure 72).

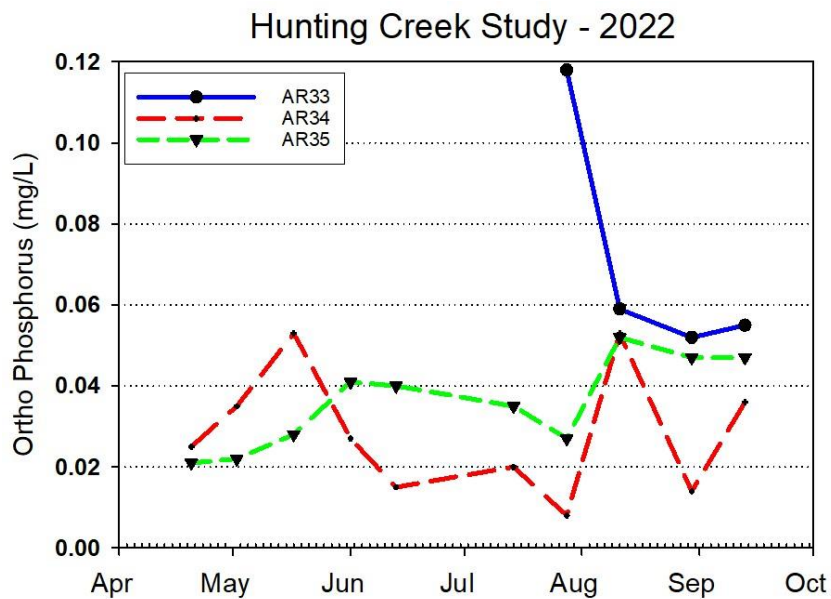


Figure 72. Ortho-Phosphorus (mg/L) AlexRenew Lab Data. Hooffs Run Axis stations. Month tick is at first day of month.

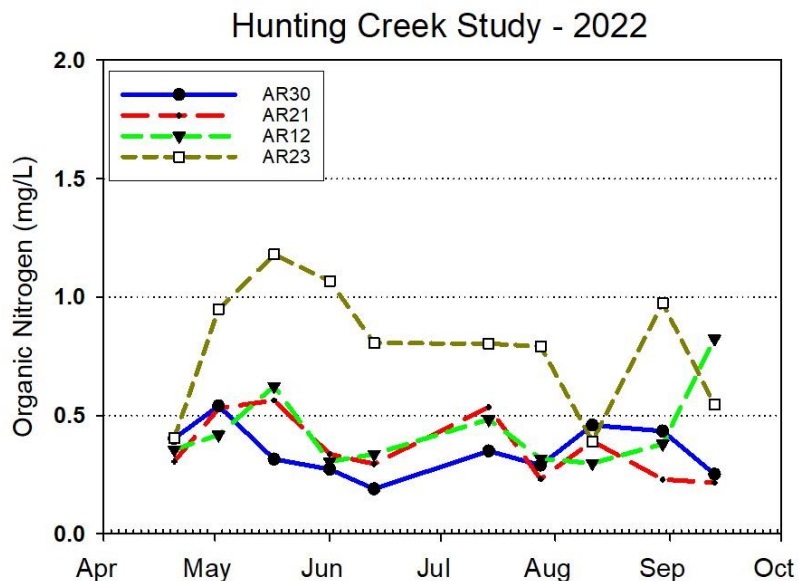


Figure 73. Organic Nitrogen (mg/L) AlexRenew Lab Data. Cameron Run Axis stations. Month tick is at first day of month.

Tributary levels of organic nitrogen are depicted in Figures 71&72. At Cameron Run Axis stations values were generally below 0.5 mg/L at most stations with little obvious pattern. However, at AR23 values were significantly higher. Hooffs Run Axis station AR35 was similar to Cameron Run Axis stations, but at AR34 higher values were observed especially in spring.

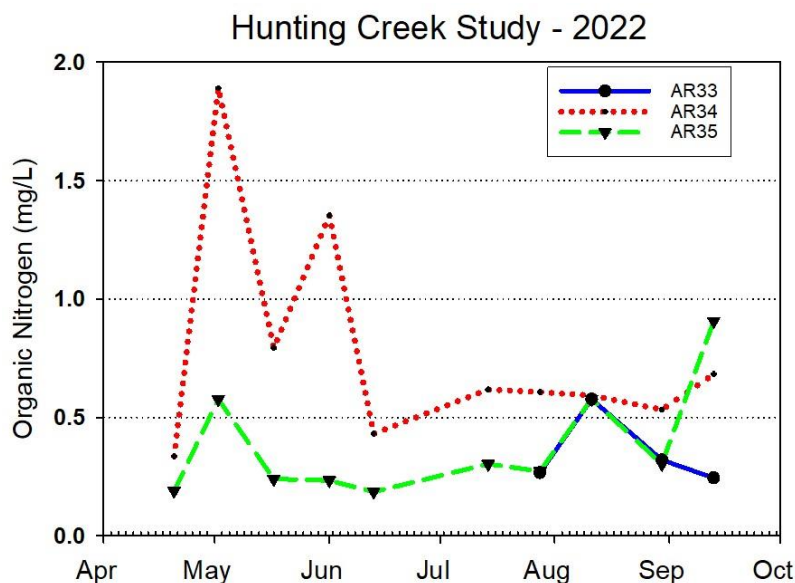


Figure 74. Organic Nitrogen (mg/L) AlexRenew Lab Data. Hooffs Run Axis stations. Month tick is at first day of month.

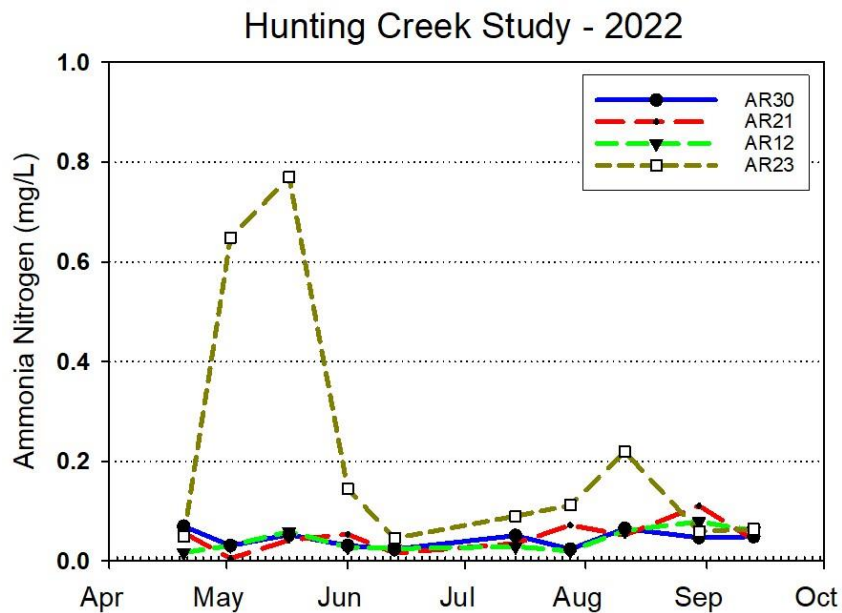


Figure 75. Ammonia Nitrogen (mg/L) AlexRenew Lab Data. Cameron Run Axis stations. Month tick is at first day of month.

Ammonia nitrogen values were generally very low at most stations on both axes (Figure 75&76). On several occasions higher values were observed at AR23 and AR34.

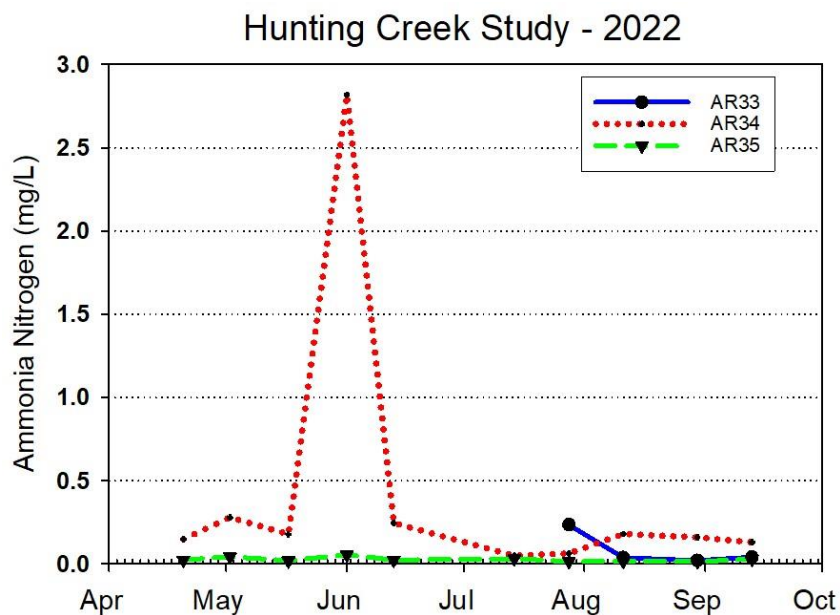


Figure 76. Ammonia Nitrogen (mg/L) AlexRenew Lab Data. Hooffs Run Axis stations. Month tick is at first day of month.

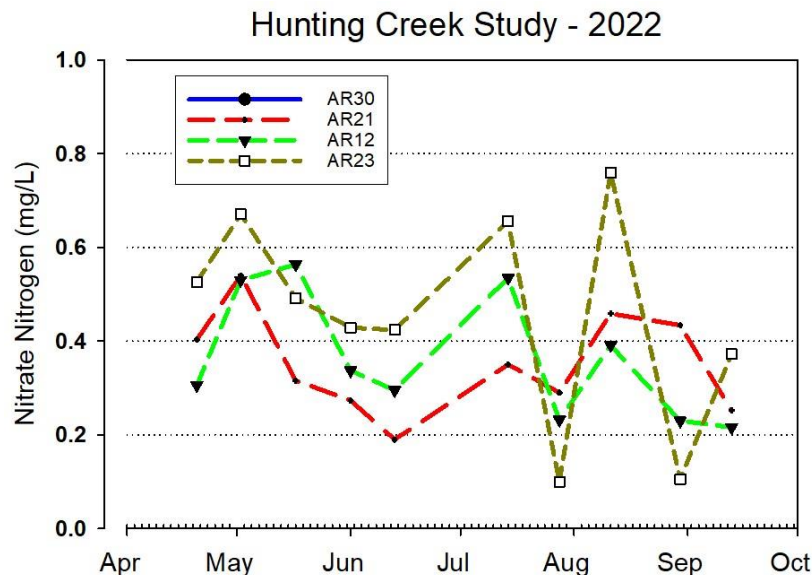


Figure 77. Nitrate Nitrogen (mg/L) AlexRenew Lab Data. Cameron Run Axis stations. Month tick is at first day of month.

Nitrate nitrogen values were generally below 0.6 mg/L along the Cameron Run Axis and showed a general decreasing trend seasonally although quite variable (Figure 77). Slightly higher values were observed at AR23. Along the Hooffs Run Axis values were consistently higher, particularly at AR 33 which averaged about 2.0 mg/L (Figure 78). The higher values for nitrate in the Hooffs Run Axis reflect the highly density residential and commercial land uses in that watershed which often have elevated nitrate levels. Interestingly nitrate nitrogen was higher at AR35 (farthest upstream) than at AR34 (farthest downstream).

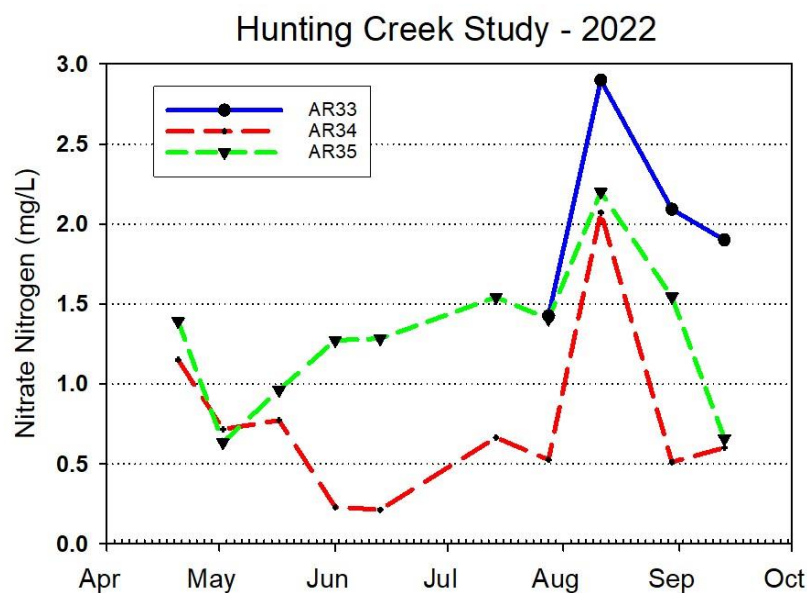


Figure 78. Nitrate Nitrogen (mg/L) AlexRenew Lab Data. Hooffs Run Axis stations. Month tick is at first day of month.

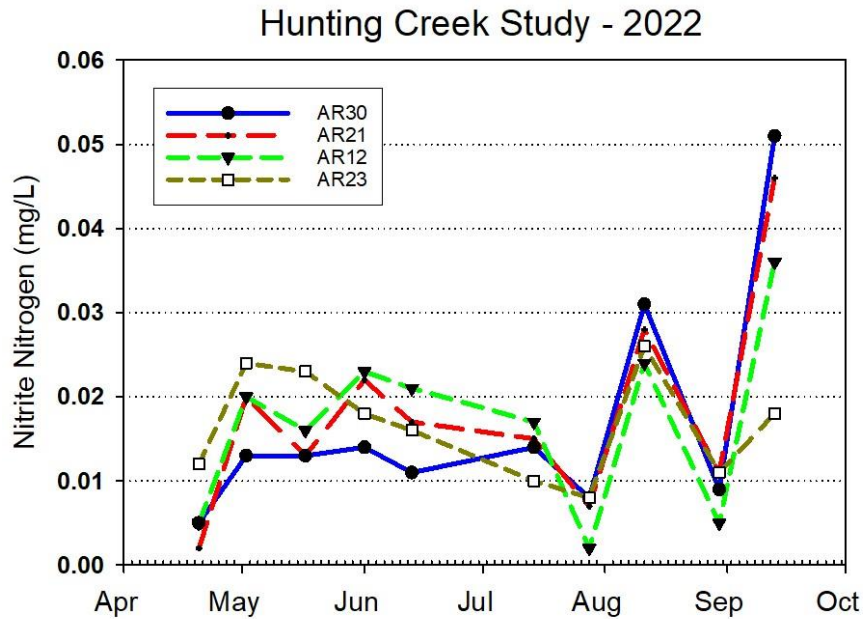


Figure 79. Nitrite Nitrogen (mg/L) AlexRenew Lab Data. Cameron Run Axis stations. Month tick is at first day of month.

Nitrite nitrogen values were generally quite low (<0.02) at all stations most of the time (Figures 79&80). Values were consistently high at AR34 perhaps because of its proximity to the AlexRenew outfall.

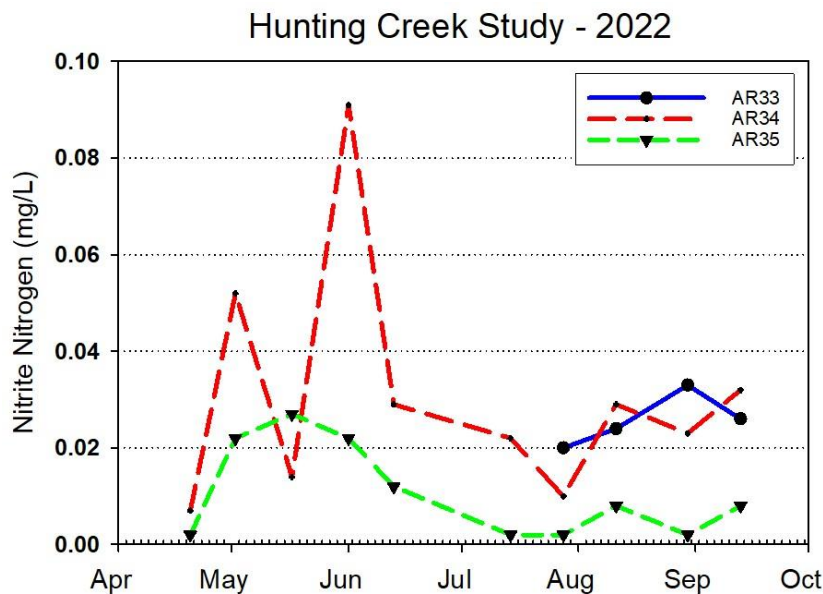


Figure 80. Nitrite Nitrogen (mg/L) AlexRenew Lab Data. Hooffs Run Axis stations. Month tick is at first day of month.

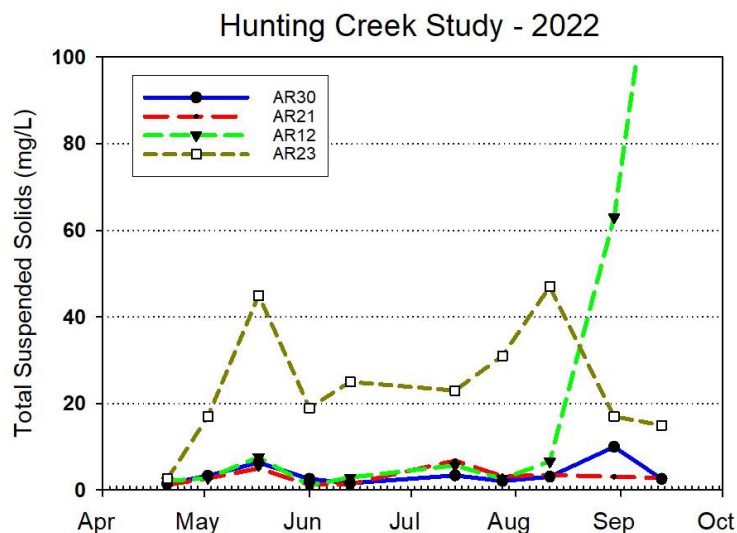


Figure 81. Total Suspended Solids (mg/L) AlexRenew Lab Data. Cameron Run Axis stations. Month tick is at first day of month.

Total suspended solids concentrations at Cameron Run Axis stations was generally below 10 mg/L (Figure 81). The exception was AR23 in upper Hunting Creek near the AlexRenew outfall which consistently had much higher values. TSS was also quite low (<10 mg/L) on most dates at AR35, the most upstream station on the Hooffs Run Axis (Figure 82). The exceptions were AR13 and AR34 in lower Hooffs Run which often had higher readings.

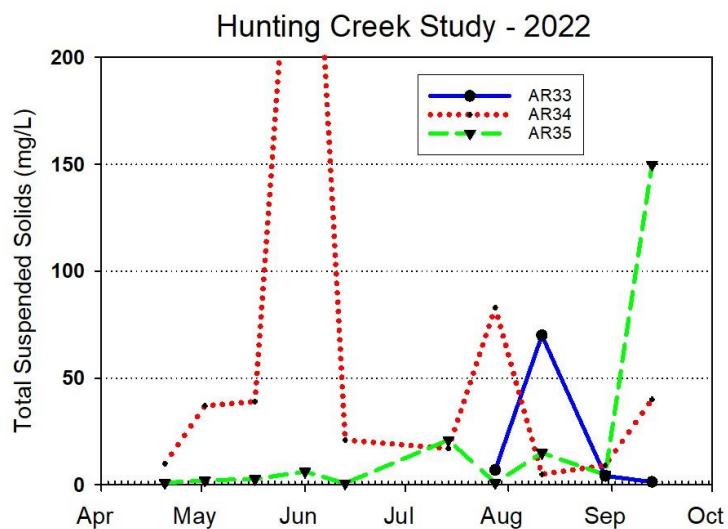


Figure 82. Total Suspended Solids (mg/L) AlexRenew Lab Data. Hooffs Run Axis stations. Month tick is at first day of month.

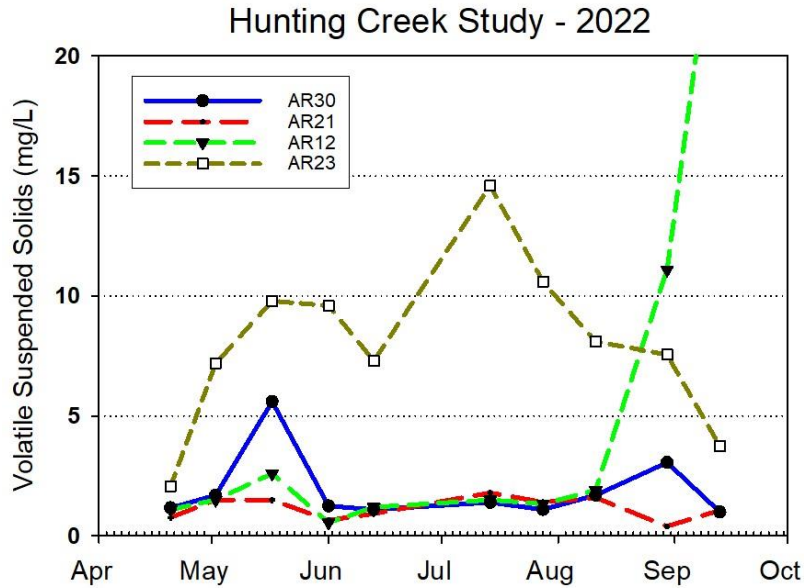


Figure 83. Volatile Suspended Solids (mg/L) AlexRenew Lab Data. Cameron Run Axis stations. Month tick is at first day of month.

VSS along the Cameron Run Axis was generally half of TSS with highest values at AR23 again (Figure 83). For the Hooffs Run Axis stations, values at AR35 were again below 5 mg/L except on the last sampling date (Figure 84). However, higher readings were observed sometimes at AR34 at the lower end of the Hooffs Run Axis.

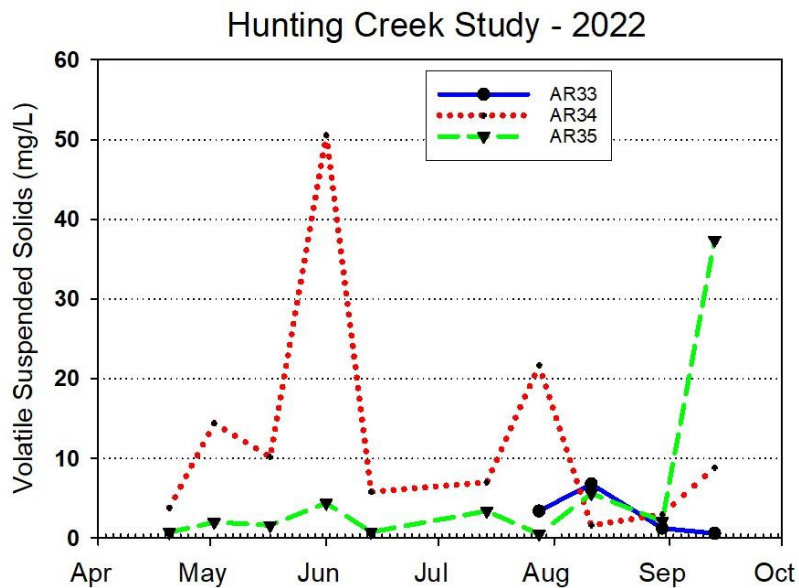
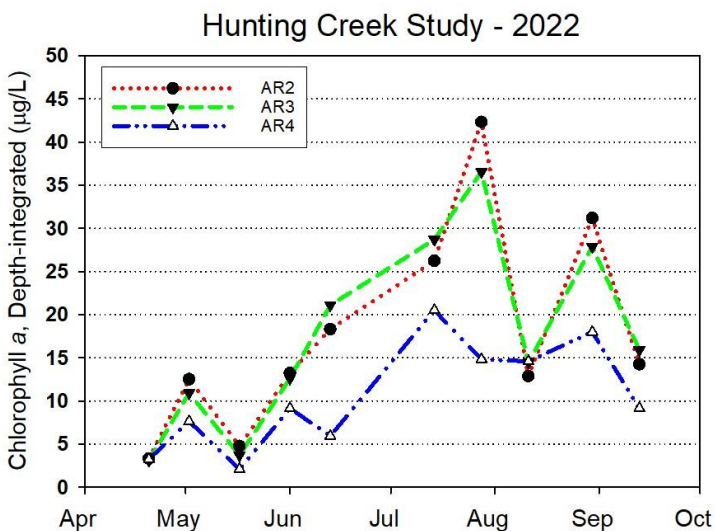


Figure 84. Volatile Suspended Solids (mg/L) AlexRenew Lab Data. Hooffs Run Axis stations. Month tick is at first day of month.

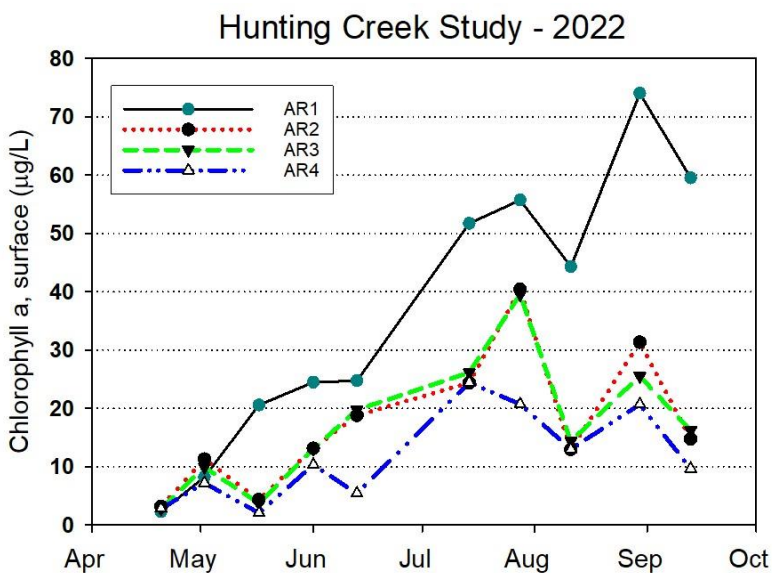
D. Phytoplankton - 2022



Chlorophyll *a* is a measure of the amount of algae growing in the water column. These suspended algae are called phytoplankton, meaning “plant wanderers”. In addition to the true algae (greens, diatoms, cryptophytes, etc.) the term phytoplankton includes cyanobacteria (sometimes known as “blue-green” algae). Both depth-integrated and surface chlorophyll values are measured due to the capacity of phytoplankton to aggregate near the surface under certain conditions.

Figure 85. Chlorophyll *a* (µg/L). Depth-integrated. GMU Lab Data. Month tick is at the first day of month.

Depth-integrated chlorophyll *a* values at AR2 and AR3 (the embayment stations) were very similar throughout the year with peak values of about 40 µg/L in late July (Figure 85). This was followed by a large decline in early August due to multiple flow pulses following storms. In the river values showed less seasonal pattern and remained at about 15-20 µg/L from early July through late August. Similar values were observed in surface chlorophyll *a* at AR2, AR3, and AR4 (Figure 86). Values at AR1 were consistently higher than the other stations and was less impacted by the early August flushing period and rebounded to even higher values in late August.



In the tidal freshwater Potomac generally, there is very little difference in surface and depth-integrated chlorophyll levels because tidal action keeps the water well-mixed which overcomes any potential surface aggregation by the phytoplankton. Summer chlorophyll concentrations above 30 µg/L are generally considered characteristic or eutrophic conditions.

Figure 86. Chlorophyll *a* (µg/L). Surface. GMU Lab Data. Month tick is at first day of month.

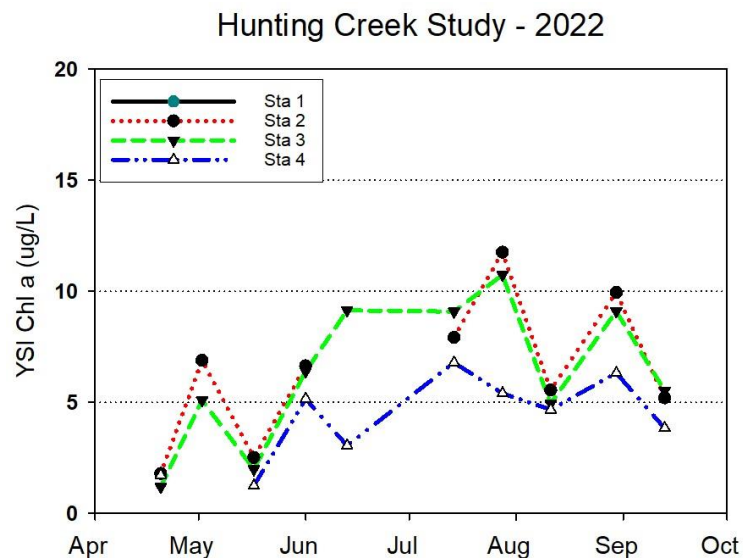


Figure 87. Chlorophyll a (ug/L). Depth-integrated. YSI sonde. Month tick is at first day of month.

YSI sonde chlorophyll a (Figure 87) followed the same general trends as Lab Extracted Chlorophyll (shown in Figures 85 and 86). Peaks were observed in early May and late July in both datasets. However, values of YSI sonde chlorophyll a were substantially lower. A correlation analysis revealed a tight relationship between the two variables (Figure 88) with an r^2 of 0.907 which was highly significant. A regression analysis revealed that YSI Chlorophyll a (YSI Chla) could be predicted from Lab Extracted Chlorophyll a (Lab Chla) using the following linear equation:

$$\text{Lab Chla} = 3.442 * \text{YSI Chla} - 4.17, n=27$$

Thus, YSI Chla would need to be multiplied by about 3.5 to equate with Lab Chla.

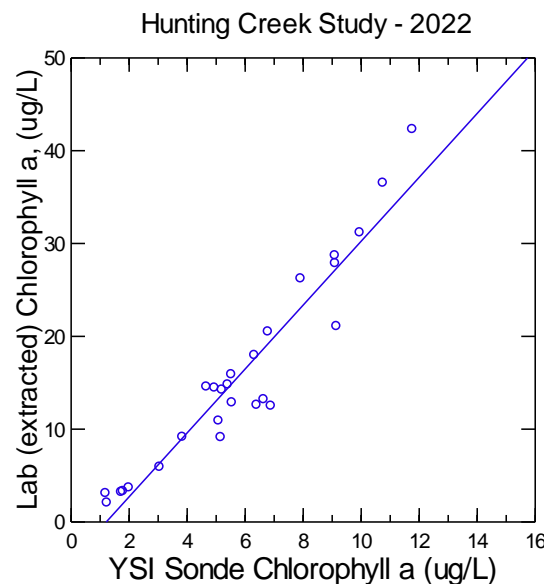


Figure 88. Relationship between Lab Chlorophyll a and YSI Sonde Field Chlorophyll a. Depth-integrated.

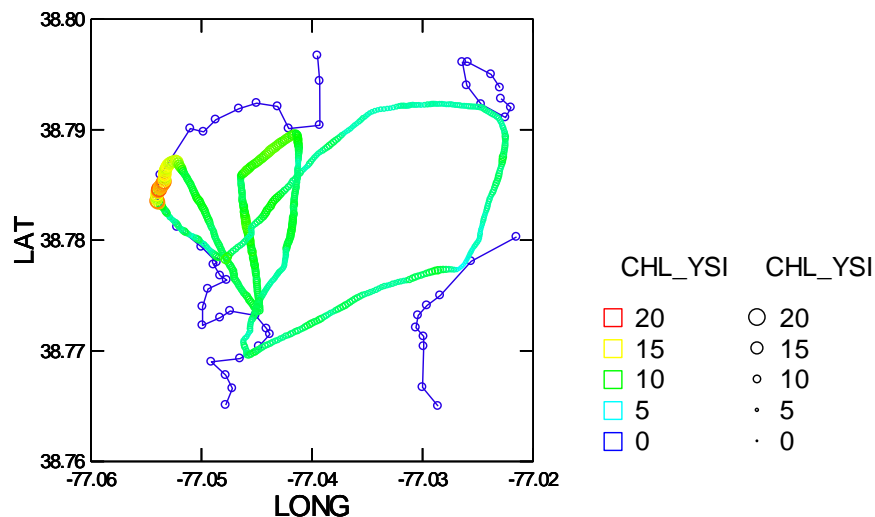


Figure 89a. Water Quality Mapping. July 18, 2022. Chlorophyll YSI ($\mu\text{g/L}$).

Water quality mapping data for July 18 indicated that YSI Chla values were generally below 15 $\mu\text{g/L}$ over the entire study area except for a hot spot in the western part of the Hunting Creek embayment just south of the GW Parkway bridge over Hunting Creek where values exceeded 20 $\mu\text{g/L}$ (Figure 89a). This would equate to about 70 $\mu\text{g/L}$ if converted to equivalent Lab chlorophyll values which was higher than any values observed in 2022 at the regular Tidal Main stations. On August 16, YSI chla below 15 $\mu\text{g/L}$ in all samples and was only slightly higher in the embayment than in the mainstem (Figure 89b). This pattern correlated well with the patterns in dissolved oxygen and pH, consistent with the hypothesis of substantial phytoplankton activity in the inner Hunting Creek area.

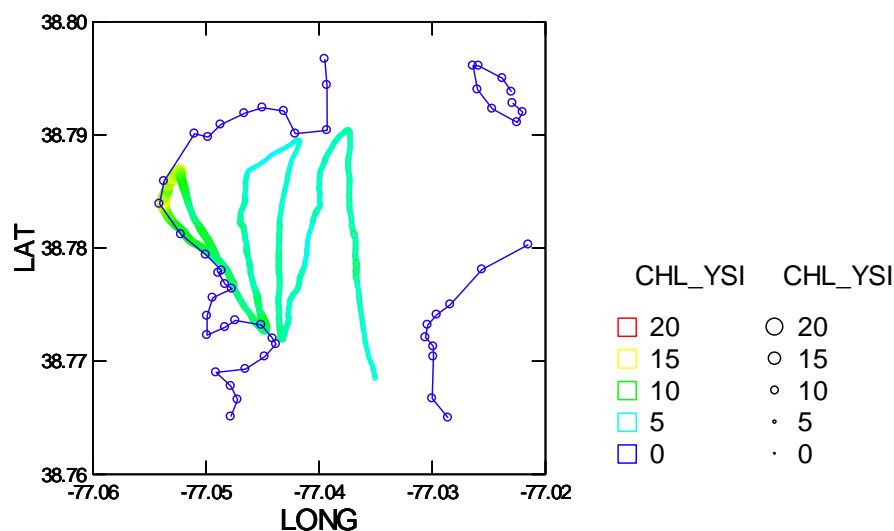


Figure 89b. Water Quality Mapping. August 16, 2022. Chlorophyll YSI ($\mu\text{g/L}$).

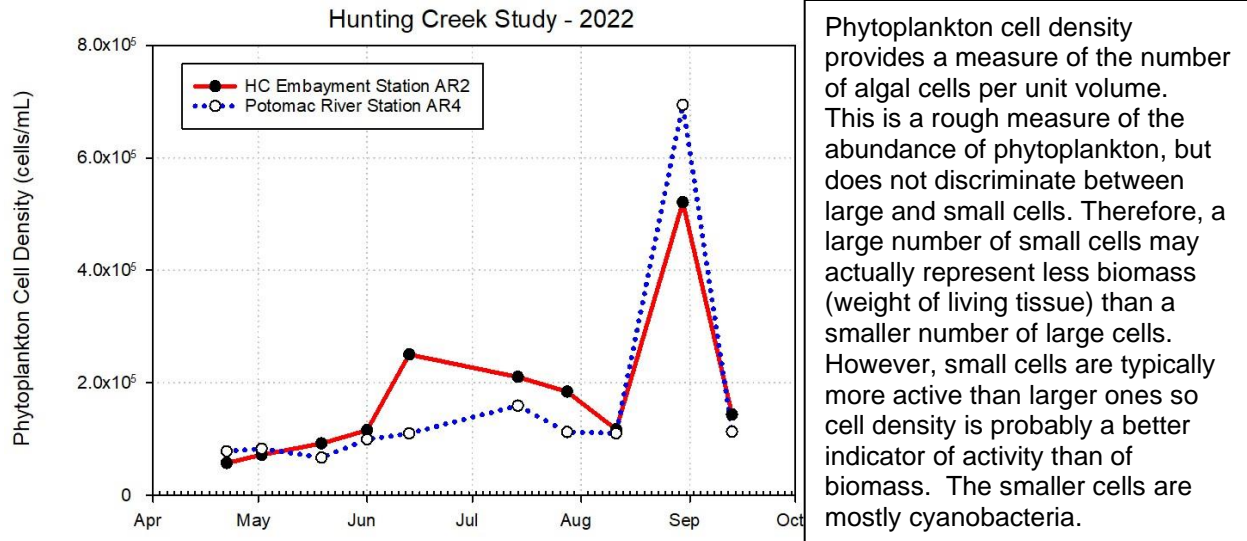


Figure 90. Phytoplankton Cell Density (cells/mL).

In 2022 phytoplankton cell density in the embayment exhibited a peak in mid-June and an even stronger peak in late August (Figure 90). In the river cell density was generally somewhat lower than in the embayment, but the late August peak was even higher in the river. Total biovolume exhibited peaks in mid-May and mid-July in the cove and lesser peaks in early June and early August in the river (Figure 91). The timing of these peaks did not closely relate to those in chlorophyll.

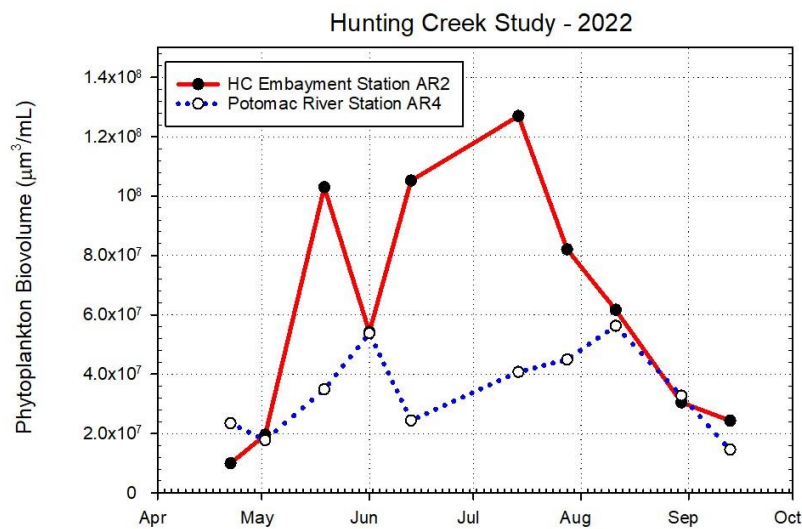


Figure 91. Phytoplankton Biovolume (um³/mL).

The volume of individual cells of each species is determined by approximating the cells of each species to an appropriate geometric shape (e.g. sphere, cylinder, cone, cube, etc.) and then making the measurements of the appropriate dimensions under the microscope. Total phytoplankton biovolume (shown here) is determined by multiplying the cell density of each species by the biovolume of each cell of that species. Biovolume accounts for the differing size of various phytoplankton cells and is probably a better measure of biomass. However, it does not account for the varying amount of water and other nonliving constituents in cells.

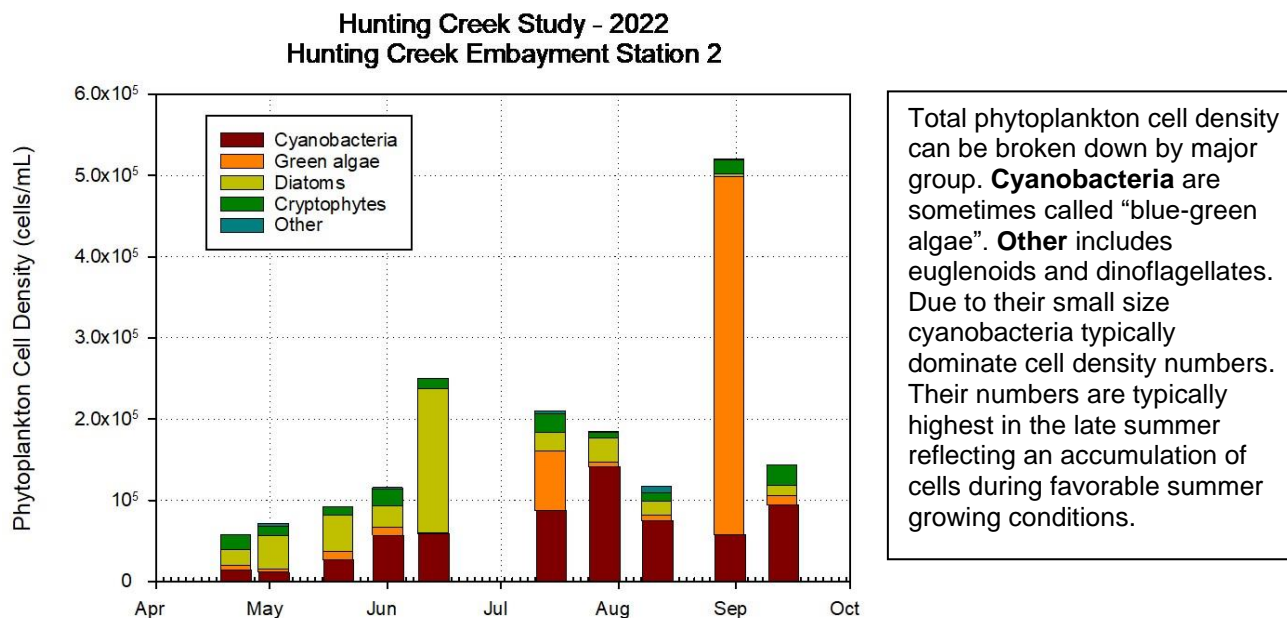


Figure 92. Phytoplankton Density by Major Group (cells/mL). Hunting Creek.

Phytoplankton cell density at AR2 was generally dominated by cyanobacteria and diatoms with diatoms assuming dominance in June (Figure 92). Green algae showed strong dominance on one date in both Hunting Creek and the river mainstem (AR4), cyanobacteria and diatoms were typically co-dominant (Figure 93).

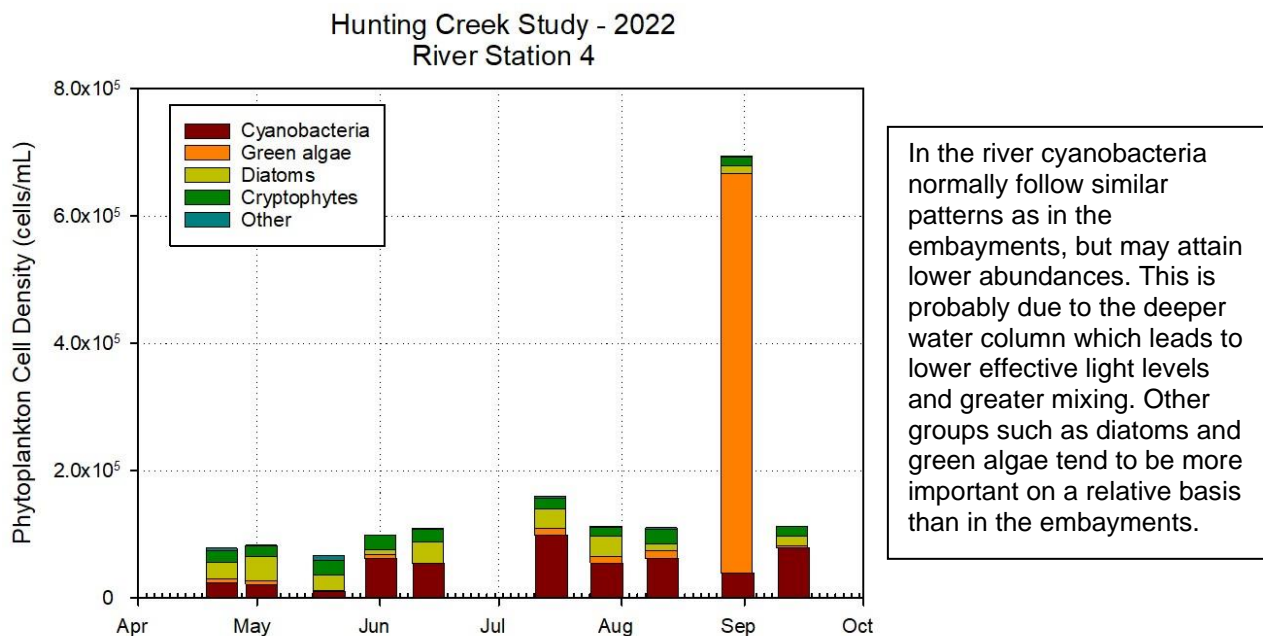


Figure 93. Phytoplankton Density by Major Group (cells/mL). River.

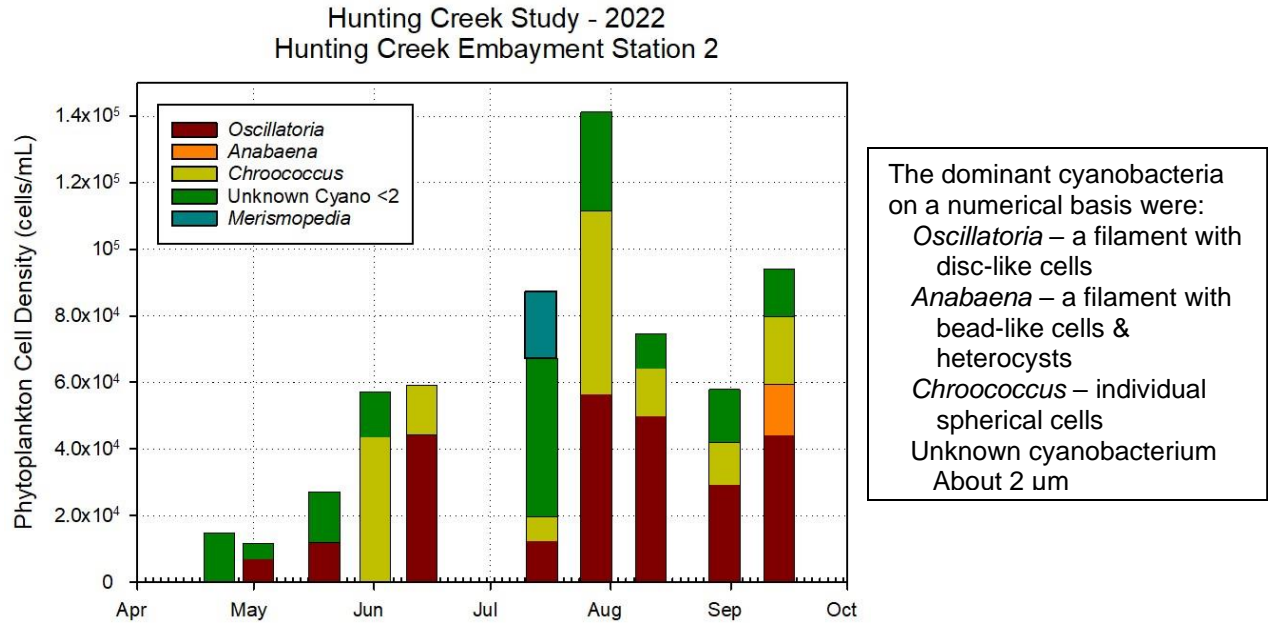


Figure 94. Phytoplankton Density by Dominant Cyanobacteria (cells/mL). Hunting Creek.

Oscillatoria and *Chroococcus*, were generally the most important cyanobacteria in cell density at the embayment station (AR2), although Unknown Cyanobacterium <2 μ m was also important on some dates (Figure 94). In the river mainstem a similar pattern of dominance in cyanobacterial cell density was also observed (Figure 95). At both stations *Anabaena*, a heterocyst-forming and therefore N-fixing species, was subdominant in mid-July.

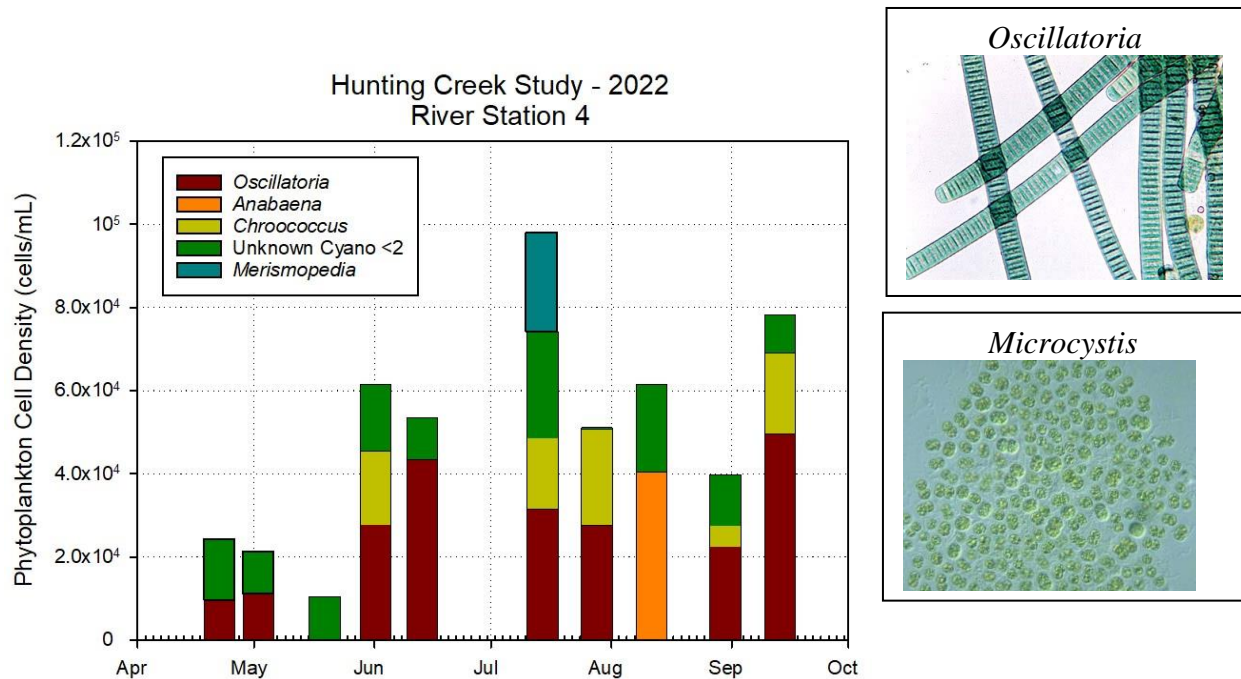


Figure 95. Phytoplankton Density by Dominant Cyanobacteria (cells/mL). River.

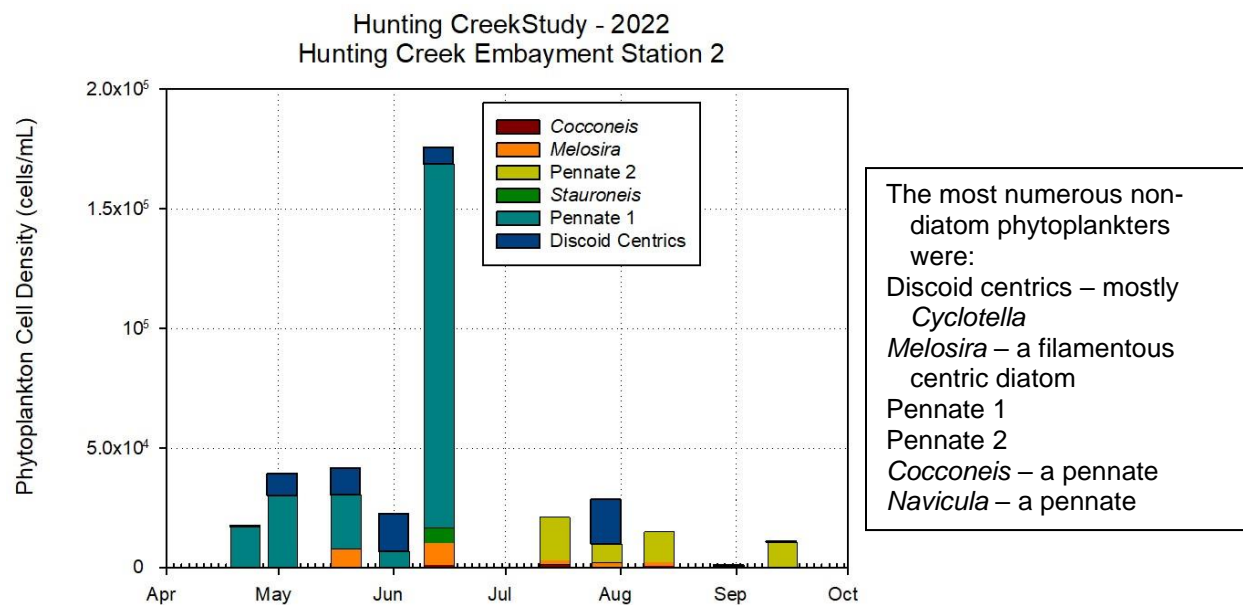


Figure 96. Phytoplankton Density (#/mL) by Dominant Diatom Taxa. Hunting Creek.

Diatom cell density dominance seemed to follow a distinct seasonal pattern. In Spring Pennate 1 and discoid centrics dominated along with some *Melosira* (Figure 96, 97). In fall Pennate 2 was most important with a sometimes significant contribution from discoid centrics. The numbers at AR2 were generally higher than at AR4, in mid-June they were much higher at AR2.

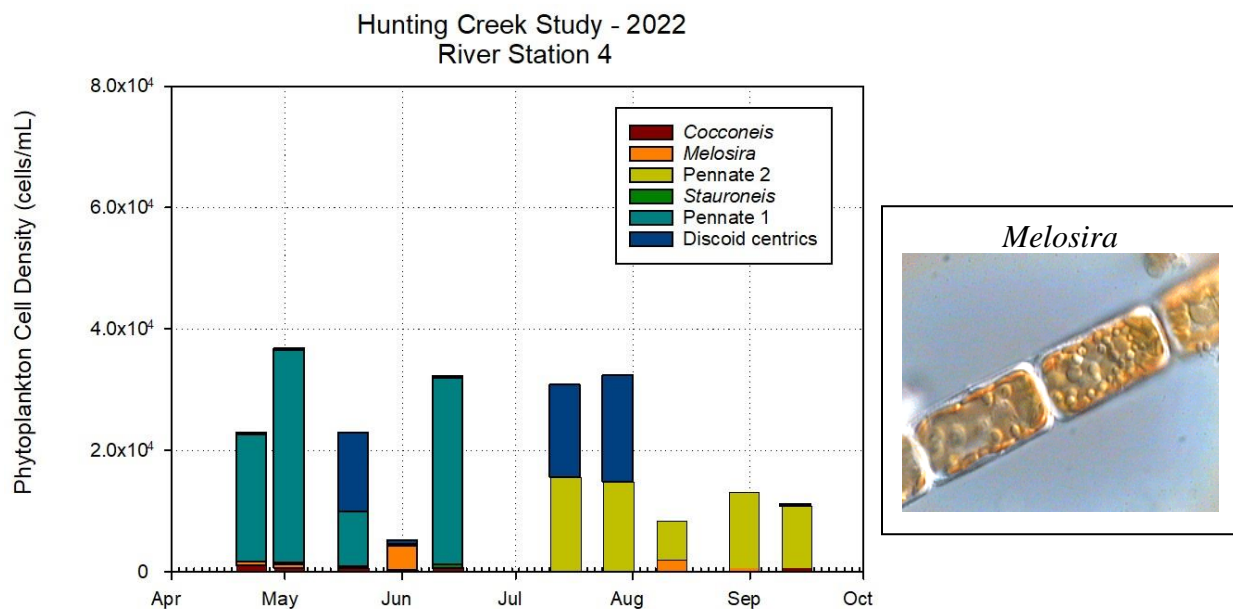


Figure 97. Phytoplankton Density (#/mL) by Dominant Diatom Taxa. River.

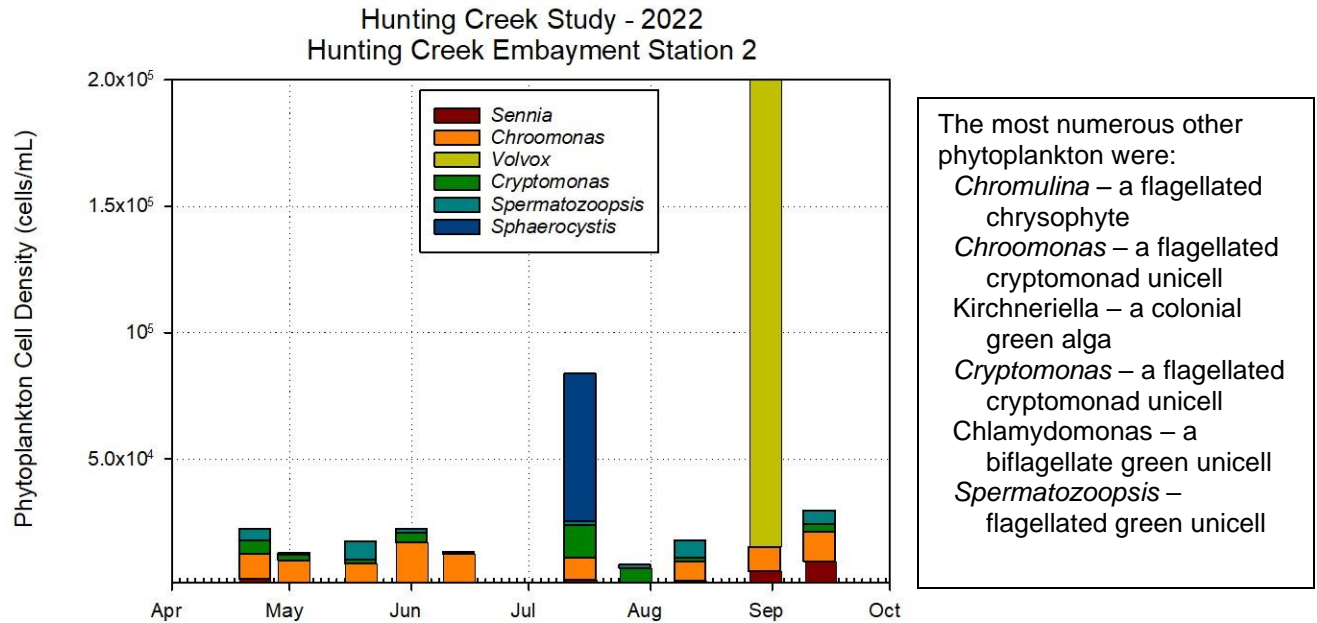


Figure 98. Phytoplankton Density (#/mL) by Dominant Other Taxa. Hunting Creek.

Phytoplankton species that were neither cyanobacteria nor diatoms were grouped together as “other” for these graphs; these included most numerous taxa of green algae, cryptophytes, euglenoids, and dinoflagellates. The cryptophyte *Chroomonas* was present and usually dominant in every month at both stations (Figures 97&99). In the late August sample at both stations the colonial green alga *Volvox*, made up of many very small cells was dominant.

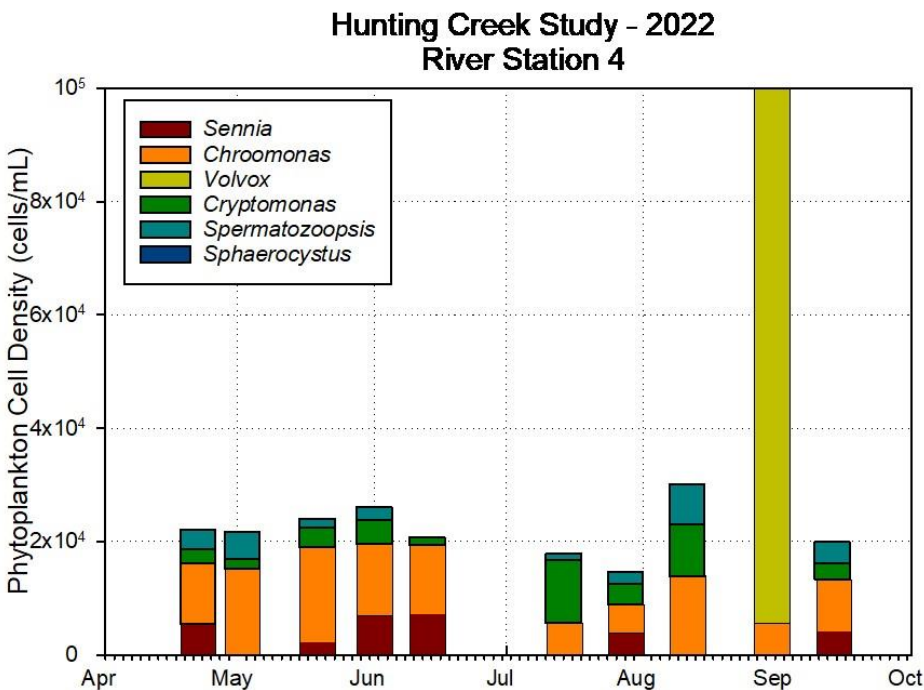


Figure 99. Phytoplankton Density (#/mL) by Dominant Other Taxa. River.

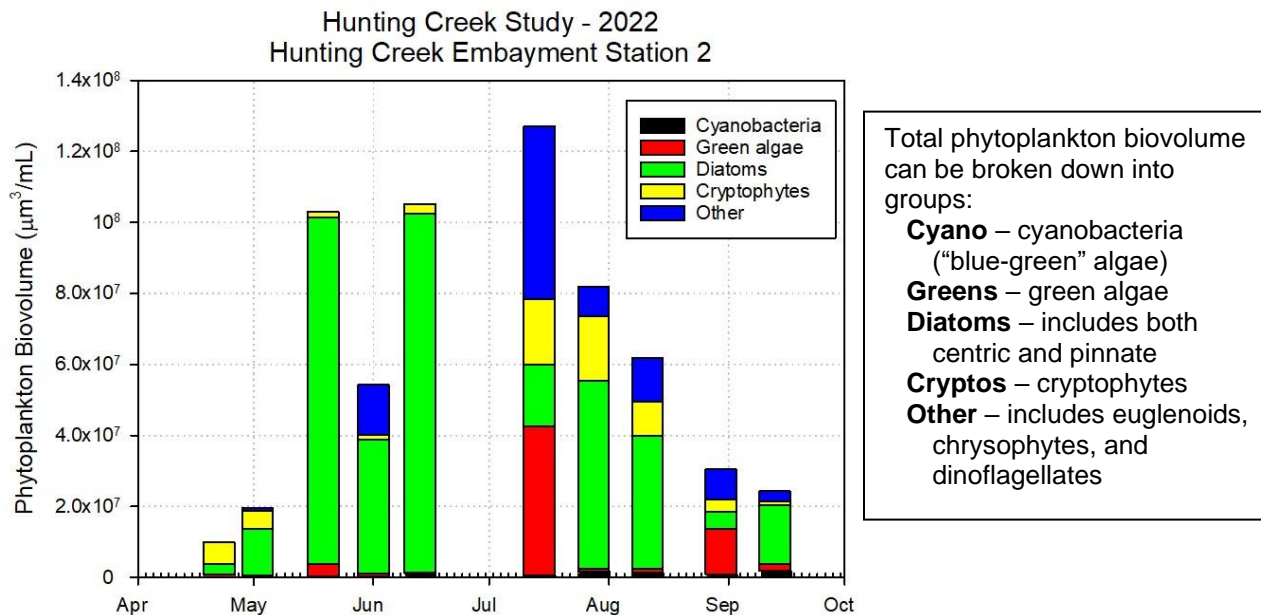


Figure 100. Phytoplankton Biovolume ($\mu\text{m}^3/\text{mL}$) by Major Groups. Hunting Creek.

In 2022 at AR2 in Hunting Creek diatoms were dominant in biovolume in almost every month (Figure 100). The exception was in mid-July when both green algae and Other algae exceeded it in biovolume. At AR4 in the river, diatoms were dominant in spring, but cryptophytes and then Green algae became greater (Figure 101).

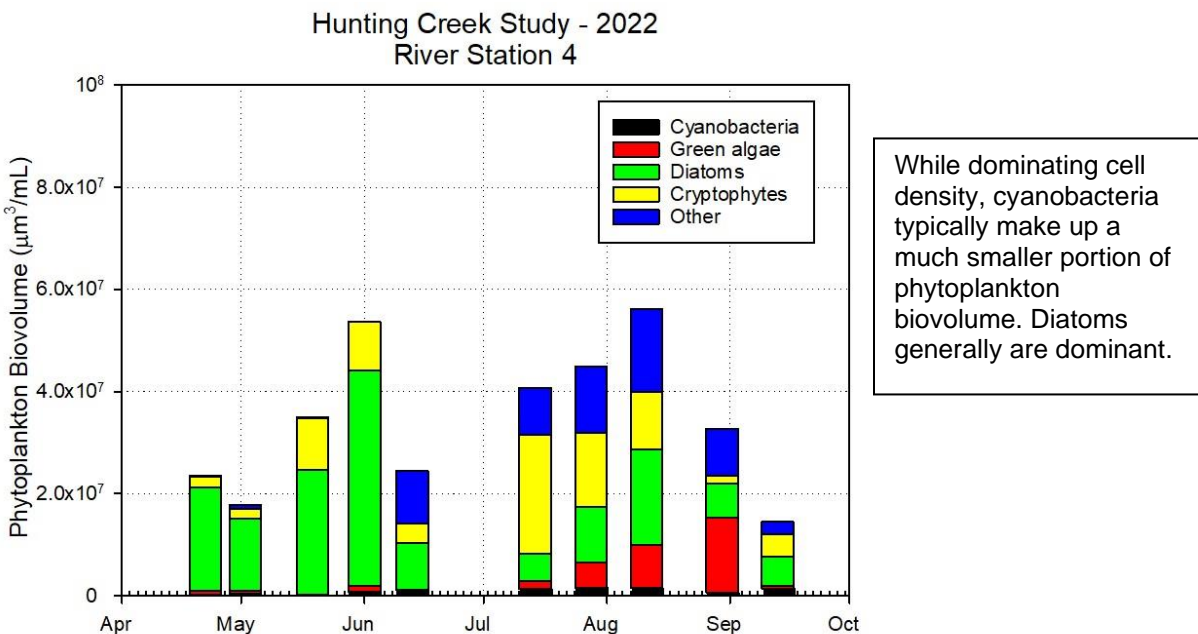


Figure 101. Phytoplankton Biovolume ($\mu\text{m}^3/\text{mL}$) by Major Groups. River.

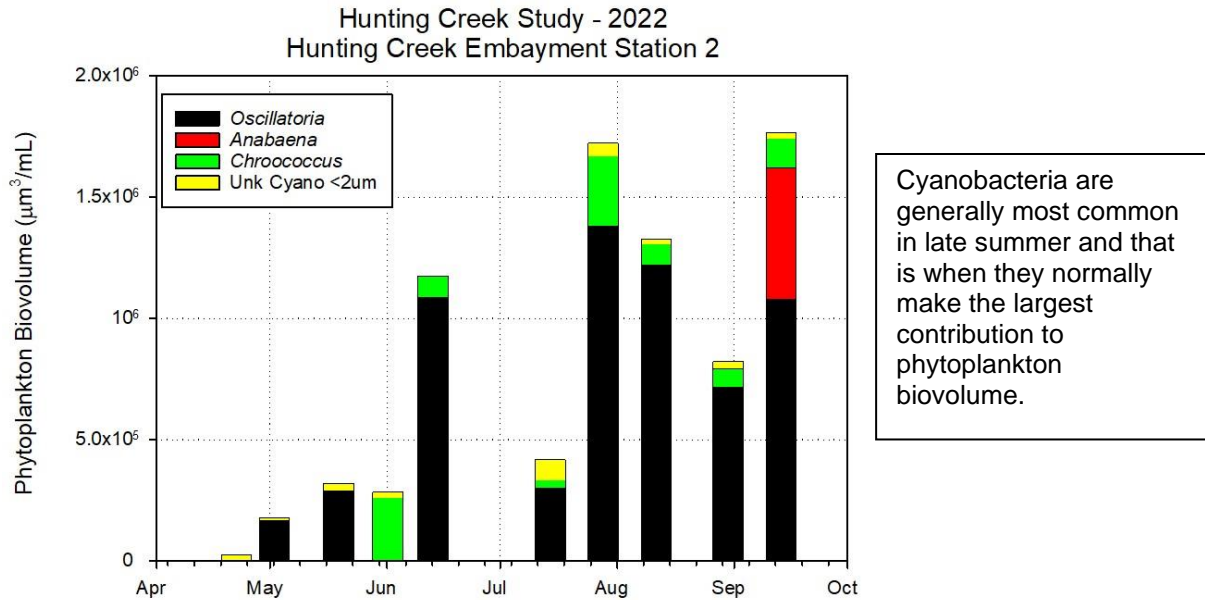


Figure 102. Phytoplankton Biovolume (um³/mL) by Cyanobacteria Taxa. Hunting Creek.

Among the cyanobacteria *Oscillatoria* was dominant on most dates at both stations (Figures 102, 103). However, in fall samples at AR4, *Anabaena* or *Merismopedia* assumed dominance or were co-dominant.

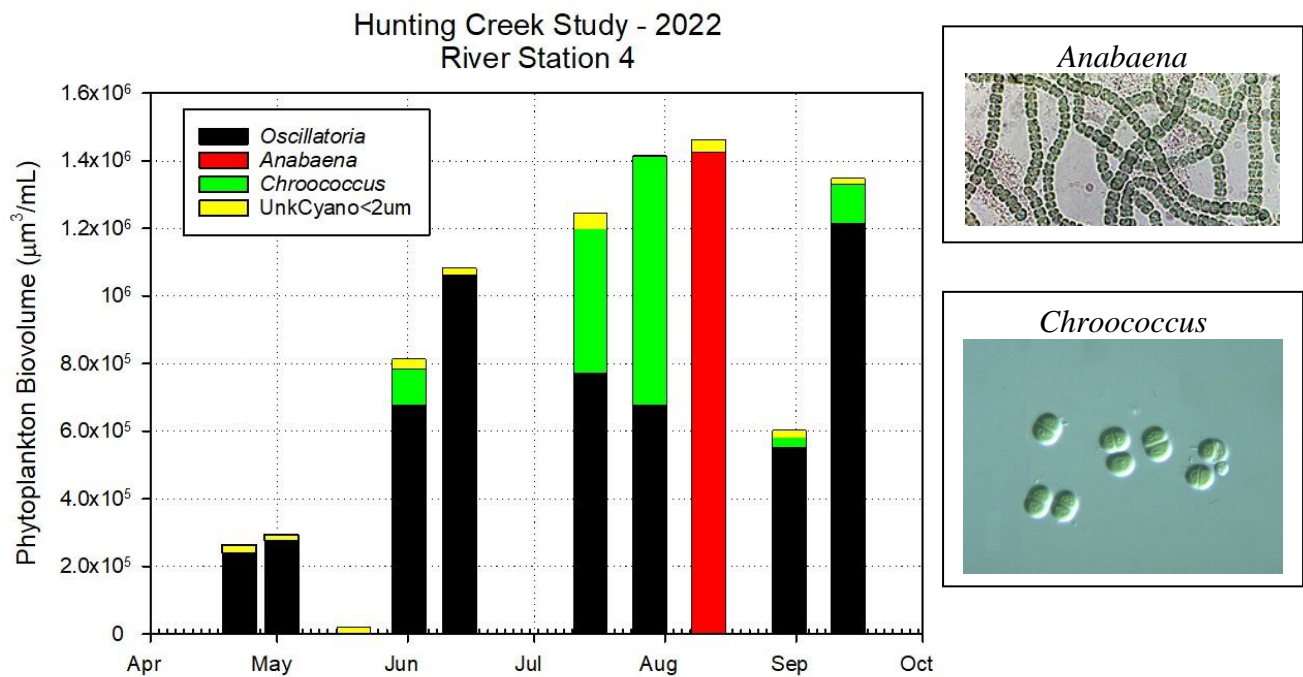


Figure 103. Phytoplankton Biovolume (um³/mL) by Cyanobacterial Taxa. River.

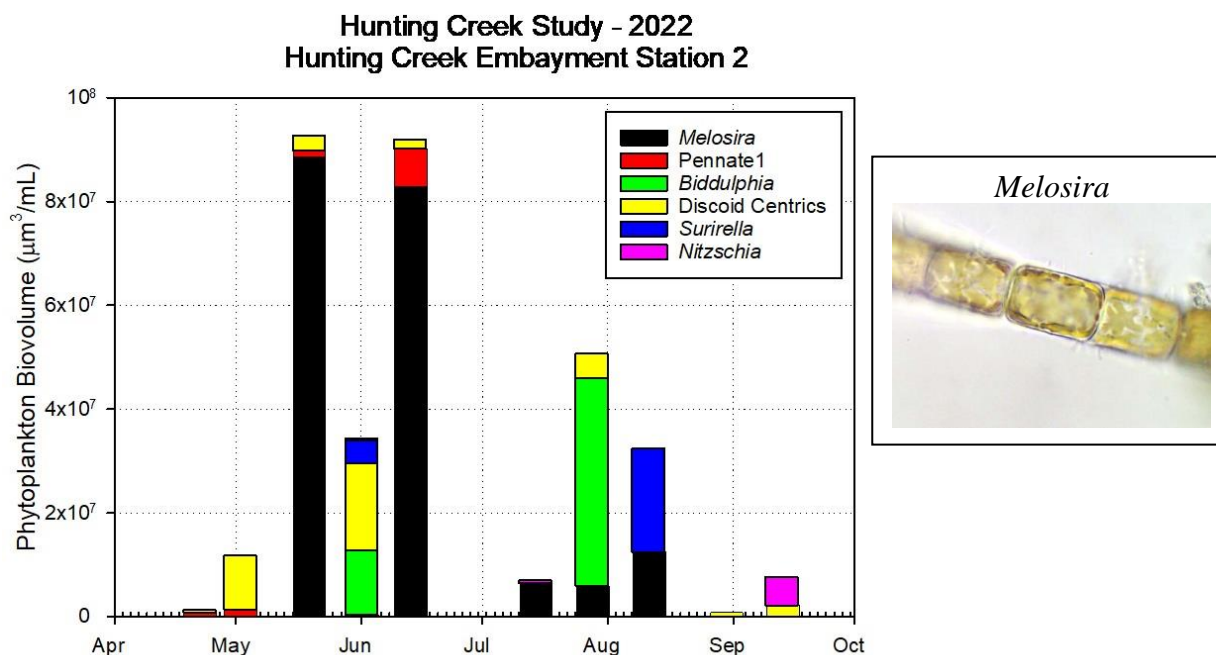


Figure 104. Phytoplankton Biovolume (um³/mL) by Dominant Diatom Taxa. Hunting Creek.

At both stations, *Melosira* was the dominant on most dates (Figures 104, 105). Discoid centrics were also important in some samples, especially in the river.

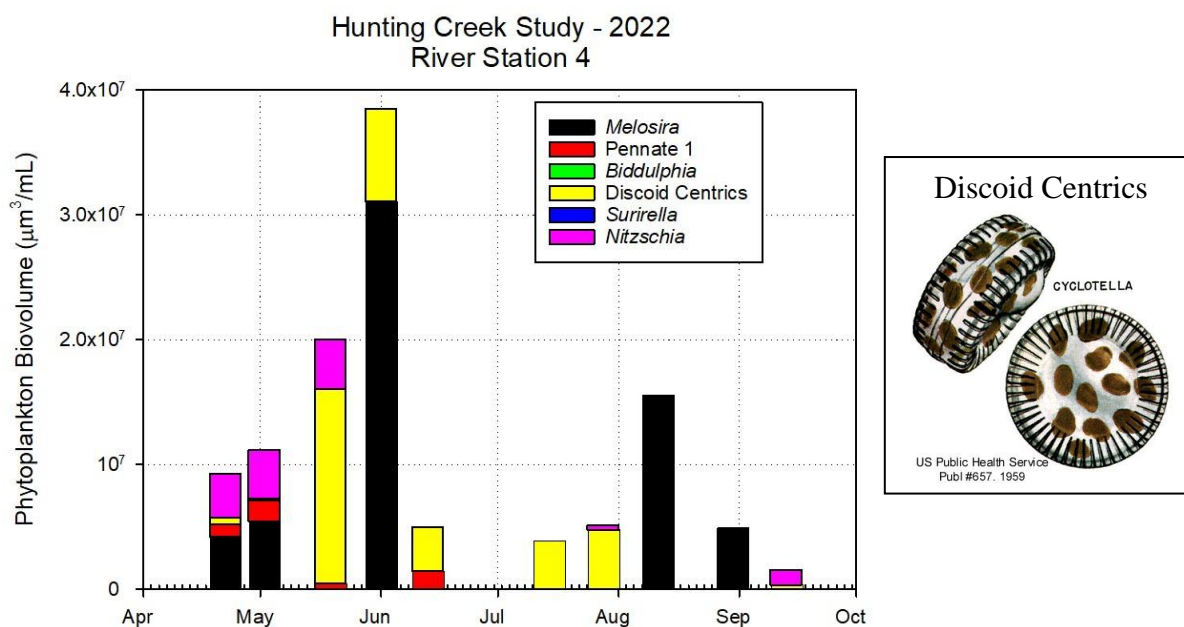


Figure 105. Phytoplankton Biovolume (um³/mL) by Dominant Diatom Taxon. River.

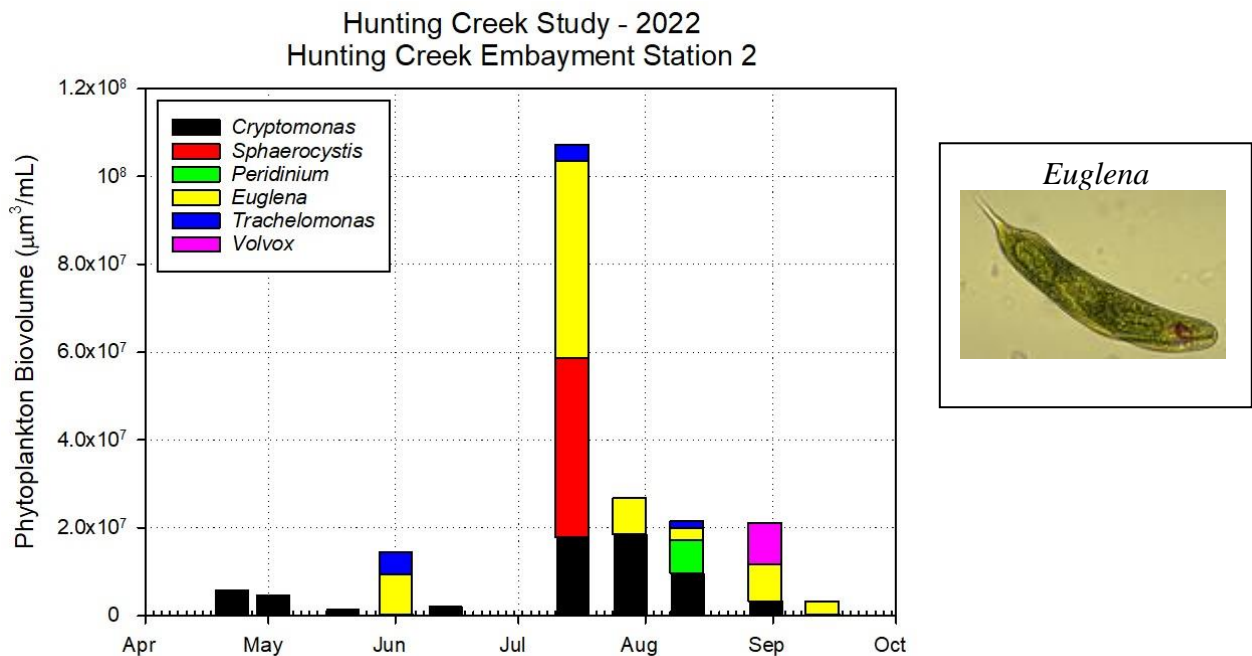


Figure 106. Phytoplankton Biovolume (um³/mL) by Dominant Other Taxa. Hunting Creek.

In the embayment the cryptophyte *Cryptomonas* was present on almost all dates and dominant on some at AR2 (Figure 106). In mid-July *Euglena* and the green alga *Sphaerocystis* made strong showings. In the river *Cryptomonas* was again dominant for most of the year with *Euglena* and *Trachelomonas* being subdominant on many occasions (Figure 107). *Volvox* was dominant in late August at AR4.

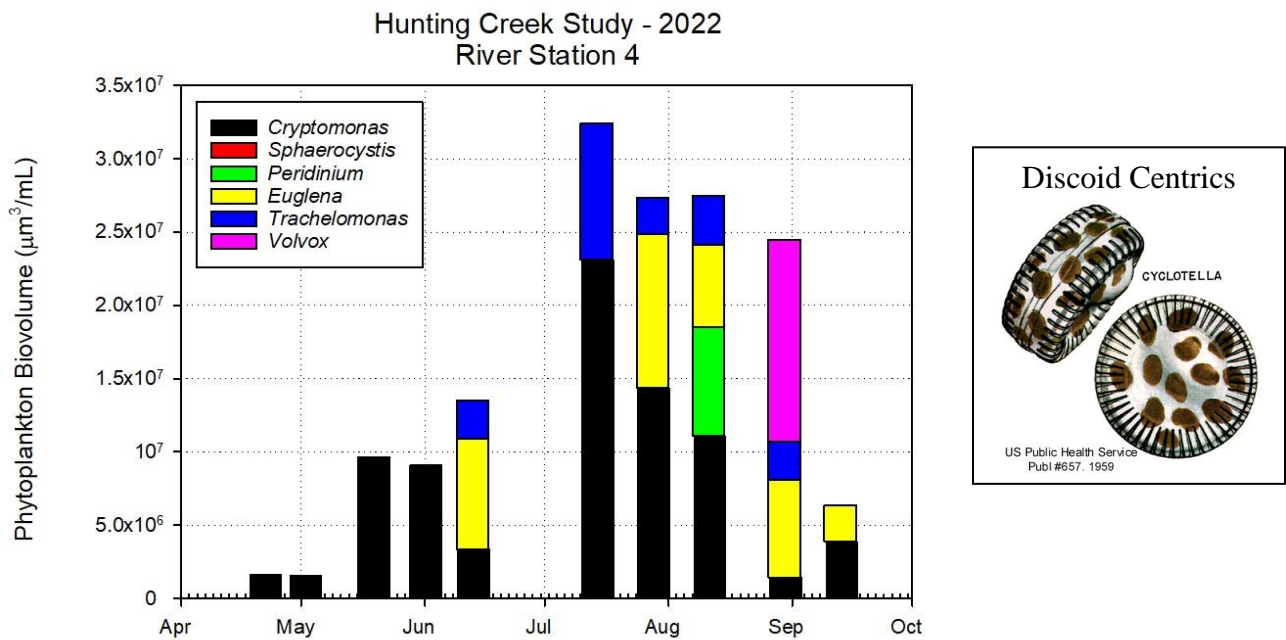


Figure 107. Phytoplankton Biovolume (um³/mL) by Dominant Other Taxon. River.

E. Zooplankton – 2022

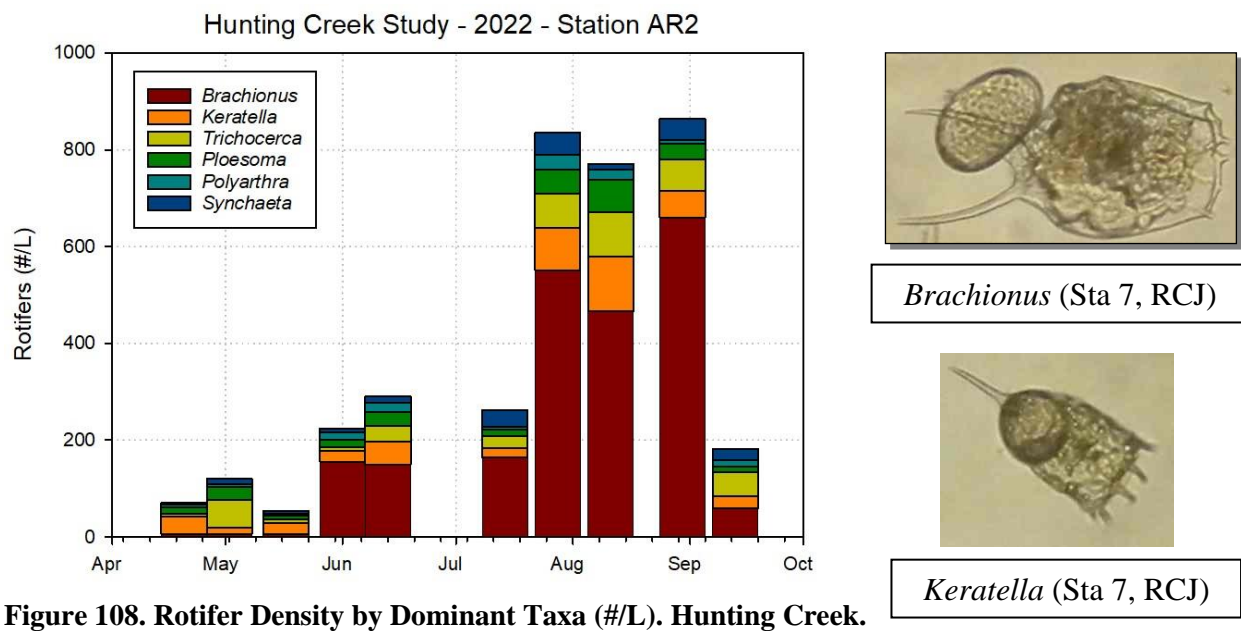


Figure 108. Rotifer Density by Dominant Taxa (#/L). Hunting Creek.

At the embayment station AR2, rotifer populations were rather low in spring and early summer, but increased markedly in late July through August reaching 800/L. *Brachionus* was dominant again on most dates with *Keratella* being dominant in spring and subdominant the rest of the year (Figure 108). In the river at AR4, rotifer population levels were less markedly seasonal and were actually greater than embayment numbers during June (Figure 109). The maximum number of rotifers was observed in August. *Brachionus* was again dominant in most samples with *Keratella* again subdominant.

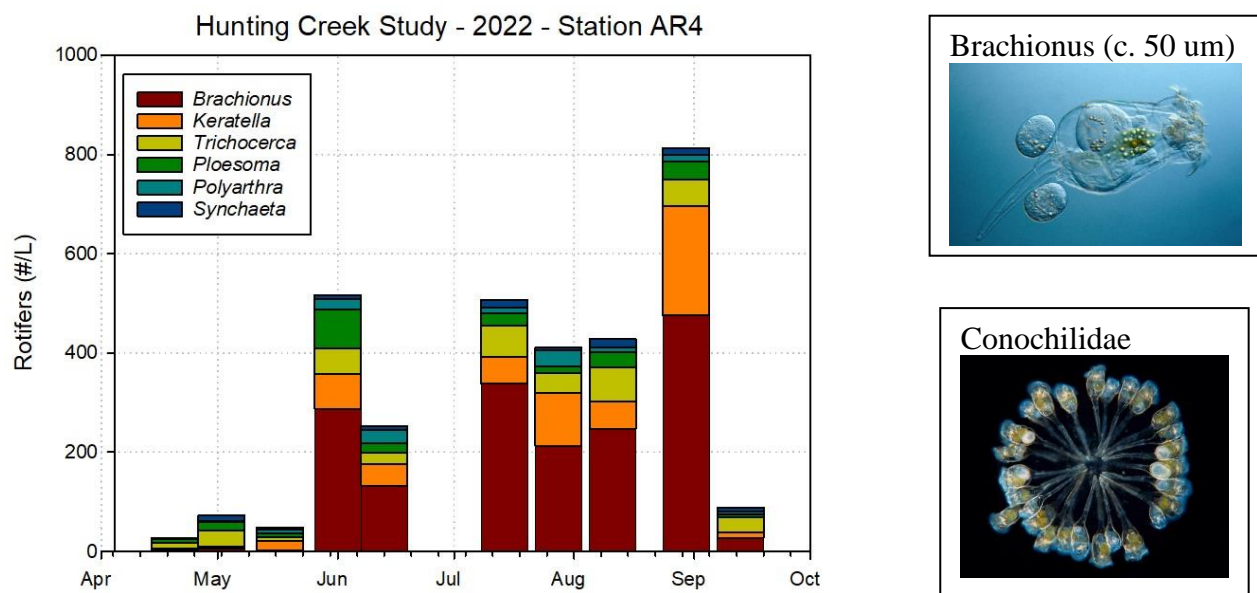


Figure 109. Rotifer Density by Dominant Taxa (#/L). River.

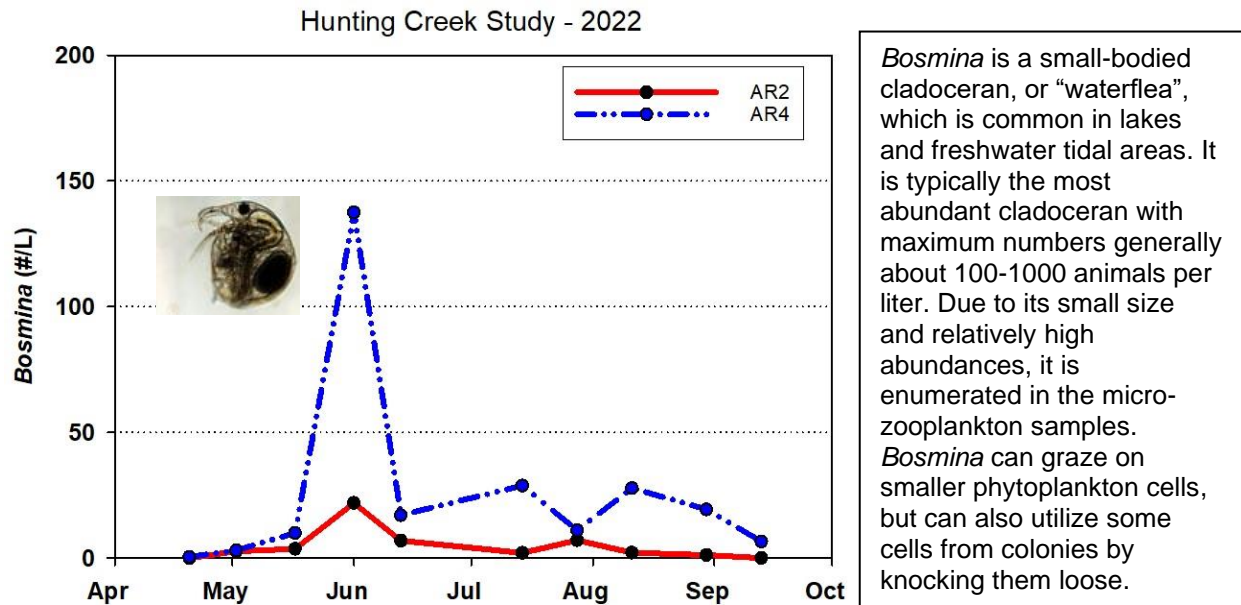


Figure 110. *Bosmina* Density by Station (#/L).

At the embayment station AR2 the small cladoceran *Bosmina* was very low all year, never exceeding 25/L (Figure 110). In the river *Bosmina* reached a clear maximum in early June at nearly 150/L and was at detectable levels for most of the year. *Diaphanosoma*, typically the most abundant larger cladoceran in the tidal Potomac, exhibited large peaks in early June (1200/L) and early August (800/L) at the embayment station but was much lower at the river station with modest peaks at the same time as those in the cove (Figure 111).

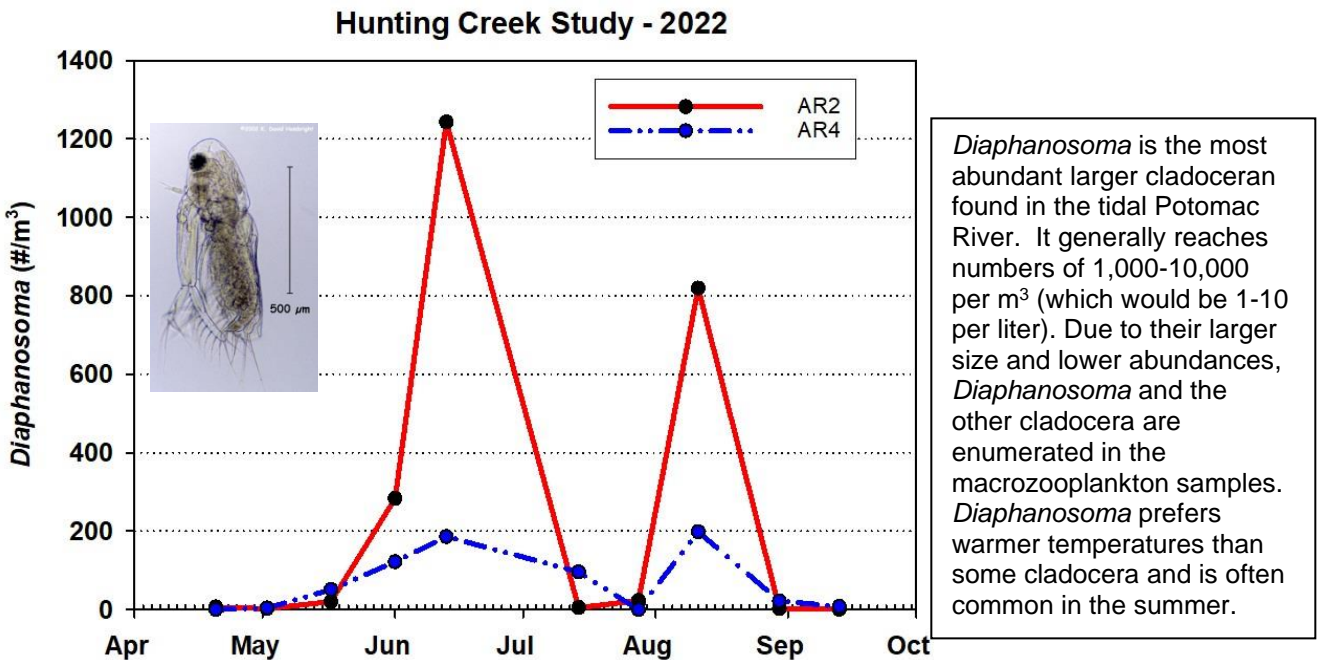
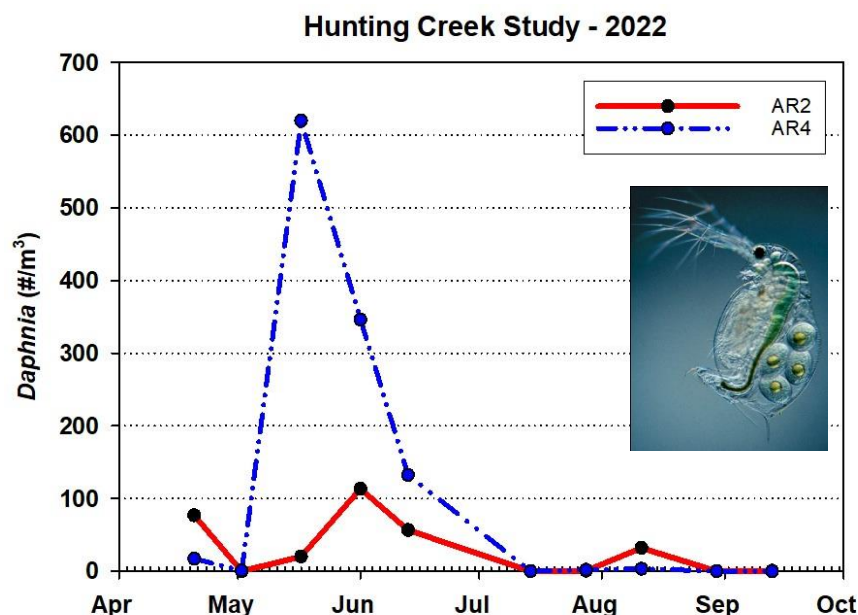


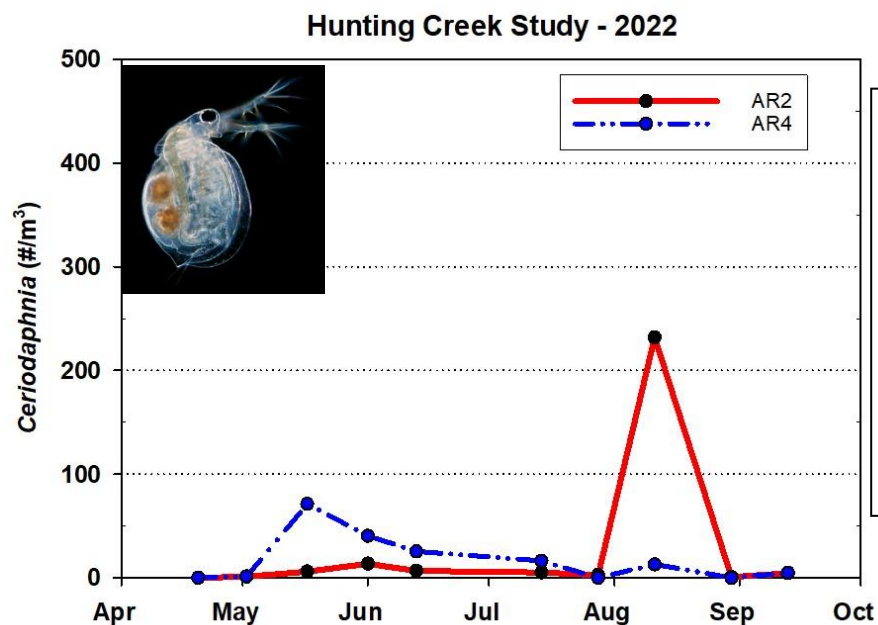
Figure 111. *Diaphanosoma* Density by Station (#/m³).



Daphnia, the common waterflea, is one of the most efficient grazers of phytoplankton in freshwater ecosystems. In the tidal Potomac River it is present, but has not generally been as abundant as *Diaphanosoma*. It is typically most common in spring.

Figure 112. *Daphnia* Density by Station (#/m³).

Daphnia was quite abundant in the river in late May at over 600/m³ and persisted at elevated levels for about a month and a half (Figure 112). In the embayment levels were much more modest. *Ceriodaphnia* showed a small peak in the embayment in early August, but otherwise was rare (Figure 113).



Ceriodaphnia, another common large-bodied cladoceran, is usually present in numbers similar to *Daphnia*. Like all waterfleas, the juveniles look like miniature adults and grow through a series of molts to a larger size and finally reach reproductive maturity. Most reproduction is asexual except during stressful environmental conditions.

Figure 113. *Ceriodaphnia* Density by Station (#/m³).

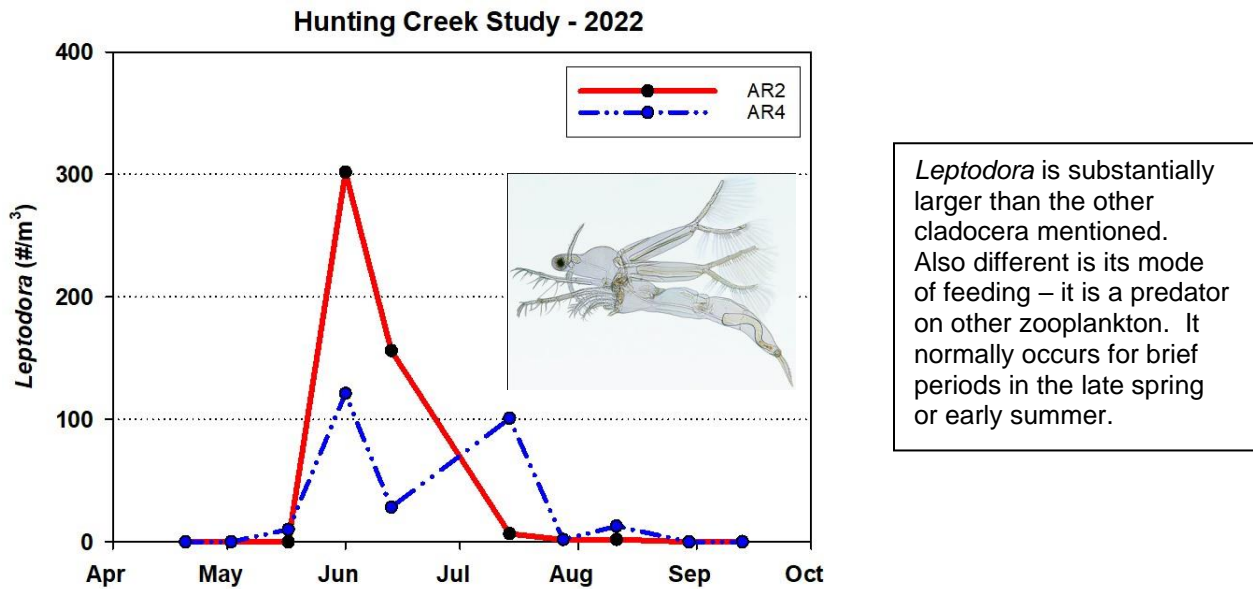


Figure 114. *Leptodora* Density by Station (#/m³).

Leptodora, the large cladoceran predator, was found in very high numbers in early June and persisted for about a month (Figure 114). It was present at somewhat lower levels in the river and persisted for a couple of weeks longer. Chydorid cladercera were found in the river at moderate levels especially during late May and early August peaks, but were almost entirely missing at AR2 (Figure 115).

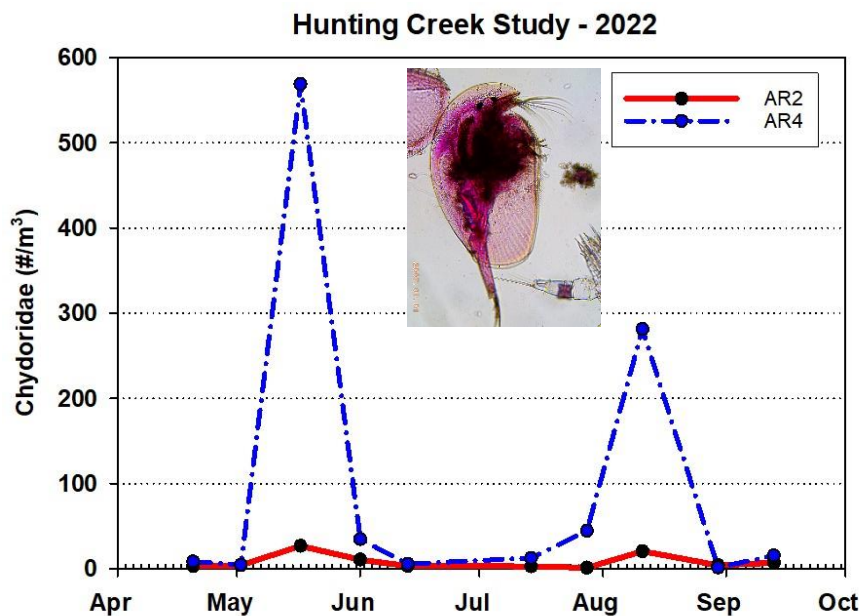
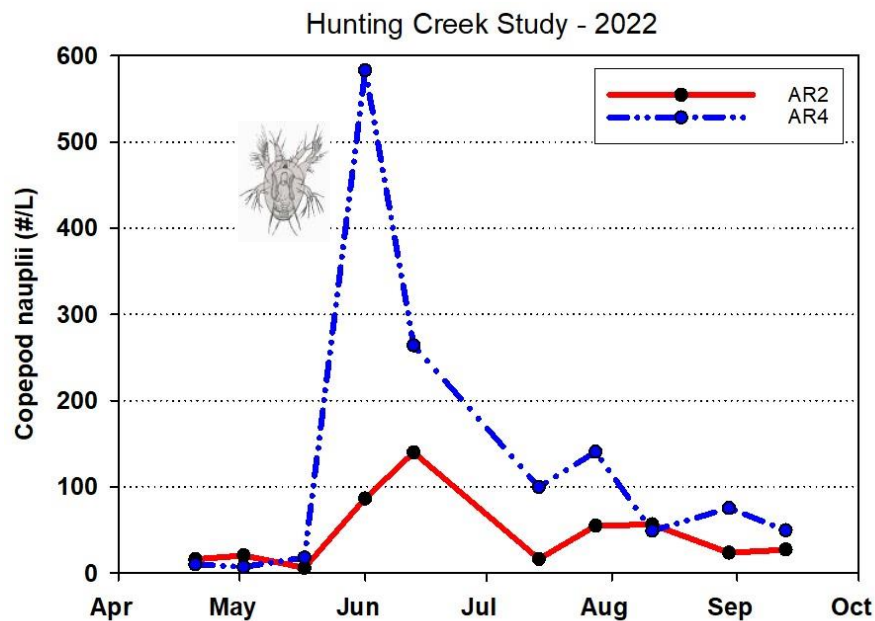


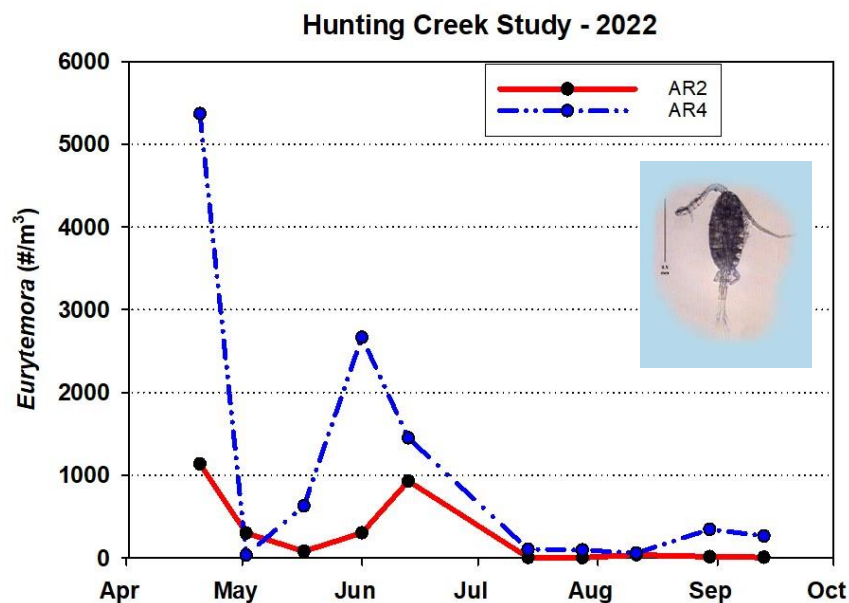
Figure 115. Chydoridae Density by Station (#/m³). (photo: L. Birsa from HC samples)



Copepod eggs hatch to form an immature stage called a nauplius. The nauplius is a larval stage that does not closely resemble the adult and the nauplii of different species of copepods are not easily distinguished so they are lumped in this study. Copepods go through 5 naupliar molts before reaching the copepodid stage which is morphologically very similar to the adult. Because of their small size and high abundance, copepod nauplii are enumerated in the microzooplankton samples.

Figure 116. Copepod Nauplii Density by Station (#/L).

Copepod nauplii, the larval stage of copepods, were the most numerous group of crustacean zooplankton. At AR2 they peaked at about 150/L in mid-June (Figure 116). They were much more abundant at AR4 peaking at nearly 600/L in early June. In the river *Eurytemora*, a large calanoid copepod, was present at high values of over 5000/m³ at AR4 on the first sampling date and after a strong decline in early May rebounded to over 2500/m³ in early June (Figure 117). Densities of *Eurytemora* were much lower in the embayment (Figure 117).



Eurytemora affinis is a large calanoid copepod characteristic of the freshwater and brackish areas of the Chesapeake Bay. *Eurytemora* is a cool water copepod which often reaches maximum abundance in the late winter or early spring. Included in this graph are adults and those copepodids that are recognizable as *Eurytemora*.

Figure 117. *Eurytemora* Density by Station (#/m³).

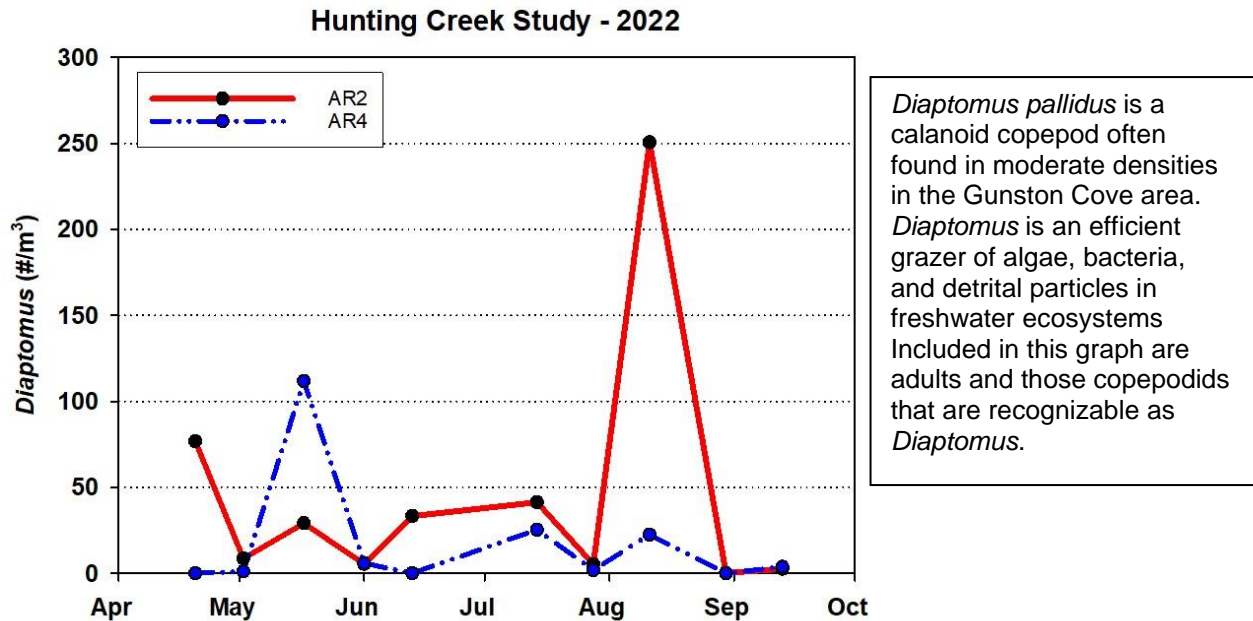


Figure 118. *Diaptomus* Density by Station (#/m³).

Diaptomus was present at only very low levels except for a modest peak in early August in the embayment (Figure 118). *Mesocyclops* was very scarce in 2022 in all samples except the early August river sample when it reached 1100/m³ (Figure 119).

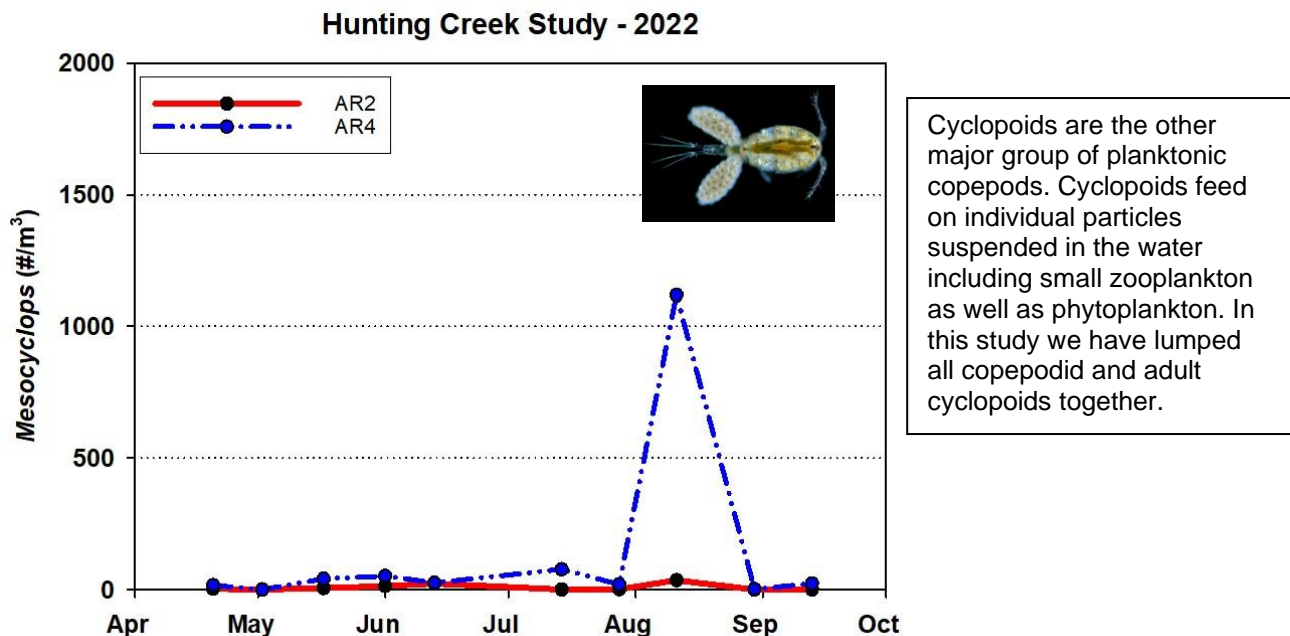


Figure 119. *Mesocyclops* by Station (#/m³).

F. Ichthyoplankton – 2022

We collected 14 samples (7 at AR2 and 7 at AR4) during the months April through July and found an average total larval density of 262 larvae of at least 10 species per 10 m³ (Table 4). The dominant family was Clupeidae, of which Gizzard Shad (*Dorosoma cepedianum*) had the highest density with an average larval density of 76 larvae per 10 m³. Unknown Clupeids had the second highest density with an average of 41 larvae per 10m³, followed by Blueback Herring (*Alosa aestivalis*) and Alewife (*Alosa pseudoharengus*) with 26 and 24 larvae per 10 m³ respectively. Another clupeid present that could positively be identified to the species level was Hickory Shad (*Alosa mediocris*) at an average of 3 larvae per 10 m³. White Perch a semi-anadromous species was also abundant in our ichthyoplankton samples with 66 larvae per 10 m³ on average, the second most abundant behind Gizzard Shad. The density of clupeid larvae has a clear seasonal pattern as a result of the spring spawning season of most clupeids that occurs higher upstream. Clupeid larvae in Figure 120 include Blueback Herring, Hickory Shad, Alewife, and Gizzard Shad. These have similar spawning patterns, so they are lumped into one group for this analysis. Clupeids peaked on the first of June and then rapidly decreased by July (Figure 120). Of these clupeids, Alewife and Blueback Herring are the two species that make up river herring, of which we describe the spawning population at the end of this report. White Perch larvae attained their highest density on average at 38 larvae per 10 m³ during mid-May (Figure 121), and decreased throughout June and July. Highest densities of other larvae (not Clupeids or Moronids) were also found on June 1st (Figure 122).

Table 5. Total larval density (#/10 m³) in Hunting Creek (AR 2) and the Potomac River (AR 4) and the mean among these stations in 2022.

Scientific Name	Common Name	AR2	AR4	Average
<i>Alosa aestivalis</i>	Blueback Herring	25.59	27.67	26.63
<i>Alosa mediocris</i>	Hickory Shad	4.96	1.72	3.34
<i>Alosa pseudoharengus</i>	Alewife	21.57	27.36	24.47
Clupeidae	unk. clupeid species	41.39	40.61	41.00
Cyprinidae	unk. cyprinidae species	0.00	0.13	0.07
<i>Dorosoma cepedianum</i>	Gizzard Shad	107.55	45.55	76.55
<i>Hybognathus regius</i>	Eastern Silvery Minnow	0.63	0.00	0.32
<i>Lepomis sp.</i>	unk. sunfish	1.12	0.00	0.56
<i>Menidia beryllina</i>	Inland Silverside	10.96	1.44	6.20
<i>Morone americana</i>	White Perch	104.99	28.48	66.73
<i>Pomoxis sp.</i>	unk. crappie species	0.63	0.00	0.32
Unidentified	unidentified	21.30	11.69	16.49
Total		340.71	184.65	262.68

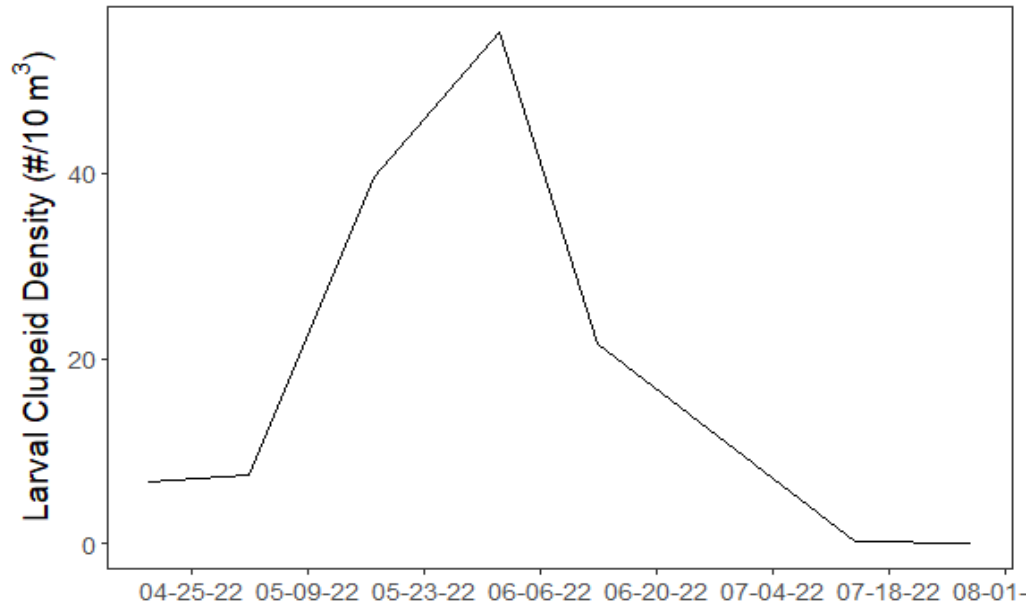


Figure 120. Density of clupeid larvae per 10m³.

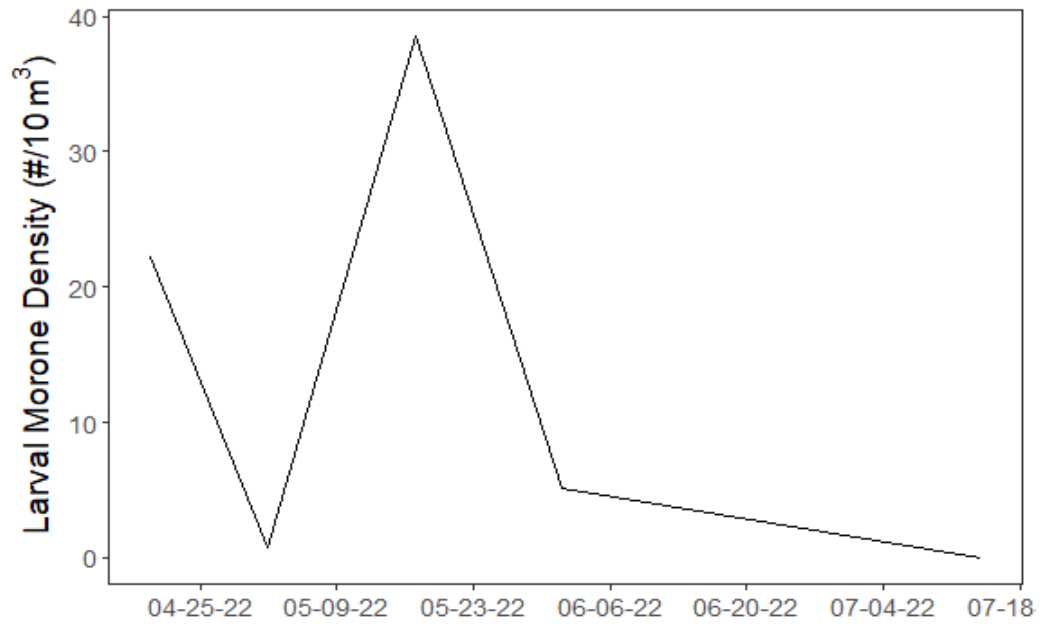


Figure 121. Density of *Morone sp.* (white perch and striped bass) per 10m³.

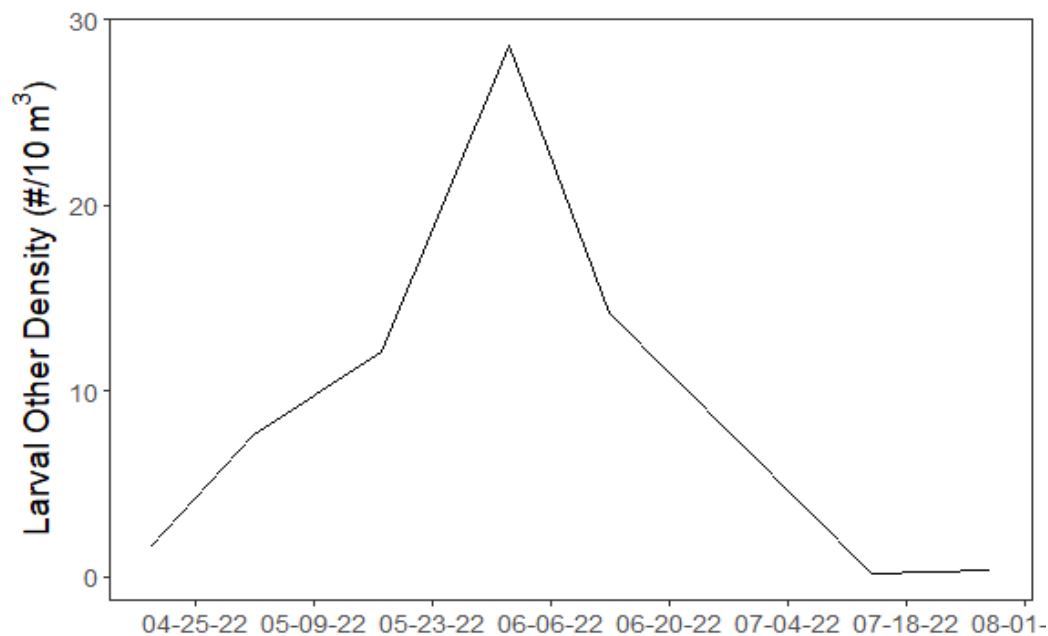


Figure 122. Density of other larvae per 10m³.

G. Adult and juvenile fishes – 2022

Trawls

Trawl sampling was conducted between April 22 and September 8 at station AR3 and AR4. A total of 2829 fishes comprising of at least 20 species were collected with trawls (Table 5). Collections were dominated by White Perch (72.98 %). The second most abundant species was Spottail Shiner (13.04 %), followed by *Alosa sp.* (6.93 %), Gizzard Shad (3.04 %), Bay Anchovy (1.56 %), and Blue Catfish (1.45 % ,Tables 5 and 6).

Our highest catch occurred on July 21, due to the high abundance of White Perch in that trawl sample (Table 6). Notable difference among AR3 and AR4 were the collection of 40 Blue Catfish at AR4, but only one at AR3 (Table 7). At both stations, we collected the highest numbers of White Perch. The catches at AR3 and AR4 were both greater than last year, with an almost 5- and 3-fold increase at AR3 and AR4 respectively, driven by White Perch collections. Similar to last year catfishes other than Blue Catfish (Brown Bullhead, Channel Catfish, and Flathead Catfish) were mostly absent in our trawl samples, only collecting 3 White Bullhead.

White Perch (*Morone americana*) was the dominant species in all months sampled, except for June, which was dominated by *Alosa sp.* (Figures 123&124). Although only the sixth most dominant species Blue Catfish were present in trawls in every month except for June.

Table 6. Adult and juvenile fish collected by trawling. Hunting Creek - 2022.

Scientific Name	Common Name	Abundance	Percent
<i>Morone americana</i>	White Perch	2064	72.98
<i>Notropis hudsonius</i>	Spottail Shiner	369	13.04
<i>Alosa sp.</i>	unk. Alosa species	196	6.93
<i>Dorosoma cepedianum</i>	Gizzard Shad	86	3.04
<i>Anchoa mitchilli</i>	Bay anchovy	44	1.56
<i>Ictalurus furcatus</i>	Blue Catfish	41	1.45
<i>Etheostoma olmstedi</i>	Tessellated Darter	7	0.25
<i>Cyprinus carpio</i>	Carp	4	0.14
<i>Ameiurus catus</i>	White Bullhead	3	0.11
<i>Lepomis gibbosus</i>	Pumpkinseed	3	0.11
<i>Lepomis macrochirus</i>	Bluegill	2	0.07
<i>Trinectes maculatus</i>	Hogchoker	1	0.04
<i>Alosa aestivalis</i>	Blueback Herring	1	0.04
<i>Carassius auratus</i>	Goldfish	1	0.04
<i>Catostomus commersonii</i>	White Sucker	1	0.04
<i>Fundulus diaphanus</i>	Banded Killifish	1	0.04
<i>Morone saxatilis</i>	Striped Bass	1	0.04
<i>Moxostoma macrolepidotum</i>	Shorthead Redhorse	1	0.04
<i>Moxostoma sp.</i>	unk. redhorse species	1	0.04
<i>Pomoxis nigromaculatus</i>	Black Crappie	1	0.04
Total		2829	100.00

Table 7. Adult and juvenile fish collected by trawling on each sampling date.

Scientific Name	Common Name	4-22	5-06	5-19	6-02	6-16	7-07	7-21	8-04	8-18	9-08	Total
<i>Alosa aestivalis</i>	Blueback Herring	0	0	0	0	0	0	0	0	0	1	1
<i>Alosa sp.</i>	unk. Alosa	0	0	0	0	196	0	0	0	0	0	196
<i>Ameiurus catus</i>	White Bullhead	0	0	0	0	1	0	0	1	1	0	3
<i>Anchoa mitchilli</i>	Bay anchovy	0	0	0	0	0	0	0	0	1	43	44
<i>Carassius auratus</i>	Goldfish	0	0	0	0	0	0	0	0	0	1	1
<i>Catostomus commersonii</i>	White Sucker	0	0	0	0	0	0	0	0	0	1	1
<i>Cyprinus carpio</i>	Carp	0	1	1	0	1	0	0	0	0	1	4
<i>Dorosoma cepedianum</i>	Gizzard Shad	0	2	0	0	0	4	74	5	1	0	86
<i>Etheostoma olmstedii</i>	Tessellated Darter	0	0	0	0	0	2	2	0	0	3	7
<i>Fundulus diaphanus</i>	Banded Killifish	0	0	0	1	0	0	0	0	0	0	1
<i>Ictalurus furcatus</i>	Blue Catfish	0	1	0	0	0	5	0	17	12	6	41
<i>Lepomis gibbosus</i>	Pumpkinseed	0	0	0	0	2	0	0	0	0	1	3
<i>Lepomis macrochirus</i>	Bluegill	0	0	1	0	0	1	0	0	0	0	2
<i>Morone americana</i>	White Perch	0	31	10	24	30	198	827	300	317	328	2064
<i>Morone saxatilis</i>	Striped Bass	0	0	0	0	0	0	1	0	0	0	1
<i>Moxostoma macrolepidotum</i>	Shorthead Redhorse	0	0	0	0	0	0	0	0	1	0	1
<i>Moxostoma sp.</i>	unk. redhorse	0	0	0	0	1	0	0	0	0	0	1
<i>Notropis hudsonius</i>	Spottail Shiner	0	7	0	1	1	1	288	0	2	69	369
<i>Pomoxis nigromaculatus</i>	Black Crappie	0	0	0	0	0	1	0	0	0	0	1
<i>Trinectes maculatus</i>	Hogchoker	0	0	0	0	0	1	0	0	0	0	1
Total		0	42	12	26	232	213	1192	323	335	454	2829

Table 8. Adult and juvenile fish collected by trawling at each station - 2022

Scientific Name	Common Name	3	4
<i>Alosa aestivalis</i>	Blueback Herring	1	0
<i>Alosa sp.</i>	unk. Alosa species	196	0
<i>Ameiurus catus</i>	White Bullhead	0	3
<i>Anchoa mitchilli</i>	Bay anchovy	39	5
<i>Carassius auratus</i>	Goldfish	0	1
<i>Catostomus commersonii</i>	White Sucker	0	1
<i>Cyprinus carpio</i>	Carp	1	3
<i>Dorosoma cepedianum</i>	Gizzard Shad	84	2
<i>Etheostoma olmstedii</i>	Tessellated Darter	7	0
<i>Fundulus diaphanus</i>	Banded Killifish	1	0
<i>Ictalurus furcatus</i>	Blue Catfish	1	40
<i>Lepomis gibbosus</i>	Pumpkinseed	3	0
<i>Lepomis macrochirus</i>	Bluegill	2	0
<i>Morone americana</i>	White Perch	1273	792
<i>Morone saxatilis</i>	Striped Bass	1	0
<i>Moxostoma macrolepidotum</i>	Shorthead Redhorse	0	1
<i>Moxostoma sp.</i>	unk. redhorse species	0	1
<i>Notropis hudsonius</i>	Spottail Shiner	292	77
<i>Pomoxis nigromaculatus</i>	Black Crappie	1	0
<i>Trinectes maculatus</i>	Hogchoker	0	1
Total		1902	927

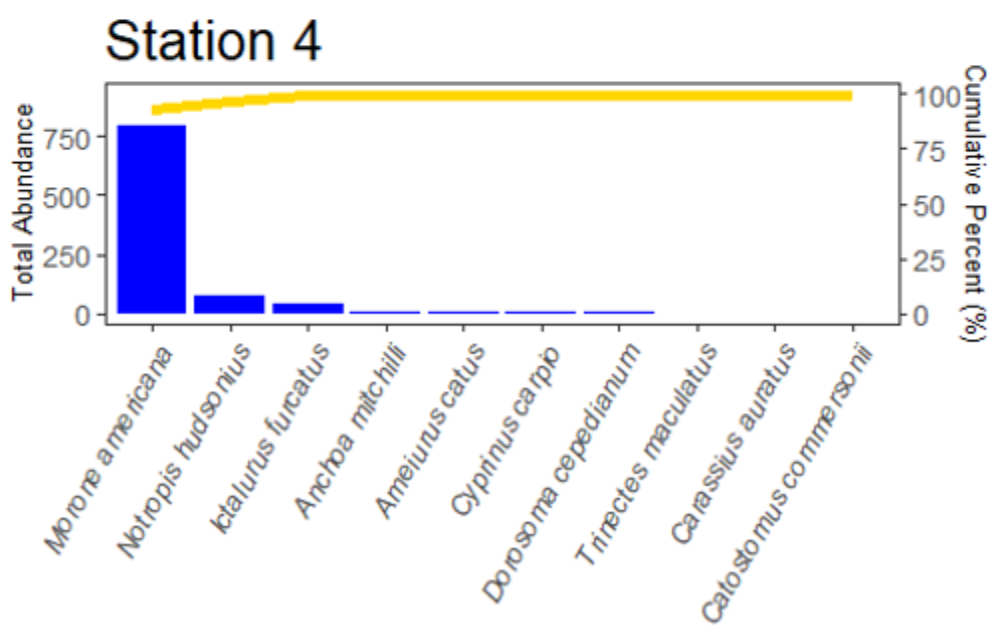
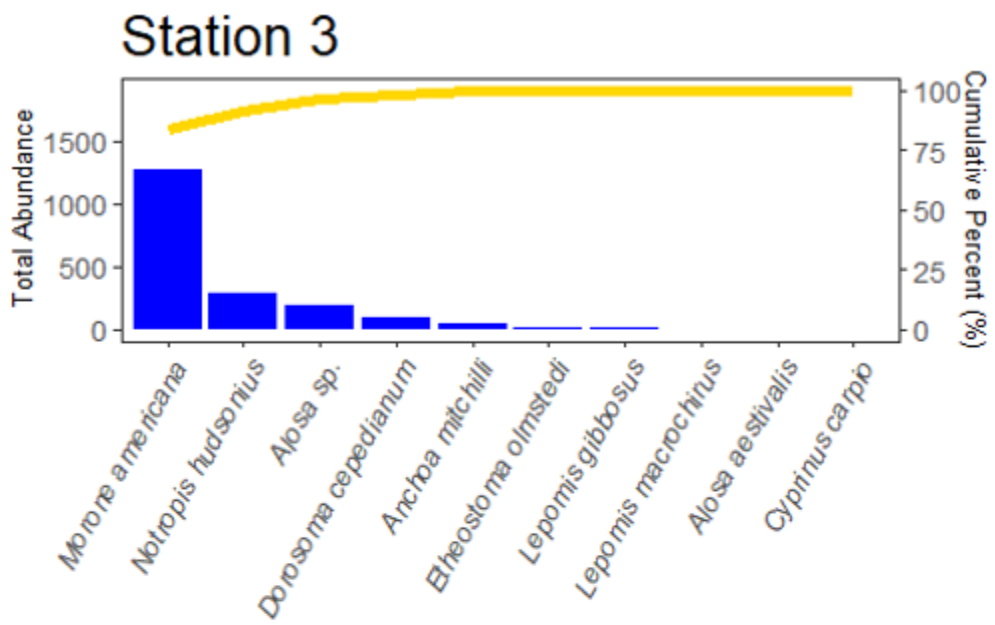


Figure 123A&B. Pareto chart of adult and juvenile fishes collected by trawling. Dominant species by station in total abundance and cumulative percentage of total for Station AR3 (top) and Station AR4 (bottom).

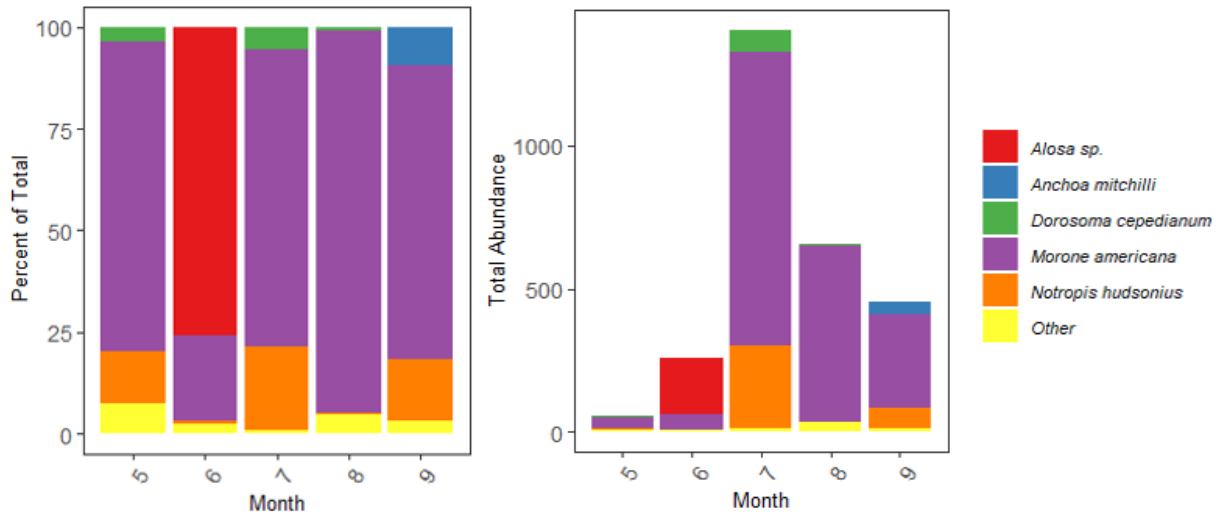


Figure 124 A&B. Adult and juvenile fishes collected by trawling. Dominant species by month in percentage of total (A) and total abundance (B).

Seines

Seine sampling was conducted between April 22 and September 8 at station AR5 and AR6; however, AR5 was somewhat problematic with many trees and debris along the shoreline. These two stations were selected as sites with shallow sloping shorelines that would enable us to tow a beach seine. The net was towed up onto the beach unless high water completely submerged the beach. In those cases, the net was towed into the boat. A total of 20 seine samples were taken (10 per station), comprising 5,748 fishes of at least 23 species (Table 8). Similar to previous years, White Perch (75.87 %) was the dominant species ($n = 4,361$) in seine catches followed by Banded Killifish (8.94 %), *Alosa* sp. (6.33 %), and Mummichog (2.82 %). This continues the trend of greater White Perch dominance seen in recent years (2019 onward) where submerged aquatic vegetation has not been present.

Banded Killifish and White Perch were collected from April to September with White Perch peaking in August at > 3000 individuals. Banded Killifish were relatively abundant (> 40 individuals) all months except April (Table 9). The total number of specimens at station 6 was higher than station 5, given that most White Perch were collected at station 6 and station 5 is more difficult to sample, likely decreasing our seining efficiency there (Table 10). More Banded Killifish were collected at station 6 as well, but Largemouth Bass and Alewife were more abundant at station 5. Evenness distribution of abundance over multiple species (Banded Killifish, *Alosa* sp., White Perch) was higher at station 5 than station 6, due to the dominance of White Perch at station 6 (Figure 61). Banded Killifish was the dominant species at station 5, while White Perch dominated at station 6. Seasonal seine collections at both sites combined were initially dominated by Banded Killifish, then *Alosa* sp., but starting in July White Perch dominated until the end of collections (Figure 62).

Table 9. Total adult and juvenile fish collected by seining - 2022

Scientific Name	Common Name	Abundance	Percent
<i>Alosa aestivalis</i>	Blueback Herring	36	0.63
<i>Alosa mediocris</i>	Hickory Shad	1	0.02
<i>Alosa pseudoharengus</i>	Alewife	6	0.10
<i>Alosa sapidissima</i>	American Shad	10	0.17
<i>Alosa sp.</i>	unk. Alosa species	364	6.33
<i>Anchoa mitchilli</i>	Bay anchovy	3	0.05
<i>Carpodes cyprinus</i>	Quillback	2	0.03
<i>Cyprinus carpio</i>	Carp	1	0.02
<i>Dorosoma cepedianum</i>	Gizzard Shad	114	1.98
<i>Dorosoma petenense</i>	Threadfin Shad	11	0.19
<i>Etheostoma olmstedii</i>	Tessellated Darter	11	0.19
<i>Fundulus diaphanus</i>	Banded Killifish	514	8.94
<i>Fundulus heteroclitus</i>	Mummichog	162	2.82
<i>Hybognathus regius</i>	Eastern Silvery Minnow	3	0.05
<i>Ictalurus furcatus</i>	Blue Catfish	1	0.02
<i>Lepomis gibbosus</i>	Pumpkinseed	14	0.24
<i>Lepomis macrochirus</i>	Bluegill	1	0.02
<i>Menidia beryllina</i>	Inland Silverside	67	1.17
<i>Micropterus salmoides</i>	Largemouth Bass	12	0.21
<i>Morone americana</i>	White Perch	4361	75.87
<i>Morone saxatilis</i>	Striped Bass	3	0.05
<i>Notemigonus crysoleucas</i>	Golden Shiner	1	0.02
<i>Notropis hudsonius</i>	Spottail Shiner	47	0.82
<i>Semotilus atromaculatus</i>	Creek Chub	3	0.05
Total		5748	100.00

Table 10. Adult and juvenile fish collected by seining on each sampling date – 2022.

Scientific Name	Common Name	4-22	5-06	5-19	6-02	6-16	7-07	7-21	8-04	8-18	9-08	Total
<i>Alosa aestivalis</i>	Blueback Herring	0	0	0	0	0	0	0	0	0	36	36
<i>Alosa mediocris</i>	Hickory Shad	0	0	0	0	0	0	1	0	0	0	1
<i>Alosa pseudoharengus</i>	Alewife	1	0	0	0	0	0	0	0	5	0	6
<i>Alosa sapidissima</i>	American Shad	0	0	0	0	1	0	0	0	9	0	10
<i>Alosa sp.</i>	unk. Alosa	0	3	192	0	169	0	0	0	0	0	364
<i>Anchoa mitchilli</i>	Bay anchovy	0	0	1	0	0	0	0	0	0	2	3
<i>Carpiodes cyprinus</i>	Quillback	0	0	0	0	1	1	0	0	0	0	2
<i>Cyprinus carpio</i>	Carp	0	0	0	0	1	0	0	0	0	0	1
<i>Dorosoma cepedianum</i>	Gizzard Shad	0	0	0	0	0	94	0	4	8	8	114
<i>Dorosoma petenense</i>	Threadfin Shad	0	0	0	0	0	0	0	3	0	8	11
<i>Etheostoma olmstedti</i>	Tessellated Darter	0	0	0	0	0	3	0	1	1	6	11
<i>Fundulus diaphamus</i>	Banded Killifish	17	114	46	41	3	12	33	119	47	82	514
<i>Fundulus heteroclitus</i>	Mummichog	4	4	5	9	0	9	70	32	0	29	162
<i>Hybognathus regius</i>	Eastern Silvery Minnow	0	0	0	0	0	0	0	0	3	0	3
<i>Ictalurus furcatus</i>	Blue Catfish	0	0	0	0	1	0	0	0	0	0	1
<i>Lepomis gibbosus</i>	Pumpkinseed	0	0	0	0	0	0	0	0	0	14	14
<i>Lepomis macrochirus</i>	Bluegill	0	0	0	0	0	0	0	0	0	1	1
<i>Menidia beryllina</i>	Inland Silverside	8	5	8	28	0	1	0	1	1	15	67
<i>Micropterus salmoides</i>	Largemouth Bass	0	0	0	0	0	2	0	0	2	8	12
<i>Morone americana</i>	White Perch	2	1	0	3	8	96	3	2250	1737	261	4361
<i>Morone saxatilis</i>	Striped Bass	0	0	0	0	1	0	0	0	1	1	3
<i>Notemigonus crysoleucas</i>	Golden Shiner	0	0	0	1	0	0	0	0	0	0	1
<i>Notropis hudsonius</i>	Spottail Shiner	3	11	0	0	0	0	0	14	5	14	47
<i>Semotilus atromaculatus</i>	Creek Chub	0	0	0	3	0	0	0	0	0	0	3
Total		35	138	252	85	185	218	107	2424	1819	485	5748

Table 11. Adult and juvenile fish collected by seining at each station – 2022

Scientific Name	Common Name	AR5	AR6
<i>Alosa aestivalis</i>	Blueback Herring	0	36
<i>Alosa mediocris</i>	Hickory Shad	1	0
<i>Alosa pseudoharengus</i>	Alewife	5	1
<i>Alosa sapidissima</i>	American Shad	7	3
<i>Alosa sp.</i>	unk. Alosa species	109	255
<i>Anchoa mitchilli</i>	Bay anchovy	1	2
<i>Carpiodes cyprinus</i>	Quillback	0	2
<i>Cyprinus carpio</i>	Carp	0	1
<i>Dorosoma cepedianum</i>	Gizzard Shad	6	108
<i>Dorosoma petenense</i>	Threadfin Shad	8	3
<i>Etheostoma olmstedii</i>	Tessellated Darter	11	0
<i>Fundulus diaphanus</i>	Banded Killifish	111	403
<i>Fundulus heteroclitus</i>	Mummichog	31	131
<i>Hybognathus regius</i>	Eastern Silvery Minnow	0	3
<i>Ictalurus furcatus</i>	Blue Catfish	1	0
<i>Lepomis gibbosus</i>	Pumpkinseed	13	1
<i>Lepomis macrochirus</i>	Bluegill	1	0
<i>Menidia beryllina</i>	Inland Silverside	13	54
<i>Micropterus salmoides</i>	Largemouth Bass	10	2
<i>Morone americana</i>	White Perch	90	4271
<i>Morone saxatilis</i>	Striped Bass	1	2
<i>Notemigonus crysoleucas</i>	Golden Shiner	0	1
<i>Notropis hudsonius</i>	Spottail Shiner	4	43
<i>Semotilus atromaculatus</i>	Creek Chub	0	3
Total		423	5325

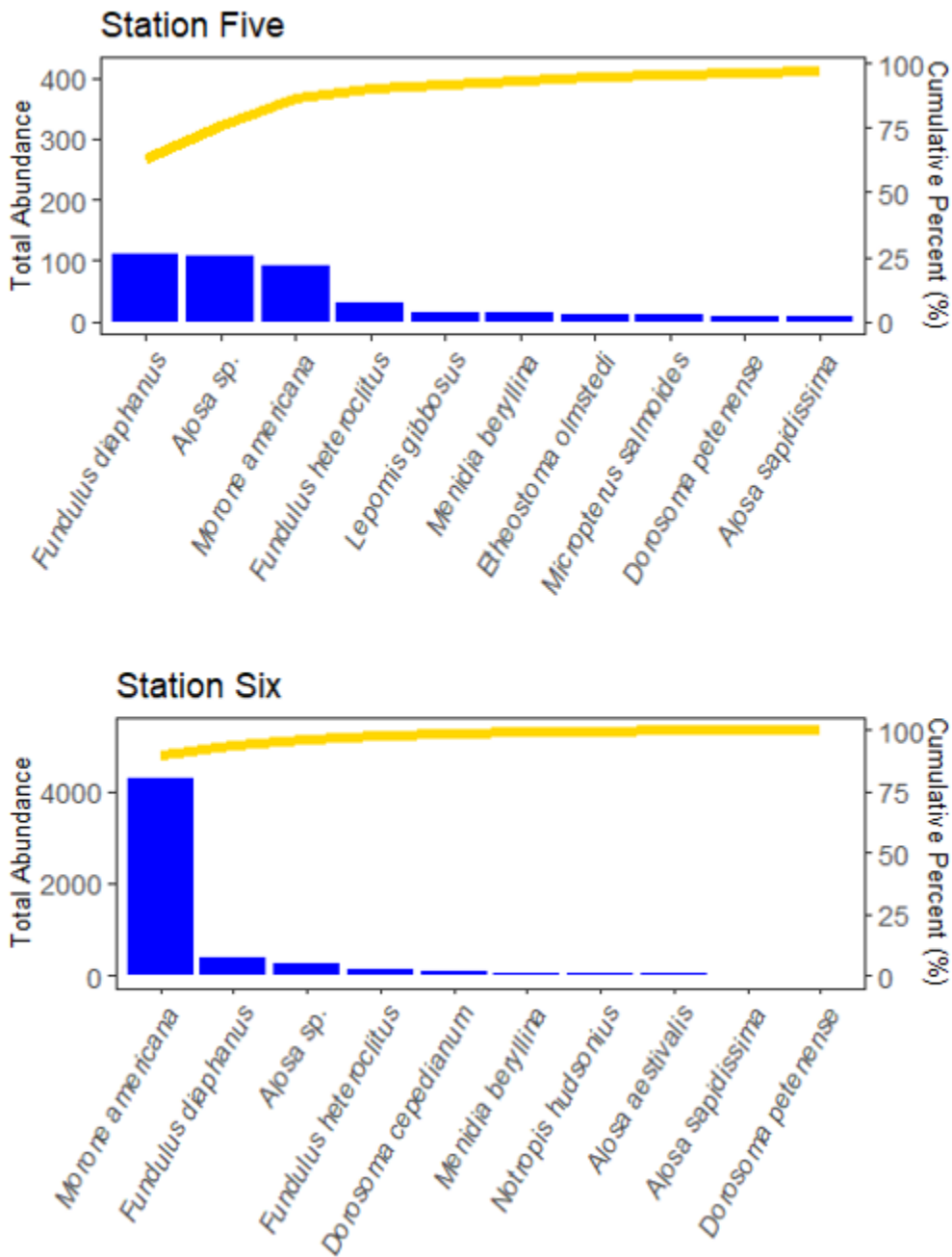


Figure 125A&B. Pareto chart of adult and juvenile fishes collected by seining. Dominant species by station in total abundance and cumulative percentage of total for AR5 (top) and AR6 (bottom).

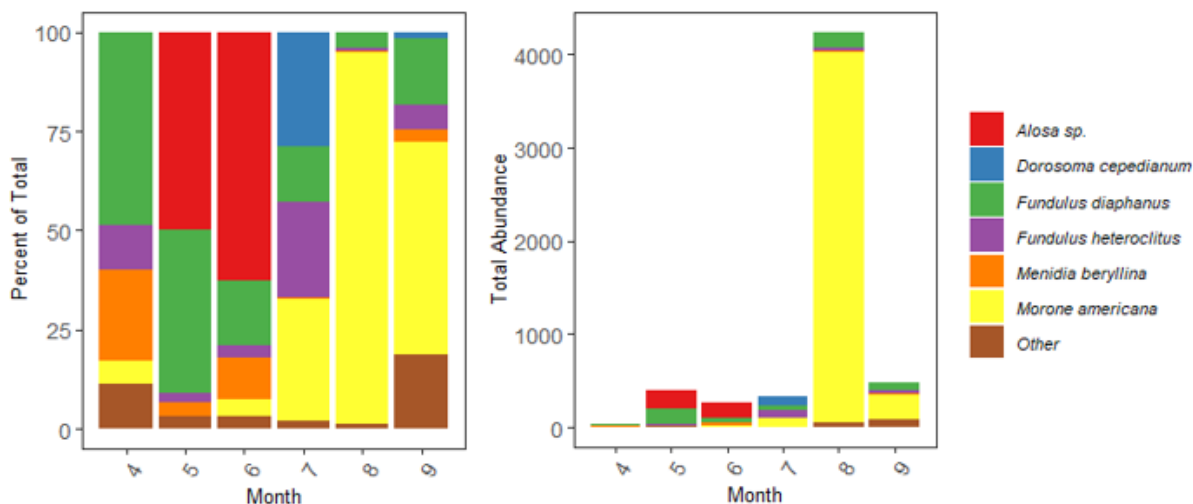


Figure 126A&B. Adult and juvenile fish collected by seining. Dominant species by month in percentage of total (A) and total abundance (B).

Fyke Nets

Fyke nets were set from April to August, but could not be set for 3 sampling periods due to inclement weather. Both fyke nets were set near trawl station 3 (Figure 1). Similar to previous years, fyke net catches were less than with the trawl or seine, given that only 305 fishes representing 8 species were collected (Table 11). Similar to trawls and seines, White Perch dominated the Fyke catch at 283 individuals. Once again, SAV cover was low in 2022, which makes the trawl more effective resulting in a higher catch, and the fyke net less effective because they are not hidden as well with less dense aquatic plant beds. This highlights the importance of using different gear types to accurately monitor species abundance trends. Previously, fyke nets were effective in 2017 when the SAV cover was much higher, with high fish abundance reflective of a diversity of species utilizing the SAV habitat.

Table 12. Adult and juvenile fish collected by fyke nets – 2022

Scientific Name	Common Name	Abundance	Percent
<i>Alosa aestivalis</i>	Blueback Herring	1	0.30
<i>Alosa pseudoharengus</i>	Alewife	1	0.30
<i>Etheostoma olmstedi</i>	Tessellated Darter	6	2.00
<i>Fundulus diaphanus</i>	Banded Killifish	1	0.28
<i>Menidia beryllina</i>	Inland Silverside	1	0.31
<i>Morone americana</i>	White Perch	283	92.86
<i>Morone saxatilis</i>	Striped Bass	4	1.19
<i>Notropis hudsonius</i>	Spottail Shiner	8	2.76
Total		305	100.00

Table 13. Adult and juvenile fish collected by fyke nets on each sampling date.

Scientific Name	Common Name	4-22	5-19	6-02	6-16	7-21	8-04	8-18	Total
<i>Alosa aestivalis</i>	Blueback Herring	0	0	0	1	0	0	0	1
<i>Alosa pseudoharengus</i>	Alewife	0	0	0	1	0	0	0	1
<i>Etheostoma olmstedii</i>	Tessellated Darter	0	0	0	1	4	1	0	6
<i>Fundulus diaphanus</i>	Banded Killifish	0	0	0	0	1	0	0	1
<i>Menidia beryllina</i>	Inland Silverside	1	0	0	0	0	0	0	1
<i>Morone americana</i>	White Perch	0	0	1	0	254	27	2	283
<i>Morone saxatilis</i>	Striped Bass	0	0	0	0	3	1	0	4
<i>Notropis hudsonius</i>	Spottail Shiner	0	0	0	0	4	4	0	8
Total		1	0	1	3	265	33	2	305

Table 14. Adult and juvenile fish collected by fyke nets at each station – 2022

Scientific Name	Common Name	Fyke Far	Fyke Near
<i>Alosa aestivalis</i>	Blueback Herring	0	1
<i>Alosa pseudoharengus</i>	Alewife	0	1
<i>Etheostoma olmstedii</i>	Tessellated Darter	5	1
<i>Fundulus diaphanus</i>	Banded Killifish	0	1
<i>Menidia beryllina</i>	Inland Silverside	1	0
<i>Morone americana</i>	White Perch	101	182
<i>Morone saxatilis</i>	Striped Bass	1	3
<i>Notropis hudsonius</i>	Spottail Shiner	5	4
Total		113	192

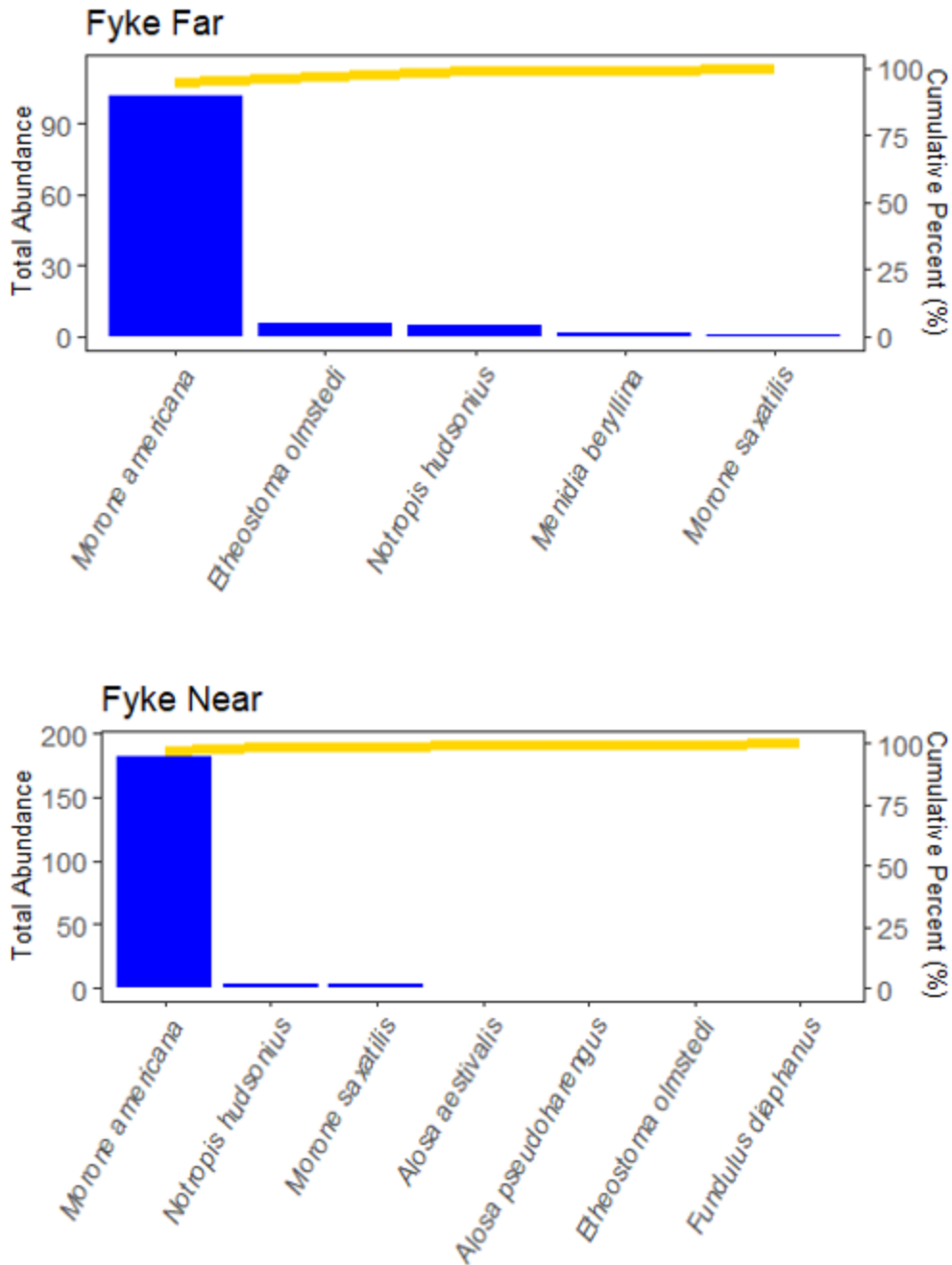


Figure 127A&B. Pareto chart of adult and juvenile fishes collected by fyke nets. Dominant species by station in total abundance and cumulative percentage of total for the Near Fyke (top) and Far Fyke (bottom).

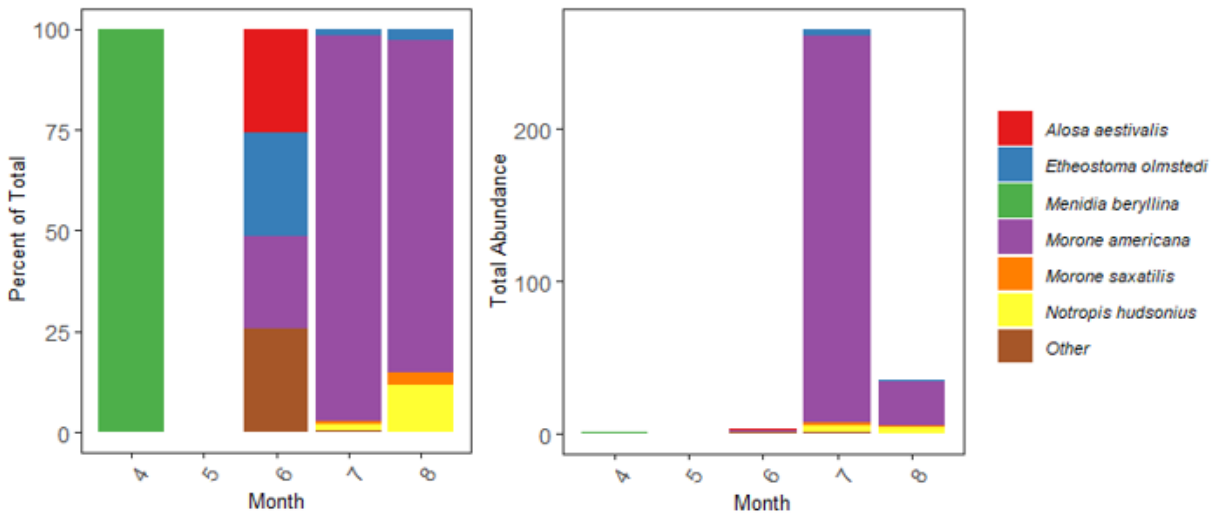


Figure 128A and B. Adult and juvenile fish collected by fyke nets. Dominant species by month in percentage of total (A) and total abundance (B).

H. Submersed Aquatic Vegetation – 2022

SAV data overflights by VIMS were conducted in 2021 and the aerial imagery is available (Figure 129). This imagery shows very little SAV coverage in 2021 compared with typical pre-2018 years. While the VIMS was not able to obtain imagery in 2022, the cruises that we conducted and the transects that were done on July 18 and August 16 (Table 12) indicate that in 2022, the SAV beds continue to be almost non-existent.



Figure 129. Aerial imagery of Hunting Creek taken in late summer 2021

<http://web.vims.edu/bio/sav/savwabmap/>
downloaded March 26, 2023.

All SAV taxa were greatly reduced in 2018 and virtually absent since then (Table 12). This decline most certainly started with the very turbid water in 2018 which obstructed light penetration. Earlier in this report we documented the major change that has occurred in the light environment in Hunting Creek since 2018.

Table 15. Average Density of Submersed Aquatic Vegetation Species in Transects. 2022

Average included all sites with water depth less than or equal to 2 m. Density scale: 0 (absent) – 4 (very abundant). On July 18, 30 sites were sampled by rake. On August 16, 28 were sampled.

Taxon Scientific Name	Taxon Common Name	Average Density per sample by SAV Species – 2022	
		July 18, 2022	Aug 16, 2022
<i>Ceratophyllum demersum</i>	Coontail	0	0
<i>Heteranthera dubia</i>	Water Stargrass	0	0
<i>Hydrilla verticillata</i>	Hydrilla	0	0
<i>Najas guadalupensis</i>	Southern Naiad	0	0
<i>Najas minor</i>	Spiny Naiad	0	0
Various	Filamentous algae	0	0

I. Benthic Macroinvertebrates - 2022

River and Embayment Samples

Triplicate petite ponar samples were collected from AR2, AR3, and AR4 monthly from May through September.

Taxonomic Groups: Annelid worms (including Oligochaetes and Leeches) were found in high numbers at each site over all dates (Table XX; Figure 130). Overall, they accounted for 68% of all benthic organisms found. Oligochaetes were by far the dominant taxonomic annelid, being found in all samples in substantial number. Leeches were less common and only found at sites AR3 and AR4 in May, August, and September. Insects were the second highest group in abundance across sites and dates, accounting for 12% of all individuals accounted for and, more importantly, for the greatest number of distinct taxa (six taxa) (Table XX). Chironomids were by far the most numerous and omnipresent insect taxon. The other insect taxa were present in only a few samples. Crustaceans (including amphipods and isopods) were the third highest group in abundance across sites and dates, accounting for 8.4% of all individuals. Gammarid amphipods (scuds) dominated this group with the isopod *Cyathura polita* being the second most common crustacean (Table XX; Figure 130). The remainder of the taxonomic groups accounted for minor components of the overall abundance and were generally most common at AR4 (Table XX). These included Bivalvia (2.6% of total abundance), Turbellaria (i.e., flatworms) (7.9%), and Gastropoda (0.8%). The bivalve group was composed of both the invasive Asian clam, *Corbicula fluminea*, and a native fingernail clam from the Sphaeriidae family. The gastropod

(i.e., snails) group was composed of invasive Japanese mystery snails (*Cipangopaludina japonica*) from the family Viviparidae and native Pleurocerid snails (*Elmina virginica*) and limpets (*Ferrissia rivularis*), all of which were only found at AR4 (Table XX).

Spatial trends: The average abundance of organisms per ponar sample was highest at AR2, but this was entirely attributable to the large number of oligochaetes at that station. AR3 had the lowest average number of organisms per ponar sample. All three sites were dominated by Annelida, driven by high abundances of Oligochaeta (Figure 130A). Site AR4 had a higher diversity of taxa (15 taxa) than either of the other sites (both of which had 6 taxa). Due to the high abundance of Annelida across all sites, additional analyses were conducted with non-Annelida taxa. All gastropods, both native and non-native, were found only at AR4. Bivalves were the most abundant at AR4, but the invasive Asian clam, *Corbicula fluminea*, was found at all sites and several native fingernail clam was present at AR3. When examining all non-Annelida taxa, Insects (driven by Chironomidae) were the dominant group in percent contribution at AR2 (89%) and AR3 (84%), while Crustaceans and Turbellarians dominated at AR4 (41% and 39%, respectively) (Figure xxC). Other taxa varied in their percent contribution by site. For example, Bivalvia were more dominant at AR3, while Gastropoda contributed little to the average abundances and were found at AR4 only.

Temporal trends: Members of Annelida, composed of oligochaetes and leeches, were the dominant taxa recorded during all months (Figure 130B). There was a seasonal increase in crustaceans driven by Gammarid amphipods, which peaked during July most likely due to recruitment. Bivalve average abundances, dominated by the invasive Asian clam *Corbicula fluminea*, were high during May and June then dropped and remained low, but relatively stable, over the rest of the sampling period. Average abundances of Turbellaria remained relatively high over the sampling period, after May, with the highest values during September. The average abundance of Insecta remained relatively stable over the sampling period; with lowest average abundances during May and highest abundances in August, mostly driven by the numbers of midge larvae (Chironomidae) found in the samples. Three gastropod species were found during the sampling period; the average abundances of these species were relatively low with the highest abundances recorded in September. Comparing percent contributions of all non-Annelida taxa across all of the sites, months were dominated by either the Insecta (May – 74%, August – 35%), Crustaceans (June – 28%, July – 61%) or the Turbellarians (June – 28%, August – 36%, September – 49%) (Figure 130D). Overall, larger increases in abundances and relative percent contributions over the sampling period for many of the taxa described above are in direct relation to seasonal changes and recruitment.

Table 16. Taxa Identified in Hunting Creek Tidal Benthic Samples.

Taxa identified with an asterisk were found on three or more station-dates and were included in the multivariate analysis (see below).

Taxon	Common Name	Average # / ponar		
		AR2	AR3	AR4
Platyhelminthes*	Flatworms	0	0	49
Nematoda	Roundworms	2	1	0
Annelida-Oligochaeta*	Oligochaete worms	180.2	77.7	76.2
Annelida-Hirudinea*	Leeches	0	1	4.3
Bivalva-Corbicula*	Asiatic clams	1	2.4	11
Bivalvia- Sphaeriidae*	Fingernail clams	0	2	3.75
Gastropoda-Viviparidae*	Mystery snails	0	0	2.8
Gastropoda-Pleuroceridae- <i>Elmina virginica</i> *	Pleurocerid snail	0	0	3.3
Gastropoda-Ancylidae- <i>Ferrissia rivularis</i> *	Limpet	0	0	2.7
Crustacea-Isopoda-Cyathura*	Isopods	0	0	5.3
Crustacea-Amphipoda-Gammarus*	Amphipods	4	0	48.2
Diptera-Chironomidae*	Midges	36.2	14.5	3.4
Ephemeroptera-Epheneridae	Common Burrower mayflies	0	0	1
Ephemeroptera-Heptageniidae	Flatheaded mayflies	0	0	1
Odonata-Gomphidae	Club-tailed dragonflies	0	0	6
Trichoptera-Leptoceridae	Long-horned caddisflies	1	0	0
Coleoptera-Elmidae	Riffle beetles	0	0	1
	TOTAL	224.4	98.6	218.95

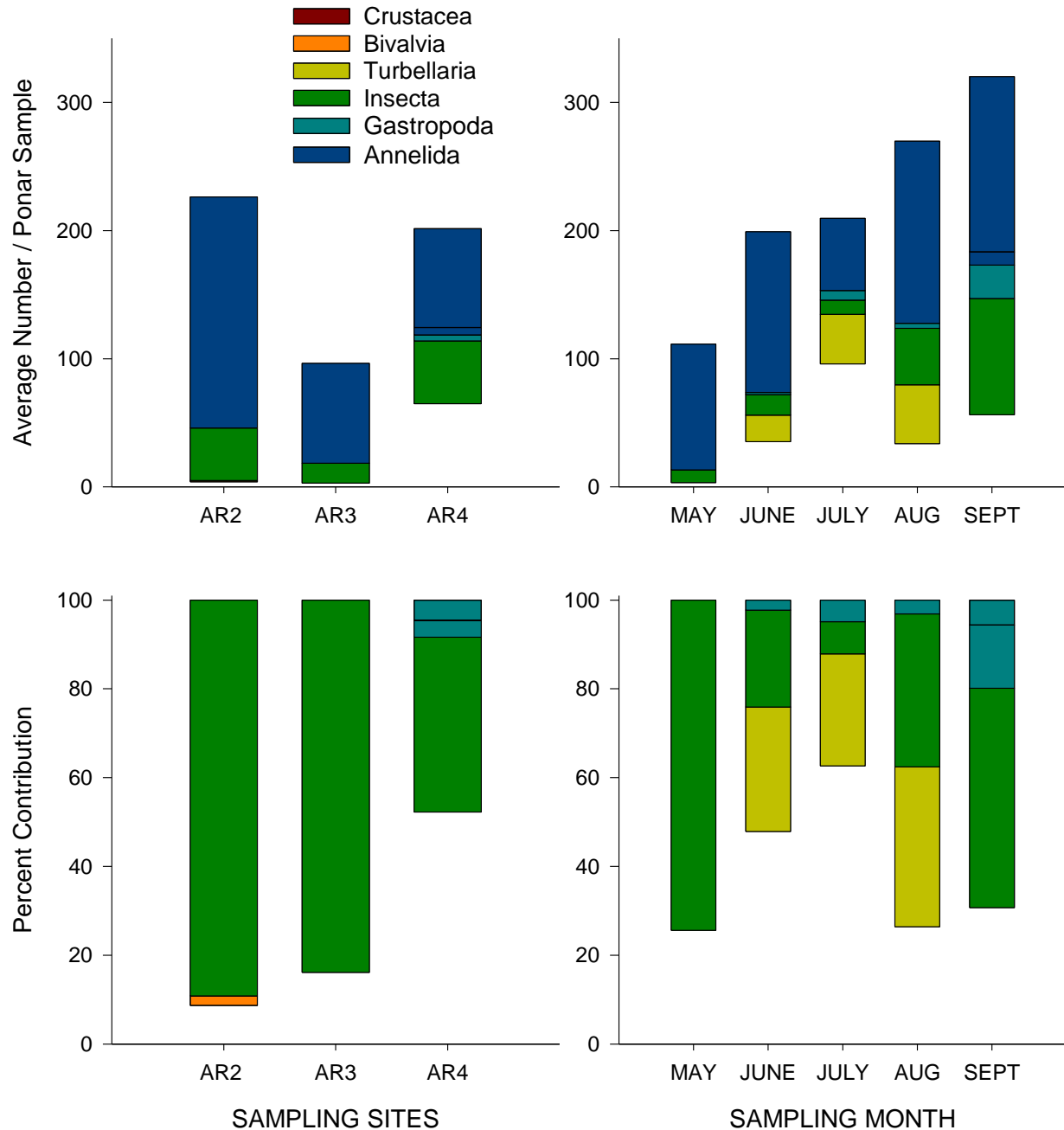


Figure 130. Average number per ponar sample of all benthic macroinvertebrate taxa (A, B) and percent contribution of all non-Annelida benthic macroinvertebrate (C, D) in petite ponar samples separated by site and month.

Multivariate analyses: Due to the multispecies aspect of benthic communities, it is often useful to use multivariate analyses or ordination to examine relationships among samples. This allows multiple taxa to be considered simultaneously when assessing these relationships. In order to get the most meaningful relationships, the full macroinvertebrate sample/taxa matrix was condensed. Taxa that were present in less than three of the original replicate sample matrix were excluded.

Then, the remaining, more consistently found taxa were used in the analysis (indicated by asterisks in Table 16, were averaged over the replicates for each date and station combination). This resulted in one set of taxa values for each station on each date. This reduced matrix (15 samples x 11 taxa) was then subjected to an ordination using a technique called Non-metric Multidimensional Scaling (nMDS). This allows relationships among samples based on their full complement of taxa to be visualized. If successful, relationships among samples can be shown on a two dimensional plot. The taxa differences responsible for the observed relationships can also be examined. The program PRIMER v.7 was used to conduct the ordinations.

The results of an nMDS ordination using the presence/absence transformed data (to decrease the importance of very abundant organisms, like *Oligochaetes*) is shown in Figure 131. In general, all of the samples separate by site (i.e., the AR4 samples cluster to the right and the AR2 and AR3 samples overlap to the left). This clustering pattern indicates that the AR4 sampling locations have distinct communities in the types and number of organisms present in every month other than May. Overall AR4 had higher taxa richness across all months (average = 9, range = 5-11) as compared to both AR2 and AR3 (AR2 average = 3, range 2-4; AR3 average = 4, range = 2-5). The higher richness at AR4 is probably due to better habitat conditions, especially large and more heterogeneous sediment particle size.

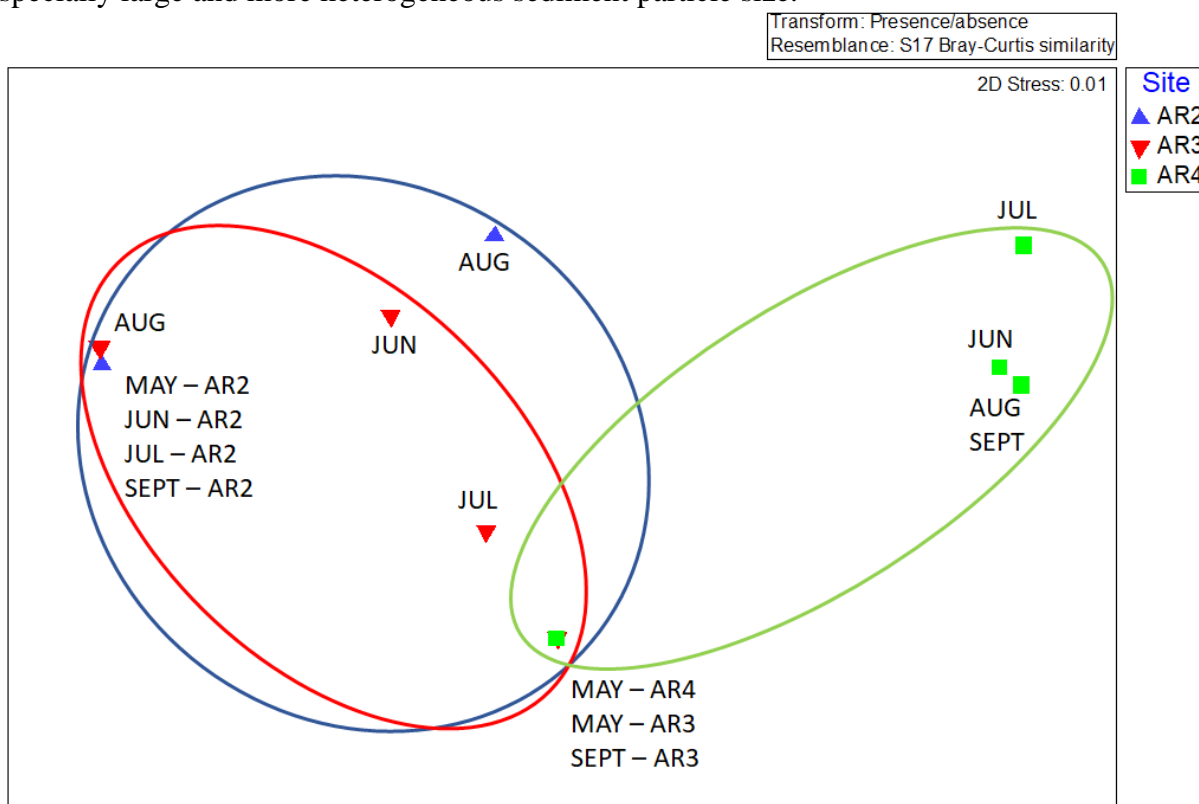


Figure 131. nMDS ordination of benthic samples from tidal stations. The sampling months (and stations, if symbols overlap) are placed above each symbol. Colors represent sites. Triplicates were averaged to get a single value for each month-station combination, and then transformed into presence/absence values. The distance measure was Hellinger.

Influence of Habitat on Community Composition: For this analysis, we assigned all materials greater than 5 mm in the petite ponar sample to one of three categories: leaves/woody debris, mollusc shells, or rocks/sand and calculated the percent contribution of each category to the overall habitat (Table 17). Submerged aquatic vegetation (SAV) was not recovered at AR2 in only one replicate in June, July, and September. AR2 was dominated by leaves and woody debris throughout the sampling period (average 83.9%), with little shells or rock/sand collected. In comparison, both AR3 and AR4 are a shelley sites (average 82.4% and 86.6%, respectively), with the shell matrix composed of mostly dead Asian clam shells. At AR2, the macroinvertebrate richness was correlated with the type of large particles available; as the percent organic matter increased and the percent shell decreased, taxa richness, but not abundance, increased ($r = 0.28$) (Table 17). Macroinvertebrate abundance was not correlated with percent organic matter ($r = 0.03$). At AR3, there was no relationship between large particle type and total abundance ($r = 0.04$) or richness ($r = 0.08$), but this station had variable amounts of large particles present (range of 37 – 98% shell and 3 – 62% leaves or woody debris). AR4 showed a positive relationship between macroinvertebrate richness and percent shell ($r = 0.67$) and abundance and percent shell ($r = 0.57$).

Summary: Similar to previous years, the macroinvertebrate community was dominated by Annelids (including Oligochaetes and Leeches) across sites, with Oligochaetes contributing most to this group. Outside of the Annelids, Crustaceans (dominated by gammarid amphipods) and Turbellarians (flatworms) were the most abundant groups at AR4, while both AR2 and AR3 were dominated by insect larvae from the Chironomidae family (midges). Each site had their own unique taxa. Insect larvae from the Leptoceridae family were only found at AR2. AR4 had the highest number of unique taxa, with nine (Turbellarians, the isopod *Cyathura polita*, three species of gastropods, including the invasive Japanese mystery snails-*Cipangopaludina japonica* and insect larvae from the families Heptageniidae, Gomphidae, Elimidae, Epheneridae). Comparing percent contributions of all non-Annelida taxa across all of the sites, months were dominated by the Crustaceans (June and July), Turbellarians (June, August, and September) or Insecta (May and August) (Figure 130). Ordination analyses of the communities indicated a separation between communities sampled from each site across the months. This could be due to the type of habitat found at each site; while the habitat at AR2 is mostly leaves and organic debris, the habitat at both AR3 and AR4 is composed of the shells of dead Asian clams. This was also reflected in the substrate analyses, with positive relationships between percent shell composition and macroinvertebrate richness and abundance at AR4. There was also a change of the community composition throughout the months, as it common for aquatic communities experiencing changes in abiotic conditions and recruitment during the summer.

Table 17. Large substrate composition vs. total abundance of benthic macroinvertebrates in individual replicate samples.

Site	Month	Replicate	% Leaves/Wood	% Shell	% Rock/Sand	Total Abundance	Total Richness
AR2	May	A	89.3	10.7	0.0	285	3
		B	66.6	32.3	0.0	141	2
		C	98.9	0.0	0.0	76	2
	June	A	95.1	2.3	1.6	324	4
		B	93.2	3.2	3.4	281	4
		C	98.5	0.1	0.0	228	4
	July	A	82.2	14.5	3.2	108	2
		B	98.8	0.8	0.3	74	2
		C	68.9	3.2	27.3	139	2
	Aug	A	93.9	1.1	4.7	339	5
		B	0.0	96.9	0.0	284	2
		C	98.7	0.2	0.0	303	2
	Sept	A	96.6	3.4	0.0	318	2
		B	94.0	0.8	5.1	218	2
		C	83.8	3.0	6.0	224	2
AR3	May	A	14.3	85.7	0.0	25	2
		B	4.7	95.3	0.0	140	5
		C	3.7	96.2	0.0	158	3
	June	A	2.4	97.5	0.0	16	1
		B	4.5	95.5	0.0	171	3
		C	5.0	95.0	0.0	54	2
	July	A	49.0	51.0	0.0	65	4
		B	3.1	96.7	0.0	39	2
		C	9.3	90.0	0.4	65	3
	Aug	A	10.1	89.9	0.0	206	2
		B	62.3	37.1	0.0	159	2
		C	15.1	82.3	0.0	108	2
	Sept	A	20.9	79.1	0.0	78	2
		B	46.9	53.1	0.0	51	2
		C	7.7	92.3	0.0	69	5
AR4	May	A	78.4	0.2	12.7	35	4
		B	39.0	60.5	0.5	14	3
		C	56.5	41.3	2.2	109	4
	June	A	0.2	99.8	0.0	146	8
		B	0.6	99.3	0.0	173	12
		C	0.5	99.5	0.0	197	9
	July	A	0.2	99.8	0.1	169	6
		B	0.2	99.8	0.1	192	8
		C	0.1	99.9	0.0	175	5
	Aug	A	0.4	99.6	0.0	230	8
		B	0.3	99.7	0.0	189	9
		C	0.1	99.9	0.0	87	10
	Sept	A	0.3	99.7	0.0	248	10
		B	0.2	99.8	0.0	279	7
		C	0.0	100.0	0.0	462	8

Tributary Samples

Duplicate kick net samples were taken in eight tributaries of Hunting Creek on November 4, 2022. The exact locations of the sampling sites are given in Table 18 and Figure 1a. Individuals from each sample were identified to lowest taxonomic unit, usually genus, except for Oligochaetes (aquatic worms) and Chironomidae (midges).

Table 18. Location of Tributary Benthos Sampling Stations

Station ID	Stream	Location on Stream
CR	Cameron Run	Just below Metrorail bridge
BR	Backlick Run	At trail bridge just upstream of the confluence with Holmes Run
TR	Turkeycock Run	In Bren Mar Park just above Edsall Road
IR	Indian Run	Just below Bren Mar Drive crossing
HR1	Holmes Run	First riffle upstream of confluence with Backlick Run
HR2	Holmes Run	Holmes Run Park just below pedestrian bridge at Pickett Street
TA	Taylor Run	In Angel Park, underneath the trail bridge
TB	Timber Branch	Just east of Ivy Hill Cemetry at W Timber Branch Parkway
PB	Pike Branch	In Jefferson Manor Park just east of Telegraph Rd

Water quality variables were measured on the date of benthic sampling (Table 19) and were generally supportive of aquatic life. It is important to note that all streams were at base flow conditions during the sampling period; water quality is expected to be more degraded during high flow.

Table 19. Water Quality Results from Tributary Benthos Sampling

Station	Temp (°C)	SpCond (uS/cm)	DO (mg/L)	DO (%)	pH	Turbidity YSI units
Cameron Run	13.9	379.9	10.88	100	7.28	0.26
Backlick Run	17.3	501	12.07	100	7.54	0.02
Turkeycock Run	14.9	327.8	10.14	100	7.37	0.40
Indian Run	15.1	401.1	9.93	98.8	7.27	2.05
Holmes Run 1	16	302.6	10.64	100	7.51	0.33
Holmes Run 2	15.7	267.6	10.58	100	7.5	0.33
Taylor Run	14.9	414.6	9.19	91.3	7.15	2.10
Timber Branch	14.0	447	9.30	90.4	6.98	0.61
Pike Branch	13.4	280.3	10.69	100	7.56	0.70

Taxonomic Groups: Across all sites, 25 different taxa were found. The five most abundant taxa observed included two groups of Tricoptera insect larvae (caddisflies of the families Hydropsychidae and Philopotamidae), a group of Dipteran insect larvae (midges of the Chironomidae family), Oligochaeta, and Turbellarians (Platyhelminthes) (Table 20, Figure 132). All of these five most abundant taxa were found at all sites. All other taxa were significantly less abundant and included Nematodes, Hirundea (leeches), Hydrachnidia (water mites), Bivalves (the invasive Asian clam, *Corbicula fluminea*, and a native fingernail clam from the Sphaeriidae family), Gastropods (native snails *Physa acuta* and limpets (*Ferrissia rivularis*), Ephemeroptera (mayflies of the family Baetidae and Caenidae), Crustaceans (Gammarid amphipods), Diptera (families Tipulidae, Simuliidae, and Empididae), Coleoptera (families Elmidae and Psephenidae

– water penny beetles), Collembola (springtails), Trichoptera (family Hydroptilidae), and Lepidopterans (family Crambidae). Of the less abundant taxa, none were present at all sites.

Spatial trends: Timber Branch had the highest average abundance of the four dominant taxa, but this was entirely due to the high abundance of Oligochaetae worms found at that location (Figure 132). Interestingly, dominant taxa differed by site. Hydropsychidae was the dominant group for Backlick Run, Holmes Run 1, Pike Branch, and Turkeycock Run, while Chironomidae was the dominant group for Cameron Run (Figure 132). Oligochaetae worms were dominant only at Holmes Run 2, Indian Run, Taylor Run, and Timber Branch. There were five taxa that were only found at a single location. For example, Hydrachnidia water mites and both Bivalve taxa were only found at Cameron Run, Odonata Calopterygidae only at Turkeycock Run, and the Crambidae moth larvae were only found at Indian Run (Table 132).

Table 20. Taxa Identified in Hunting Creek Stream Benthic Samples.

Taxon	Common Name	Average # / kicknet								
		Backlick Run	Cameron Run	Homes Run 1	Holmes Run 2	Indian Run	Pike Branch	Taylor Run	Timber Branch	Turkeycock Run
Platyhelminthes*	Flatworms	1.5	30.5	25	15.5	28	10	5.5	4	6.5
Nematoda	Round worms	1.5	0	0	0.5	0	0	0	1.5	0.5
Annelida-Oligochaeta*	Oligochaete worms	28.5	4	15	45.5	40.5	8	61	119	21.5
Annelida-Hirundea	Leeches	0	9.5	0	0	0	0	18.5	0	0
Arthropoda-Hydrachnidia	Water mites	0	3	0	0	0	0	0	0	0
Bivalva-Corbicula*	Asiatic clams	0	3.5	0	0	0	0	0	0	0
Bivalvia- Sphaeriidae	Fingernail clams	0	0.5	0	0	0	0	0	0	0
Gastropoda-Ancylidae-Ferrissia rivularis	Limpets	0	1.5	0	0	0	0	1.5	0	0
Gastropoda-Physidae-Physa acuta	Physid snail	0	0	0	0	0	0	4.5	0	1
Crustacea-Amphipoda-Gammarus*	Amphipods	0	13	27	17.5	0.5	0	0	0	0
Collembola	Springtails	0	0	0	0	0	0	0.5	0.5	0
Ephemeroptera-Baetidae	Small minnow mayflies	0.5	6	1	1	0.5	1	0.5	0	2.5
Ephemeroptera-Caenidae	Small squaregill mayflies	0	0.5	1	0	0	0	0	0	1.5
Diptera-Tipulidae*	Crane flies	0	1	0	0	0	1	6	0.5	3.5
Diptera-Chironomidae*	Midges	54	58.5	26.5	29.5	26	32	51	26	25.5
Diptera-Empididae*	Dagger flies	1.5	0	0	0	0	0	0	0.5	0
Diptera-Simuliidae	Black flies	2	0	0.5	11	8.5	5	3.5	0.5	4.5
Coleoptera-Psephenidae	Water-penny beetles	0	0	0.5	0	0	0	0	0	0
Coleoptera-Elmidae	Riffle beetles	0	3	0	0	0	0.5	0	0	2.5
Odonata-Calopterygidae	Broad-winged damselflies	0	0	0	0	0	0	0	0	0.5
Odonata-Coenagrionidae	Narrow-winged damselflies	0	0.5	0.5	0	1.5	0.5	0	0	0
Trichoptera-Hydroptilidae	Microcaddisflies	7.5	14.5	9.5	32	0.5	0.5	0	0.5	0
Trichoptera-Hydropsychidae*	Hydropsychid caddisflies	86	56.5	72	30.5	9.5	68.5	24	42.5	83
Trichoptera-Philopotamidae*	Finger-net caddisflies	7	4	18.5	18.5	11	17.5	9	1.5	44
Lepidoptera-Crambidae	Grass moths	0	0	0	0	0.5	0	0	0	0
	TOTAL	190	210	197	201.5	127	144.5	185.5	197	197
	TAXA RICHNESS	10	17	12	10	11	11	12	11	13

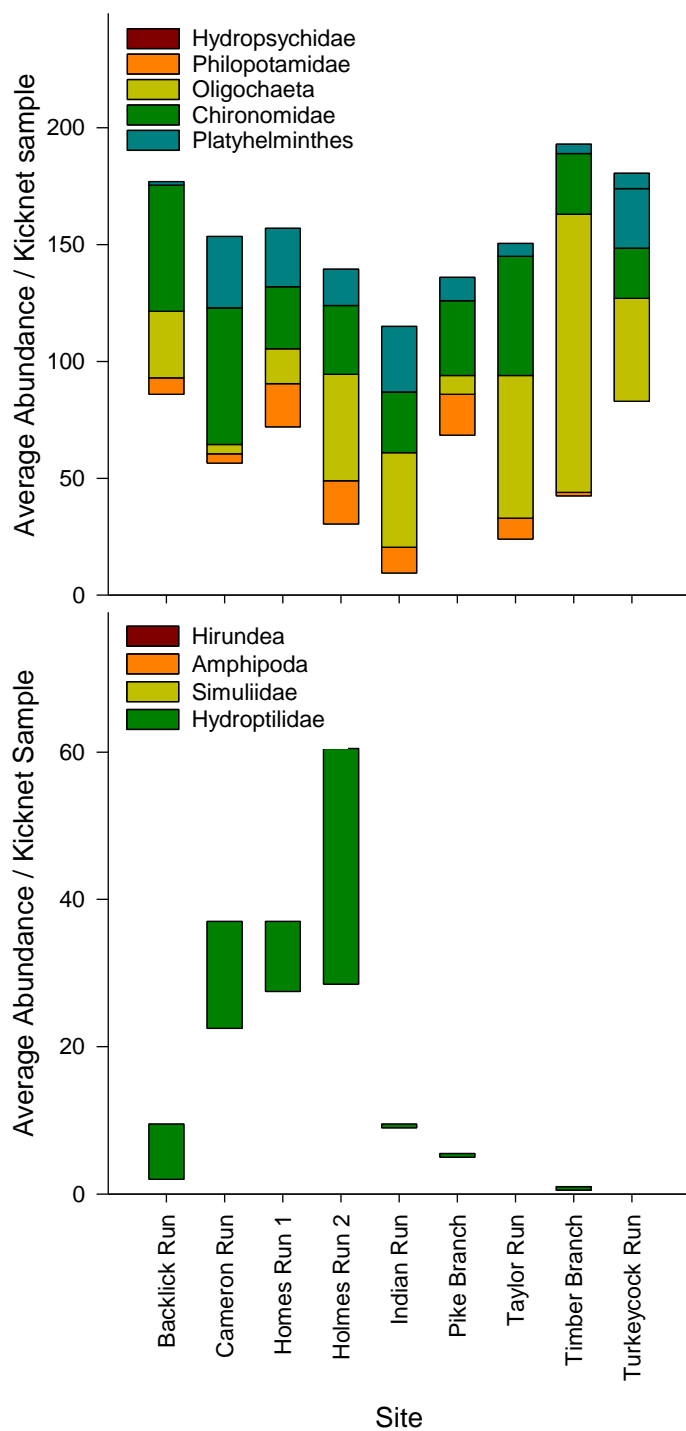


Figure 132. TOP: Average abundance per kicknet sample of the four dominant benthic invertebrate taxa in tributary kick samples. BOTTOM: Average abundance per kicknet sample of four less dominant benthic invertebrate taxa in tributary kick samples. Note the different scales of the y-axes between the two graphs.

Benthic Invertebrate Community Metrics: In general, increasing taxa richness reflects increasing water quality, habitat diversity, or habitat suitability. Taxa richness across all nine sites ranged from 10 to 17 taxa, with lowest richness at Backlick Run and Holmes Run 2 and highest richness at Cameron Run. “Good” sites were classified as having more than 14 taxa, while “moderate” sites had between 7 and 13; “poor” sites had less than 6 taxa present (Table 21).

A subset of abundance, EPT richness is the number of species from the generally more environmentally sensitive Insecta groups Ephemeroptera, Plecoptera, and Trichoptera. In general, if the EPT richness is ≤ 2 , then conditions are poor. If between 3 and 5, then conditions are moderate. If ≥ 5 , then conditions are good. EPT richness at all sites had at least three species. Backlick Run, Holmes Run 2, Indian Run, and Turkeycock Run had four species, while Cameron Run and Holmes Run 1 had five species.

Calculating the percentage of total organisms that are from the Ephemeroptera, Plecoptera, and Trichoptera groups, without including the family Hydropsychidae, provides another metric for stream condition. In this case, if the value is $>9.3\%$, then conditions are good. If the value is between 4.7 and 9.3%, then conditions are moderate. If the value is $<4.7\%$, then conditions are poor. Only Timber Branch had a value (1%) below the threshold of 4.7%. Two sites, Backlick Run and Taylor Run, had moderate conditions. The rest of the sites had a relatively high percent of EPT taxa, without the family Hydropsychidae included (9.4 – 25.6%).

Examining the Trichopteran families (without Hydropsychidae) closer can provide more detail about the site conditions, as this insect group has a range of tolerance values for abiotic conditions. Here, good conditions are when the percentage of total organisms $>50\%$, moderate are 25 – 50%, and poor are $<25\%$. No sites had percent Trichopteran values higher than 50%, and only one sites was “moderate” (Holmes Run 2). The rest of the sites were considered poor.

Looking at the Coleopteran (beetle) family can also tell us about the stream conditions. In this case, good conditions are values above 1.5, moderate values are 0.75-1.5, and poor conditions are values less than 0.75. Beetles were not found at the majority of sites; only Turkeycock Run and Cameron Run had “moderate” percentages of beetles (Elmidae larvae).

The Family Biotic Index (FBI) estimates the overall tolerance of the community in a sampled area toward organic (nutrient) enrichment, weighted by the relative abundance of each taxonomic group (family, genus, etc.). Organisms are assigned a tolerance number from 0 to 10 pertaining to that group's known sensitivity to organic pollutants; 0 is most sensitive, 10 is most tolerant. Low HBI values reflect a higher abundance of sensitive groups, thus a lower level of pollution. Family-level tolerance values from USEPA (Barbour et al. 1999) were used for organisms that could not be identified to the genus level because of size or condition. Taxa with tolerance values ≤ 3 were considered *intolerant*, whereas those with values ≥ 7 were considered *tolerant*. Low FBI (≤ 4.7) values reflect a higher abundance of sensitive groups, indicative of a lower level of pollution. None of the locations had values less than 4.7 (i.e., “good” FBIs). The majority of the locations (Holmes Run 1 and 2, Pike Branch, Timber Branch, and Turkeycock Run) fell into the “moderate” category (values 4.7 – 5.4), indicating some organic pollution is probable. Four of the locations were categorized as “poor” (values >5.4) (Backlick Run, Cameron Run, Indian Run, and Taylor Run), indicating that very substantial pollution was likely (Table 22).

In most cases, as the diversity of a community declines, a select few taxa will dominate the assemblage. Tolerant taxa can replace specialized species, and these communities are indicative

of poor stream quality. Percent dominance is calculated as the total number of individuals in the top four most abundant taxa divided by the total number of individuals. A percent dominance above 79% is considered “poor” quality, a value between 57 and 79 is “moderate”, and anything below 57% is “good.” This year, the top four taxa were the Trichopteran families Hydropsychidae and Philopotamidae, the Chironomidae and the Oligochaeta. All of sites were dominated by one of these top four taxa, but there were four sites that were categorized as “moderate”, including Cameron Run, Holmes Run 1 and 2, Indian Run, and Taylor Run.

The percent of organisms that are clingers, which are those that have fixed retreats or adaptations for attachment to surfaces in flowing water, is another indicator of environmental quality. While this metric would normally also include the percent of organisms are from the Plecoptera group (which are one of the first groups to disappear as human disturbance increases), none of the organisms sampled this year were from that group. Increasing metric values indicate increasing substrate stability. In this case, if the value is >14%, then conditions are good. If the value is between 7 and 14%, then conditions are moderate. If the value is <7%, then conditions are poor. All of the locations had values >14%, indicating good substrate stability.

Shredder taxa are those that tear apart organic material, usually leaves, and dominate low-velocity, high-retention pools. Sites were categorized as “poor” if the percent of shredders was <2, as “moderate” if the percent was between 2 and 4, and as “good” if the percent was higher than 4. As Chironomidae are considered shredder taxa, and that was a dominant group this year, all locations had high percentages of shredders indicating good conditions.

Predator taxa are at the top of the food web and depend on a reliable source of other invertebrate prey items. The percentage of taxa that are obligate predators can provide a measure of how trophically complex a site is. Less distributed sites support a greater abundance and diversity of prey items, thus supporting a greater number and diversity of predators. Sites were categorized as “poor” if the percent of predators was <3.2, as “moderate” if the percent was between 3.2 and 6.5, and as “good” if the percent was higher than 6.5. All sites were classified as “poor” except for Cameron Run and Taylor Run, both of which had relatively high numbers of Hirundea. This may be due to the fact that only five identified taxa were recognized as predators (Hirundea, Tipulidae, Empididae, Calopterygidae, and Coenagrionidae), and these organisms were not very common across sampled locations.

Using these 10 measures of biological health, we can calculate a summary statistic of relative overall health of these streams. In this case, we assign values of high (6), moderate (3), or low (0) health for each metric at each site, sum these values for each site and divide by 60 (i.e., the maximum score achievable). Streams characterized as “excellent” would achieve summary statistics of 80-100% of the maximum summary statistic. “Good” streams would be between 60 and 79%, “fair” streams would come in at between 40 and 59% of the summary statistic, while “poor” streams would be between 20 to 39%. Using the criteria for each metric laid out above, only one stream was categorized as “good” (i.e., Cameron Run), six were categorized as “fair”, and two were categorized as “poor” (i.e., Backlick Run and Timber Branch) (Table 22). Those that are “good” are slightly degraded sites with decreasing numbers of intolerant species. “Fair” sites have a marked decrease in intolerant species, and the community has shifted to be dominated by a few species. Lastly, “poor” sites lack intolerant species and have an overall low

number of taxa.

Table 21. Benthic invertebrate community metrics on the sum total of organisms found from both replicate kicknets. EPT include the Insecta from Ephemeroptera, Plecoptera, and Trichoptera. Color shading indicates relatively good (green), moderate (yellow), or poor (dark brown) conditions for each of the metrics and the summary statistic.

	Abundance	Taxa Richness	EPT Richness	% EPT w/o Hydropsychidae	% Trichoptera w/o Hydropsychidae	% Coleoptera	Family Biotic Index	% Dominance	% Clingers + % Plecoptera	% Shredders	% Predators
Backlick Run	190	10	4	7.9	7.6	0.0	5.9	92.4	54.2	32.4	0.8
Cameron Run	210	17	5	11.9	8.8	1.4	6.1	58.6	40.5	35.2	5.2
Holmes Run 1	197	12	5	15.2	14.2	0.3	4.9	67.0	51.5	18.3	0.3
Holmes Run 2	201. 5	10	4	25.6	25.1	0.0	5.2	61.5	46.2	30.5	0.0
Indian Run	127	11	4	9.4	9.1	0.0	5.9	68.5	23.6	21.3	1.2
Pike Branch	144. 5	11	4	13.1	12.5	0.3	5.4	87.2	65.1	23.2	1.0
Taylor Run	185. 5	12	3	5.1	4.9	0.0	6.5	78.2	23.2	30.7	13.2
Timber Branch	197	11	3	1.0	1.0	0.0	5.4	95.9	23.1	13.7	0.5
Turkeycock Run	197	13	4	24.4	22.3	1.3	4.8	88.3	71.1	14.7	2.0

Table 22. Index scores of the benthic invertebrate community metrics on the sum total of organisms found from both replicate kicknets. Color shading indicates relatively good (green), moderate (yellow), or poor (red) conditions for each of the metrics and the summary statistic.

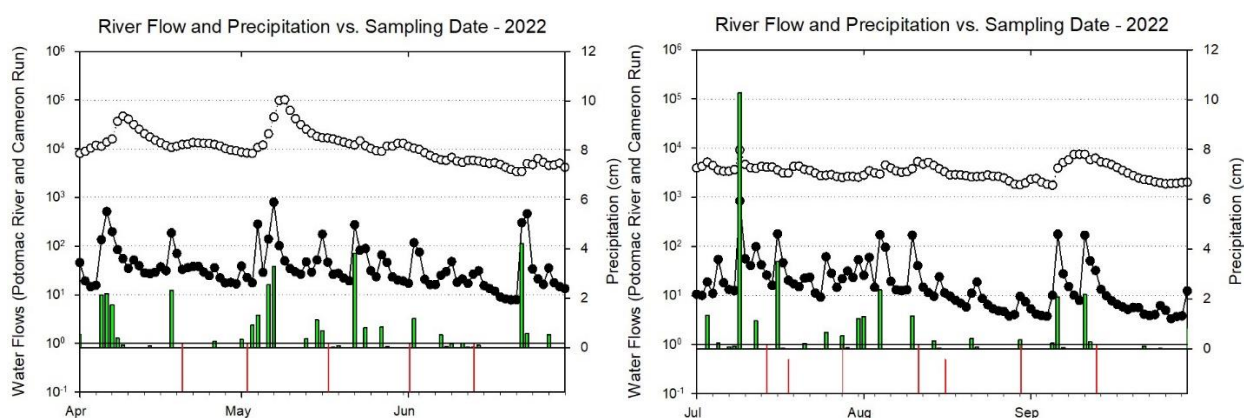
	Taxa Richness	EPT Richness	% EPT w/o Hydropsychidae	% Trichoptera w/o Hydropsychidae	% Coleoptera	Family Biotic Index	% Dominance	% Clingers + % Plecoptera	% Shredders	% Predators	Index Score
Backlick Run	3	3	3	0	0	0	0	6	6	0	35%
Cameron Run	6	6	6	0	3	0	3	6	6	3	65%
Holmes Run 1	3	6	6	0	0	3	3	6	6	0	55%
Holmes Run 2	3	3	6	3	0	3	3	6	6	0	55%
Indian Run	3	3	6	0	0	0	3	6	6	0	45%
Pike Branch	3	3	6	0	0	3	0	6	6	0	45%
Taylor Run	3	3	3	0	0	0	3	6	6	6	50%
Timber Branch	3	3	0	0	0	3	0	6	6	0	35%
Turkeycock Run	3	3	6	0	3	3	0	6	6	0	50%

Summary: Twenty-five taxa were identified across all sites in 2022. In general, the top four most abundant taxa observed across all sites stayed the same as in previous years. In 2022, Cameron Run had the highest abundance and diversity of all macroinvertebrates, mostly composed of the Insecta families Chironomidae and Hydropsychidae. Timber Branch had the highest number of the top five macroinvertebrate taxa found. Hydropsychidae larvae (caddisflies) were the dominant group at the majority of the sites (5/9 sites). Taxa richness across all sites ranged from 10 to 17 taxa, with lowest richness at Backlick Run and Holmes Run 2 and highest richness at Cameron Run. Using 10 measures of biological health, we calculated a summary statistic of relative overall health of these streams. Using the criteria for each metric laid out above, one streams was categorized as “good” (Cameron Run), six were categorized as “fair”, and two were categorized as “poor” (Backlick Run and Timber Branch).

DISCUSSION

A. 2022 Synopsis

In 2022 air temperature was above normal in all months except August (Table 3). There were 34 days with maximum temperature above 32.2°C (90°F) in 2022 which is well above the median number over the past decade. Precipitation and resulting tributary inflow was closer to normal in 2022 than in the extremely wet year 2018. However, it was again well above normal, especially in May and July. This was reflected by Cameron Run inflows which were also well above normal in May and July which could have direct impacts on water quality-plankton sampling dates during those months (Figure 133).



Figures 133. Precipitation (green bars), Cameron Run flows (solid circles), Potomac River flows (open circles), water quality/plankton sampling events (longer red lines at bottom), and datamapping dates (shorter red lines at the bottom).

Water temperature followed a typical seasonal pattern at all tidal stations with highest values approaching 30°C in late July and August. Specific conductance exhibited a gradual upward trend at most tidal stations except for AR1, AR24, and 25 which were quite variable, probably due to the variable impact of the AlexRenew effluent and Cameron Run discharge. Chloride patterns closely followed those in specific conductance. Dissolved oxygen (DO) followed a seasonal decline when expressed in mg/L at all tidal stations, but DO as percent saturation was less seasonal especially at AR2 and AR3. Apparently, at these two stations active photosynthesis kept DO higher in the summer, but it rarely exceeded saturation. However, water quality mapping on July 18 indicated an area of supersaturation in the middle of the Hunting Creek embayment. Field pH measured in the semimonthly cruises showed little evidence, but an area of high pH was observed on July 18 corresponding to the same area as the elevated DO, consistent with high photosynthesis. Total alkalinity was in the 60-100 range with a modest upward seasonal trend at most of the tidal river sites. But at AR1 values were generally variable and often below 60 mg/L.

Light penetration was generally somewhat higher in the river than in the embayment. At all tidal main stations there was a consistent decline in Secchi disk depth and light attenuation coefficient

over the year. A strong decline in light penetration was observed in early August following two moderately large runoff events in Cameron Run. Field turbidity readings also reflected these trends.

Ammonia nitrogen was quite variable seasonally at all stations. Generally, AR1 had the highest values being immediately below the AlexRenew outfall. However, on one occasion values at AR24 and AR25 spiked even higher. Nitrate showed a general pattern of decline from April into August which is probably attributable to less input and uptake by phytoplankton and other biota. Nitrite was low at all stations, but showed a clear upward seasonal trend. Organic N was showed a seasonal increase from April to July and then a steady decrease at most tidal stations. As with some other variables, AR1, AR24 and AR25 were generally higher and more variable. Total P exhibited a similar pattern. All ortho-P values were quite low, but showed little spatial or temporal patterns. N/P ratio showed a general decline consistently pointed to P limitation, with values generally in the 10-30 range being greater than 7.2 threshold in all samples. BOD was consistently below 4 mg/L at most stations. TSS values did not vary consistently at most tidal stations, but there were extreme fluctuations at AR1, AR4, AR24, AR25 some of which corresponded to high flows in mid-August.

The grouping of tidal stations into Tidal Main Stations and Tidal Impact Stations did not reveal any major differences in any variables other than perhaps more variability at the Tidal CSO Impact stations. However, the timing and volume of CSO discharges was not known.

In the tributaries, seasonal temperature patterns were similar to the tidal stations with the marked drop in late June, but somewhat reduced maximum values near 25°C. In contrast to the tidal stations, specific conductance exhibited a marked seasonal decline especially at the Cameron Run Axis stations probably due to the slow flushing of road salt residuals from surface groundwater. The patterns in chloride, a main component of road salt, backed up these trends in specific conductance. Dissolved oxygen was 60-100% saturation at the tributary stations except for AR34 which is at the lower end of the Hooffs Run Axis and influenced by the AR effluent and perhaps by near shore tidal Hunting Creek stations. AR34 showed values at low as 1 mg/L or 20% saturation. Field pH was fairly constant, slightly lower than field pH, and generally differed little among stations being 7.0-7.5. Lab pH values were even more consistent over time and stations, centered slightly below 7.5. YSI turbidity was very low at all tributary stations on all dates except for AR23, AR13, and AR34. These stations are at the lower end of their axes and near the influence of the AR effluent. Total alkalinity was quite consistent at most stations and throughout the year. Again, the exception was AR23 which often showed elevated values. Chloride declined seasonally from a high of about 120 mg/L in April to about 40 mg/L.

Total phosphorus values were frequently below 0.1 mg/L except at AR23 and AR34. Ortho-P values in the Cameron Run Axis stations were generally below 0.03 mg/L and were quite variable over time at all stations, but they were correlated in their variability. Organic N at most stations was below 0.5 mg/L and did not show much seasonal change. Exceptions again were AR23 and AR34 which had substantially higher and more variable values. Ammonia N was generally very low (<0.1 mg/L) with a few exceptions at AR23 and AR34. AR23 was often higher. Nitrate on the Hooffs Run Axis was definitely higher, especially at AR33 in the middle

of a residential area which was consistently higher over 2.5 mg/L. Nitrate was even high at AR35 which has a suburban/park-like drainage area. Many stations reached a maximum in mid-August when stream flows were high suggesting sources in the watershed. Nitrite N was consistently very low. Nitrite N was generally less than 0.03 mg/L but underwent two peaks late in the year: mid-August and September stations in the Cameron Run Axis. TSS and VSS were consistently low (<10 mg/L) at most Cameron Run Axis tributary stations. Values were consistently higher and more variable at AR23. TSS and VSS were variable at the Hoofs Run Axis stations especially at AR34. Unexplained very high values were found at two stations in September: AR35 and AR12.

Phytoplankton biomass as indicated by chlorophyll *a* exhibited two distinct maxima at Hunting Creek embayment stations (AR2 and AR3) in late July and late August. The late July peak occurred following a period of low rainfall and corresponded with high dissolved oxygen and high pH observed in both semimonthly cruises and datamapping indicating strong photosynthesis by phytoplankton. This peak in late July of 40 µg/L is similar to that attained in 2020 and 2022 which are among the highest values observed in the nine years of study. At the river station AR4 chlorophyll values rose seasonally to a peak of about 20 µg/L in early July. YSI sonde chlorophyll followed similar patterns as solvent-extracted chlorophyll. However, YSI sonde *in situ* chlorophyll *a* was found to underestimate extracted chlorophyll by about 3.5 times meaning a sonde value of 10 corresponded with an extracted value of about 30 µg/L. Phytoplankton cell density at AR2 peaked in late August at the same time as the second peak in chlorophyll *a* at AR2. At this time green algae led by the colonial alga *Volvox* dominated. At AR4 phytoplankton cell density peaked on the same date led by the colonial green alga *Volvox*. Phytoplankton biovolume was generally dominated by diatoms including *Melosira* and *Biddulphia* unidentified pennate diatoms at both AR2 and AR4. Other algae such as discoid centrics, *Cryptomonas*, and *Euglena* were also dominant on some occasions.

Peak rotifer abundance of 850/L in late August was much less than the 8000/L at AR2 and as was the maximum of about 800/L at AR4. As is typical, *Brachionus* was the dominant rotifer representing over half of the individuals in any given sample. The small cladoceran *Bosmina* had a high short-lived peak in early June at AR4 of about 150/L. *Diaphanosoma* was the dominant large cladoceran and was very abundant at both AR2 reaching maxima in mid-June and early August and early June, at about 1000/m³. *Leptodora* reached a modest peak of about 300/m³ in early June. *Daphnia* had a large peak in late May at AR4. Chydorids experienced two large peaks in the river. Among the copepods the immature copepod nauplii reached a strong peak of about 600/L in early June at AR2 and then showed a slow decline thereafter. *Eurytemora* as the most abundant larger copepod had a maximum of over 5000/m³ in April and a secondary peak in early June of 2500/m³ at AR4. Highest values of 1000/m³ were found in April and mid-June at AR2. *Mesocyclops* was also abundant at AR4 in early August.

B. Correlation Analysis of Hunting Creek Data: 2013-2022

To better understand the ecological relationships in Hunting Creek and the nearby Potomac River, relationships among parameters were assessed using correlation analysis. Since all samples were collected by PEREC personnel at the same time, it was possible to pool the data on all field and lab water quality parameters at the level of depth-averages and/or surface samples. Three tables were constructed: PEREC field and lab parameters correlated against each other, AlexRenew lab parameters correlated against each other, and all water quality parameters correlated against Cameron Run flow. This final set of correlations will determine the effect of freshwater flow pulses into Hunting Creek on the water quality variables.

Table 21 shows the correlations among PEREC-collected water quality parameters from the regular sampling with data from the embayment stations AR2 and AR3 combined. These reflect relationships over all ten years of the study. Indicators of photosynthesis (DOPPM, DOSAT, Field pH) were highly intercorrelated. Measures of particles in the water column and resultant water clarity (turbidity, TSS, Secchi disk depth, and extinction coefficient) were also highly intercorrelated. Indicators of phytoplankton abundance (CHLDI, CHLSF, and VSSSF) were fairly highly intercorrelated. Similar patterns were found for the river station (Table 22).

Table 21. Correlations among PEREC collected water quality parameters from regular sampling. Depth-integrated samples unless otherwise indicated. AR2 and AR3 pooled. 2013-2022. April-September.

Data for the following results were selected according to
SELECT (STATION = 2) OR (STATION = 3)

Pearson Correlation Matrix

	TEMPC	SPC	DOPPM	DOSAT	FLDPH	SECCHI	EXTCOEF	YSITURB	YSICHL	CHLDI	CHLSF	DRYWTSF	AFDWSF
TEMPC	1.000												
SPC	0.397	1.000											
DOPPM	-0.353	-0.147	1.000										
DOSAT	0.045	0.004	0.913	1.000									
FLDPH	0.200	0.081	0.613	0.730	1.000								
SECCHI	-0.044	0.316	0.068	0.048	0.165	1.000							
EXTCOEF	-0.031	0.352	0.042	0.024	0.227	0.831	1.000						
YSITURB	-0.037	-0.352	-0.054	-0.065	-0.242	-0.618	-0.791	1.000					
YSICHL	0.329	0.245	0.010	0.160	0.237	-0.082	-0.083	0.067	1.000				
CHLDI	0.491	0.273	-0.045	0.140	0.096	-0.269	-0.311	0.124	0.450	1.000			
CHLSF	0.484	0.253	-0.069	0.116	0.077	-0.289	-0.333	0.138	0.467	0.988	1.000		
DRYWTSF	0.003	-0.287	-0.088	-0.096	-0.397	-0.746	-0.847	0.723	-0.050	0.381	0.399	1.000	
AFDWSF	0.197	-0.064	-0.062	0.015	-0.212	-0.548	-0.689	0.533	0.070	0.608	0.623	0.844	1.000

TEMP – water temperature (°C), SPC – specific conductance (µS), DOPPM – dissolved oxygen (mg/L), DOSAT – dissolved oxygen (% saturation), FLDPH – field pH, SD – secchi disk depth (m), EXTCO (light attenuation coefficient (m⁻¹), CHLDI – depth-integrated chlorophyll a (µg/L), CHLSF – surface chlorophyll a (µg/L), , DRYWTSF - TSS on surface samples (mg/L), AFDWSF – VSS on surface samples (mg/L) YSITUR – Turbidity as measured by YSI sonde *in situ*.

Table 22. Correlations among PEREC collected water quality parameters from regular sampling. Depth-integrated samples unless otherwise indicated. AR4, 2013-2022. April-September.

Data for the following results were selected according to
SELECT (STATION = 4)

Pearson Correlation Matrix

	TEMPC	SPC	DOPPM	DOSAT	FIELDPH	SECCHI	EXTCOEF	YSITURB	YSICHL	CHLDI	CHLSF	DRYWTSF	AFDWSF
TEMPC	1.000												
SPC	0.585	1.000											
DOPPM	-0.833	-0.594	1.000										
DOSAT	-0.463	-0.430	0.871	1.000									
FIELDPH	-0.254	-0.236	0.467	0.535	1.000								
SECCHI	-0.142	0.161	0.082	0.017	0.002	1.000							
EXTCOEF	0.064	0.164	-0.059	-0.007	0.030	0.722	1.000						
YSITURB	-0.028	0.028	-0.072	-0.142	-0.103	-0.245	-0.310	1.000					
YSICHL	0.370	0.298	-0.192	0.024	0.116	-0.017	0.151	-0.068	1.000				
CHLDI	0.574	0.491	-0.345	-0.078	0.047	-0.104	0.017	-0.074	0.671	1.000			
CHLSF	0.588	0.499	-0.370	-0.100	0.006	-0.109	0.022	-0.098	0.639	0.977	1.000		
DRYWTSF	-0.085	-0.034	0.124	0.122	0.131	-0.406	-0.519	0.412	0.055	0.046	0.010	1.000	
AFDWSF	0.120	0.149	0.029	0.129	0.079	-0.169	-0.152	0.089	0.251	0.450	0.407	0.635	1.000

For abbreviations code, see Table 23.

The correlation coefficients among AlexRenew lab parameters are shown in Tables 23 and 24. Among the most highly correlated variables in this dataset were TSS and VSS. Total P was positively correlated with organic N, TSS and VSS. Most phosphorus is bound to particles so these correlations make sense. TP was negatively correlated with N to P ratio and this makes sense since it is in the denominator of this ratio. Organic N was highly correlated with TSS, VSS, and BOD in the embayment, but not in the channel VSS and TSS were highly correlated with BOD.

Table 23. Correlations among AlexRenew Lab analyzed water quality parameters from regular sampling. Depth-integrated samples unless otherwise indicated. AR 2 and AR 3 combined. 2013-2022. April-September. For abbreviation codes, see Table 26.

Data for the following results were selected according to
SELECT (STATION = 2) OR (STATION = 3)

Pearson Correlation Matrix													
	PHLAB	ALK	TP	OP	ON	NO3	NH4	NO2	CLD	TSS	VSS	BOD	NTOP
PHLAB	1.000												
ALK	0.254	1.000											
TP	-0.229	-0.156	1.000										
OP	-0.138	-0.276	-0.051	1.000									
ON	-0.178	0.014	0.509	-0.237	1.000								
NO3	-0.081	-0.029	0.282	0.124	-0.223	1.000							
NH4	-0.383	-0.360	0.308	0.327	-0.016	0.435	1.000						
NO2	-0.146	0.039	0.187	-0.100	0.295	-0.005	0.084	1.000					
CLD	-0.074	0.139	-0.013	-0.149	0.269	-0.301	0.027	0.008	1.000				
TSS	-0.325	-0.044	0.703	-0.067	0.509	0.326	0.334	0.193	-0.024	1.000			
VSS	-0.206	0.037	0.605	-0.070	0.561	0.157	0.236	0.140	0.119	0.791	1.000		
BOD	-0.153	-0.082	0.268	-0.090	0.478	-0.131	0.039	0.050	0.207	0.343	0.413	1.000	
NTOP	0.029	0.178	-0.608	0.062	-0.389	0.214	-0.001	-0.147	0.033	-0.317	-0.309	-0.176	1.000

Table 24. Correlations among AlexRenew Lab analyzed water quality parameters from regular sampling. Depth-integrated samples unless otherwise indicated. AR4. 2013-2022. April-September.

Data for the following results were selected according to
SELECT (STATION = 4)

Pearson Correlation Matrix													
	PHLAB	ALK	TP	OP	ON	NO3	NH4	NO2	CLD	TSS	VSS	BOD	NTOP
PHLAB	1.000												
ALK	0.336	1.000											
TP	0.038	-0.066	1.000										
OP	-0.273	-0.508	0.039	1.000									
ON	0.113	-0.008	0.215	-0.121	1.000								
NO3	0.103	0.061	0.101	0.055	-0.318	1.000							
NH4	-0.297	-0.099	0.243	0.131	-0.040	-0.194	1.000						
NO2	-0.079	0.319	0.047	-0.174	0.178	-0.293	0.196	1.000					
CLD	-0.054	0.463	-0.045	-0.320	0.059	-0.428	0.087	0.395	1.000				
TSS	0.077	0.021	0.620	-0.012	0.256	0.105	0.049	-0.001	-0.141	1.000			
VSS	0.100	0.054	0.593	-0.010	0.267	0.015	0.051	0.051	-0.076	0.925	1.000		
BOD	0.095	0.199	-0.082	-0.143	0.206	-0.080	-0.120	0.008	0.131	-0.124	-0.026	1.000	
NTOP	0.087	0.140	-0.684	-0.132	0.038	0.280	-0.175	-0.164	-0.047	-0.319	-0.342	0.096	1.000

PHLAB – lab pH, ALK – total alkalinity (mg/L as CaCO₃), TP – total phosphorus (mg/L), OP – orthophosphorus (mg/L), NO₃N – nitrate nitrogen (mg/L), NH₄N – ammonia nitrogen (mg/L), NO₂N – nitrite nitrogen (mg/L), CLD – chloride (mg/L), TSS – total suspended solids (mg/L), VSS – volatile suspended solids (mg/L), NTOP – nitrogen to phosphorus ratio by mass.

Since the study began in 2013 it has been noted that certain water quality variables appear to be impacted by major rainfall and runoff events. In this year's report we have tested the correlations between recent runoff coming down Cameron Run and a wide array of water quality variables (Table 25). This analysis reveals that many variables are strongly correlated with recent stream flow. Specific conductance, chloride, pH, and alkalinity are all significantly reduced by increased streamflow, probably due to the dilution effects of the runoff on the water already in the river. Turbidity, Secchi depth, light attenuation, and TSS are all increased by runoff because solids are either brought in or resuspended by the higher runoff resulting in poorer light penetration. Ammonia nitrogen is increased at all except AR4; the reason for this is unclear.

Table 25. Pearson Correlation Coefficients between Water Quality Parameters and Log₁₀(5 day flow) where 5-day flow is the average stream flow on Cameron Run as measured at USGS Gaging Station 01653000 for the day of sampling and the 5 previous days. N=67-100.
 ¶ Parameters correlated against Log (3-day Flow)

Water Quality Parameter	AR 1 ¶ GW Pkwy Br	AR 2 N. Hunting Cr	AR 3 S. Hunting Cr.	AR 4 River Mainstem
Temperature (°C)	-0.333	-0.364**	-0.347**	-0.35
Sp. Conductance (µS/cm)	-0.525	-0.606**	-0.720**	-0.687
Dissolved Oxygen (mg/L)	-0.029	0.015	-0.076	0.295
Dissolved Oxygen (%sat)	-0.220	-0.130	-0.216	0.138
Field pH	-0.115	-0.311	-0.315	0.032
Secchi Disk Depth (m)	-----	-0.291	-0.303	-0.227
Light Atten. Coef. (m ⁻¹)	-----	-0.312	-0.414	-0.218
YSI Turbidity (NTU)	0.497**	0.347**	0.359	0.080
YSI Chlorophyll (µg/L)	0.205	-0.068	-0.087	-0.085
Chlorophyll a, DI (µg/L)	-----	-0.126	-0.147	-0.201
Chlorophyll a, Surf (µg/L)	-----	-0.093	-0.126	-0.219
TSS, Surf, GMU (mg/L)	0.183	0.389*	0.258	0.080
VSS, Surf, GMU (mg/L)	0.081	0.132	0.084	-0.017
pH Lab	-0.297	-0.330	-0.414	-0.328
Total Alk. (mg/L as CaCO ₃)	-0.621	-0.564	-0.543	-0.525
Total Phosphorus (mg/L)	0.182	0.282	0.237	0.057
Ortho Phosphorus (mg/L)	0.203	0.250	0.259	0.372
Organic Nitrogen (mg/L)	-0.011	-0.022	0.029	-0.130
Nitrate Nitrogen (mg/L)	0.067	0.288	0.234	0.218
Ammonia Nitrogen (mg/L)	0.375	0.394	0.468	0.163
Nitrite Nitrogen (mg/L)	-0.042	-0.015	0.010	-0.224
Chloride (mg/L)	-0.105	-0.170	-0.267	-0.355
TSS, DI, ARE (mg/L)	0.219	0.356	0.171	0.023
VSS, DI, ARE (mg/L)	0.193	0.226	0.083	-0.007
BOD (mg/L)	0.205	0.181	0.112	0.173
N to P ratio	-0.170	-0.079	-0.112	0.009

C. Water Quality: Comparison among Years

Since ten years of data are now available for the Hunting Creek area, comparisons were made for each parameter among years. In order to assess overall patterns in the data among years and stations, scatter plots were constructed with the values for each station plotted by year and trend lines were run through the data using LOWESS.

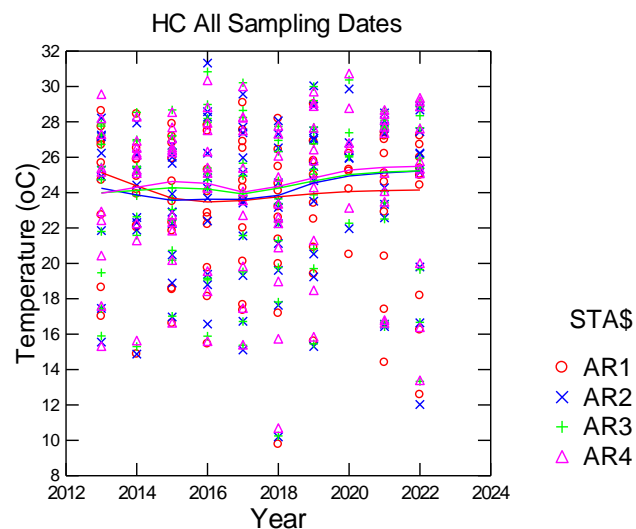


Figure 134. Scatterplots comparing values of Temperature among years. April through September. 2013-2022.

Temperature did not show much difference among the years with the trend lines staying within the 24-26°C range at all sites and years (Figure 134). Specific conductance showed clear differences among stations in most years with AR 1 consistently higher due to input from AlexRenew effluent (Figure 135). In 2022 values at all stations were similar to most years and higher than the wet year 2018.

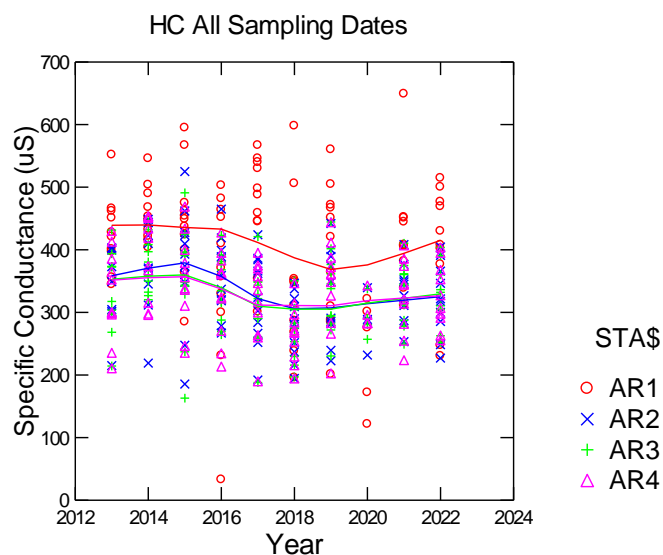


Figure 135. Scatterplots comparing values of Specific Conductance among years. April through September. 2013-2022.

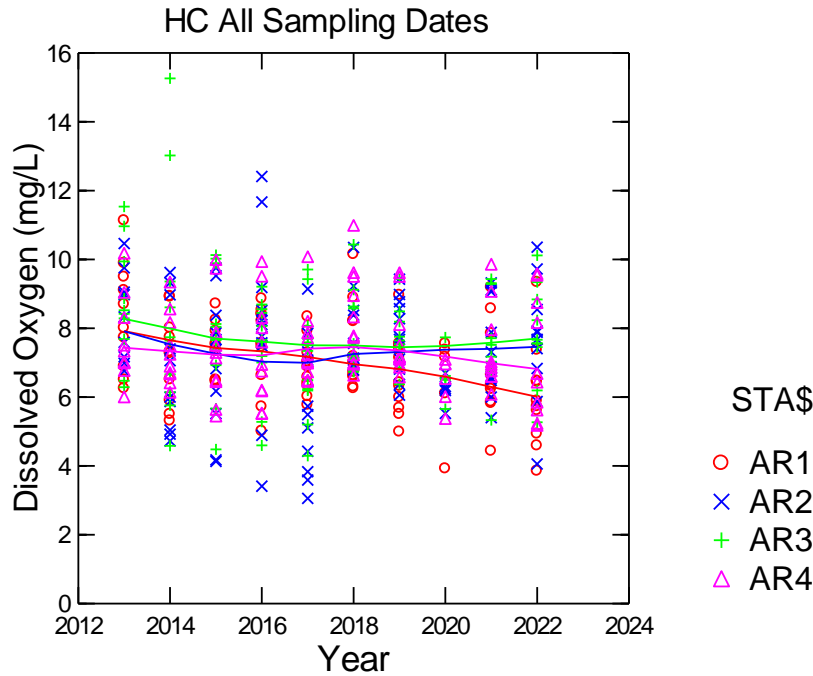


Figure 136. Scatterplots comparing values of dissolved oxygen as mg/L among years. April through September. 2013-2022.

Dissolved oxygen showed little difference among stations AR2, AR3, and AR4 in 2022, but the trend line for AR1 continued a drop begun in 2018 (Figure 136). A similar pattern was observed in dissolved oxygen (as percent saturation) (Figure 137).

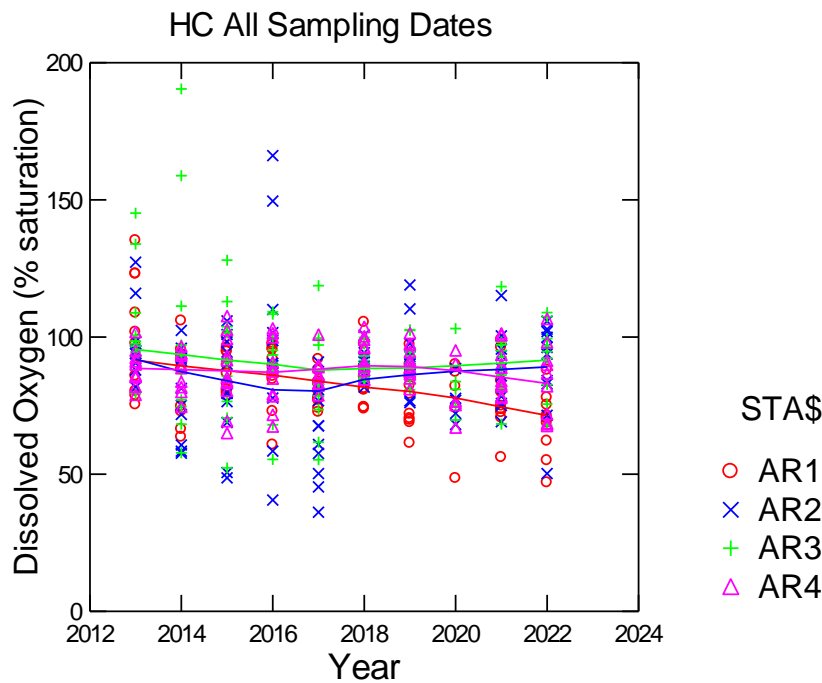


Figure 137. Box plots comparing values of dissolved oxygen as percent saturation among years. April through September. 2013-2022.

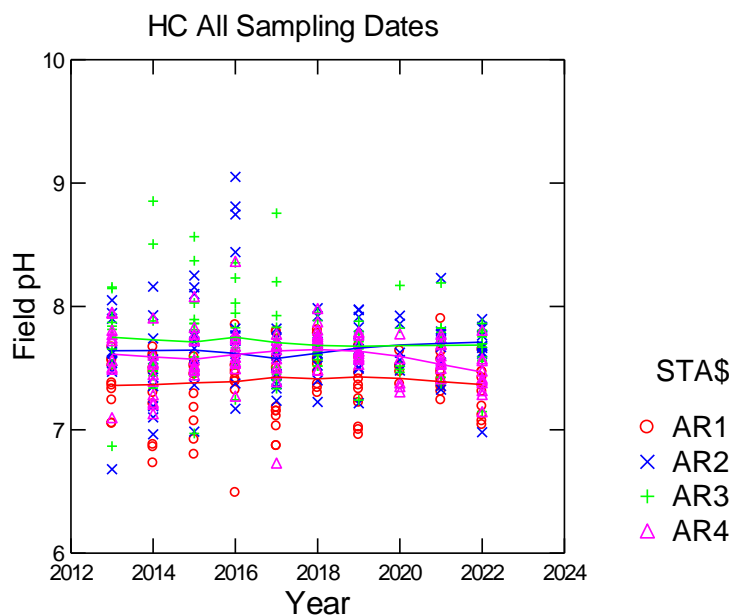


Figure 138. Scatterplots comparing values of field pH among years. April through September. 2013-2022.

Field pH values fell into a relatively narrow range in 2022 as in 2018-2020 (Figure 138). During the period 2013-2017 median values at AR2 and AR3 were often much higher than at the other two stations. This was attributed to photosynthesis by SAV which tends to increase pH since the high values were observed in July and August when SAV was most abundant. In the period 2018 to 2022 SAV was minimal in Hunting Creek and pH hardly ever exceeded 8. Lab pH showed a similar pattern in 2013-2017 period. In 2020 and 2021 Lab pH had some lower values. (These were the years that the PW Mooney lab ran the samples).

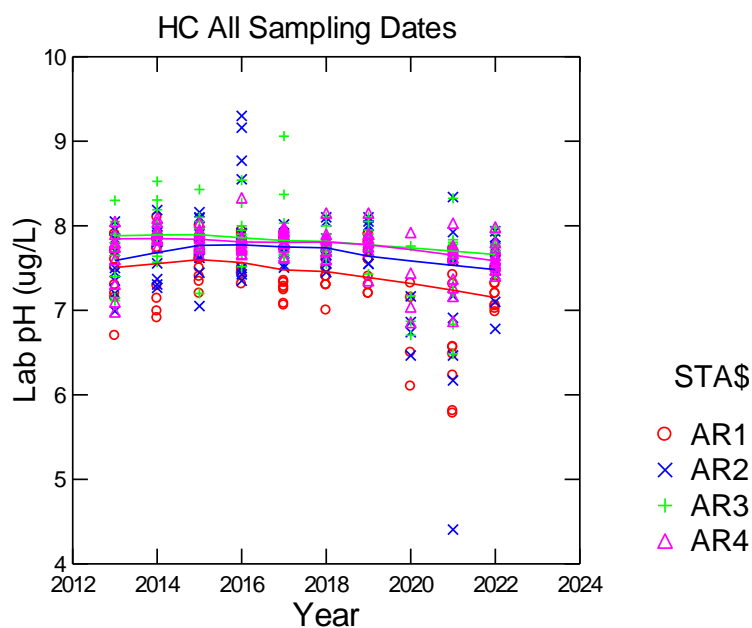


Figure 139. Scatterplots comparing values of lab pH among years. April through September. 2013-2022.

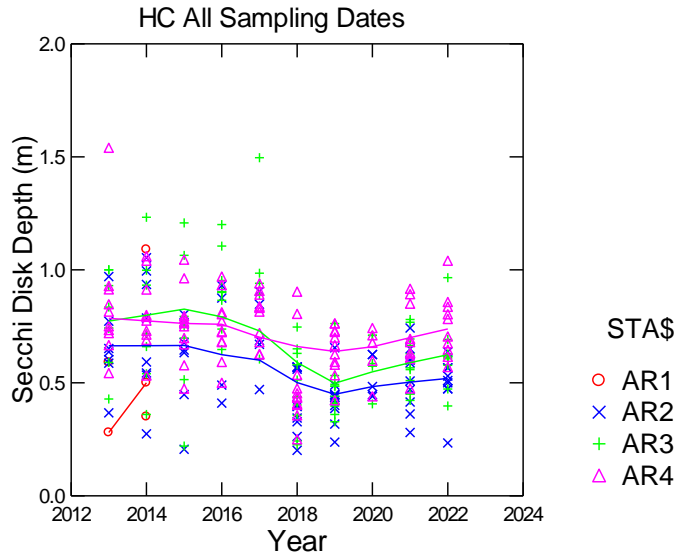


Figure 140. Scatterplots comparing values of Secchi disk depth among years. April through September. 2013-2022.

Secchi disk depth (Figure 140) has generally shown major and consistent differences between stations, attributable to major differences in SAV abundance between the stations. In particular AR3 was often much higher than the other stations. However, starting in 2018 coincident with the disappearance of SAV and continuing through 2022, Secchi depths were lower overall and were generally lower at AR2 and AR3 (in the embayment) than at AR4 in the river channel. Light attenuation coefficient is another way of measuring water clarity: less negative values of light attenuation coefficient indicate clearer water. Median values in light attenuation coefficient were similar from year to year until 2018 (Figure 141). As with Secchi disk depth, values for light attenuation in 2018 to 2022 showed much reduced water clarity than previous years at AR2 and AR3.

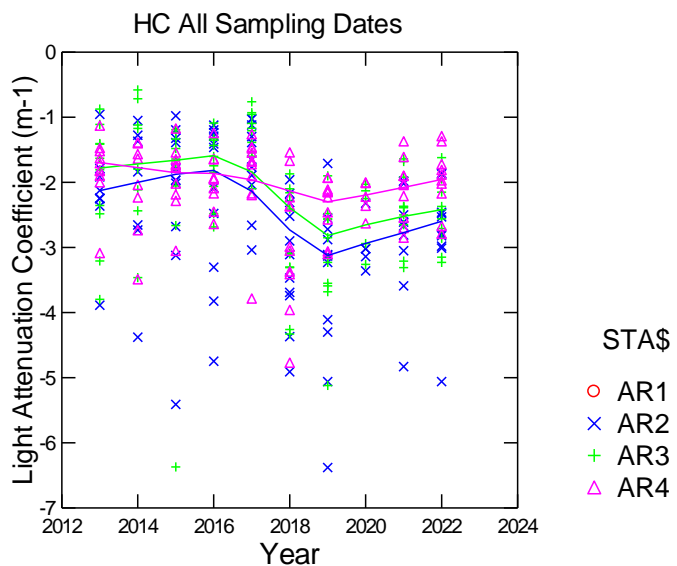


Figure 141. Scatterplots comparing values of Light Attenuation Coefficient among years. April through September. 2013-2022.

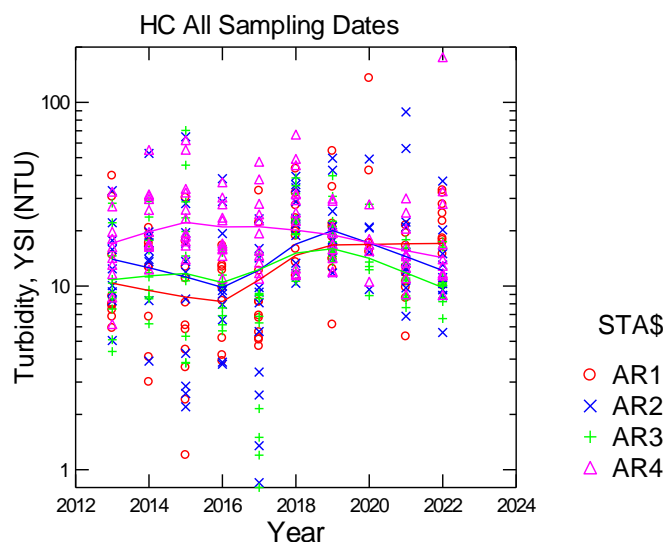


Figure 142. Scatterplots comparing values of Turbidity among years. April through September. 2013-2022.

Turbidity, another measure of water clarity, continued to exhibit higher values at AR2 and AR3 in 2022 as compared to 2013-2017 (Figure 142). Values at AR4 did not show a clear trend. After a strong decline in 2019, YSI Chlorophyll *a* resumed values similar to previous years (Figure 143).

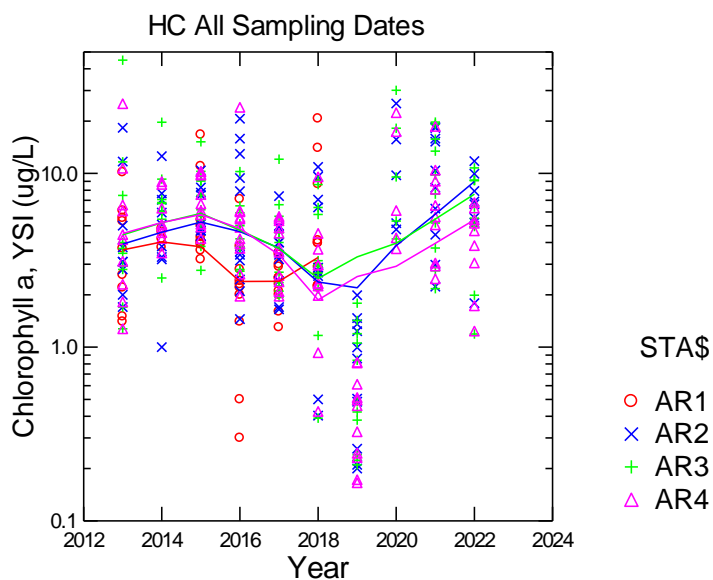


Figure 143. Scatterplots comparing values of YSI Chlorophyll a between years. April through September. 2013-2022.

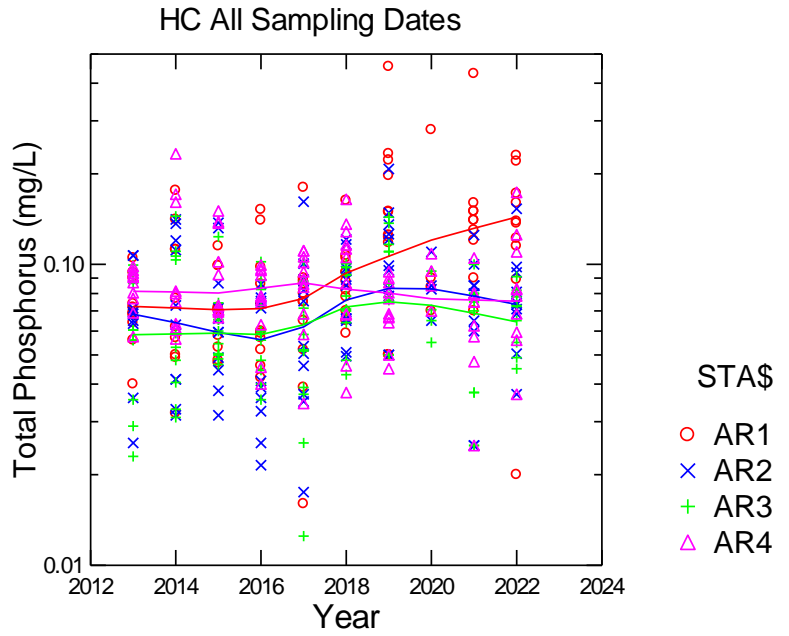


Figure 144. Scatterplots comparing values of Total Phosphorus among years. April through September. 2013-2022.

Total phosphorus has shown little trend at the river station AR4 over the study period, but the embayment stations AR2 and AR3 have shown a clear transition to higher values beginning in 2018. And AR1 has increased steadily since 2017. Ortho-Phosphorus has shown little consistent pattern at any station over the study. Note that in 2020 and 2021 samples were analyzed by the PW Mooney plant which had a higher detection limit than the AlexRenew Lab so many results were concentrated at the detection limit.

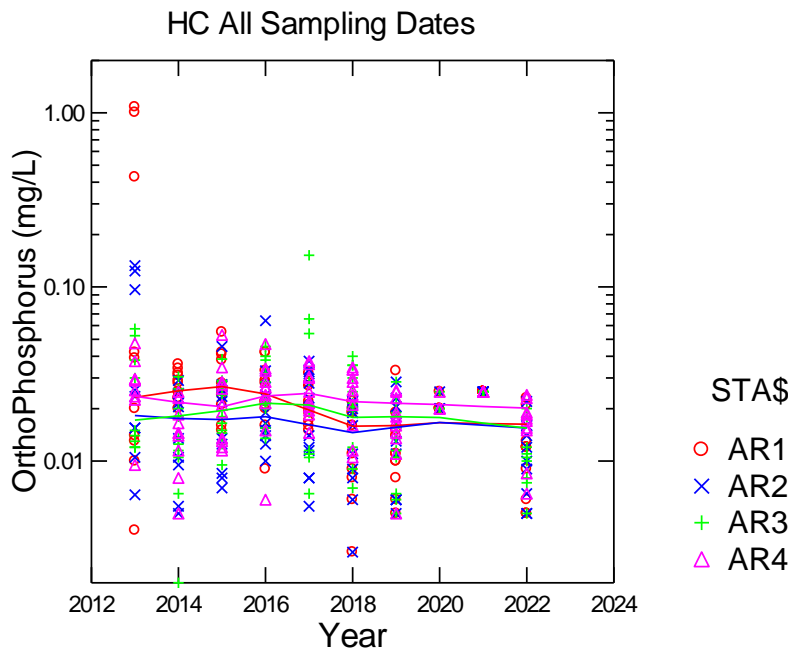


Figure 145. Scatterplots comparing values of Ortho-Phosphorus among years. April through September. 2013-2022.

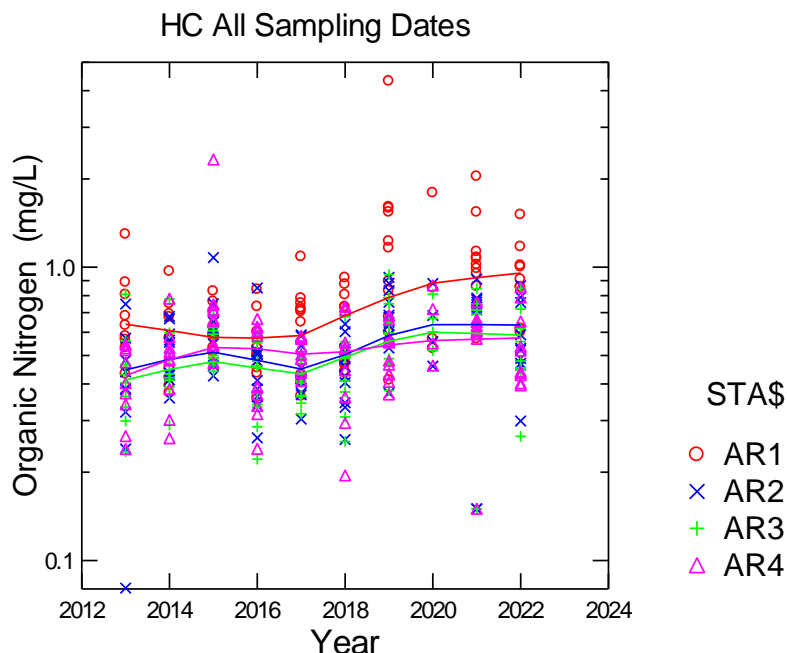


Figure 146. Scatterplots comparing values of Organic Nitrogen among years. April through September. 2013-2022.

Organic nitrogen values in 2022 overlapped extensively with the ranges from previous years (Figure 146). Since 2018 there was the suggestion of an increase at AR2 and AR3. A clear spatial pattern was observed with AR1 highest and greater than normal, while AR4 was little changed compared with previous years. Nitrate nitrogen values in 2022 continued a decline begun in 2019 at all stations (Figure 147).

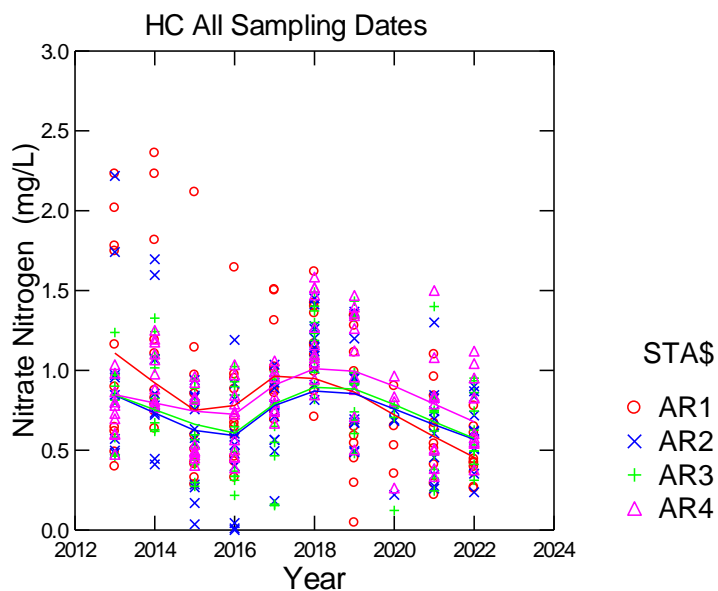


Figure 147. Scatterplots comparing values of Nitrate Nitrogen among years. April through September. 2013-2022.

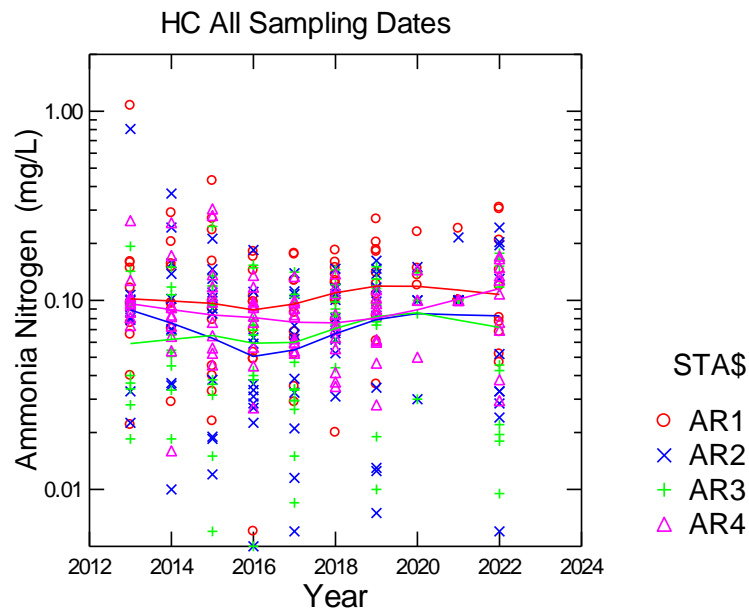


Figure 148. Scatterplots comparing values of Ammonia Nitrogen among years. April through September. 2013-2022.

Ammonia nitrogen values in 2022 appeared to stabilize at AR2 and AR4 after increasing since 2017 (Figure 148). AR1 and AR4 did not evince much of a trend over the period. Nitrite nitrogen values in 2022 were in the middle of the range for previous years and did not vary much among stations (Figure 149).

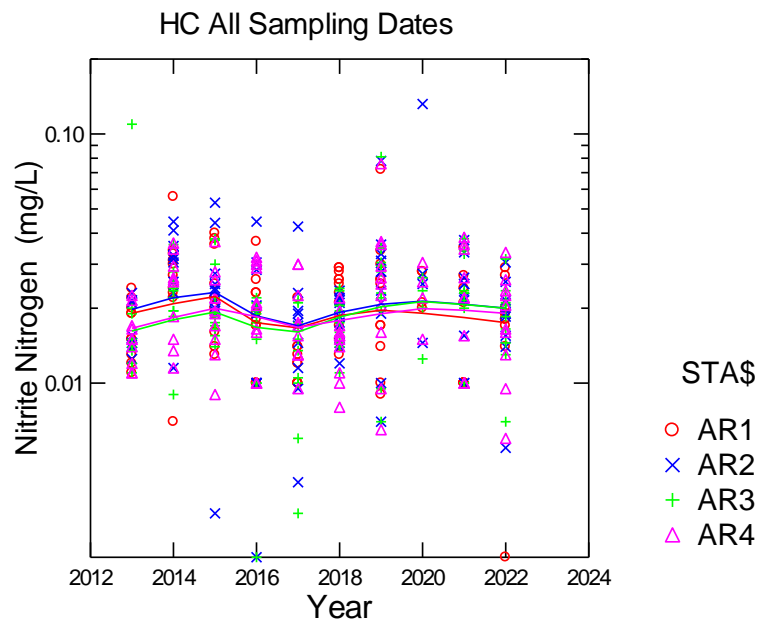


Figure 149. Scatterplots comparing values of Nitrite Nitrogen among years. April through September. 2013-2022.

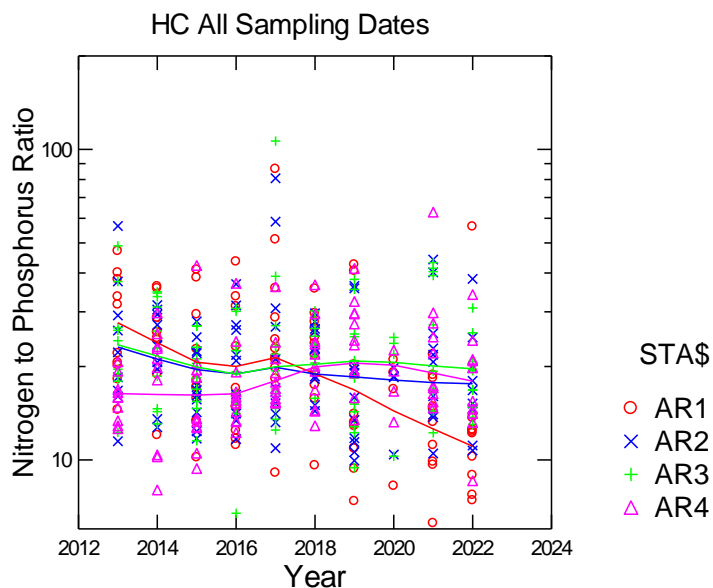


Figure 150. Scatterplots comparing values of N to P ratio among years. April through September. 2013-2022.

N to P ratio for 2022 was in the lower range of values from previous years, but still within the range indicating phosphorus limitation (Figure 150). Since 2019 N:P ratio values have shown a consistent decline at AR1, while AR2, AR3, and AR4 do not exhibit an obvious change over the years. BOD has shown a strong upward trend at AR1 since 2016 (Figure 151). AR2 and AR3 have maintained slightly higher values than AR4 over the last few years.

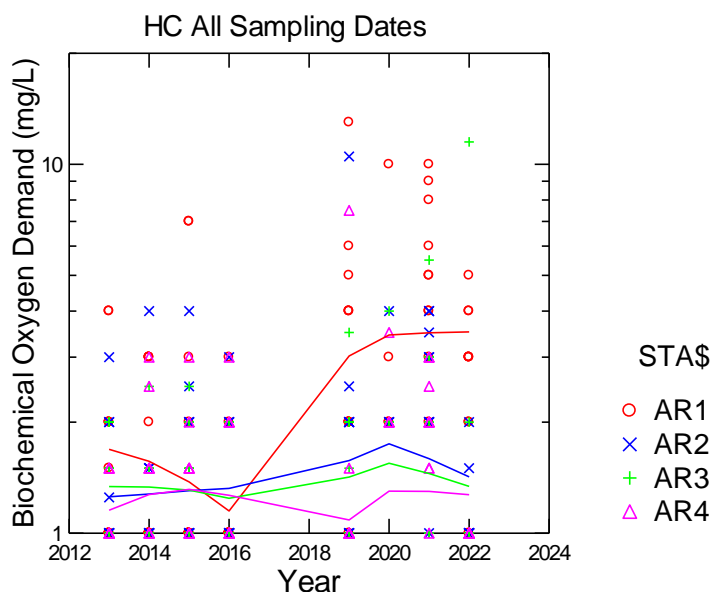


Figure 151. Scatterplots comparing values of BOD among years. April through September. 2013-2022.

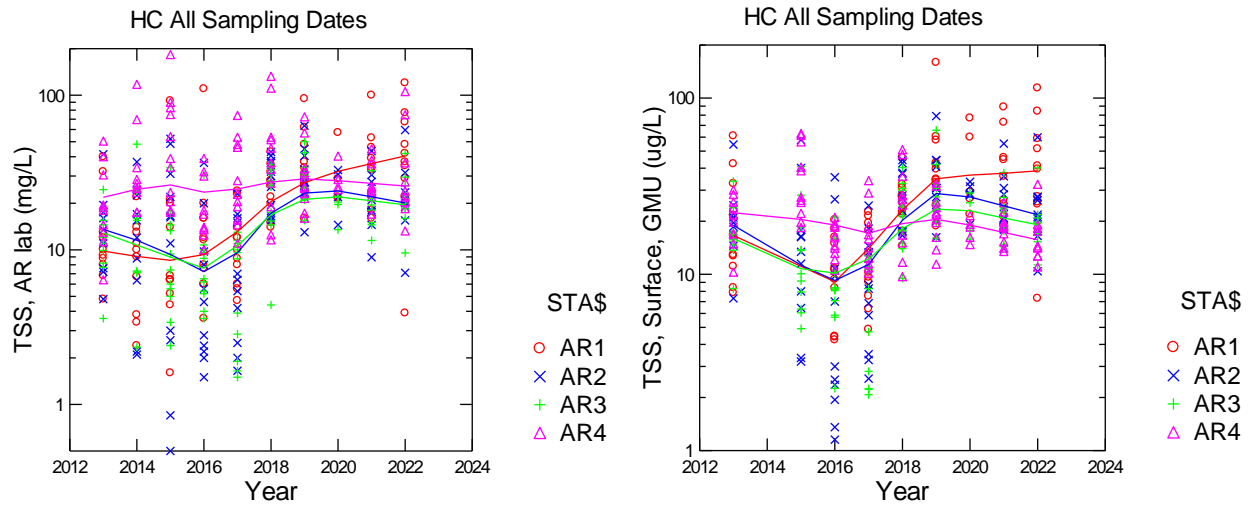


Figure 152. Scatterplots comparing values of Total Suspended Solids among years. Alex Renew data (a. left) and GMU data (b. right). June through September.

As in 2018 through 2022 total suspended solids (TSS) at AR1, AR2, and AR3 continued to have a higher trend line in 2022 than in previous years (Figure 152a,b). The patterns were similar in samples analyzed by both Alex Renew and GMU. Volatile suspended solids (VSS) in 2022 was similar to 2018-2021 and higher than in pre-2018 years (Figure 153a,b).

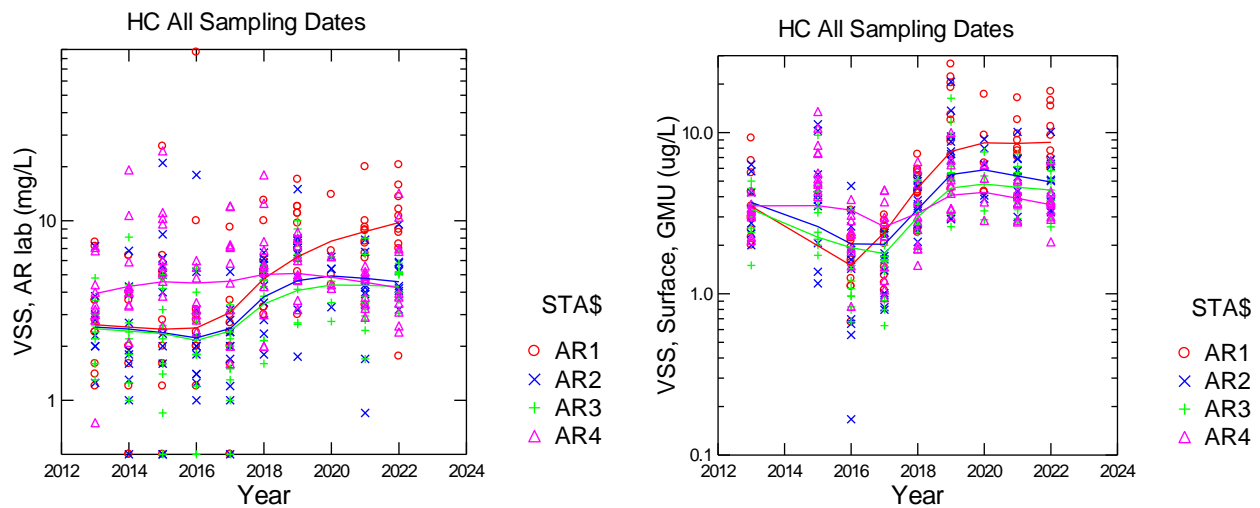


Figure 153. Scatterplots comparing values of Volatile Suspended Solids among years. Alex Renew Lab data (a. left) and GMU Lab data (b. right). April through September. 2013-2022.

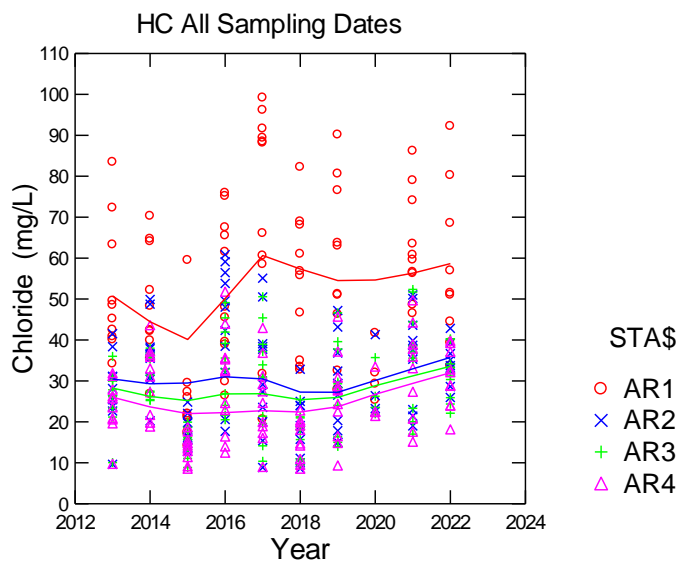


Figure 154. Box plots comparing values of Chloride among years. April through September. 2013-2022.

As in most previous years, chloride was higher at AR1 than at the other stations (Figure 154). None of the stations showed evidence of a long-term trend. Total alkalinity was about equal to the early years of the study (Figure 155). In contrast to chloride, total alkalinity was generally lower at AR1 than at the other stations. And at AR4 maintained about 10 mg/L difference compared to AR2 and AR3.

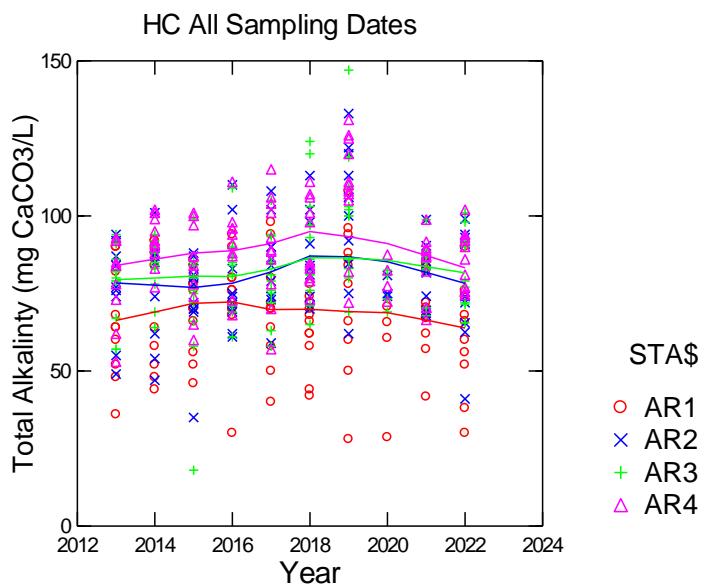


Figure 155. Box plots comparing values of Total Alkalinity among years. April through September. 2013-2022.

In 2018 frequent very high flows scoured and washed all of the SAV out of the Hunting Creek embayment. They have not become re-established and have not been detected at all in the datamapping cruises. To understand the impact of this fundamental change in ecosystem structure the data set was divided into two periods: 2013-2017 and 2018-2022, with 2020 omitted due to a COVID-induced incomplete data set. Most of the significant differences between the two periods were found for Stations AR2 and AR3 during the period June-September and involved changes in the ambient light environment due to increased suspended solids and phytoplankton. Box plots of some of the most significant parameters are shown below (Figures 156-158). Note that indicators of light transparency (Secchi Disk and Light Attenuation Coefficient) have decreased substantially and consistently at both AR2 and AR3 since 2018. Also, TSS has increased indicating more suspended sediments in the water column which contributes to poor light penetration. With no competition from SAV, phytoplankton chlorophyll has increased.

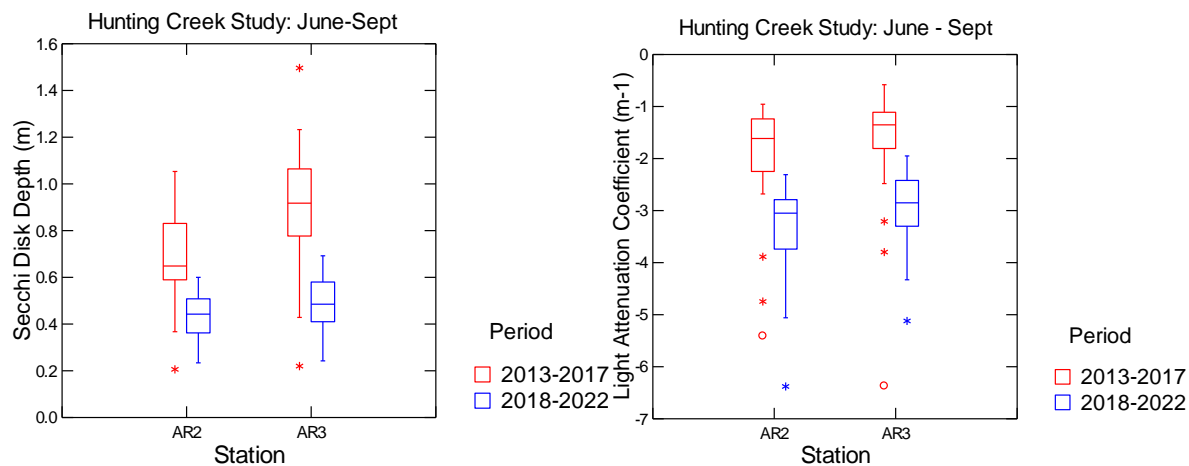


Figure 156. Measures of Light Transparency at Hunting Creek Embayment Stations Comparing 2013-2017 to 2018-2022. June-Sept data (2020 excluded).

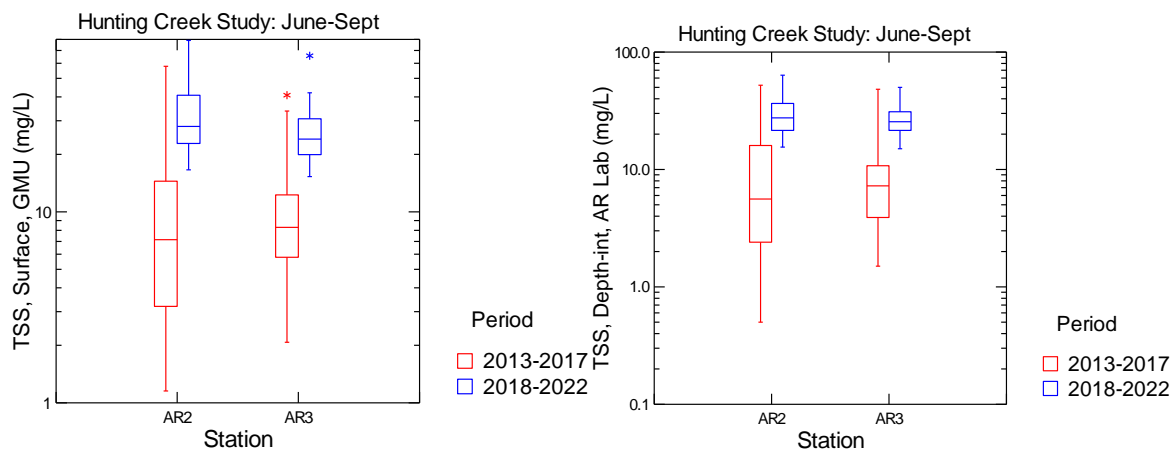


Figure 157. Measures of Suspended Solids at Hunting Creek Embayment Stations Comparing 2013-2107 to 2018-2022. June-Sept data (2020 excluded)

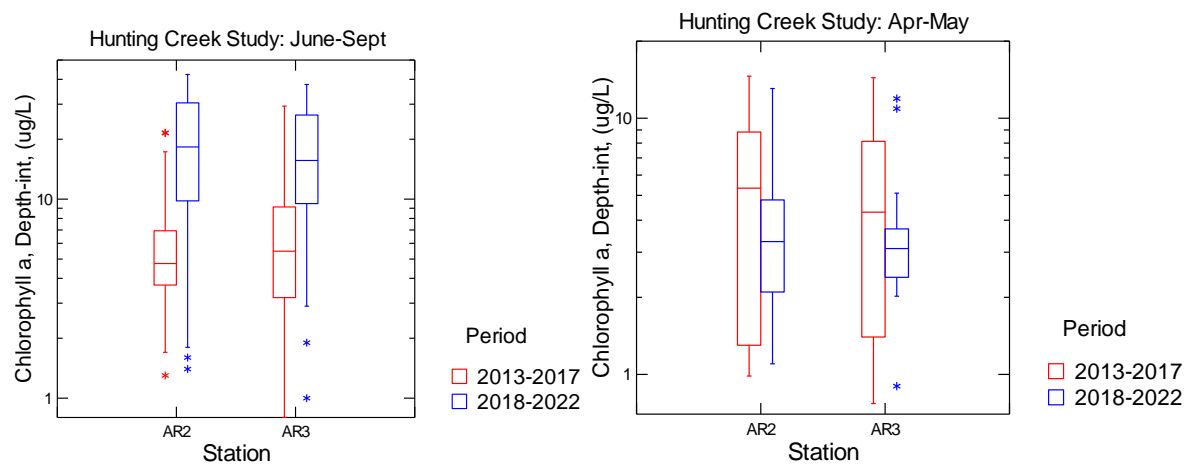


Figure 158. Measures of Phytoplankton Chlorophyll a at Hunting Creek Embayment Stations Comparing 2013-2017 to 2018-2022. Left: June-Sept. data. Right: Apr-May data. (2020 data excluded.)

D. Phytoplankton: Comparison among Years

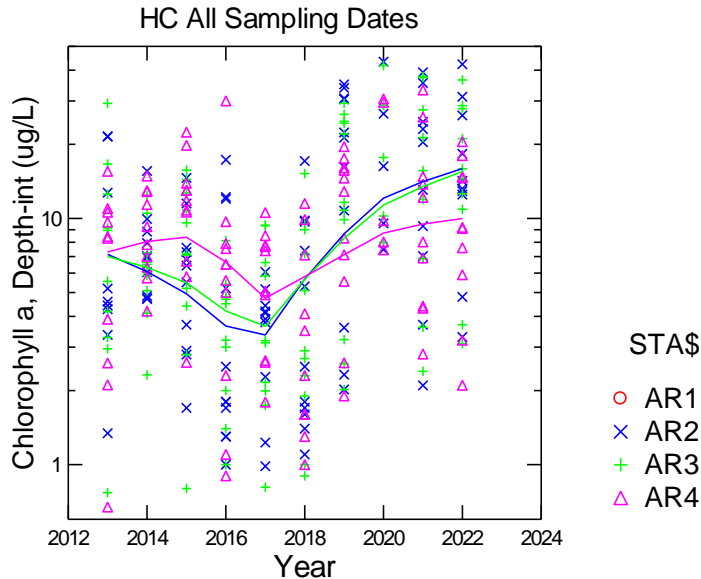


Figure 159. Scatterplots comparing values of depth-integrated Chlorophyll *a* among years.

In 2022 chlorophyll *a* levels were similar to 2019 through 2021, reflecting a strong rebound from the generally low levels found in 2018 and were among the highest of all previous years (Figure 159,160). Similar results were observed with surface chlorophyll. Chlorophyll values in the water are a measure of phytoplankton populations which compete with SAV for light and nutrients. Since SAV is now absent in the embayment, phytoplankton have increased. And their continued presence at higher levels will impede the re-establishment of SAV. Interestingly, the highest values have been recorded recently at AR1.

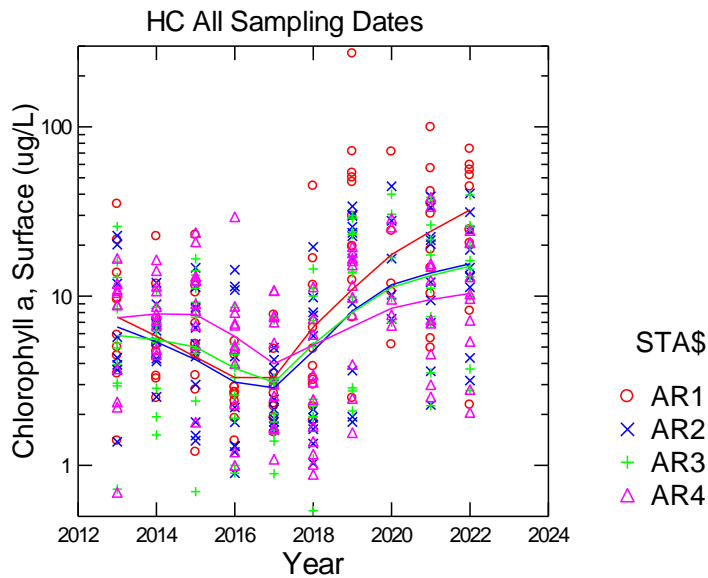


Figure 160. Satterplots comparing values of surface Chlorophyll *a* over the years.

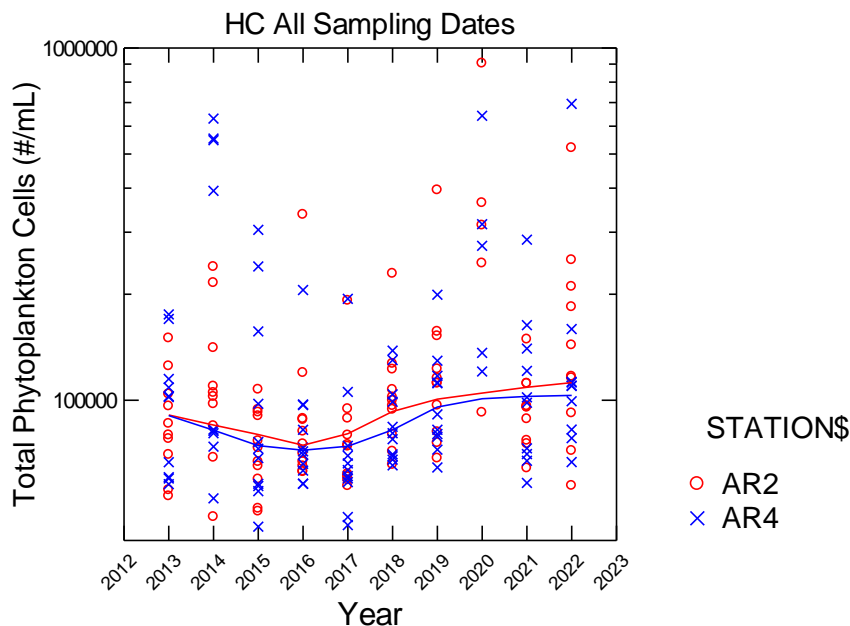


Figure 161. Scatterplots comparing values of Total Phytoplankton Density over the years.

Phytoplankton counts are done only at AR2 in the embayment and AR4 in the river channel. The trend lines for both stations have followed a very similar trend with recent values at the higher end and AR2's trend line maintaining a slight edge (Figure 161). The high 2020 values may be partially due to the fact that data were only available for the July to September period which often has the highest densities. Total cyanobacterial cell density over the period followed a similar pattern to total phytoplankton density, cyanobacteria being smaller in general (Figure 162).

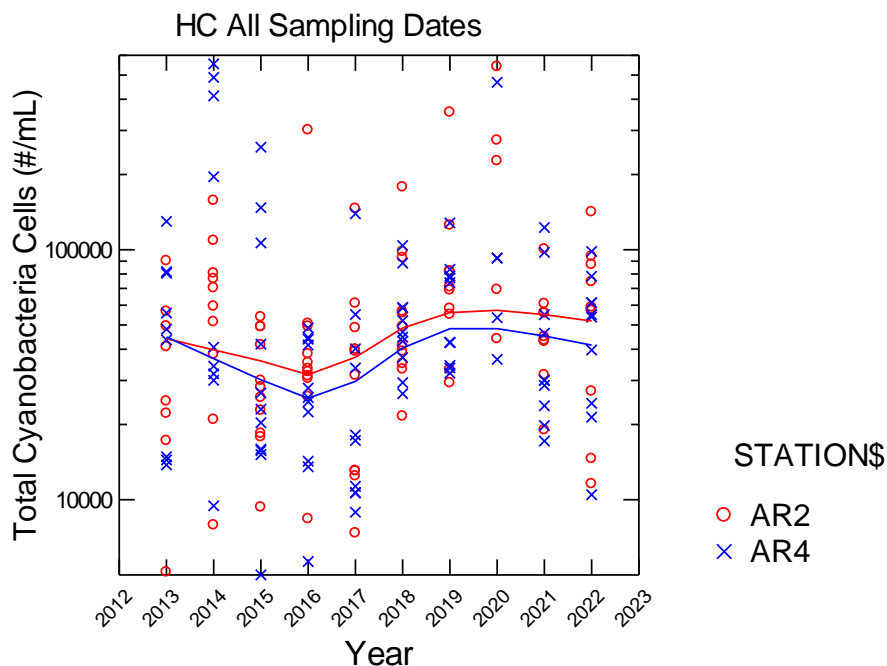


Figure 162. Scatterplots comparing values of Cyanobacterial Density over the years.

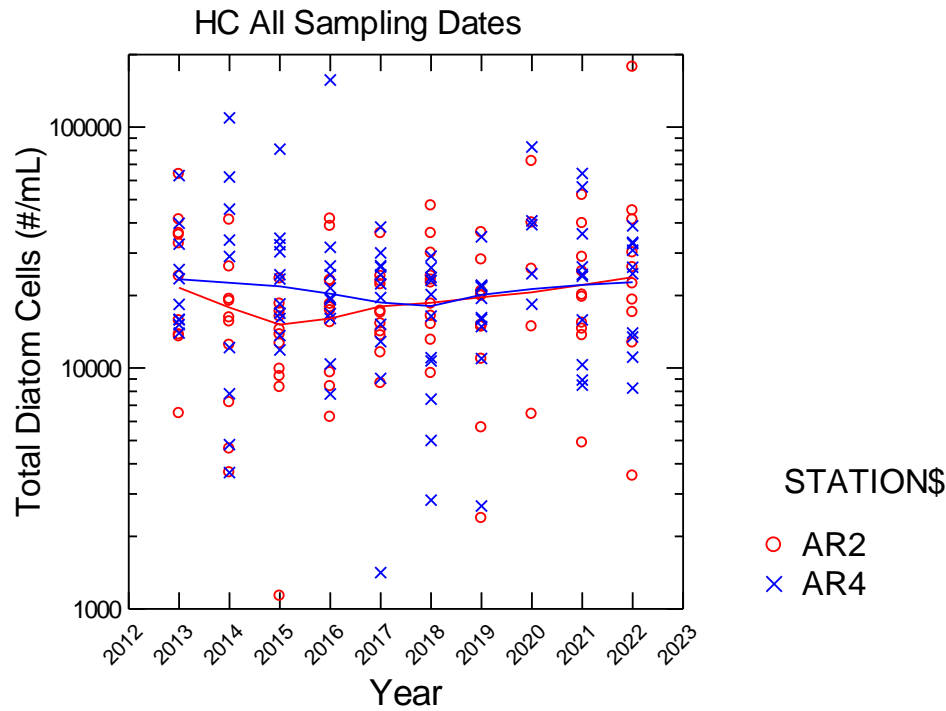


Figure 163. Scatterplots comparing values of Diatom Density over the years.

Diatom densities have shown little change over the study period and little difference in the trend lines between AR2 and AR4 (Figure 163). Green algal cell density trend line has shown a very slow, but persistent decline over the study period at both stations and little consistent difference between the two stations (Figure 164).

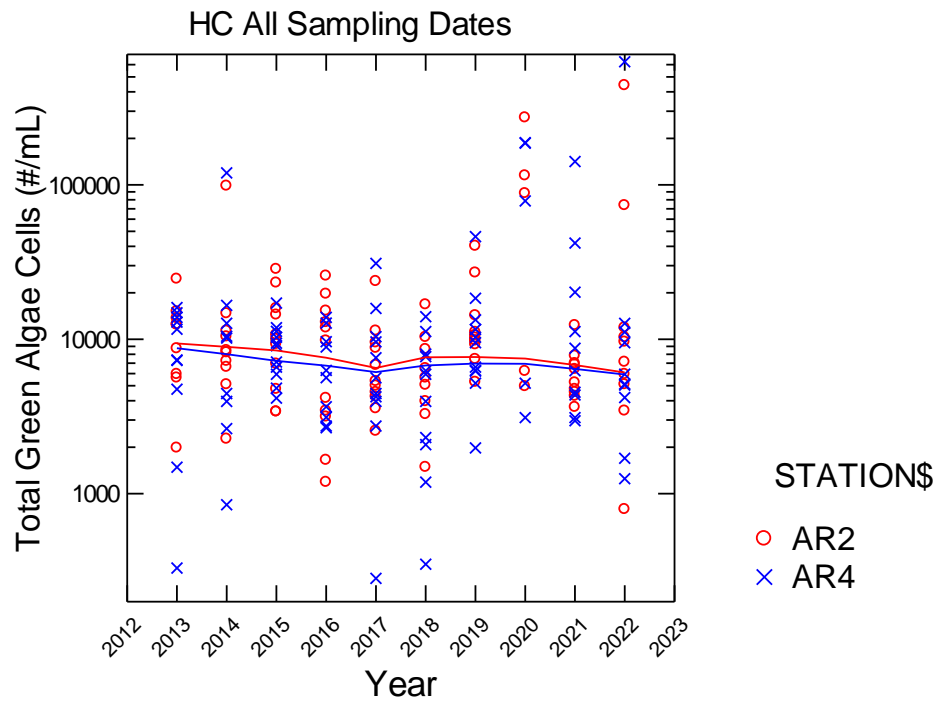


Figure 164. Scatterplots comparing values of Green Algal Density over the years.

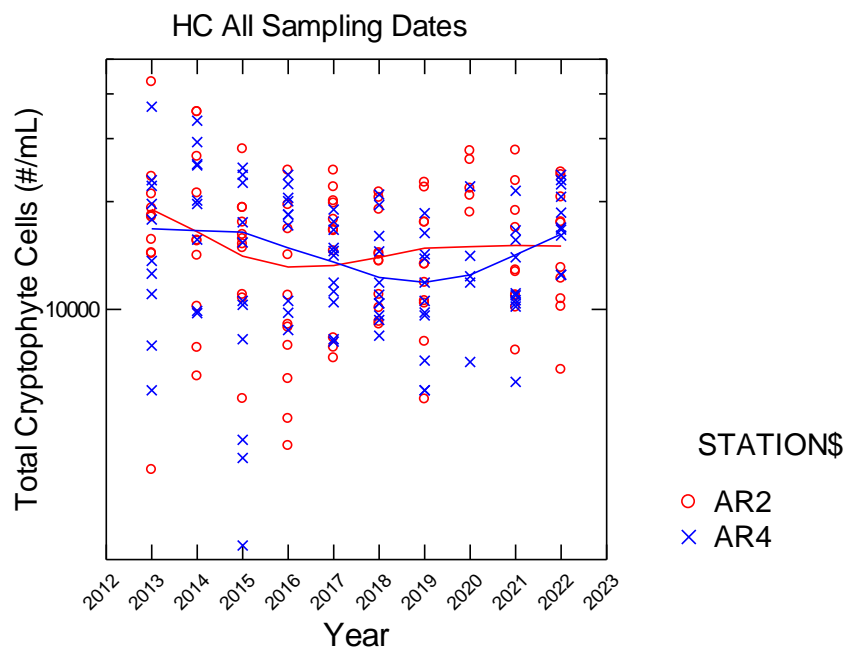


Figure 165. Scatterplots comparing values of Cryptophyte Density over the years.

Cryptophyte cell densities at AR2 have remained relatively consistent over the study period (Figure 165). At AR4 the cryptophyte density trend line has moved above and below the AR2 line, but has not shown a consistent trend. Other taxa includes those species of phytoplankton in groups not tallied above. These are mainly dinoflagellates, chrysophytes and euglenoids whose abundances are somewhat sporadic in the study area. Nonetheless, the trend lines for this group have shown a small net increase over the study period (Figure 166).

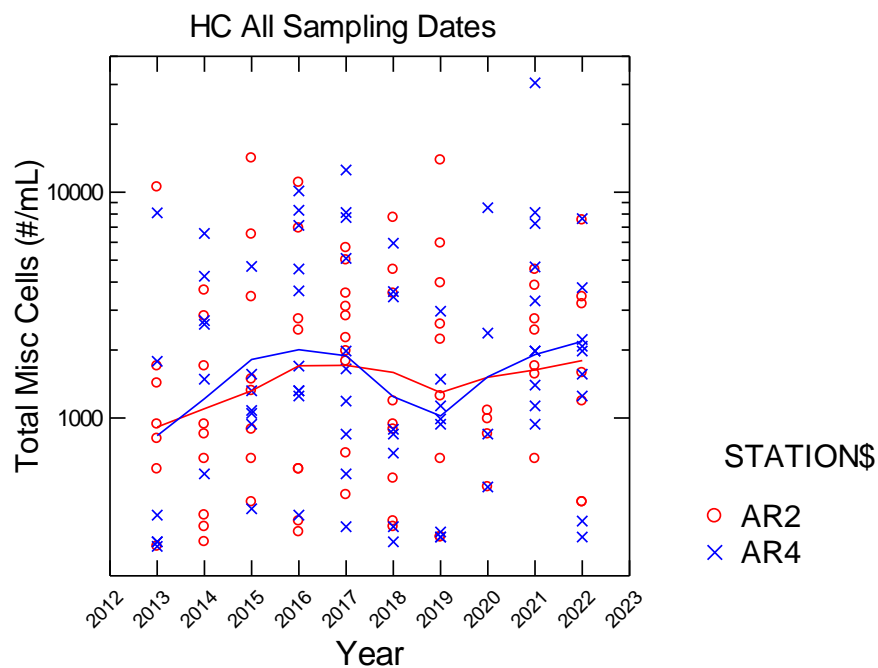


Figure 166. Scatter plots comparing values of Miscellaneous Taxa Density over the years.

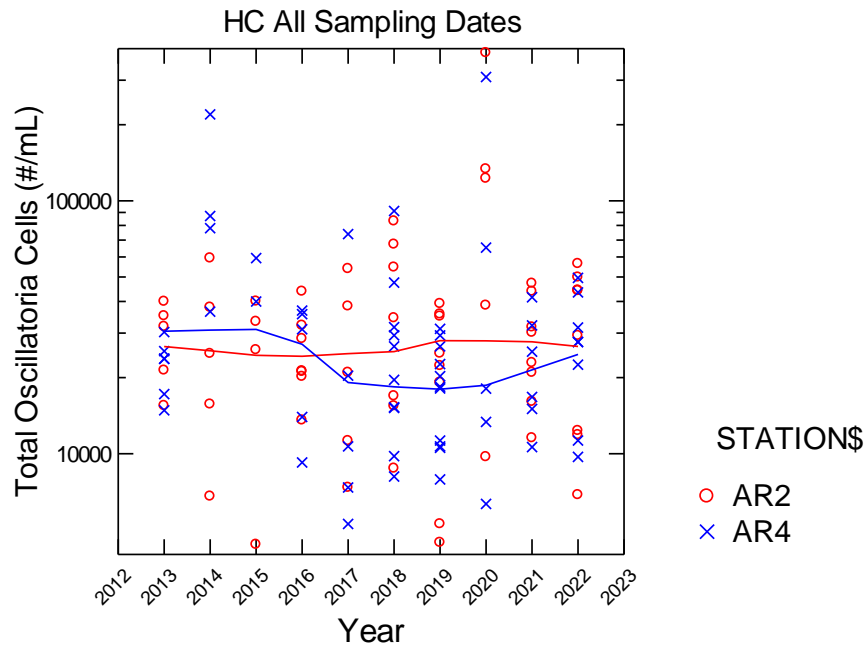


Figure 167. Scatterplots comparing values of *Oscillatoria* Cell Density over the years.

Oscillatoria has been the most abundant cyanobacterium during the course of this study. The trend line for *Oscillatoria* at AR2 has remained very steady at about 25,000 cells/mL over the entire study period (Figure 167). At AR4 there was a decline from 2015 to 2018 followed by a recent increase. *Chroococcus* has shown a net increase over the study period with the trend line for AR2 being above that for AR4 (Figure 168).

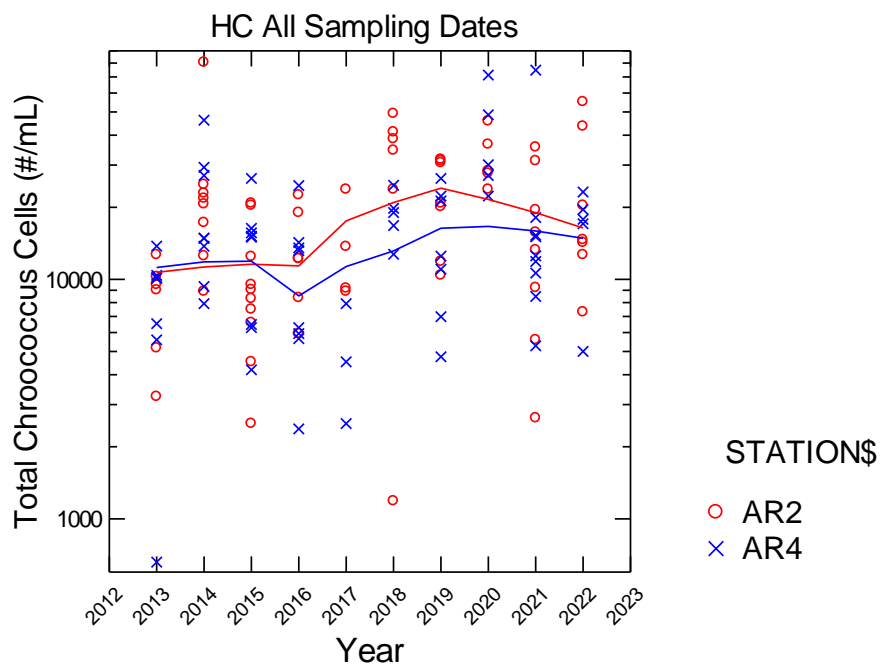


Figure 168. Scatterplots comparing values of *Chroococcus* Cell Density over the years.

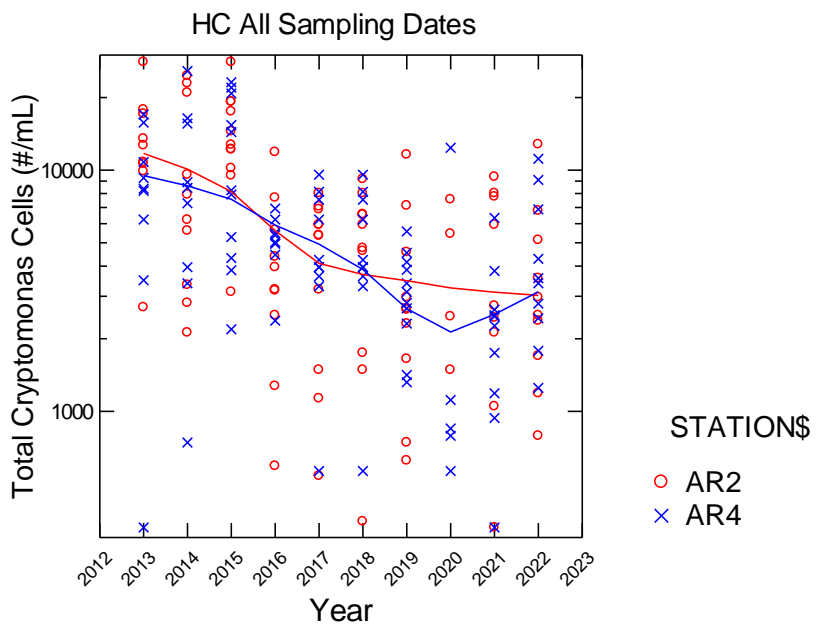


Figure 169. Scatterplots comparing values of *Cryptomonas* Cell Density over the years.

Cryptomonas cell density has show a clear and marked decline over the study period at both stations (Figure 169). The trend lines dropped from 10,000 cells/mL to 2,000 to 3,000 cells/mL over the period. *Chroomonas* maintained a steady trend line at 8,000-10,000 cells/mL over the period at both stations (Figure 170).

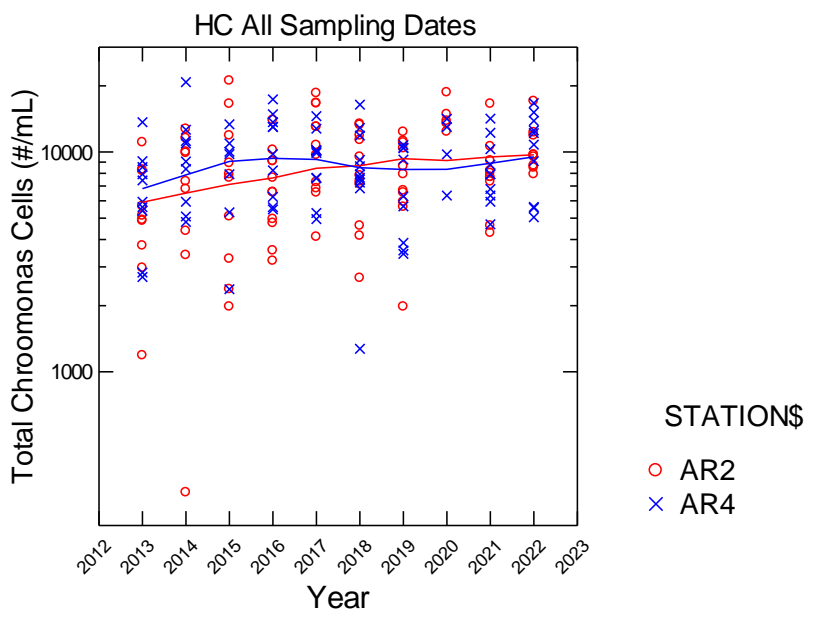


Figure 170. Scatterplots comparing values of *Chroomonas* Cell Density over the years.

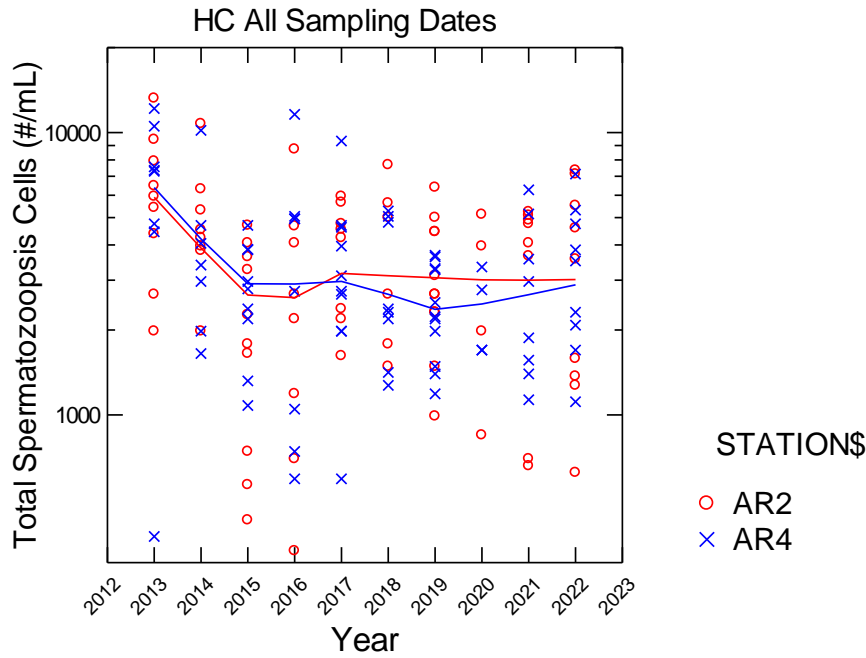


Figure 171. Scatterplots comparing values of *Spermatozoopsis* Cell Density over the years.

Spermatozoopsis, one of the more common green algae, has shown a similar trend at both stations, declining markedly in the first three years of the study and then stabilizing (Figure 171). *Melosira*, the most common diatom, has shown a steady decline over the study period at both stations, from about 10,000 cells/mL in 2013 to less than 2000 cells/mL at AR4 and about 3,000 cells/mL at AR2 (Figure 172).

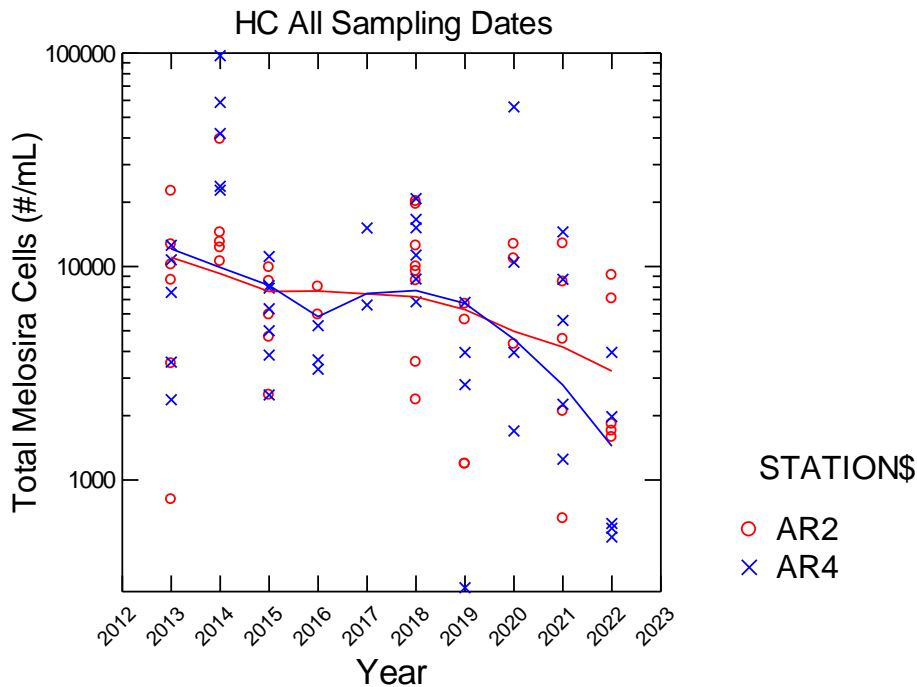


Figure 172. Scatterplots comparing values of *Melosira* Cell Density over the years.

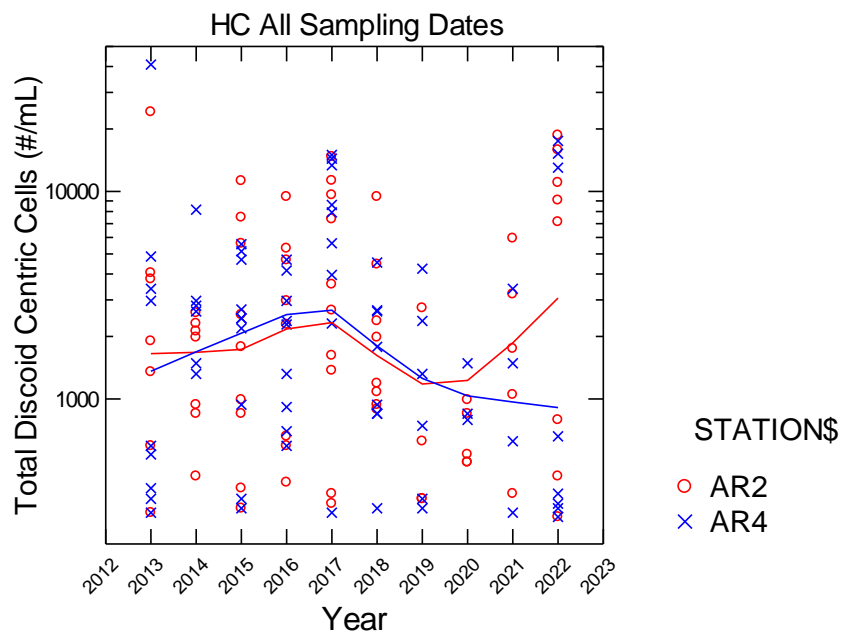


Figure 173. Scatterplots comparing values of Discoid Centrics Cell Density over the years.

Discoid centric diatoms exhibited a steady increase at both stations during the early years of the study, but started declining in 2018 (Figure 173). In 2020 they started to increase again at AR2 and reached their highest values to date. In contrast they continued to decline at AR4. Pennate 1 cells were fairly constant until 2018 and have since increased (Figure 173).

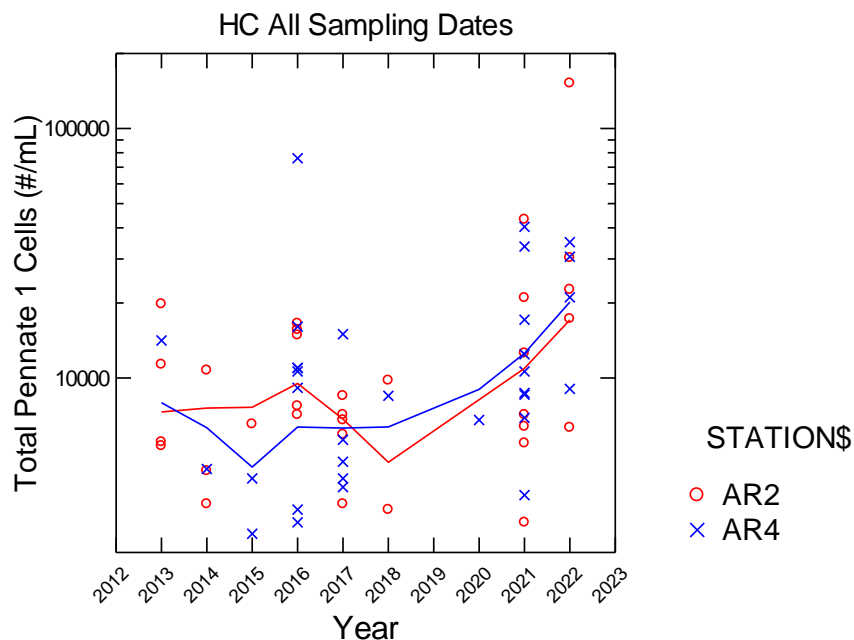


Figure 173. Scatterplots comparing values of Pennate 1 Cell Density over the years.

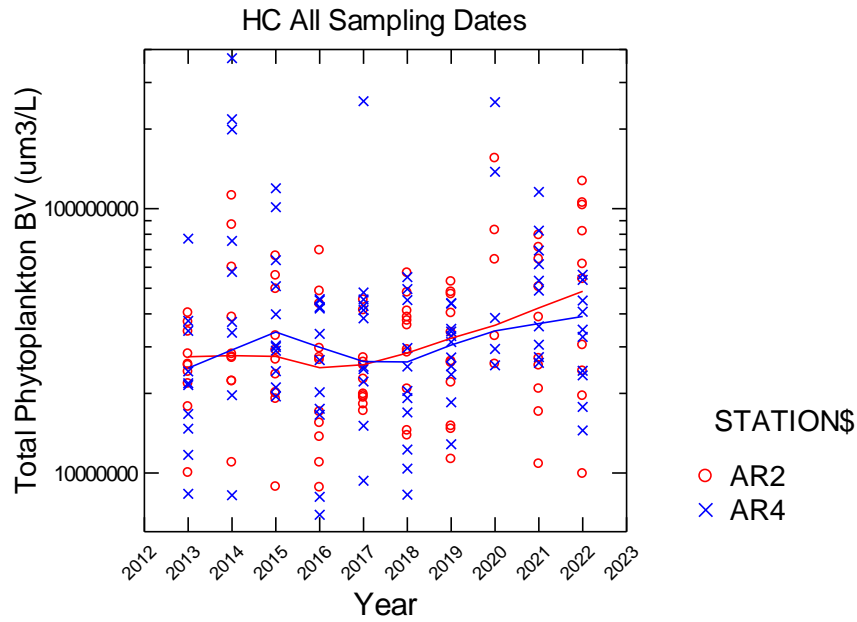


Figure 174. Scatterplots comparing values of Total Phytoplankton Biovolume over the years.

Biovolume takes into account both the number of cells and their relative size. In 2022 total biovolumes were at the higher end of the range of previous years similar to 2014 and 2020 (Figure 174). Total cyanobacterial biovolume median in 2022 declined from 2020 values which were among the highest observed to date (Figure 175).

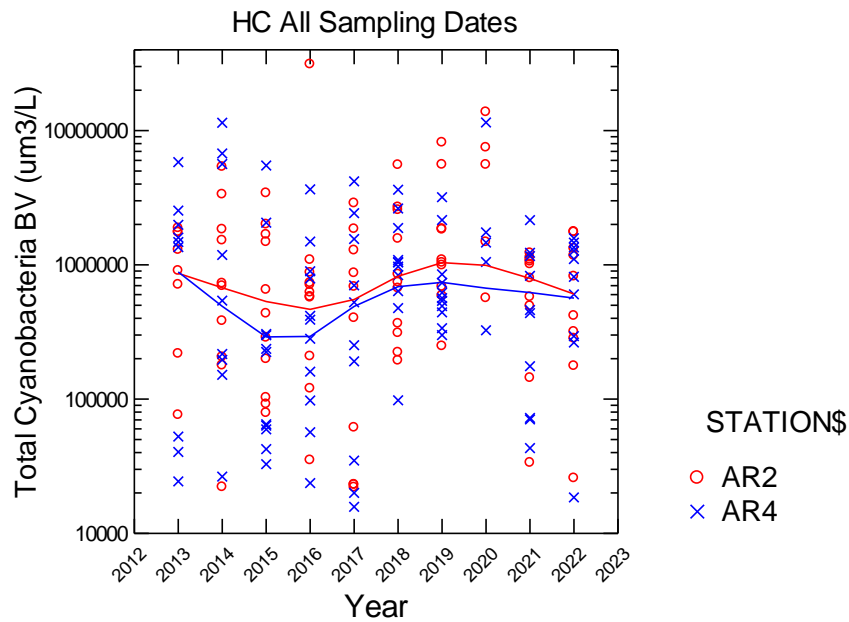


Figure 175. Scatterplots comparing values of Cyanobacterial Biovolume over the years.

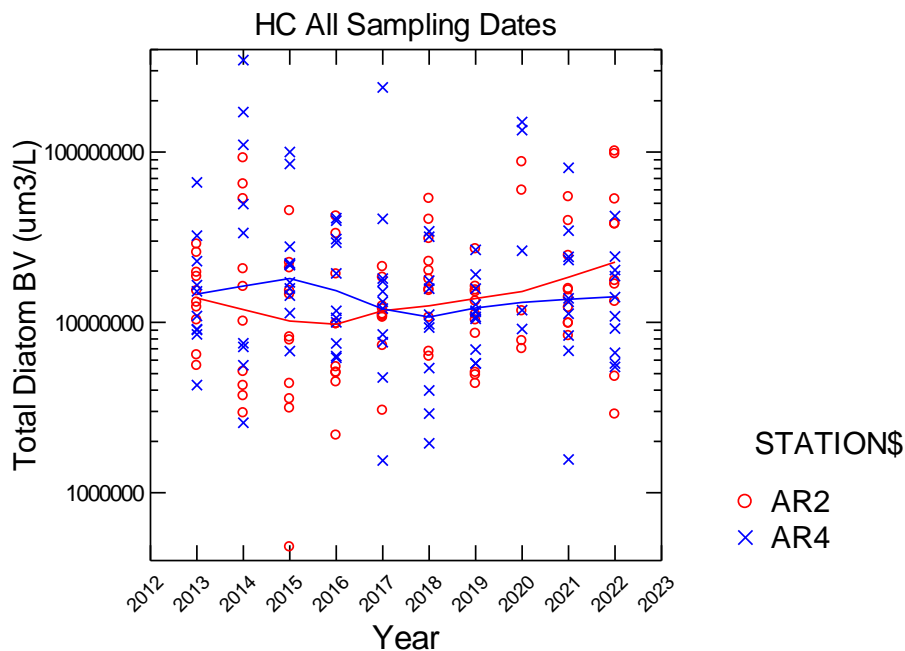


Figure 176. Scatterplots comparing values of Diatom Biovolume over the years.

Median diatom biovolume in 2022 was similar at both stations, falling within the range of previous years (Figure 176). The trend line for AR2 continued to rise while it was flat for AR4. Median values in green algal biovolume were also very similar between the two stations and much reduced at AR2 from 2020 (Figure 177).

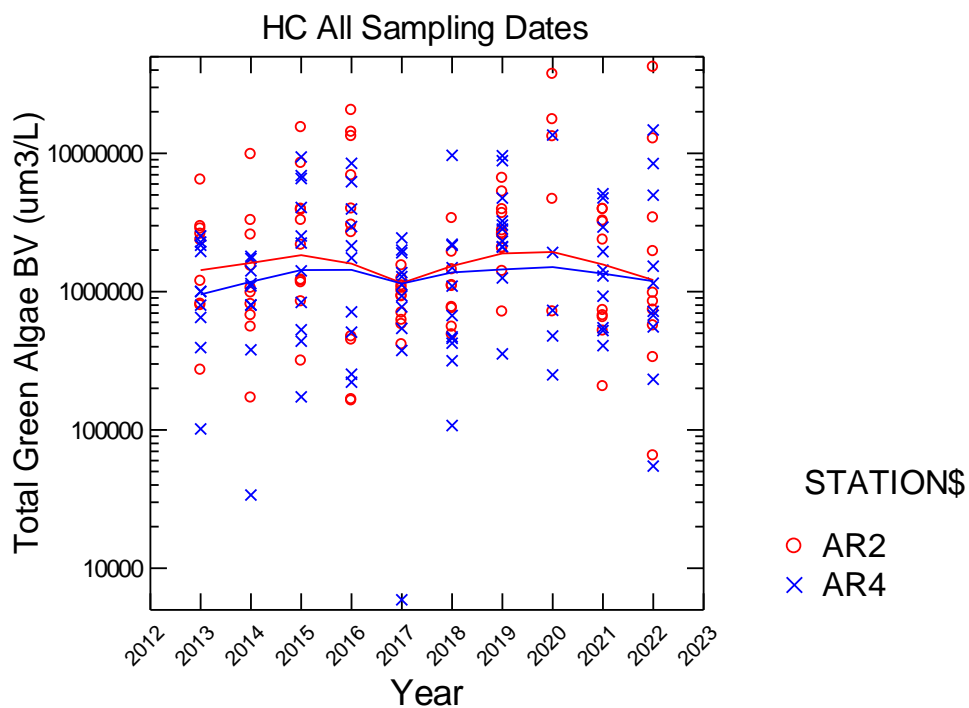


Figure 177. Scatterplots comparing values of Green Algal Biovolume over the years.

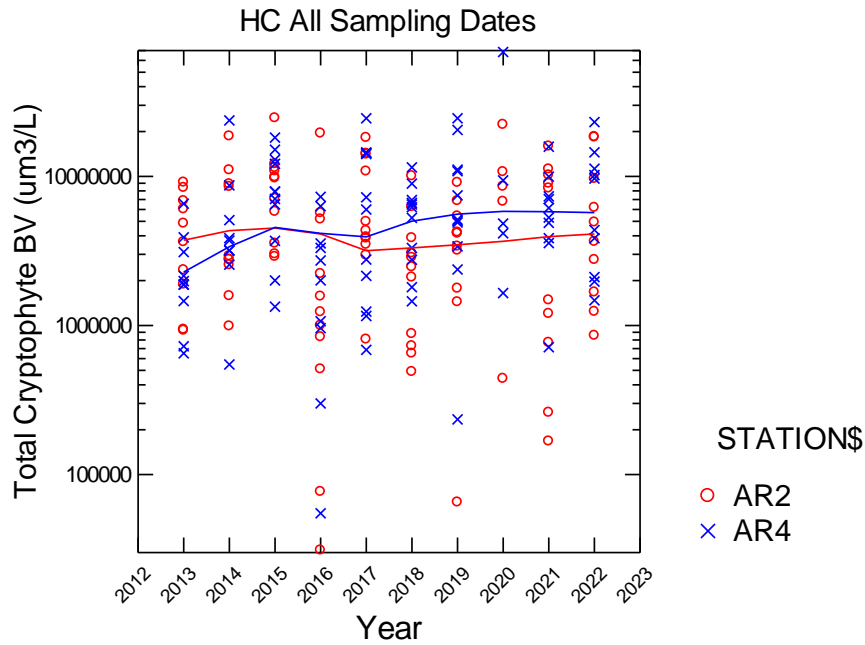


Figure 178. Scatterplots comparing values of Cryptophyte Biovolume over the years.

Cryptophyte biovolume at both stations showed a stable trend line with AR4 slightly above AR2 (Figure 178). Levels at AR4 were somewhat higher and more in line with previous years. The patterns in Miscellaneous Taxa Biovolume were steady in 2022 after higher levels were found in 2021 (Figure 179).

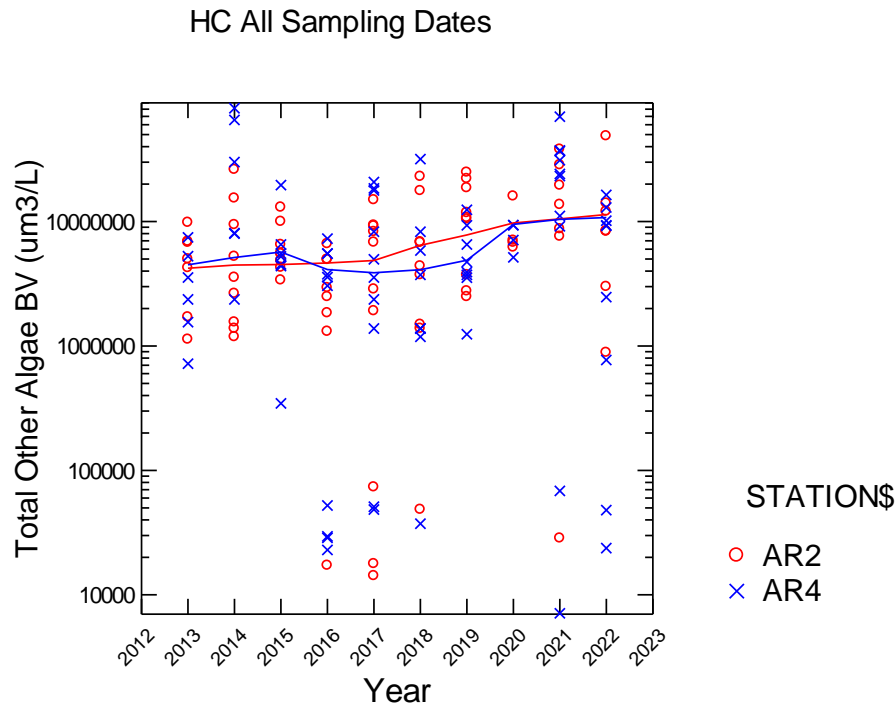


Figure 179. Scatterplots comparing values of Miscellaneous Biovolume over the years.

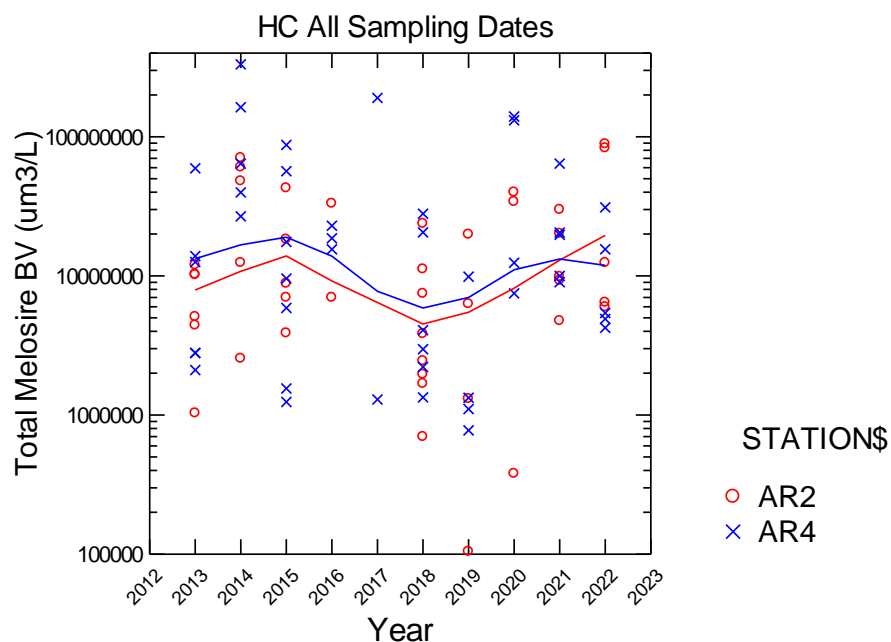


Figure 180. Scatterplots comparing values of *Melosira* Biovolume over the years.

An analysis of interannual and seasonal effects also done for selected individual taxa. Median biovolume values of the filamentous diatom *Melosira* showed a clear peak in 2014 at both stations, then declined steadily through 2019, but came back strongly in the 2020-2022 period (Figure 180). Discoid centric biovolume in 2022 was similar at both stations and showed a slight upward trend line (Figure 181).

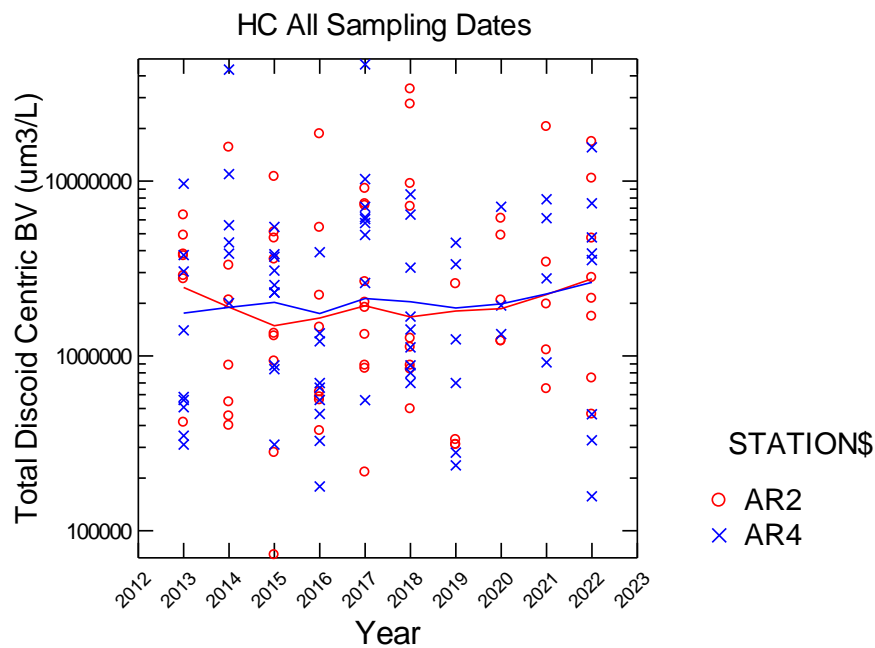


Figure 181. Scatterplots comparing values of Discoid Centric Diatom Biovolume over the years.

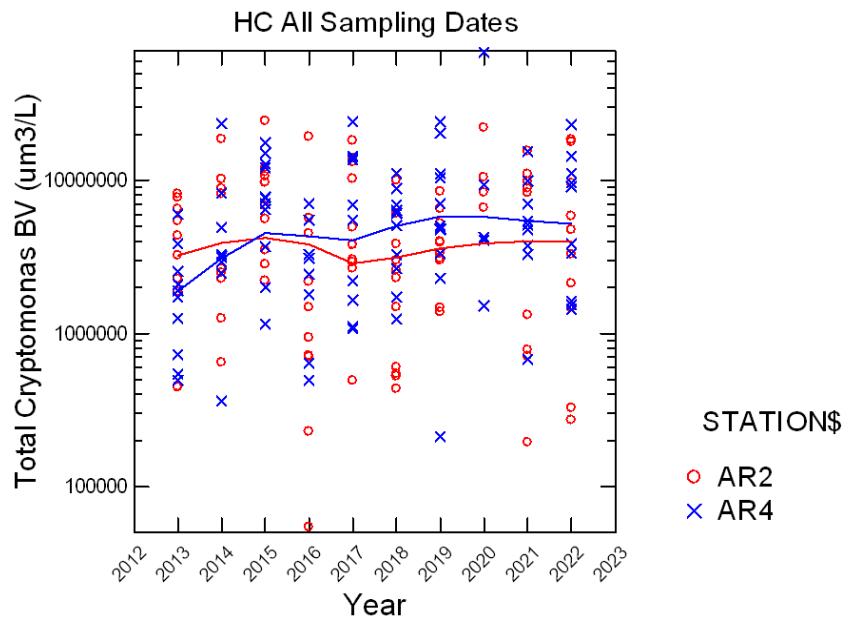


Figure 182. Scatterplots comparing values of *Cryptomonas* Biovolume over the years.

Cryptomonas biovolume at both stations was similar and in the same range as previous years (Figure 182). *Trachelomonas* has undergone substantial cycles with values at AR4 generally higher than at AR2.

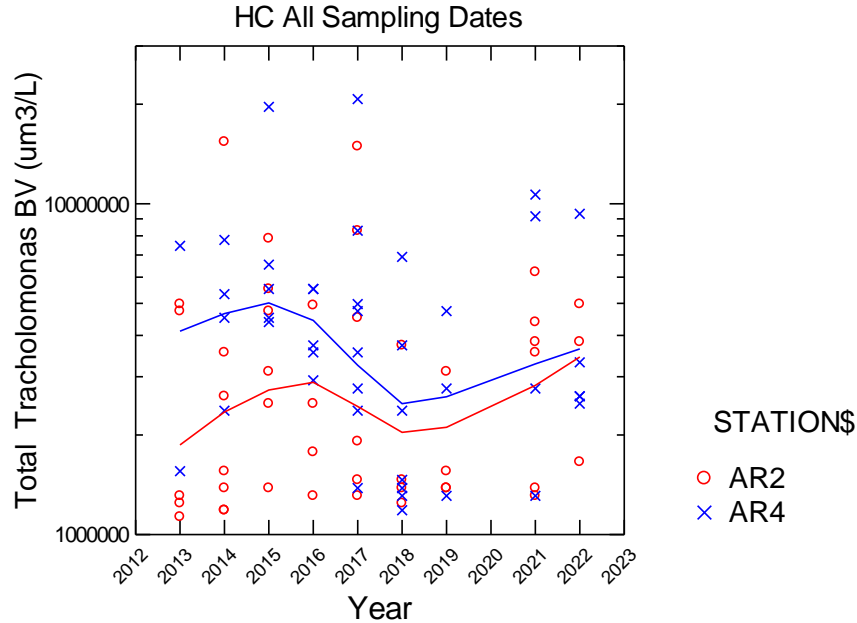


Figure 183. Scatterplots comparing values of *Trachelomonas* Biovolume over the years.

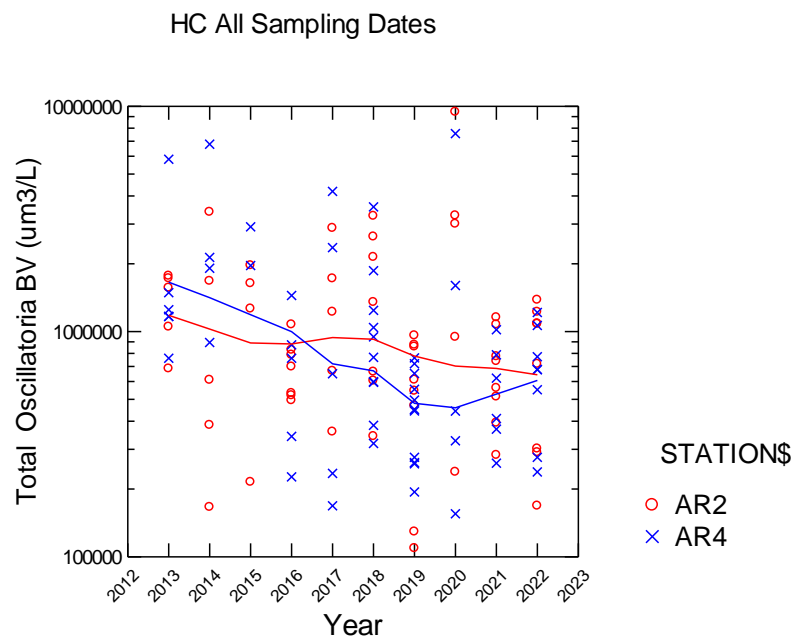


Figure 184. Scatterplots comparing values of *Oscillatoria* Biovolume over the years.

Oscillatoria is the most consistently abundant cyanobacterium in the study area. Levels at AR2 have remained fairly constant, while at AR4 they have showed a strong and consistent decline through 2020 with a strong recovery in 2021 and 2022 (Figure 184). *Anabaena*, a heterocystous cyanobacterium, has been sporadic and variable over the study period at both stations (Figure 185).

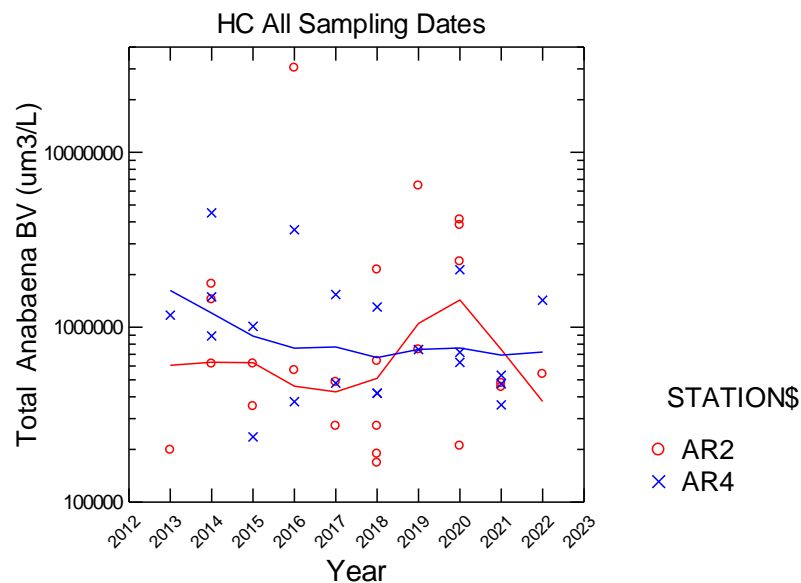


Figure 185. Scatterplots comparing values of *Anabaena* Biovolume over the years.

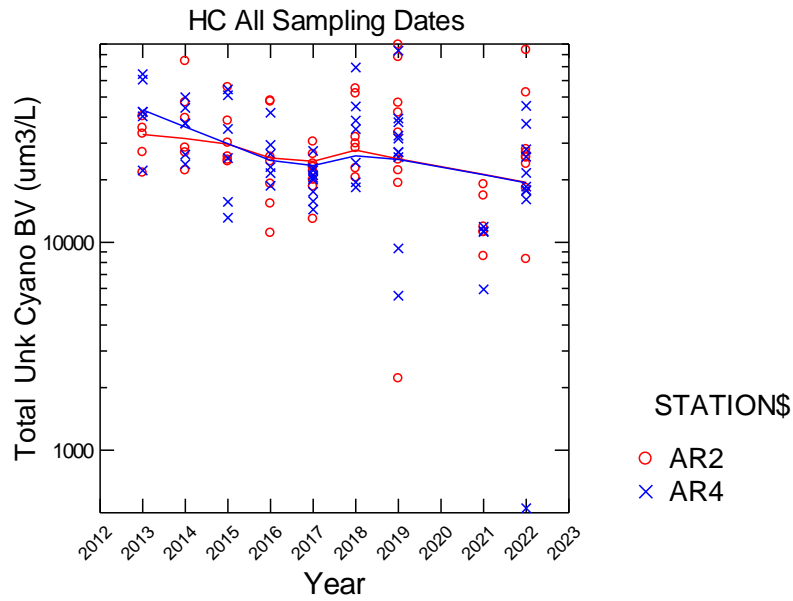


Figure 186. Scatterplots comparing values of Unkown Cyanobacterium <2um. Biovolume over the years.

A commonly occurring cyanobacterium (Unknown Cyano <2u) has been present in most samples from both stations (Figure 186). Another common cyanobacterium, *Chroococcus*, has maintained fairly steady populations over the study period with consistently higher amounts at the embayment stations AR2 (Figure 187).

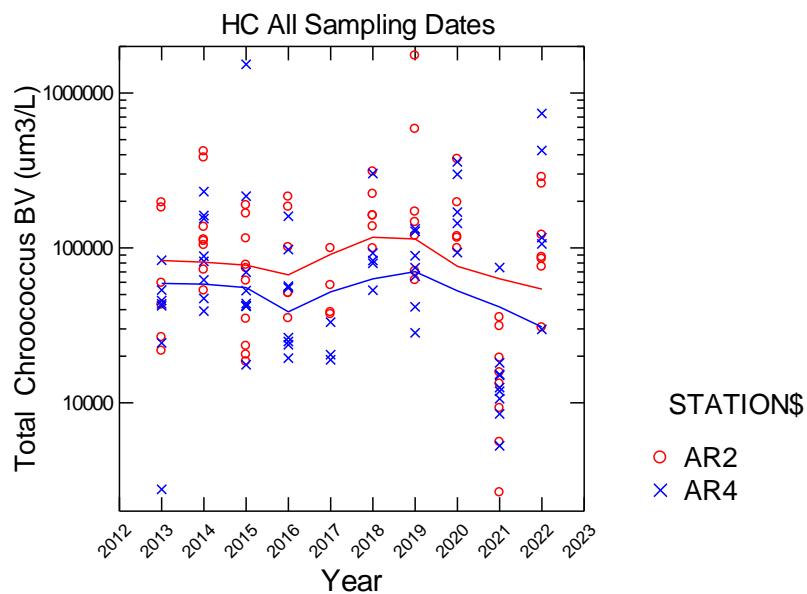


Figure 187. Scatterplots comparing values of *Chroococcus* Biovolume over the years.

E. Zooplankton: Comparison among Years

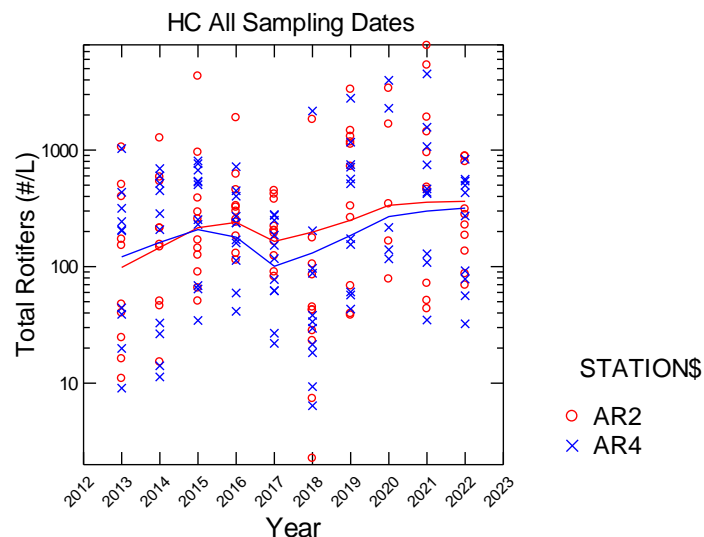


Figure 188. Scatterplots comparing values of Total Rotifers over the years.

Total rotifer densities were a little lower than in 2022 than in some recent years, but the trend line continues to rise from a density of about 100/L in 2013 to about 400/L in 2022 (Figure 188). Of particular interest was the strong recovery from the record low values of 2018 which were probably a result of the high rainfall and subsequent flushing of organisms observed that year. Episodic flushing occurred in 2019-2021 and may have actually stimulated the rotifers. The common rotifer *Brachionus* (Figure 189) was the dominant taxon and displayed a similar trend as total rotifers with 2019-2021 levels very high and 2018 the lowest year to date. *Brachionus* exhibited similar values at both station in most years. The trend lines went from about 10/L in 2013 to 100/L in 2022.

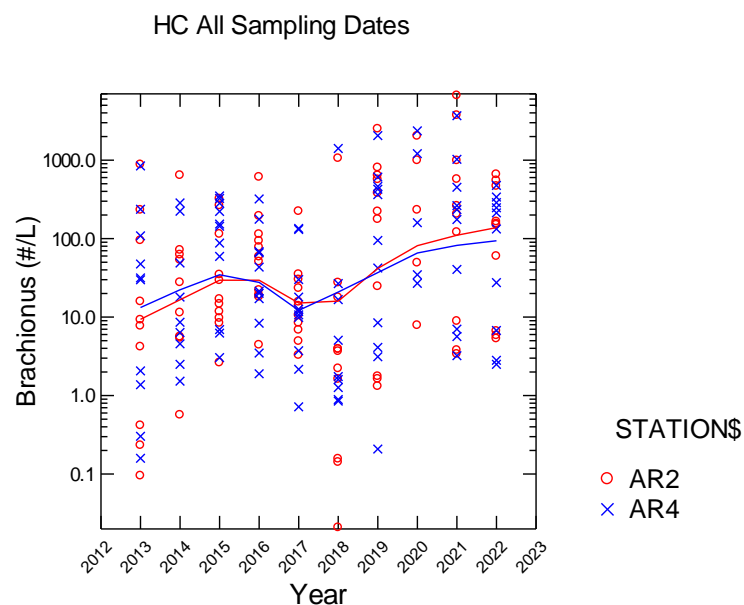


Figure 189. Scatterplots comparing values of *Brachionus* over the years.

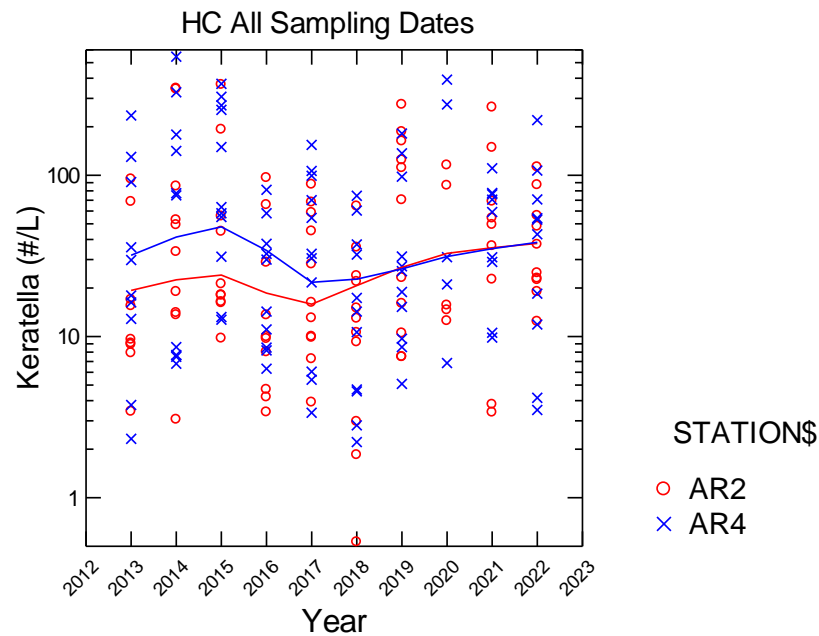


Figure 190. Scatterplots comparing values of *Keratella* over the years.

Another common rotifer *Keratella* has shown a fairly steady trend line over the years (Figure 190). In the early years AR4 was much higher than AR2, but the two stations now have similar trend lines. *Polyarthra*, consistently observed, but less common than *Brachionus* or *Keratella*, also showed a continued rebound from low 2018 levels (Figure 191).

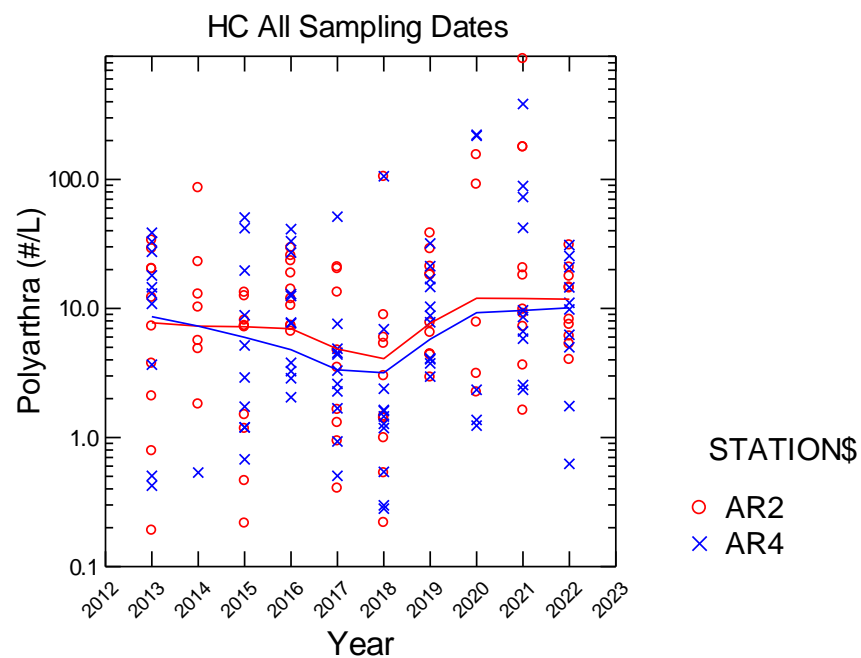


Figure 191. Scatterplots comparing values of *Polyarthra* over the years.

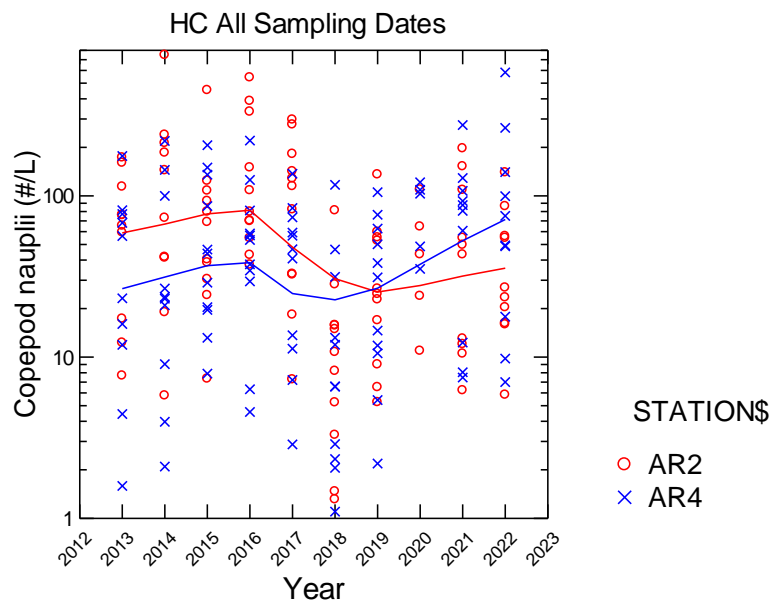


Figure 192. Scatterplots comparing values of Copepod Nauplii over the years.

Nauplii are the juvenile stages of copepods. As such it is hard to identify them to species since they do not have mature characteristics so they have been lumped for all copepod taxa. Before 2018, nauplii were consistently much higher in the embayment than in the river, but in recent years that has shifted as AR2 values have declined and AR4 values have increased (Figure 192). *Bosmina* is a small cladoceran enumerated in the 44 μm samples, but related to *Daphnia* and *Diaphanosoma* collected in the 202 μm nets. Except for the very low values in 2018, *Bosmina* levels have been fairly consistent over time (Figure 193). There were consistently more *Bosmina* in the river than in the embayment.

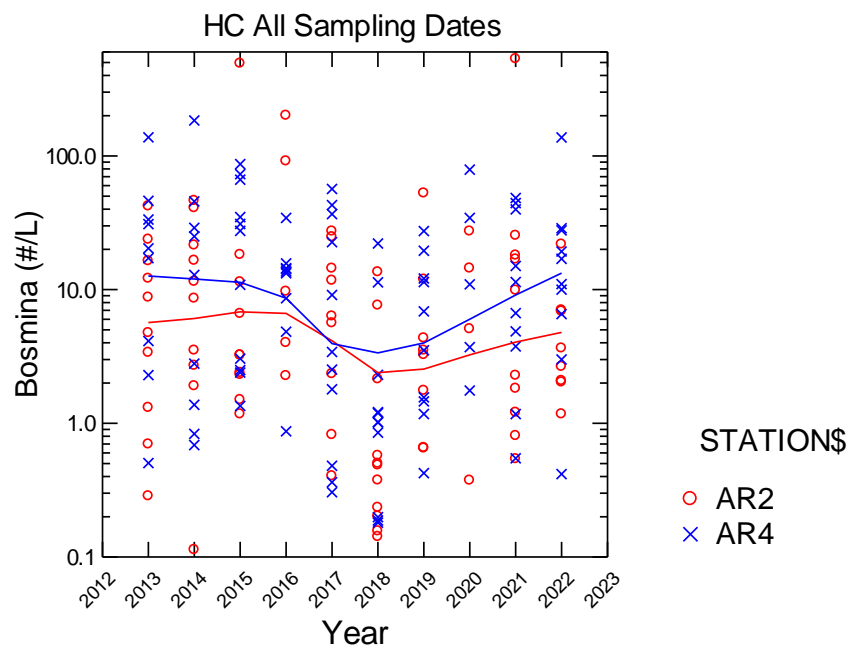


Figure 193. Scatterplots comparing values of *Bosmina* over the years.

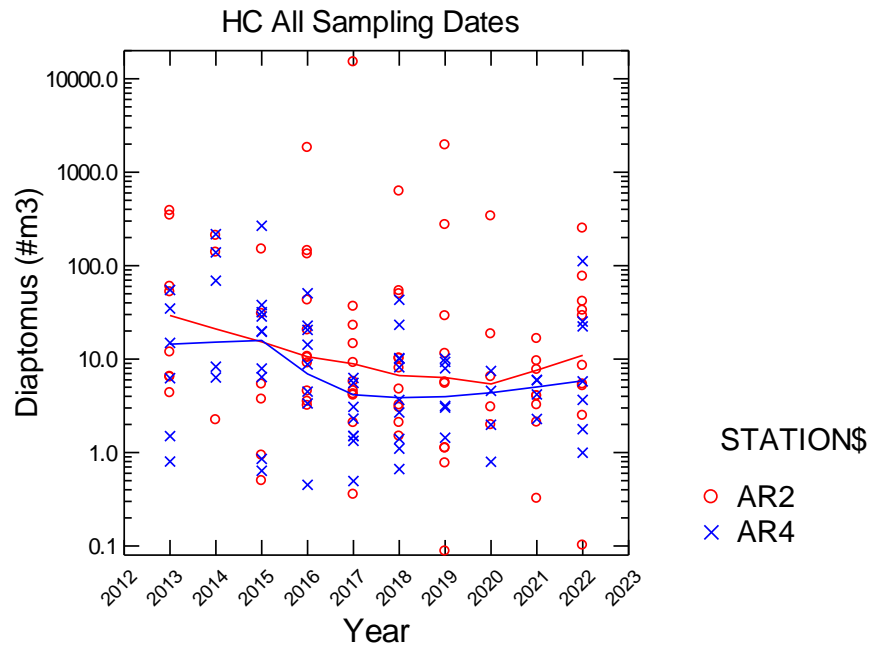


Figure 194. Scatterplots comparing values of *Diaptomus* over the years.

Diaptomus densities exhibited an upturn in 2022 after several years of decline at both stations (Figure 194). *Eurytemora* is the most common calanoid copepod (Figure 195). It consistently was more abundant at the river station AR4 than at AR2 in Hunting Creek with the trend lines being almost an order of magnitude apart. *Eurytemora* did not exhibit much response to the very different flow regimes of 2018 and to the changes in SAV since 2018.

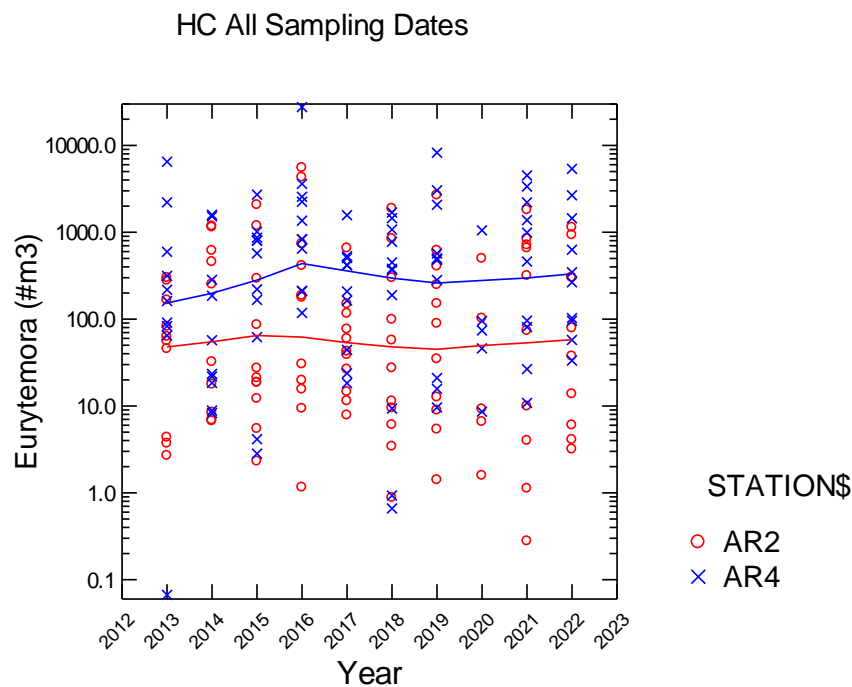


Figure 195. Scatterplots comparing values of *Eurytemora* over the years.

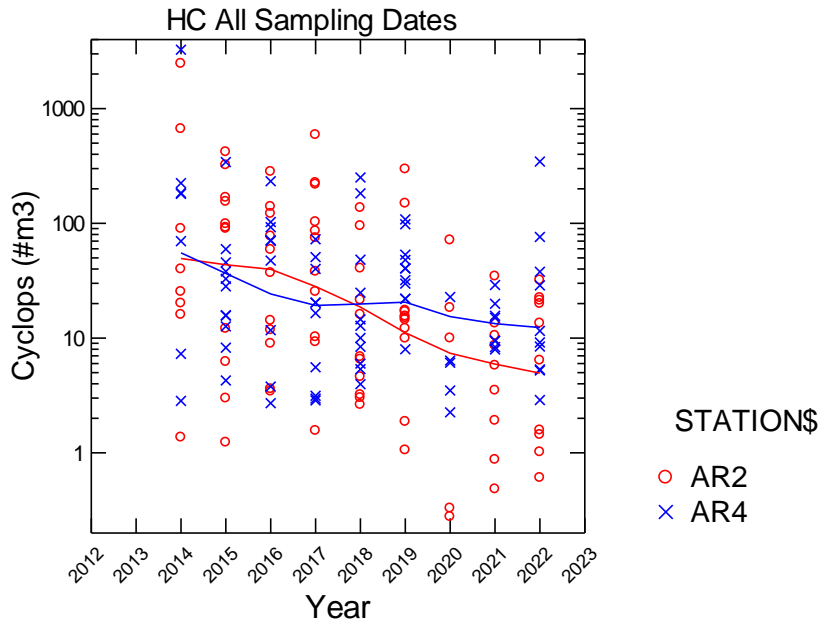


Figure 196. Scatterplots comparing values of *Cyclops* over the years.

The copepod *Cyclops* continued a downward trend at AR2 which has resulted in a decline from about 50/m³ to 5/m³ over the study period (Figure 196). At AR4 values have declined, but at a much slower rate. *Mesocyclops* is the other common cyclopoid copepod. It has shown a consistent decline in the embayment from about 20/m³ to 4 /m³ (Figure 197). At AR4 there has been an opposite trend with the trend line rising by almost an order of magnitude.

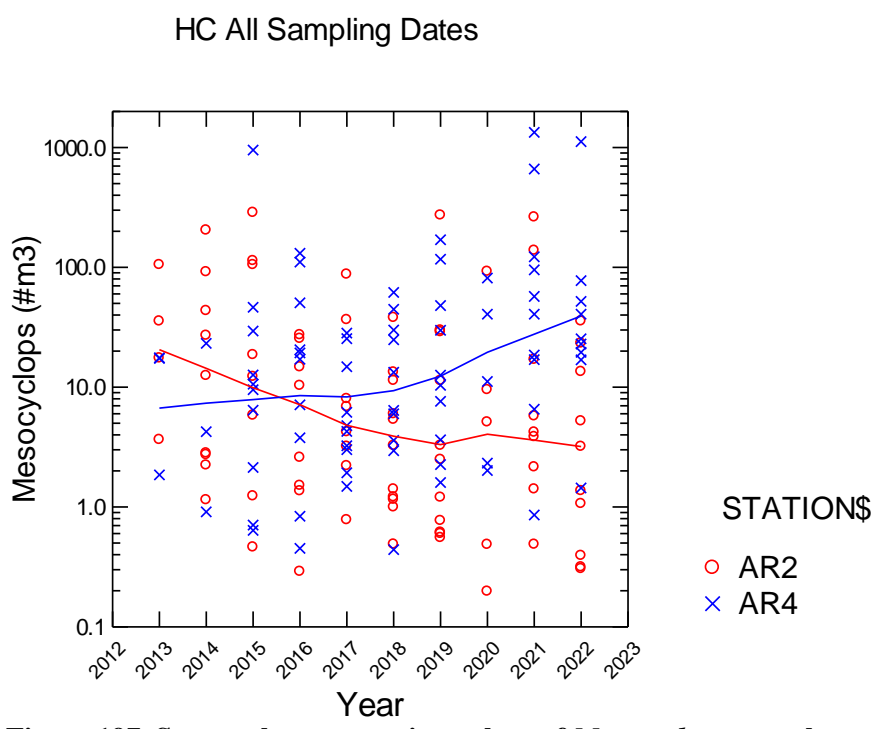


Figure 197. Scatterplots comparing values of *Mesocyclops* over the years.

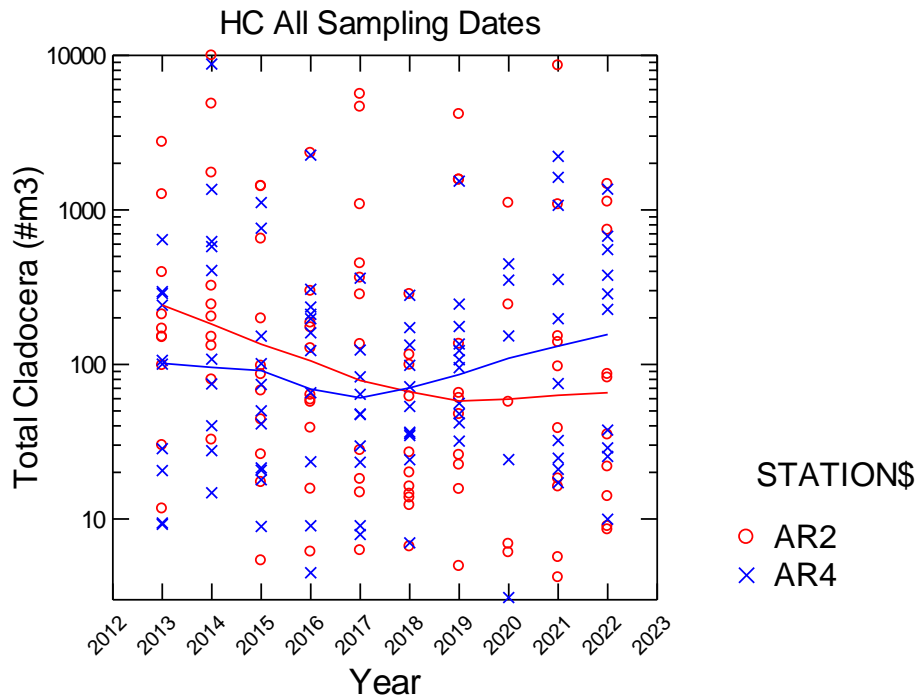


Figure 198. Scatterplots comparing values of Total Cladocerans over the years.

Total cladoceran values (excluding *Bosmina*) at AR2 continued to recover in 2022 at AR4 after the low levels in 2018, but were still below pre-2018 values (Figure 198). Values at AR2 continued to be lower than in the earliest years of the study. *Daphnia* exhibited a steady and marked decline at AR2 in the early years of the study, but has recently undergone a recovery (Figure 199). At AR4 *Daphnia* levels started out markedly less than at AR2, but have since followed a similar trend.

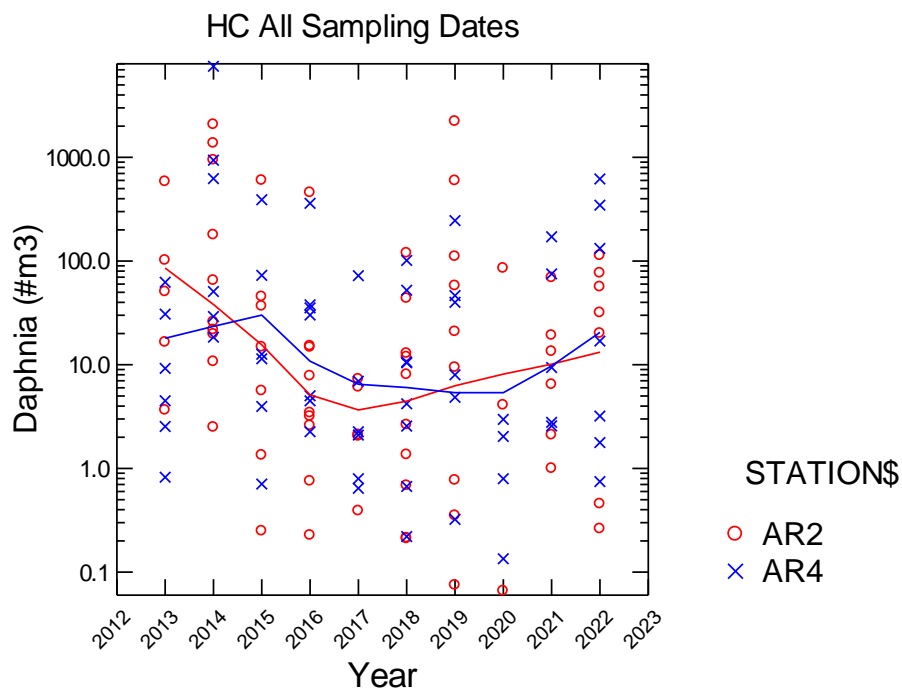


Figure 199. Scatterplots comparing values of *Daphnia* over the years.

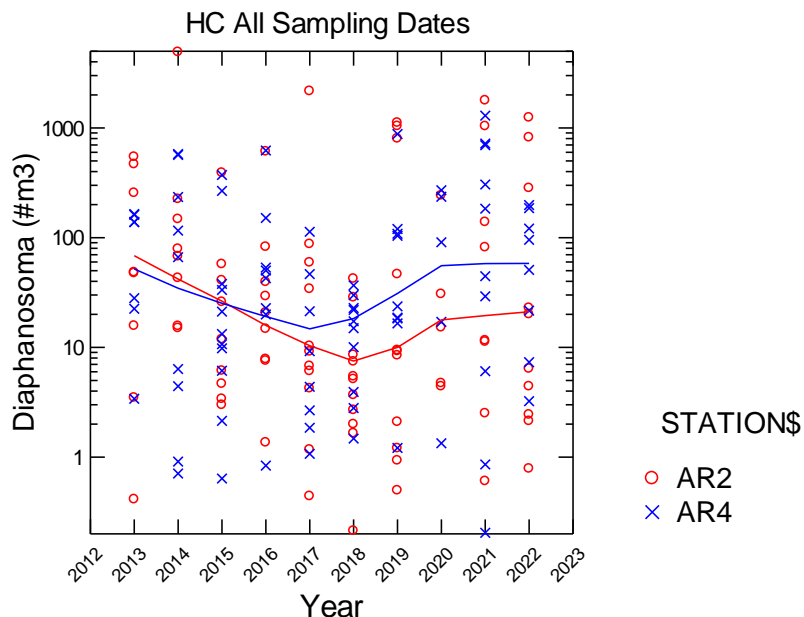


Figure 200. Scatterplots comparing values of *Diaphanosoma* over the years.

Diaphanosoma is a very abundant cladoceran in Gunston Cove, but has proven to be less abundant in the Hunting Creek area, although still important. *Diaphanosoma* levels at AR2 were at record lows in 2018, and have demonstrated some recovery at AR2, but even more at AR4 (Figure 200). Levels at AR4 were also higher in 2020-2022 than in 2018 and among the highest of the entire study period. *Sida* was generally less abundant than *Diaphanosoma*, It suffered a marked decline in 2018 and has continued to decline at both stations (Figure 201).

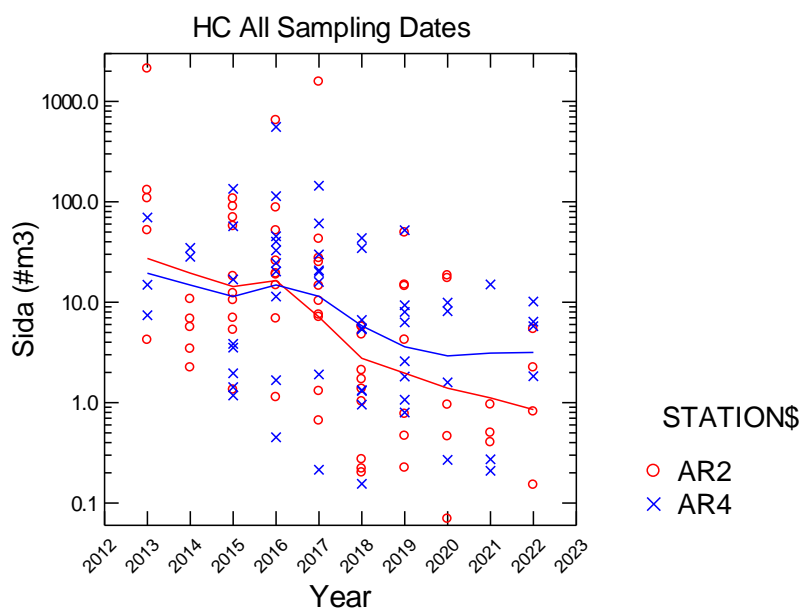


Figure 201. Scatterplots comparing values of *Sida* over the years.

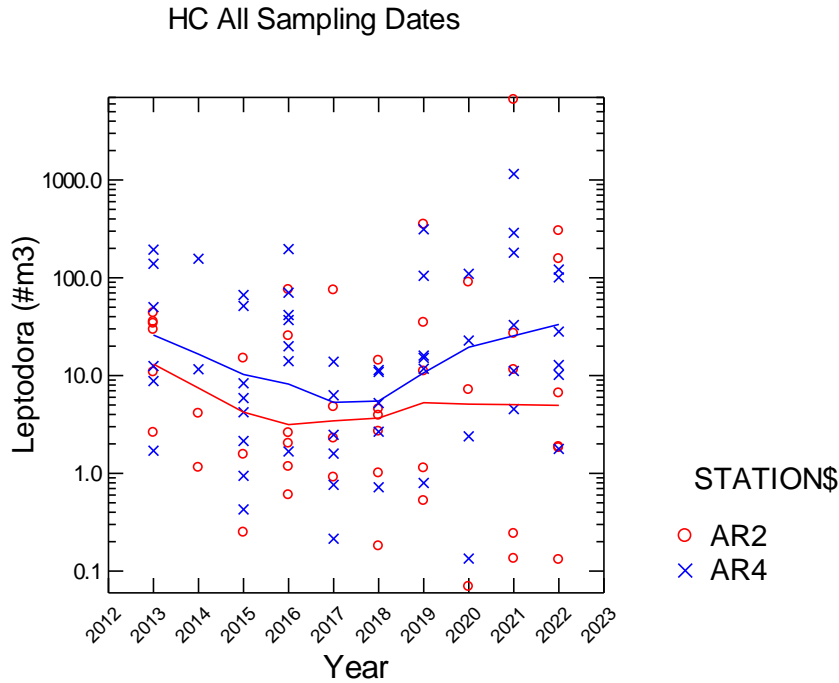


Figure 202. Scatterplots comparing values of *Leptodora* among over the years.

Leptodora is a large predacious cladoceran which occurs consistently in the study area (Figure 202). Values in 2022 were among the highest observed to date, particularly at AR4 and were distinctly higher than in 2017 and 2018. Total macrozooplankton, those collected in the 202 μm net indicates that AR4 has maintained steady populations while AR2 has declined over the study period (Figure 203).

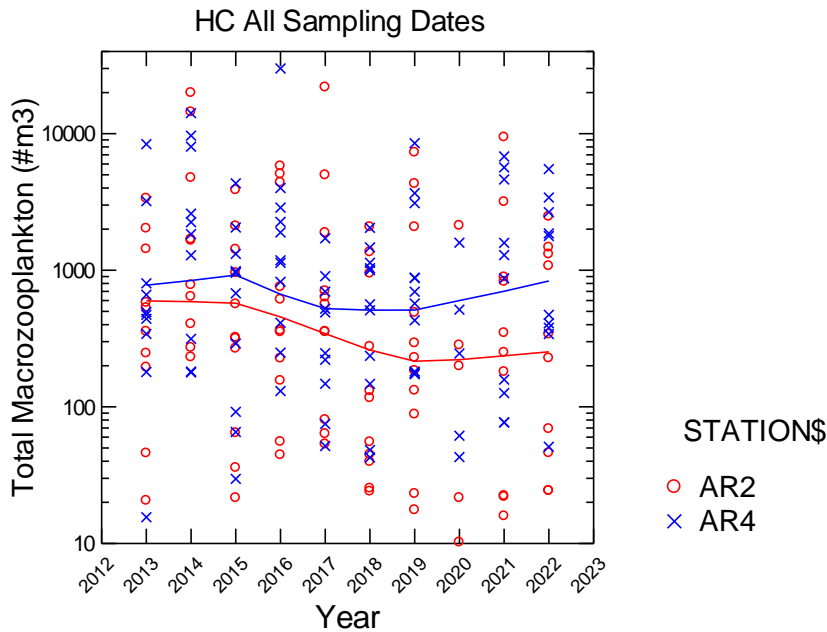


Figure 203. Scatterplots comparing values of Total Macrozooplankton over the years.

F. Ichthyoplankton: Comparison among Years

2022 marks the tenth year of our fish collections in Hunting Creek. Both trends and inter-annual variability become apparent when comparing the years of data. Total larval density is similar to 2021, but lower than previous years except for 2018 and 2020, which were poorly represented (Table 28). Although total abundance was lower, River Herring and other Clupeids remained the most abundant species similar to previous years. Interestingly, White Perch larvae was the most abundant we have seen throughout the course of this study, matching the trends in adult and juvenile fishes seen this year. Although abundances were somewhat diminished, three out of the four anadromous *Alosa* species were collected in Hunting Creek, demonstrating that this waterbody remains an important nursery habitat for these imperiled species of concern.

Table 28. Density of larvae collected all years.

Scientific Name	Common Name	2013	2014	2015	2016	2017	2018	2019	2020	2021	2022
<i>Alosa aestivalis</i>	Blueback Herring	61.69	200.35	382.05	91.54	205.29	56.54	271.72	4.89	112.14	53.27
<i>Alosa mediocris</i>	Hickory Shad	4.80	4.13	12.11	9.63	4.28	1.58	11.36	0.00	5.93	6.68
<i>Alosa pseudoharengus</i>	Alewife	139.80	57.71	265.97	78.52	81.75	38.85	214.34	3.65	103.19	48.94
<i>Alosa sapidissima</i>	American Shad	0.12	1.32	0.61	1.97	2.80	0.15	0.00	0.00	0.35	0.00
<i>Alosa</i> sp.	unk. Alosa	0.00	18.49	0.00	0.00	0.00	0.00	0.00	0.00	0.17	0.00
<i>Carassius auratus</i>	Goldfish	56.78	0.89	0.00	0.30	7.02	0.00	0.00	0.00	0.00	0.00
<i>Carpionidae</i>	Quillback	0.00	0.00	0.00	0.78	0.00	0.92	8.14	0.00	0.19	0.00
Catostomidae	unk.	0.00	0.00	0.00	0.00	0.00	0.00	0.17	0.00	0.00	0.00
Centrarchidae	unk.	0.00	0.00	0.00	0.13	0.00	0.00	0.00	0.00	0.00	0.00
Clupeidae	unk.	422.94	781.67	444.54	175.5	193.3	129.35	169.13	5.55	152.75	82.00
Cyprinidae	unk.	1.14	0.00	0.59	0.00	0.00	0.00	0.00	0.00	0.00	0.13
<i>Cyprinus carpio</i>	Carp	0.00	0.00	0.00	0.00	2.98	0.00	0.00	0.00	0.00	0.00
<i>Dorosoma cepedianum</i>	Gizzard Shad	438.39	381.85	592.25	221.5	293.5	83.18	1999.48	0.98	172.51	153.09
Eggs	eggs	0.16	3.09	2.69	17.80	25.66	11.17	62.25	0.00	0.00	0.00
<i>Enneacanthus gloriosus</i>	Bluespotted Sunfish	0.00	0.24	0.00	0.00	0.00	0.00	0.00	0.00	0.00	0.00
<i>Etheostoma olmstedii</i>	Tessellated Darter	0.00	0.00	0.00	0.13	0.00	0.00	0.00	0.00	0.00	0.00
<i>Etheostoma</i> sp.	unk. darter species	0.00	0.00	0.00	0.00	0.00	0.00	0.19	0.00	0.00	0.00
<i>Fundulus diaphanus</i>	Banded Killifish	0.00	0.00	0.00	0.00	0.50	0.00	0.00	0.00	0.00	0.00
<i>Hybognathus regius</i>	E. Silvery Minnow	0.00	0.00	0.00	0.00	0.50	0.00	0.19	0.00	0.00	0.63
<i>Lepisosteus osseus</i>	Longnose Gar	0.00	0.00	0.00	0.00	0.25	0.00	0.00	0.00	0.00	0.00
<i>Lepomis cyanellus</i>	Green Sunfish	0.00	0.00	0.00	0.41	0.50	0.00	0.00	0.37	0.00	0.00
<i>Lepomis gibbosus</i>	Pumpkinseed	0.00	0.00	0.00	1.62	0.99	0.39	0.35	0.00	0.00	0.00
<i>Lepomis macrochirus</i>	Bluegill	0.00	0.00	0.00	0.00	0.50	0.00	0.00	2.38	0.00	0.00
<i>Lepomis</i> sp.	unk. sunfish	0.60	2.83	0.49	0.00	8.23	0.00	0.19	0.31	0.19	1.12
<i>Menidia beryllina</i>	Inland Silverside	2.48	3.32	1.98	20.36	60.78	0.66	1.21	1.78	4.89	12.40
<i>Morone americana</i>	White Perch	0.00	5.90	15.93	8.60	17.54	15.48	66.30	0.14	33.67	133.47
<i>Morone saxatilis</i>	Striped Bass	0.00	4.02	0.00	1.10	7.71	0.00	0.00	0.00	0.00	0.00
<i>Morone</i> sp.	unk. perch/bass	39.06	43.46	4.32	14.11	3.71	0.00	0.00	0.00	0.00	0.00
<i>Notemigonus crysoleucas</i>	Golden Shiner	0.00	0.84	0.00	0.00	0.00	0.00	0.00	0.00	0.00	0.00
<i>Notropis hudsonius</i>	Spottail Shiner	0.00	0.00	0.00	0.39	2.48	4.94	0.23	0.00	0.00	0.00
<i>Perca flavescens</i>	Yellow Perch	38.22	1.41	0.00	0.65	0.50	0.74	0.73	0.00	0.58	0.00
<i>Pomoxis</i> sp.	unk. crappie	0.00	0.00	0.00	0.00	0.00	0.00	0.00	0.00	0.00	0.63
<i>Strongylura marina</i>	Atlantic Needlefish	0.00	0.12	0.00	0.00	0.13	0.00	0.00	0.00	0.00	0.00
Unidentified	unidentified	11.45	84.35	27.42	34.65	84.23	6.43	126.74	1.03	10.77	32.99
Total		1218	1596	1751	680	1005	350	2933	21	597	525

G. Adult and Juvenile Fish: Comparison among Years

The total number of adult and juvenile fishes collected in 2022 was the most we have collected in the decade that this project has run. Once again, White Perch was the dominant species collected, continuing a trend that started in 2019 (Table 29). Banded Killifish abundances were higher than 2021, but lower than early years when SAV was present in Hunting Creek. In 2022, we collected our highest numbers of White Perch to date, which was driven by high abundances in our August collections. Similar to 2021, we also collect a large number of *Alosa sp.* All four *Alosa* species (Blueback Herring, Alewife, Hickory Shad, and American Shad) were also collected in our trawl and seine surveys, demonstrating the importance of Hunting Creek as nursery habitat for these imperiled species. Continued monitoring of these trends will indicate if the moratorium on fishing has resulted in population level responses and the data we gather as part of this long-term monitoring will directly contribute to fishery management decisions.

The continued low Banded Killifish numbers, coupled with the elevated White Perch abundance is likely a result of the SAV loss in 2018 that has not reestablished in the system. Looking at our long-term trends in species percentages, it is clear that the community was dominated by Banded Killifish (Figure 204) prior to this loss, but now remains dominated by White Perch (Figures 204, 206, 207). The opposite trend was seen in the longer survey record of Gunston Cove (Jones and De Mutsert 2018), which seems mostly due to SAV resurgence since 2005. The decline in SAV cover in Hunting Creek in recent years could be a reason for the decreasing Banded Killifish abundances and increasing White Perch abundances. This loss of SAV may also be favoring other open water species like the Blue Catfish (Figure 205), which was once again present in high numbers this year, when compared to earlier collection seasons (Table 29, Figure 205). Investigating the impacts of this invasive species on the fish community assemblage would be a valuable avenue for future work. Furthermore, predation studies to determine if Blue Catfish are predated upon the imperiled River Herring should also be conducted to protect these imperiled species.

Table 29. Abundances of species collected all years.

Scientific Name	Common Name	2013	2014	2015	2016	2017	2018	2019	2020	2021	2022
<i>Alosa aestivalis</i>	Blueback Herring	16	8	12	29	0	0	33	0	291	38
<i>Alosa mediocris</i>	Hickory Shad	0	0	0	0	0	0	8	4	0	1
<i>Alosa pseudoharengus</i>	Alewife	6	23	28	12	0	14	69	113	26	7
<i>Alosa sapidissima</i>	American Shad	208	32	163	19	2	2	12	0	2	10
<i>Alosa sp.</i>	unk. Alosa species	299	8	55	12	3	433	822	18	89	560
<i>Ameiurus catus</i>	White Bullhead	0	0	0	2	0	8	1	4	2	3
<i>Ameiurus natalis</i>	Yellow Bullhead	0	0	0	0	0	0	4	0	0	0
<i>Ameiurus nebulosus</i>	Brown Bullhead	3	2	3	3	5	13	2	1	0	0
<i>Anchoa mitchilli</i>	Bay anchovy	69	70	7	0	0	0	86	8	22	47
<i>Anguilla rostrata</i>	American Eel	1	3	2	0	0	1	2	0	0	0
<i>Brevoortia tyrannus</i>	Atlantic Menhaden	0	0	0	0	0	0	30	0	12	0
<i>Carassius auratus</i>	Goldfish	20	39	2	9	107	1	0	0	2	1
<i>Carpionodes cyprinus</i>	Quillback	9	19	2	0	0	0	72	13	6	2
<i>Catostomus commersonii</i>	White Sucker	0	0	0	0	0	0	0	0	0	1
<i>Cyprinella spiloptera</i>	Spotfin shiner	0	0	1	0	0	0	0	0	0	0
<i>Cyprinus carpio</i>	Carp	0	3	1	14	3	2	4	0	5	5
<i>Dorosoma cepedianum</i>	Gizzard Shad	5	1	3	0	0	50	52	71	22	200
<i>Dorosoma petenense</i>	Threadfin Shad	0	0	0	0	0	0	0	24	29	11
<i>Erneacanthus gloriosus</i>	Bluespotted Sunfish	0	0	0	0	47	0	0	0	0	0
<i>Erimyzon oblongus</i>	Creek Chubsucker	0	0	0	0	0	1	0	0	0	0
<i>Etheostoma olmstedi</i>	Tessellated Darter	292	49	39	8	35	221	30	11	29	24
<i>Fundulus diaphanus</i>	Banded Killifish	1798	2382	2723	1547	769	777	424	147	343	516
<i>Fundulus heteroclitus</i>	Mummichog	53	152	174	16	62	20	14	4	50	162
<i>Gambusia holbrooki</i>	Mosquitofish	11	69	19	0	1	0	7	6	1	0
<i>Hybognathus regius</i>	Eastern Silvery Minnow	0	6	31	4	40	14	6	0	0	3
<i>Ictalurus furcatus</i>	Blue Catfish	12	4	4	1	6	57	93	61	56	42
<i>Ictalurus punctatus</i>	Channel Catfish	0	0	2	0	0	2	2	3	0	0
<i>Lepisosteus osseus</i>	Longnose Gar	0	0	3	1	1	0	0	0	1	0
<i>Lepomis auritus</i>	Redbreast Sunfish	0	0	1	2	0	0	0	0	0	0
<i>Lepomis cyanellus</i>	Green Sunfish	0	0	2	0	7	0	0	0	0	0
<i>Lepomis gibbosus</i>	Pumpkinseed	6	17	11	22	180	100	22	6	4	17
<i>Lepomis macrochirus</i>	Bluegill	12	52	21	20	188	81	5	1	6	3
<i>Lepomis megalotis</i>	Longear Sunfish	0	0	0	0	1	0	0	0	0	0
<i>Lepomis microlophus</i>	Redear Sunfish	6	11	5	8	0	0	0	0	0	0
<i>Lepomis sp.</i>	unk. sunfish	5	12	5	85	169	2	4	1	0	0
<i>Menidia beryllina</i>	Inland Silverside	15	6	73	210	124	120	86	4	44	68
<i>Micropogonias undulatus</i>	Atlantic Croaker	1	0	0	0	0	0	0	0	1	0
<i>Micropterus punctulatus</i>	Spotted Bass	1	0	0	0	0	0	0	0	0	0
<i>Micropterus salmoides</i>	Largemouth Bass	8	12	9	11	72	24	13	6	6	12
<i>Micropterus sp.</i>	unk. bass species	1	0	0	0	0	0	0	0	0	0
<i>Morone americana</i>	White Perch	574	107	693	57	439	675	1364	2920	1378	6709
<i>Morone saxatilis</i>	Striped Bass	2	0	2	5	8	2	6	0	2	8
<i>Morone sp.</i>	unk. perch/bass species	0	1	0	0	0	0	0	0	13	0
<i>Moxostoma erythrum</i>	Golden Redhorse	0	0	0	0	0	0	3	0	0	0
<i>Moxostoma macrolepidotum</i>	Shorthead Redhorse	0	0	0	0	0	1	0	0	0	1
<i>Moxostoma sp.</i>	unk. redhorse species	0	0	0	0	0	0	0	0	0	1
<i>Notemigonus crysoleucas</i>	Golden Shiner	2	3	13	2	2	5	1	0	0	1
<i>Notropis hudsonius</i>	Spotail Shiner	338	666	87	17	13	125	113	96	69	424
<i>Perca flavescens</i>	Yellow Perch	22	16	7	7	2	37	6	0	0	0

<i>Pomoxis nigromaculatus</i>	Black Crappie	0	0	4	1	0	3	4	0	0	1
<i>Pylodictis olivaris</i>	Flathead Catfish	0	0	0	0	0	0	0	1	0	0
<i>Sander vitreus</i>	Walleye	0	0	0	0	0	1	0	0	0	0
<i>Semotilus atromaculatus</i>	Creek Chub	0	0	0	0	0	0	0	0	0	3
<i>Strongylura marina</i>	Atlantic Needlefish	2	4	3	0	9	1	2	0	1	0
<i>Trinectes maculatus</i>	Hogchoker	0	0	0	0	0	0	0	0	1	1
Unidentified	unidentified	2	0	0	0	0	0	0	0	0	0
Total		3798	3777	4210	2125	2294	2794	3402	3524	2512	8882

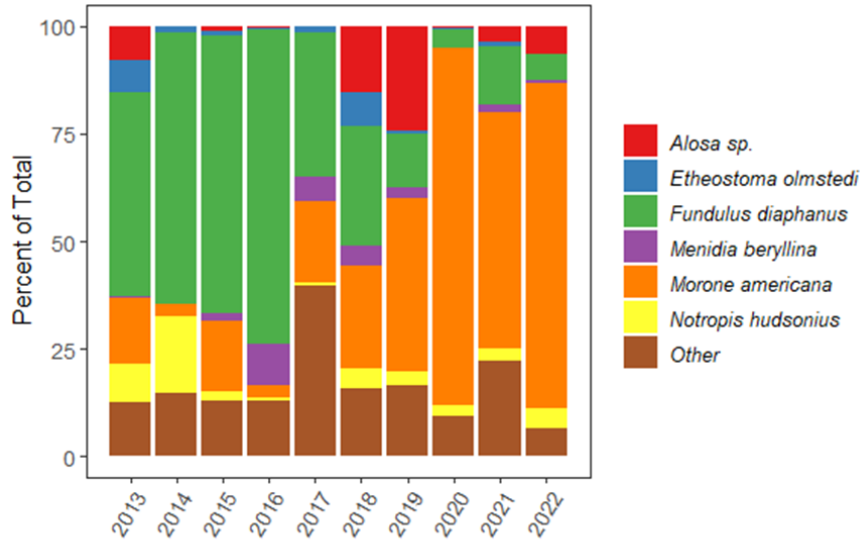


Figure 204. Percentage of total of dominant species collected in all years.

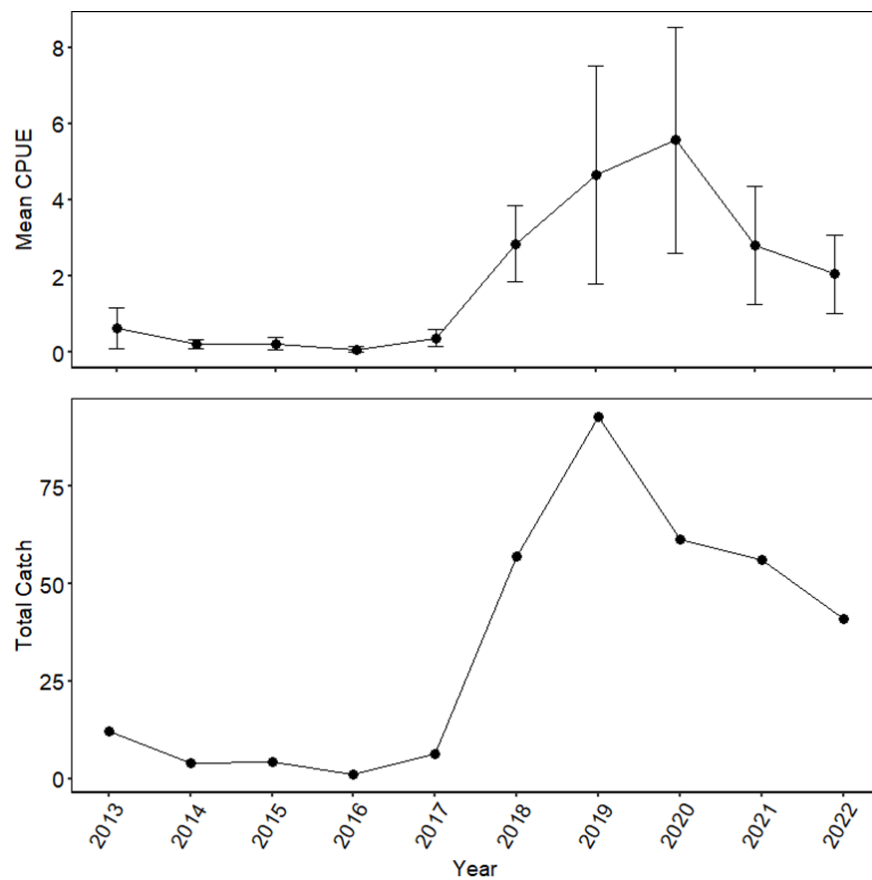


Figure 205. Mean \pm 1 SE (top) catch per unit effort (CPUE) and total catch (bottom) of Blue Catfish from trawls for all years of study.

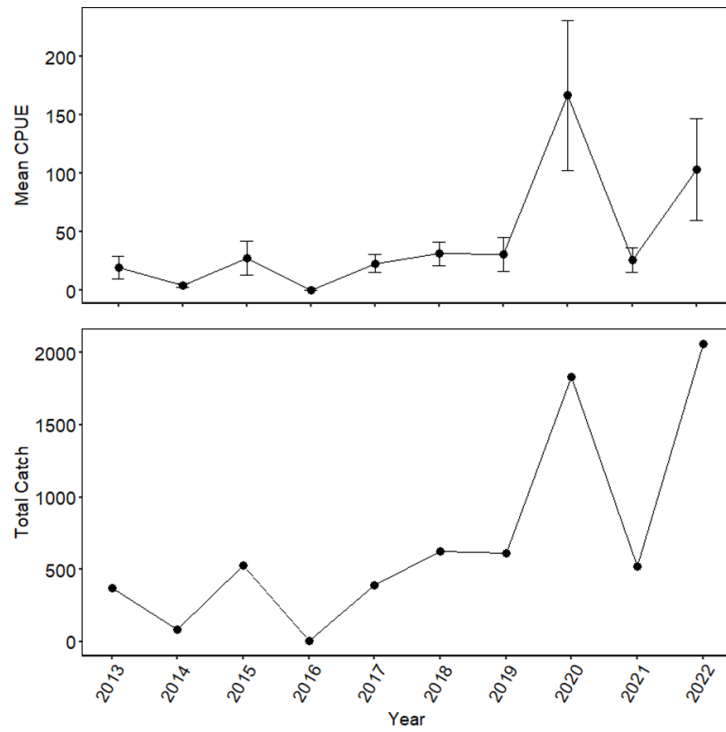


Figure 206. Mean ± 1 SE (top) catch per unit effort (CPUE) and total catch (bottom) of White Perch from trawls for all years of study.

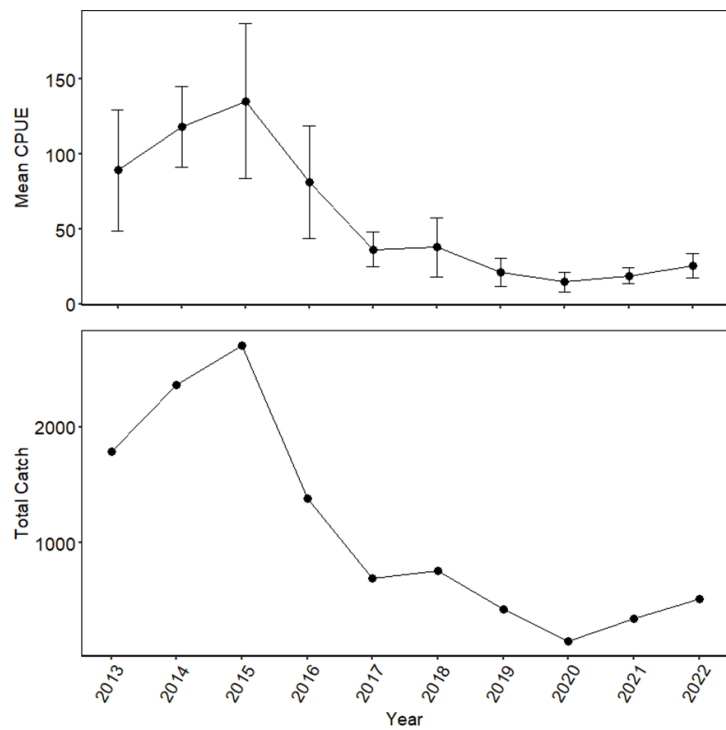


Figure 207. Mean ± 1 SE (top) catch per unit effort (CPUE) and total catch (bottom) of Banded Killifish from seines for all years of study.

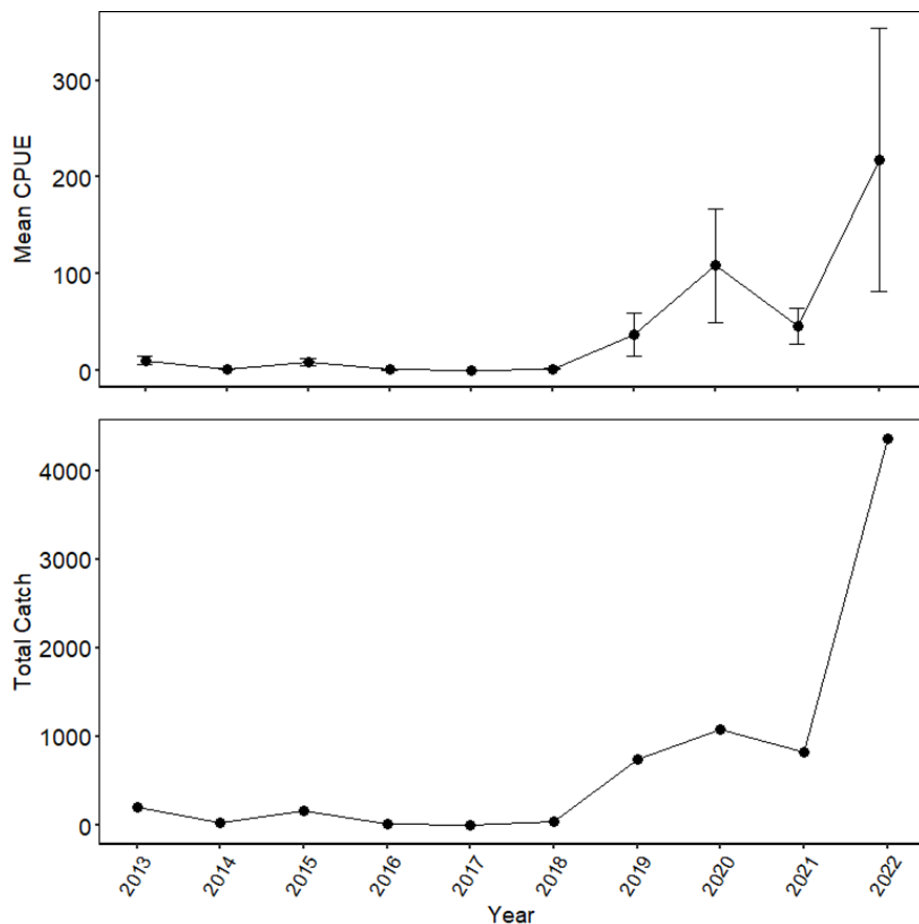


Figure 208. Mean \pm 1 SE (top) catch per unit effort (CPUE) and total catch (bottom) of White Perch from seines for all years of study.

In 2022, we collected at least 29 different species, an improvement over our 2021 collections. The Simpson's Index of Diversity (calculated as $1 - (\sum (n_i/N)^2)$) was calculated for all years based on adult and juvenile abundances (Figure 209). Note that in the 2016 report the Simpson's index (D) was reported, in which communities with higher diversity or evenness approach zero. In the reports since 2016 we calculated the Simpson's Index of Diversity, which is $1 - D$. In this index the communities with higher diversity have higher values (approaching 1) which is more intuitive to interpret. While evenness was reduced each year of sampling before 2017, 2017 and 2018 showed high Simpson's Index of Diversity values, with 2019 slightly lower but still very close to that (Figure 209). 2020 remains the lowest on record with a value of 0.309, which should not be interpreted as a reflection of true diversity. However, in 2022, our Simpson's diversity index was only 0.419, the second lowest in the last decade, driven by the high abundance of White Perch this year (Figure 209, Table 30).

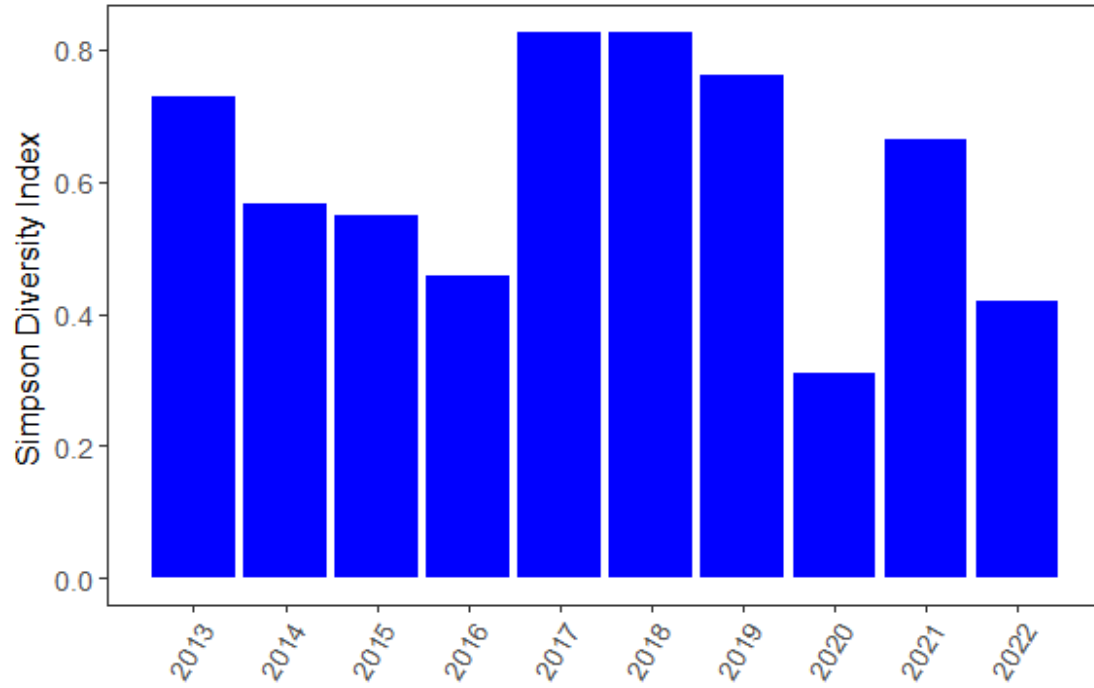


Figure 209. Simpson Diversity Index of fish species collected in Hunting Creek all years.

Table 30. Simpsons Diversity Index Values for each year of the study.

Year	Simpson
2013	0.730
2014	0.567
2015	0.550
2016	0.457
2017	0.825
2018	0.827
2019	0.761
2020	0.309
2021	0.663
2022	0.419

H. Submersed Aquatic Vegetation: Comparison among Years

According to annual reports of the Virginia Institute of Marine Science (VIMS) SAV Monitoring Program (<http://web.vims.edu/bio/sav/maps.html>), virtually the entire surface area of the Hunting Creek embayment was covered with submersed aquatic vegetation during the first five years of this study (2013-2017). In 2018 there was a severe decline in SAV coverage. Furthermore, due to the frequent rainfall events and resulting poor water clarity, VIMS was unable to conduct the aircraft remote sensing so we were not able to make direct comparisons of 2018 coverage with 2016 and 2017. In 2019 VIMS was able to obtain aerial imagery which appears to show no SAV growing in Hunting Creek. In 2016-2022 mapping of species was done via boat in association with the water quality mapping surveys (Table 31). In 2017 the native SAV species *Ceratophyllum demersum* was substantially more abundant than the exotic species *Hydrilla verticillata* in contrast to 2016 when they had a similar abundance. The boat transects studies in 2018-2022 confirmed the severe dieback has persisted. Transects were done in 2022 as well with no SAV species observed.

Table 31. Average Density of Submersed Aquatic Vegetation Species in Transects.

Average included all sites with water depth less than or equal to 2 m. 2017-2021. Density scale: 0 (absent) – 4 (very abundant).

Taxon Scientific Name	Taxon Common Name	Average Density per sample by SAV Species – 2020/21	
		Aug 21, 2020	Aug 9, 2021
<i>Ceratophyllum demersum</i>	Coontail	0	0
<i>Heteranthera dubia</i>	Water Stargrass	0	0
<i>Hydrilla verticillata</i>	Hydrilla	0	0
<i>Najas guadalupensis</i>	Southern Naiad	0	0
<i>Najas minor</i>	Spiny Naiad	0	0
Various	Filamentous algae	0	0

Taxon Scientific Name	Taxon Common Name	Average Density per sample by SAV Species - 2019	
		July 16	August 19
<i>Ceratophyllum demersum</i>	Coontail	0	0
<i>Heteranthera dubia</i>	Water Stargrass	0	0
<i>Hydrilla verticillata</i>	Hydrilla	0.04	0
<i>Najas guadalupensis</i>	Southern Naiad	0	0
<i>Najas minor</i>	Spiny Naiad	0	0
Various	Filamentous algae	0	0

Taxon Scientific Name	Taxon Common Name	Average Density per sample by SAV Species - 2018	
		July 16	August 28
<i>Ceratophyllum demersum</i>	Coontail	0.20	0.10
<i>Heteranthera dubia</i>	Water Stargrass	0.07	0
<i>Hydrilla verticillata</i>	Hydrilla	0.43	0.27

<i>Najas guadalupensis</i>	Southern Naiad	0.02	0.07
<i>Najas minor</i>	Spiny Naiad	0.07	0
Various	Filamentous algae	0.09	0

Average Density per sample by SAV
Species - 2017

Taxon Scientific Name	Taxon Common Name	July 12	August 10
<i>Ceratophyllum demersum</i>	Coontail	1.76	1.74
<i>Heteranthera dubia</i>	Water Stargrass	0.19	1.19
<i>Hydrilla verticillata</i>	Hydrilla	0.78	0.32
<i>Najas guadalupensis</i>	Southern Naiad	0.20	0
<i>Najas minor</i>	Spiny Naiad	0.45	0.21
Various	Filamentous algae	0.03	0.43

I. Benthic Macroinvertebrates: Comparison among Years

River and Embayment Samples

Comparison among Years: As we expected, the macroinvertebrate community from the embayment of Hunting Creek has been dominated by Oligochaete worms across all sites and years (Figure 210). However, if Annelids are removed and we examine the other dominant taxon groups, we see a few different trends in dominant taxa between the three Hunting Creek sites across years (Figure 211). In general, AR2 is dominated by the insect larvae of Chironomids (midges), AR3 is dominated by Gastropods (mostly composed of the invasive Japanese mystery snails), Chironomids, and Gammarid amphipods, and AR4 is dominated by Platyhelminthes flatworms and Gammarid amphipods. AR2 is the site closest to the outflow from Hunting Creek, and across years, this site is mostly dominated by Chironomids (2013, 2014, 2018, 2019, 2020, 2021, and 2022), but some years Gammarid amphipods (2016 and 2017) and Gastropods (2015) dominate (Figure 212). The AR4 site is the closest to the Potomac River and has been consistently dominated by Gammarid amphipods between 2014 and 2019 and 2021; however, in 2020 and most recently the 2022 summer, this site was dominated by the Turbellarians (flatworms). Only in 2013 were the samples dominated by Chironomid insect larvae (Figure 212). The AR4 site also has the highest relative abundances of Bivalvia (mostly driven by the invasive Asian clam *Corbicula fluminea*) and Isopoda (Crustacean) compared to the other two sites. AR4 receives higher water flow and movement, which many species of Bivalvia require, and may help explain why there are higher abundances of Bivalvia located closer to the Potomac River. The site with the most fluctuations in percent contributions of macroinvertebrate taxa was AR3, which is located in the middle of the embayment. In any given year, dominant macroinvertebrate groups change from Gastropods (2013, 2015, and 2016) to Gammarid amphipods (2014, 2017, 2018, and 2020) or Chironomid insect larvae (2019, 2021, and 2022). AR3 is also the only site where Gastropods dominate the community composition frequently. This site is probably influenced by both the Potomac River, through the daily movement of the tidal freshwater water body, and by the outfall of Hunting Creek, which moves nutrients and sediments from terrestrial sources. Only in a few years do AR2 and AR3 share the same

dominant taxa; in 2015, they were both dominated by Gastropods (mostly composed of the invasive Japanese mystery snails), in 2017 by Gammarid amphipods, and in 2019, 2021, and 2022 by Chironomid insect larvae. In comparison, AR4 seems to show different patterns of dominance than either of the other two sites further in the embayment. The relative importance of both of these waterbodies on determining benthic macroinvertebrate community structure probably also varies annually due to climatic events.

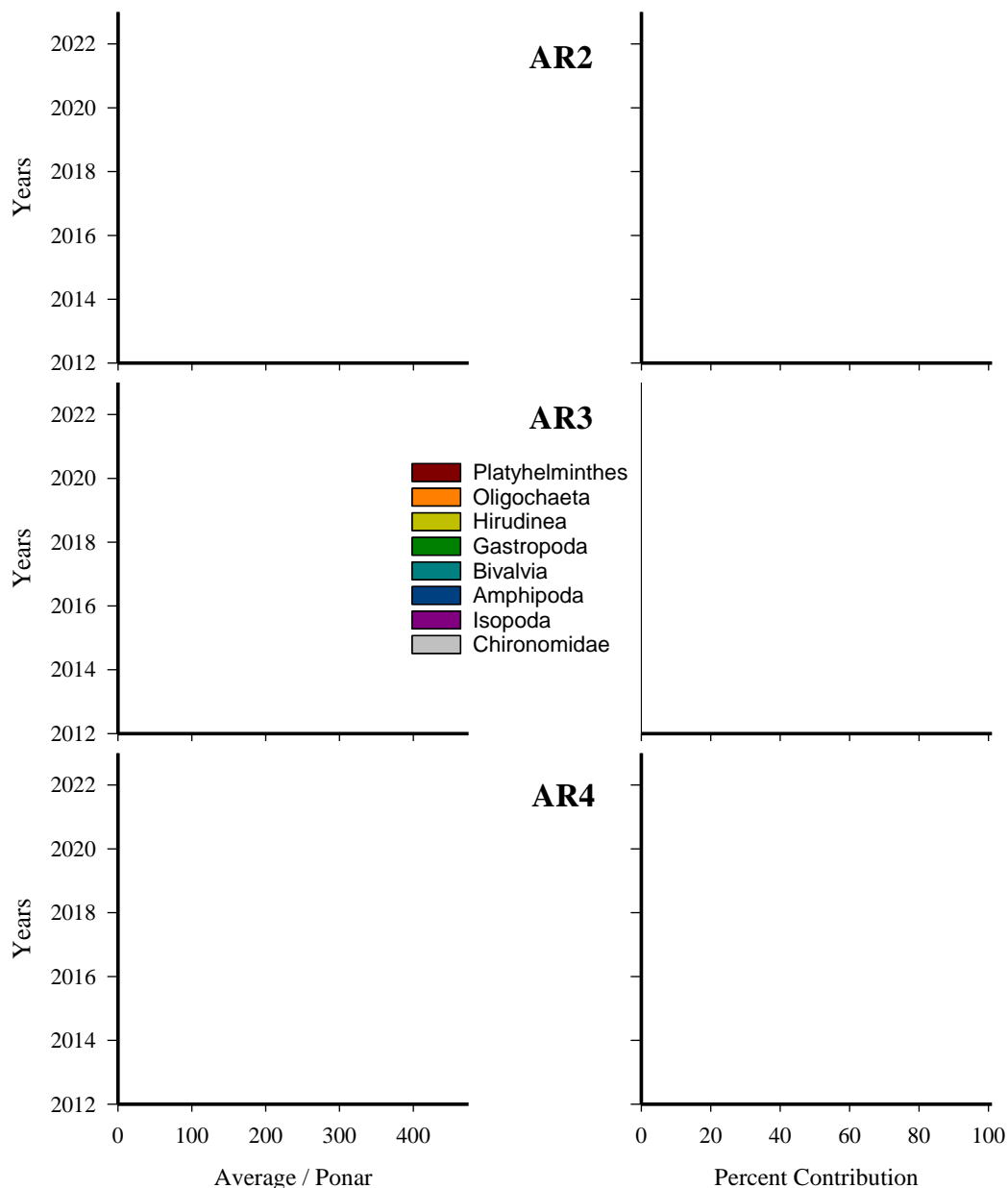


Figure 210. Average number per ponar sample (Left) and percent contribution (Right) of the eight dominant benthic invertebrate taxa in Hunting Creek embayment samples collected between 2013 and 2022 separated by site and year. Note the dominance of the Oligochaeta (worms).

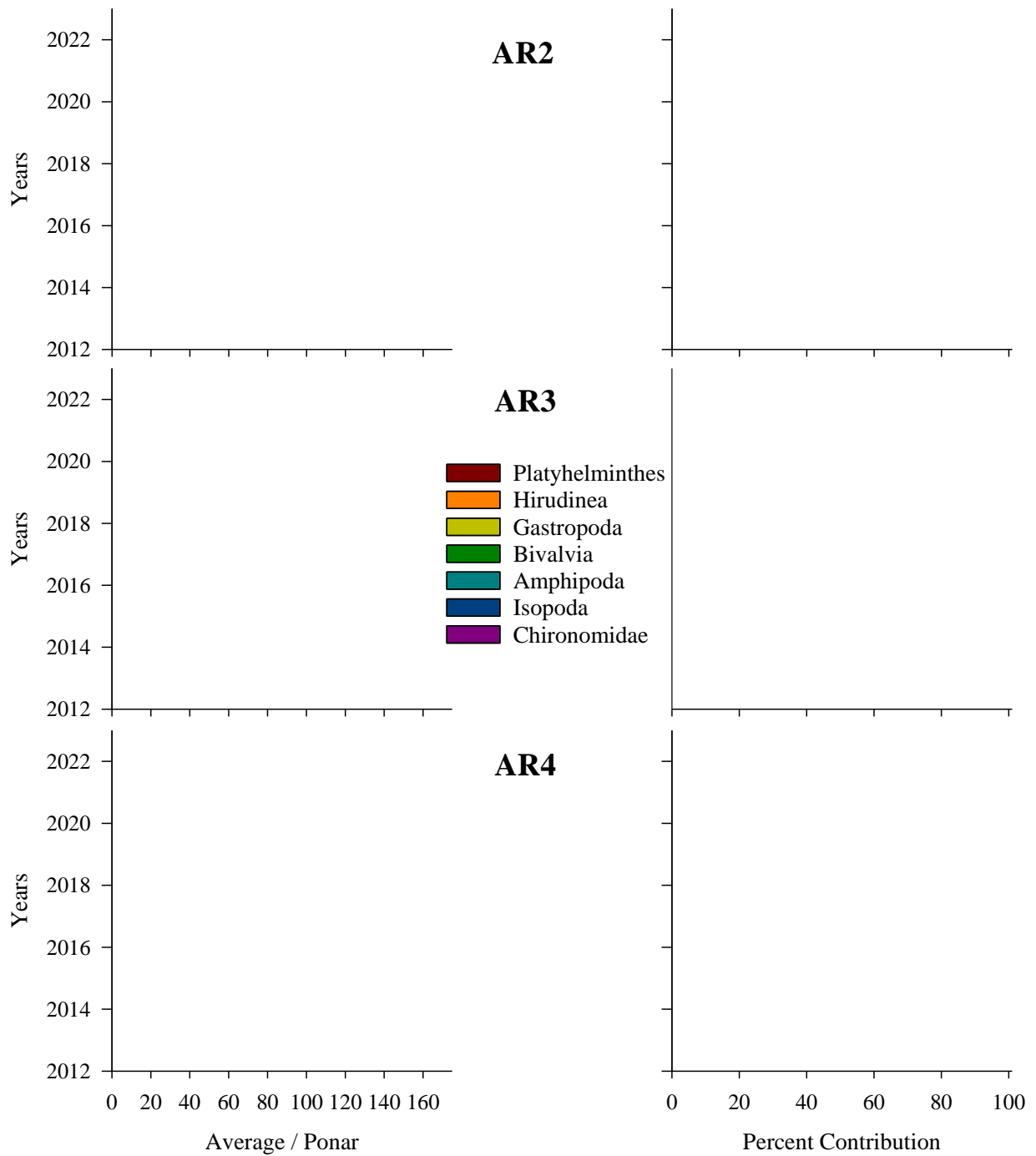


Figure 212. Without Oligochaeta, average number per ponar sample (Left) and percent contribution (Right) of the dominant benthic invertebrate taxa in Hunting Creek embayment samples collected between 2013 and 2022 separated by site and year.

Tributary Samples

Comparison among Years: We have been collecting benthic macroinvertebrate samples from the original six streams emptying into Hunting Creek since 2016. Taylor Run, Timber Branch, and Pike Branch are excluded from the analyses here, as Taylor Run and Timber Branch were first sampled in 2018 and Pike Branch in 2022. Looking across all sites and years, the taxa that dominates are members of the Insecta family Hydropsychidae. They are the most dominant group 40% of the time across all years and sites. Members within this family are net-spinning caddisflies, which live in debris and under stones and spin concave silken nets that face upstream to capture floating or swimming prey. This year, the majority of sites were dominated by Hydropsychidae (Backlick Run, Cameron Run, Holmes Run 1, and Turkeycock Run). The next most dominant group across all sites and years are members of the Insecta family Chironomidae (26% across all years and sites), known as midges. Chironomid larvae are filter-feeders and often live in tubes in the mud. Cameron Run was dominated by Chironomidae in 2022. Other macroinvertebrate groups can dominate a site during particular years. For example, Oligochaetes (worms) have been the most frequently encountered group at Cameron Run during 2017 and at Holmes Run-1 and Turkeycock Run in 2018. Turbellarians (flatworms) have only been the most dominant group at Holmes Run-1 during 2016 and at Turkeycock Run in 2019. Members of the Insecta family Philopotamidae and Baetidae are rarely the most dominant group at a site; although Philopotamidae were the most frequently encountered group at Indian Run in 2019 and 2021 (accounting for 43% of organisms counted), Cameron Run in 2020 (41% of organisms counted), and Holmes Run 2 in 2021. In general, across all years, Cameron Run is dominated by Chironomidae, and both Holmes Run sites are dominated by Hydropsychidae. Backlick Run is dominated by either Chironomidae or Hydropsychidae. Depending on the year, Indian Run fluctuates in being dominated by either of the two Trichopteran families – either Hydropsychidae or Philopotamidae. Turkeycock Run is an interesting site, as it has been dominated by all of the groups, except the Trichopteran family Philopotamidae, at some point over the last seven years of sampling. All of these sites are probably influenced by differences in the types and amounts of nutrients and sediments moving from terrestrial sources, the flow of water, and anthropogenic impacts to the system. The relative importance of a variety of abiotic factors on determining benthic macroinvertebrate community structure probably varies annually, and even monthly, due to climatic events. Therefore, site-level trends may be apparent with continued annual sampling.

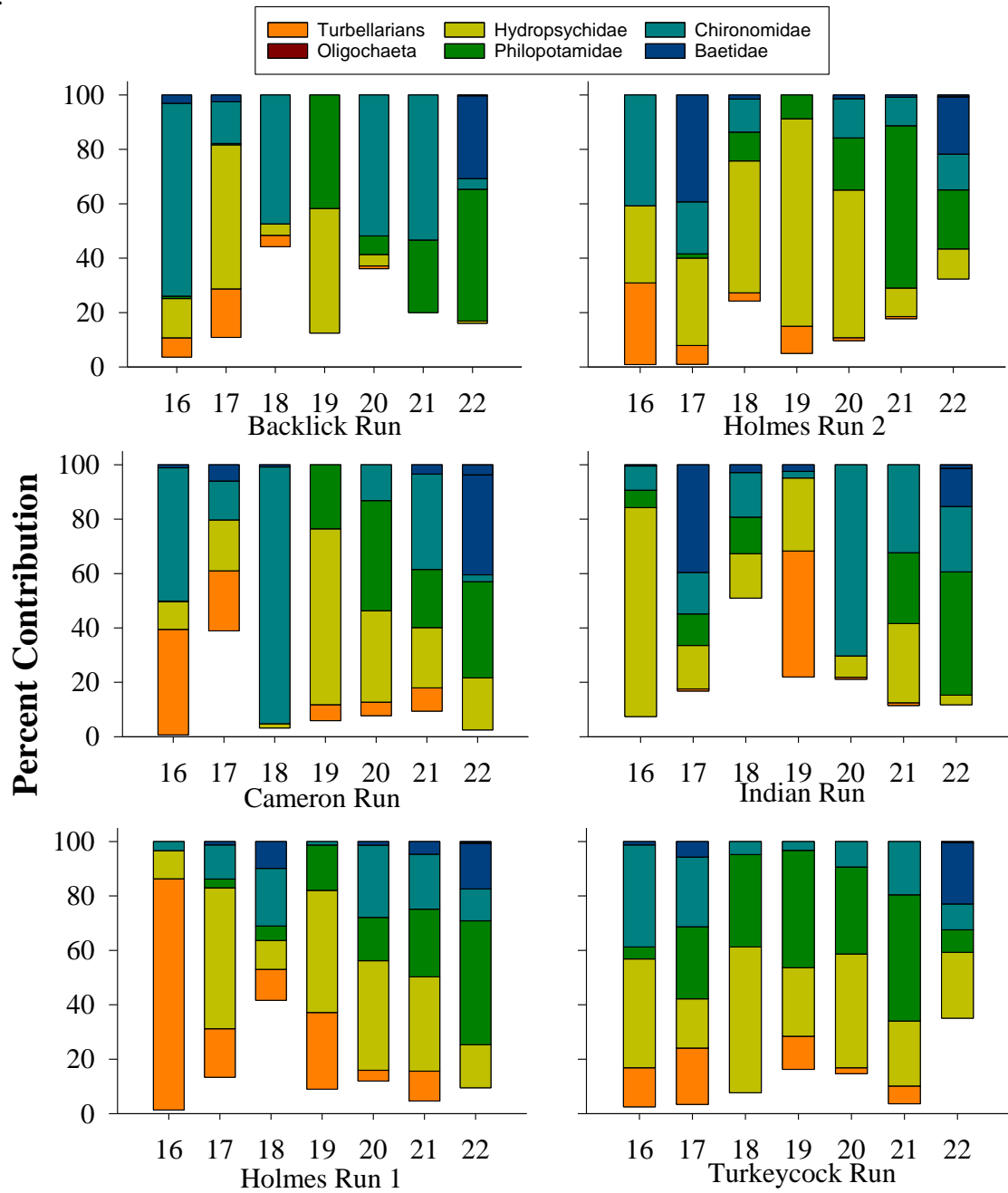


Figure 213. Percent contribution of of the six dominant benthic invertebrate taxa in tributary kick samples collected between 2016 and 2022 separated by site and year.

LITERATURE CITED

- Bigelow, H.B. and W.C.Schroeder. 1953. Fishes of the Gulf of Maine. Fishery bulletin No. 74, Vol. 53. U.S. Government Printing Office. Washinton, D.C. 577 pp.
- Carter, V., P.T. Gammon, and N.C. Bartow. 1983. Submersed Aquatic Plants of the Tidal Potomac River. Geological Survey Bulletin 1543. U.S. Geological Survey. 63 pp.
- Chesapeake Bay Program. 2006 Ambient water quality criteria for dissolved oxygen, water clarity, and chlorophyll *a* for the Chesapeake Bay and its tidal tributaries. 2006 Addendum. Downloaded from Bay Program website 10/13/2006.
- Cummings, H.S., W.C. Purdy, and H.P. Ritter. 1916. Investigations of the pollution and sanitary conditions of the Potomac watershed. Treasury Department, U.S. Public Health Service Hygienic Laboratory Bulletin 104. 231 pp.
- Dahlberg, M.D. 1975. Guide to coastal fishes of Georgia and nearby states. University of Georgia Press. Athens, GA 187 pp.
- Douglass, R.R. 1999. A Field Guide to Atlantic Coast Fishes: North America (Peterson Field Guides). Houghton Mifflin Harcourt, Boston. 368 pp.
- Eddy, S. and J.C. Underhill. 1978. How to know the freshwater fishes. 3rd Ed. W.C. Brown Co. Dubuque, IA. 215 pp.
- Froese, R. and D. Pauly (Eds.). 2012. Fish Base. World Wide Web electronic publication. www.fishbase.org, version (04/2012).
- Hildebrand and Schroeder. 1928. Fishes of the Chesapeake Bay. U.S. Bureau of Fisheries Bulletin 53, Part 1. Reprinted 1972. T.F.H. Publishing, Inc. Neptune, NJ. 388 pp.
- Hogue, J.J, Jr., R.Wallus, and L.K. Kay. 1976. Preliminary guide to the identification of larval fishes in the Tennessee River. Technical Note B19. Tennessee Valley Authority. Knoxville, TN.
- Huntley, M., K. Tande, and H.C. Eilertsen. 1987. On the trophic fate of *Phaeocystis pouchetii* (Hariot). Grazing rates of *Calanus hyperboreus* (Kroyer) on diatoms and different size categories of *Phaeocystis pouchetii*. J. Exp. Mar. Biol. Ecol. 110: 197-212.
- Islam, S. 2001. Seasonal dynamics of micro-, nanno-, and picoplankton in the tidal freshwater Potomac River in and around Gunston Cove. Ph.Dissertation. George Mason University. 127 pp.
- Jenkins, R.E. and N.M. Burkhead. 1994. The freshwater fishes of Virginia. American Fisheries Society. Washington, DC. 1080 pp.
- Jones, P.W., F.D. Martin, and J.D. Hardy, Jr. 1978. Development of fishes of the Mid-Atlantic bight. Volumes I-VI. Fish and Wildlife Service, U.S. Department of the Interior. FWS/OBS-78/12.
- Kraus, R.T. and R.C. Jones. 2011. Fish abundances in shoreline habitats and submerged aquatic vegetation in a tidal freshwater embayment of the Potomac River. Environmental Monitoring and Assessment. Online: DOI 10.1007/s10661-011-2192-6.
- Kelso, D.W., R.C. Jones, and P.L. deFur. 1985. An ecological study of Gunston Cove - 1984-85. 206 pp.
- Lippson, A.J. and R.L. Moran. 1974. Manual for identification of early development stages of fishes of the Potomac River estuary. Power Plant Siting Program, Maryland Department of Natural Resources. PPSP-MP-13.
- Loos, J.J., W.S. Woolcott, and N.R. Foster. 1972. An ecologist's guide to the minnows of the freshwater drainage systems of the Chesapeake Bay area. Association of Southeastern

- Biologists Bulletin 19: 126-138.
- Lund, J.W.G., C. Kipling, and E.C. LeCren. 1958. The inverted microscope method of estimation algal numbers and the statistical basis of estimations by counting. *Hydrobiologia* 11: 143-170.
- Mansueti, A.J. and J.D. Hardy, Jr. 1967. Development of fishes of the Chesapeake Bay region: an atlas of egg, larvae and juvenile stages: Part 1. Natural Resources Institute. University of Maryland. 202 pp.
- Merritt, R.W. and K.W. Cummins. 1984. An introduction to the aquatic insects of North America. 2nd edition. Kendall/Hunt Publishing Co., Dubuque, IA. 722 pp.
- Pennack, R.W. 1978. Fresh-water invertebrates of the United States. 2nd ed. Wiley-Interscience. New York, NY.
- Schloesser, R.W., M.C. Fabrizio, R.J. Latour, G.C. Garman, G.C., B. Greenlee, M. Groves and J. Gartland. 2011. Ecological role of blue catfish in Chesapeake Bay communities and implications for management. *American Fisheries Society Symposium* 77:369-382.
- Scott, W.B. and E.J. Crossman. 1973. Freshwater fishes of Canada. Bulletin 184. Fisheries Research Board of Canada. Ottawa, Canada. 966 pp.
- Standard Methods for the Examination of Water and Wastewater. 1980. American Public Health Association, American Waterworks Association, Water Pollution Control Federation. 15th ed. 1134 pp.
- Thorp, J.H. and A.P. Covich, eds. 1991. Ecology and classification of North American Freshwater Invertebrates. Academic Press. San Diego, CA. 911 pp.
- Wetzel, R.G. 1983. *Limnology*. 2nd ed. Saunders. 767 pp.
- Wetzel, R.G. and G.E. Likens. 1991. *Limnological analyses*. 2nd ed. Springer-Verlag. 391 pp.

Anadromous Fish Survey Cameron Run: 2022

T. Reid Nelson

Assistant Professor, Department of Environmental Science and Policy
Potomac Environmental Research and Education Center

Introduction

Anadromous river herring and shad live as adults in the coastal ocean and return to freshwater creeks and rivers to spawn. In the mid-Atlantic region, four species are present: American Shad (*Alosa sapidissima*), Blueback Herring (*Alosa aestivalis*), Alewife (*Alosa pseudoharengus*), and Hickory Shad (*Alosa mediocris*). Two other Clupeids are semi-anadromous and spawn in Potomac River tributaries. These are Gizzard Shad (*Dorosoma cepedianum*) and Threadfin Shad (*Dorosoma petenense*). Previous reports describe the history of herring populations in the Potomac River watershed (Jones et al. 2019).

The focus of the Cameron Run fish survey is river herring, the collective name of Blueback Herring and Alewife. River herring populations have declined drastically over their range, spurring conservation efforts since 1970, which have been intensified since 2005 with implementation of moratoria. Identifying all areas used as spawning habitat by Alewife and/or Blueback Herring is an important component of their conservation. Since 1988, George Mason University researchers have focused a monitoring program on the spawning of these species in other tributaries such as Pohick Creek, Accotink Creek, and, less regularly, Dogue Creek. With this study Cameron Run was added in 2013, which has not been monitored for presence of river herring or other anadromous species by either George Mason or other fisheries biologists before the start of this study (Jim Cummins, pers. comm.). Historically, local anglers reported anadromous fishes spawning in Cameron Run (Neves et al. 1988); however, our 2013 survey provided the first confirmation of Cameron Run as River Herring spawning habitat (Alan Weaver, VDGIF, pers. comm.). Use of Cameron Run by river herring upstream from where the effluent of Alexandria Renew Enterprises enters Cameron Run signifies that the effluent does not deter river herring from using Cameron Run as spawning habitat. In 2014 we moved the collection site approximately 500 m downstream (still above the Alexandria Renew Enterprises effluent), which increased our catches, and allows us to estimate the size of the spawning population. The new location proved successful and remains our collection site.

Methods

We conducted weekly sampling trips from March 10 to May 12 in 2022. During each trip (when conditions allowed it) a hoop net was set with wings blocking the complete creek (referred to as block net) to collect adults swimming upstream, and ichthyoplankton nets were set to collect larvae floating downstream. Cross-section and flow were measured to calculate discharge, and physical parameters were measured using a handheld YSI. When heavy rainfall occurs near weekly sampling dates, we are unable to set the block nets, given that it is unsafe for our field

crew and the flashy flow of Cameron Run renders our nests useless, sweeping them away. Although this is the case, on many occasions when large block nets cannot be set, we still collect larval fish, abiotic conditions, and water quality parameters. Table 1 provides the information on which procedures were completed each sampling day in 2022. The sampling location was chosen to be upstream from the Alex Renew effluent, and downstream of the first dam in Cameron Run (Figure 1).

Table 1. Procedures completed each sampling date

Date	Block Net	Plankton	Flow
3/10/2022	No Net Set	10 mins	Yes
3/17/2022	No Net Set	10 mins	Yes
3/23/2022	No Net Set	20 mins	Yes
3/31/2022	24 hours	20 mins	Yes
4/6/2022	No Net Set	No	No
4/14/2022	24 hours	20 mins	Yes
4/21/2022	24 hours	20 mins	Yes
4/28/2022	24 hours	20 mins	Yes
5/5/2022	No Net Set	20 mins	Yes
5/12/2022	24 hours	20 mins	Yes

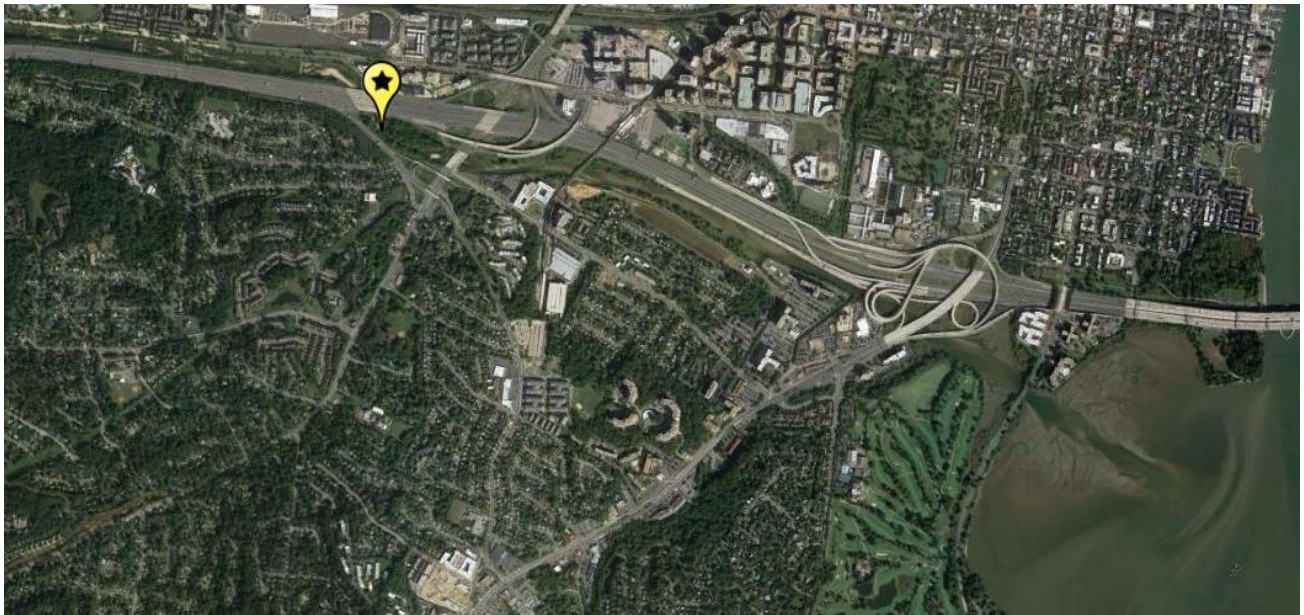


Figure 1. Sampling location Cameron Run.

We collected ichthyoplankton by setting two conical plankton net with a mouth diameter of 0.25 m and a square mesh size of 0.333 mm in the stream current for 20 minutes. To estimate water volume filtered by the net, we suspended a mechanical flow meter designed for low velocity measurements in the net opening. The number of rotations of the flow meter attached to the net opening was multiplied by 5760 and then divided by 999999 to gain volume filtered (m³) based on the correction equations provided by the General Oceanics flow meter user manual (https://www.forestry-suppliers.com/Documents/588_msds.pdf). Larval density (#/m³) per species was calculated using the following formula: Larval density (#/m³) = number of larvae in one sample (#) /volume filtered (m³).

We collected 2 ichthyoplankton samples per trip, and these were spaced out evenly along the stream cross-section. Coincident with plankton samples, we calculated stream discharge rate from measurements of stream cross-section area and current velocity using the following equation:

$$\text{Depth (m)} \times \text{Width (m)} \times \text{Velocity (m/s)} = \text{Discharge (m}^3\text{/s)}$$

We measured velocity using a handheld digital flow meter that measures flow in cm/s, which had to be converted to m/s to calculate discharge. We measured depth and current velocity at 12 to 20 locations along the cross-section. During each sampling trip, we recorded other physical parameters (water temperature, dissolved oxygen, pH, and specific conductivity) as well.

We preserved ichthyoplankton samples in 70% ethanol and transported them to the GMU laboratory for identification and enumeration. To identify larvae, we used multiple taxonomic resources: primarily Lippson & Moran (1974), Jones et al. (1978), and Walsh et al. (2005). River herring (both species) have semi-demersal eggs (tend to sink to the bottom) that are frequently adhesive. As this situation presents a significant bias, we are not treating egg abundance in the samples as a reliable estimate of egg abundance, and this is not used in population productivity estimates. We estimate total larval production (P) during the period of sampling by multiplying the larval density (m⁻³) with total discharge (m³) during the spawning period, which we assume is represented with our sampling period.

The block net was deployed once each week in the morning and retrieved the following morning (Figure 2). Fish in the block net were identified, enumerated, and measured.

Since the net was set 24 hours per week during the spawning season (1 day), and the spawning season is estimated to last 10 weeks, we approximated total abundance of spawning river herring during the spawning season by extrapolating the mean catch per day per species over the total collection season (10 weeks) as follows:

$$(\text{total spawning River Herring collected} / \text{adult spawning sampling days}) * \text{total season days (70)} \\ = \text{total abundance of spawners}$$

We assumed our total collection period to be a good approximation of the total time of the river herring spawning run.

In response to problems with animals tearing holes in our nets in previous sampling experiences, we used a fence device in front of the mouth of the net that significantly reduces this problem. The device effectively excluded wildlife such as otters and turtles, while it has slots that allowed up-running fish to be captured.



Figure 2. Hoop net deployed in new location in Cameron Run. The hedging is angled downstream in order to funnel up-migrating herring into the opening of the net.

Results and Discussion

During the sampling period, we only collected 5 Alewife across two sampling days April 14th and 21st (Table 2). Unfortunately, this low abundance of Alewife was similar to low numbers collected in pre fishing moratorium years, but we may have missed spawning events early in the season given that nets could not be set because of rain. Although we did not intercept any adult Blueback Herring this year, we did collect larval Blueback Herring and Alewife indicating that this creek was used for spawning by both species. Since the spawning populations are small and sampling variability high (for larval density, a small portion of the water column is sampled for 20 minutes per week), sampling over multiple years provides us with increasingly better estimates of the spawning population of Alewife and Blueback Herring in Cameron Run. Given that we only collected adult Alewife, we were only able to estimate the Alewife spawning population.

We collected more larvae this year than we did in 2019, unfortunately the 2020 field season was cancelled as a result of COVID-19 so we have a gap in our data for that year. In our samples, we positively identified 219 Alewife, and 11 Blueback Herring larvae (Table 3), which is almost identical to our 2019 numbers of each species respectively (211, 10). The unidentified larvae could have also been river herring potentially increasing our numbers. Once again, the collection of Blueback Herring larvae confirms that they were spawning in Cameron Run, even though we did not intercept any adults. In addition to river herring, we also collected Gizzard Shad, Goldfish, Spottail Shiners, White Perch, Common Carp, Inland Silversides, and Quillback (Table 3).

Table 2. Species collected in Cameron Run with hoop net during weekly sampling.

Date	ScientificName	CommonName	Count
2022-04-14	<i>Alosa pseudoharengus</i>	Alewife	2
2022-04-14	<i>Lepomis sp.</i>	unk. sunfish	1
2022-04-21	<i>Alosa pseudoharengus</i>	Alewife	3
	Total		6

We positively identified 710 Alewife, and 9 Blueback Herring larvae (Table 3) from our larval fish samples, collecting more total larvae than in 2021 or 2019. Additionally, the Alewife larvae we collected was roughly 3 times greater than 2021 (n = 219) or 2019 (n = 211), while Blueback Herring numbers were similar (2019 = 10, 2021 = 11). This large number of Alewife larvae couple with their first occurrence on 3-31-23, indicates that we likely missed a large pulse of spawning Alewife earlier in the season given our one day a week sampling interval and inability to sample in adverse flashy flow conditions. Some of the unidentified larvae, especially unknown Clupeids, may have also been river herring potentially increasing our numbers. Once again, the collection of Blueback Herring larvae confirms that they were spawning in Cameron Run, even though we did not intercept any adults. In addition to river herring, we also collected Spottail Shiners, White Perch, and an Inland Silverside (Table 3).

Table 3. Larvae collected in Cameron Run. Herring larvae (river herring and other clupeids) are in bold. Fish larvae too damaged for identification to species level were identified at the highest level possible. NA volume numbers represent a date of little to no flow in Cameron Run, which still resulted in fish egg and one larvae collected.

Date	Scientific Name	Common Name	Count	Volume	AveDensity
2022-03-17	Unidentified	Unknown fish larvae	1	31.736	0.024
2022-03-31	<i>Alosa pseudoharengus</i>	Alewife	4	20.188	0.193
2022-03-31	Eggs	Eggs	23	20.188	1.347
2022-04-14	<i>Alosa aestivalis</i>	Blueback Herring	9	46.185	0.166
2022-04-14	<i>Alosa pseudoharengus</i>	Alewife	702	46.185	13.761
2022-04-14	Catostomidae	Unk. sucker	1	46.185	0.017
2022-04-14	Clupeidae	Unk. Herring/Shad	135	46.185	2.454
2022-04-14	Cyprinidae	Unk. minnow	9	46.185	0.166
2022-04-14	Eggs	Eggs	127	46.185	2.895
2022-04-14	Unidentified	Unknown fish larvae	9	46.185	0.191
2022-04-21	Eggs	Eggs	11	7.954	NA
2022-04-28	<i>Alosa pseudoharengus</i>	Alewife	4	31.767	0.117
2022-04-28	Cyprinidae	Unk. minnow	5	31.767	0.123
2022-04-28	Eggs	Eggs	7	31.767	0.229
2022-04-28	<i>Notropis hudsonius</i>	Spottail Shiner	5	31.767	0.218
2022-05-05	Eggs	Eggs	13	NA	NA
2022-05-05	<i>Menidia beryllina</i>	Inland Silverside	1	NA	NA
2022-05-12	Eggs	Eggs	13	8.140	3.340
2022-05-12	<i>Morone americana</i>	White Perch	14	8.140	1.051
2022-05-12	<i>Notropis hudsonius</i>	Spottail Shiner	1	8.140	0.075
	Total		1,094		

We measured creek discharge and other physical parameters at the same location and times where ichthyoplankton samples were taken, which was about 100 m downstream from the block net (Table 4). Mean creek discharge was less than 2019 and 2021, but in the same range as previous years. Mean discharge in 2022 was $0.302 \text{ m}^3 \text{ s}^{-1}$, ranging from $0.05 \text{ m}^3 \text{ s}^{-1}$ to $0.59 \text{ m}^3 \text{ s}^{-1}$. Water temperature was above $10 \text{ }^\circ\text{C}$ on all sampling days, which is the presumed minimum temperature for river herring spawning, and rapidly warmed after April. Dissolved oxygen (DO), and pH were in the benign range for occurrence of river herring throughout the sampling period (Table 4).

Table 4. Physical parameters measured at Cameron Run during each sampling week. No data was taken on 2022-04-06 given adverse creek conditions.

Date	Discharge $\text{m}^3 \text{s}^{-1}$	Temperature $^{\circ}\text{C}$	Spcond $\mu\text{S s}^{-1}$	DO mg L^{-1}	pH
2022-03-10	0.17	10.9	616.0	12.33	7.74
2022-03-17	0.59	12.0	1447.0	11.48	7.53
2022-03-23	0.05	11.9	615.0	10.98	8.57
2022-03-31	0.41	13.3	583.0	11.88	7.78
2022-04-06	NA	NA	NA	NA	NA
2022-04-14	0.39	22.5	502.0	10.62	8.82
2022-04-21	0.25	17.3	493.6	11.51	8.69
2022-04-28	0.32	14.1	511.0	11.66	7.70
2022-05-05	0.09	18.4	468.3	10.02	7.37
2022-05-12	0.45	19.2	425.6	10.65	7.91

During the sampling period of 10 weeks, the total discharge was estimated to be on the order of 1.82 million cubic meters (Table 5), less than 2021 and 2019. Although we did not sample in peak flow conditions given unsafe working environments. Given the observed mean densities of larvae (1.42 m^{-3}), the total production of river herring larvae was estimated at approximately 2.6 million for Cameron Run (Table 5). Note that the estimate is based on a small sample of the total discharge. With 5 adult Alewife collected and extrapolating over period of the spawning run as explained in the methods, this could mean that the river herring spawning population in 2019 was 70 individuals, which was lower than 2019 and 2021. However, not sampling earlier in the season may have led to this low estimate and the high numbers of larvae present indicate that more adults likely spawned earlier in the season.

Table 5. Estimation of river herring (alewife and blueback herring) larval production and spawner abundance from Cameron Run during spring 2022.

Parameter	Cameron Run
Mean discharge (m^3s^{-1})	0.301
Total discharge, (m^3)	1819987.227
Total plankton nets volume sampled (m^3)	161.414
Mean Alosa larvae density (m^3)	1.424
Total river herring production (# larvae)	2591202.417
Total adult river herring (#)	70.000

Conclusions

After we found that Cameron Run is used as river herring spawning habitat with just one adult river herring and seven larvae in 2013, we were able to confirm this finding by collecting more river herring adults and larvae from 2014-2022 (Figure 3), albiet except for 2020 when sampling did not occur because of COVID-19. By moving our sampling site approximately 500 m downstream in 2014 we have found a better sampling location. Even further downstream Cameron Run becomes too deep and wide for our sampling strategy.

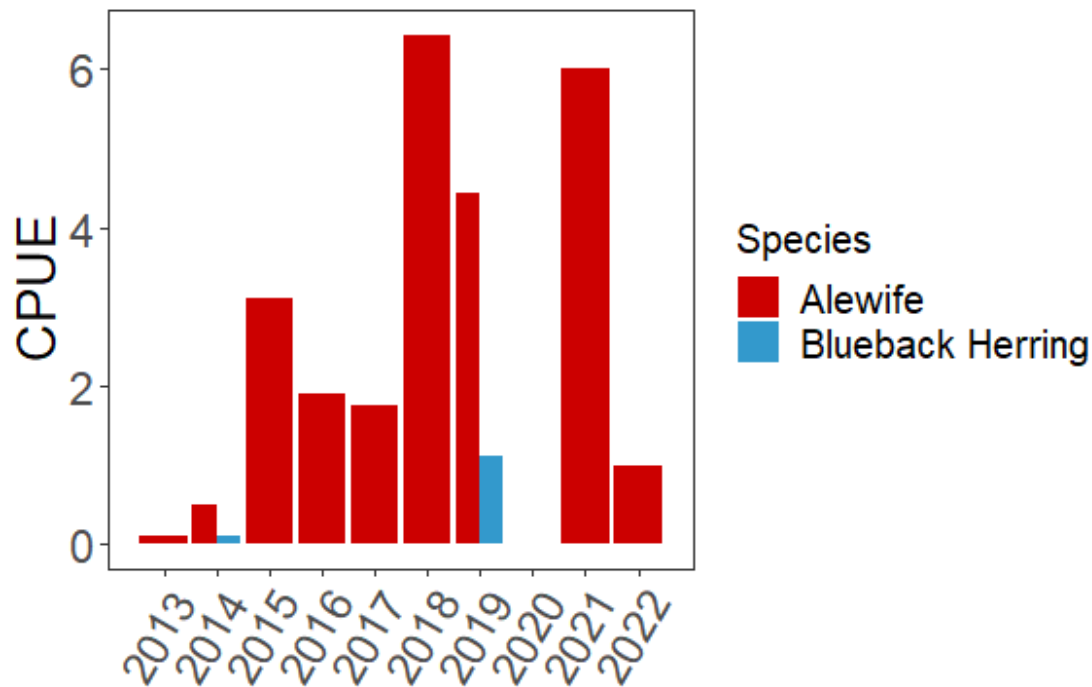


Figure 3. Catch per Unit Effort of Alewife and Blueback Herring (number of individuals per block net) collected with the block net in each year.

The finding of river herring adults and larvae in an area above the outflow of the Alexandria Renew Enterprises wastewater reclamation facility signifies that the water of Cameron Run is clean enough to use as spawning habitat for these species of concern. These finding will not affect AlexRenew, but will affect the terms of construction permits in and around Cameron Run (i.e. some construction activities may be restricted by the Virginia Department of Wildlife Resources (VADWR) during the annual spawning period (mid-March to mid-May) of river herring (Alan Weaver, VADWR, pers. comm.).

Although the current evidence suggests that the importance of Cameron Run may be marginal to Alewife and Blueback Herring populations, it is important to recognize that marginal habitats may sustain fish populations during periods of declining abundance and low recruitment (Kraus and Secor 2005). Due to the moratorium on river herring set in place bay-wide in 2012, annual

estimation of spawner abundance should be a continued priority for annual monitoring of this and other Potomac River tributaries. In 2015, 3 years after the 2012 moratorium, Alewife CPUE greatly increased, which is about the time it takes for Alewife to grow to adulthood and return to their spawning grounds. This peak has been seen in other tributaries to the Potomac River as well (Jones and De Mutsert 2016) and could signify the effect of the release from the fishery. This effect was not seen throughout Virginia however (Alan Weaver, VDGIF, pers. comm.), and was not maintained to the same level in the subsequent years (2016 and 2017). Anadromous fishes typically exhibit strong year-class fluctuations, and we expected a high return of river herring in 2018 if the offspring of the successful 2015 year-class was able to return. We indeed saw even higher numbers return in 2018, which is a sign that the high abundance in 2015 may have given a lasting boost to the population. It is a good sign that the same level of return spawners was registered in 2019, and that adult Blueback Herring were among the river herring collected this year. Unfortunately, we were not able to collect fishes during 2020, but our trends from 2021 also indicate many Alewife spawners, continuing this three year trend. Although we did not collect nearly as many fish in 2022, this lower number matched the 3-year cycle we have observed for the last decade. Furthermore, the spawners we collected came from a limited sample size given environmental constraints on our sampling methods and the overall spawning population may have been even higher than detected. While our total adult Alewife population numbers were less than 2019 and 2021, the larval production of Alewife was much higher potentially indicating better spawning and larval survival conditions. Additional years of data collection will allow us to see if this cycle continues and helps with the slow built-up of river herring populations.

Literature Cited

- General Oceanics. ND. General Oceanics digital flowmeter mechanical and electronic operators manual. https://www.forestry-suppliers.com/Documents/588_msds.pdf.
- Jones, P. W., F. D. Martin, and J. D. Hardy, Jr. 1978. Development of fishes of the Mid-Atlantic Bight: an atlas of egg, larval, and juvenile stages, volume 1. Acipenseridae through Ictaluridae. U.S. Fish and Wildlife Service, FWS/OBS-78/12.
- Jones, R. C., De Mutsert, K., and G. D. Foster. 2014. An Ecological Study of Hunting Creek-2013. Final report to Alexandria Renew Enterprises, Alexandria, VA. 123 p.
- Jones, R. C. and De Mutsert, K. 2016. An Ecological Study of Gunston Cove-2015. Final report. Potomac Environmental research and education Center, Fairfax, VA.
- Kraus, R. T. and D. H. Secor. 2005. Application of the nursery-role hypothesis to an estuarine fish. *Marine Ecology Progress Series* 290:301-305.
- Neves, R. J., M. Cooper, Odom, J. J. Ney, and Virginia. Dept. of Transportation. 1988. Use of Virginia's tributaries of the Potomac River by anadromous fishes : final report for phase four of an analysis of the impediments to spawning migrations of anadromous fish in Virginia rivers.

ESCHERICHIA COLI ABUNDANCES IN HUNTING CREEK/CAMERON RUN AND ADJACENT POTOMAC RIVER - 2022

Final Report

By

Benoit Van Aken

Associate Professor, Department of Chemistry & Biochemistry
George Mason University

1. Introduction

During 2022, in connection with examination of ecological and chemical parameters, a study of *Escherichia coli* in waters in the areas of Hunting Creek/Cameron Run and adjacent waters of the Potomac River was continued with samples being collected at 16 sites. These sites included 9 sites sampled in the period 2016 – 2018 (AR-1, AR-2, AR-3, AR-4, AR-10, AR-12, AR-21, AR-23, and AR-30). AR-11 (outlet of Lake Cook) was not sampled beyond 2019 because it was considered redundant with a nearby downstream site in Camron Run: AR-21. Note that AR-22, sampled in 2016 and 2017, was not accessible since 2018 due to existence of large-scale construction projects and earthwork along the stream bank of Huntington Park. Similarly, AR13 was not sampled in 2022 because of large-scale construction projects and earthwork along Timber Branch of Hooffs Run at the level of Jamieson Ave. Three new sites sampled since 2019 included one off-shore site: AR-32 (Potomac Mainstem downstream of Outfall 001) and two shore sites: AR-33 (Hooffs Run at Linden St) and AR-34 (Hooffs Run at Alex Renew). Note that site AR-31 (Potomac Mainstem upstream of Outfall 001), which was sampled in 2019, was not sampled in 2020 and 2021. AR-33 site was gated in 2022 by the City of Alexandria and not accessed until July 28, 2022. In 2020, four new sites were added, including three shore sites: AR-24 and AR-25 by the Hunting Creek Embayment near shore just west and east of Royal St combined sewage outfall (CSO), respectively, and AR-35 by the Timber Branch of Hooffs Run at downstream end of Ivy Hill Cemetery, and one off-shore site in the Potomac River at Daingerfield Island (marker '6'): AR-38.

This work provides current microbiological water quality information in these aquatic ecosystems adjacent to and receiving water from the wastewater reclamation facility operated by Alexandria Renew Enterprises (hereafter AlexRenew). The research continues to determine if these waters are impaired under the Clean Water Act in terms of their uses as designated by the Commonwealth of Virginia.

The text of the Virginia Water Quality Standards (9 VAC 25-260-10) is as follows:

"All state waters, including wetlands, are designated for the following uses: recreational uses, e.g., swimming and boating; the propagation and growth of a balanced, indigenous population of aquatic life, including game fish, which might reasonably be expected to inhabit them; wildlife; and the production of edible and marketable natural resources, e.g., fish and shellfish" (VSWCB 2011).

Section 9VAC25-260-170 of the Virginia Water Quality Standards (amended as of January 2011) specifies the bacteriological criteria for *E. coli* that apply to primary contact recreational use surface waters:

1. "*E. coli* bacteria shall not exceed a monthly geometric mean of **126 CFU/100 mL** in freshwater [...]."
2. "Geometric means shall be calculated using all data collected during any calendar month with a minimum of four weekly samples."
3. "If there are insufficient data to calculate monthly geometric means in freshwater, no more than 10% of the total samples in the assessment period shall exceed **235 *E. coli* CFU/100 mL** [...]."
5. "For beach advisories or closures, a single sample maximum of **235 *E. coli* CFU/100 mL** in freshwater [...] shall apply." (VSWCB 2011b)

Of all of the conditions in rivers and streams which can lead to a listing of 'impaired water', the one criterion that, more than any other, results in such a listing is coliform bacteria or *E. coli* abundances (USEPA 2014). Both Hunting Creek and Cameron Run were listed as impaired under the Clean Water Act for exceedances of Virginia's water quality criterion for *E. coli* bacteria (VADEQ, 2012), although the earlier impairment listing of Hunting Creek was based on the then applicable fecal coliform criterion (VADEQ 2010). The fecal coliform criterion was subsequently changed to *E. coli* based on the understanding that this subset of fecal coliforms is more specifically associated with fecal material from humans and other warm-blooded animals. The U.S. EPA (USEPA 2012) recommended and the Commonwealth of Virginia accepted *E. coli* as the better indicator of health risk related to recreational water contact. That is the current microbiological water quality criterion.

Due to this impairment, total maximum daily load (TMDL) allocations for *E. coli* were developed for both of these watersheds in late 2010 (VADEQ 2010). The City of Alexandria is working toward achieving the bacteriological criteria for these waters through a variety of programs including a storm water program, minimizing combined storm water sewer system overflows and eventually eliminating those discharges, reductions in pet waste sources, and discovery of illegal discharges. Because the sources of *E. coli* to water systems are many and varied, including wildlife sources which are generally not controlled unless at a nuisance level, continued monitoring of *E. coli* in these waterways is an important aspect of maintaining and improving water quality. The results reported here add to the understanding of the microbiological quality of these systems.

2. Methods

Sampling Regime & Methods

In the prior years, the approach was to sample on a biweekly basis in May through September with one sampling in April. In 2022, samples were collected on 10 dates, from April 20, 2022 to September 13, 2022. The last scheduled sampling on September 28, 2022 was a backup date in case of inclement weather on one of the prior dates, which was not necessary (**Table EC1**). Water samples were collected at 15 or 16 stations on each sampling day (AR-33 was not accessed until July 28). Station identifiers and locations are shown in **Table EC2** (the map of EC sampling stations is provided in Appendix A, **Figure A1**). Samples were collected in clean, steam sterilized (autoclaved), 1-liter, wide-mouth polypropylene bottles. Ten stations were approached from the shore: AR-1, AR-12, AR-21, AR-23, AR-24, AR-25, AR-30, AR-33, AR-34, and AR-35, and 6 stations were sampled from a small, outboard-powered research vessel: AR-2, AR-3, AR-4, AR-10, AR-32, and AR-38. Among the shore stations, stations AR-21, AR-24, AR-25, AR-30, and AR-35 were sampled from the shore without wading into the stream. At

these stations, samples were collected as grab samples using the 1-liter bottle. Sampling was operated in the most active flow zone that could be reached from the shore. At station AR-1, AR-23, and AR-34, samples were collected remotely using a sterilized, 1- or 4-liter round, polypropylene wide-mouth bottle fitted with a harness and nylon line. At station AR-1, the sample bottle was deployed from atop the George Washington Parkway Bridge over Hunting Creek on the downstream side approximately at mid-span. At stations AR-23 and AR-34, the sample bottle was deployed from the shore and thrown to about 5-10 yards into the water. When accumulation of surface debris prevented the collection of grab samples, AR-25 was also sampled using a bottle fitted with a harness and nylon line. Collection at two shore-approached sites was achieved wading in the streams: AR-12 and AR-33. At station AR-12, we waded into the water downstream of the collection site to approximately midstream, waited for the current to carry away any disturbed sediment and then collected the sample by submerging the 1-liter bottle upstream of the sample collector. At station AR-33, the bottom of the stream is entirely paved with concrete. At this site, we waded to approximately midstream. After waiting for any disturbed sediment to be washed away, the sample was collected again by submerging the sterile 1-liter bottle in the stream. Boat-approached sites, AR- 2, AR-3, AR-4, AR-10, AR- 32, and AR-38, were sampled by submerging the collection bottles over the side of the research vessel as the vessel coasted on final approach to the station.

In all cases, the bottles were rinsed twice with sample water and then the final sample was collected. Immediately after collection, samples were placed in dark, insulated containers packed with ice. Samples were returned to the George Mason University at the Potomac Science Center, where they were processed within about 4 hours after collection.

Table EC1. Sampling Dates

Date	Date Codes
20-apr-2022	20220420
2-may-2022	20220501
17-may-2022	20220517
1-jun-2022	20220601
13-jun-2022	20220613
14-jul-2022	20220714
28-jul-2022	20220728
11-aug-2022	20220811
30-aug-2022	20220830
13-sep-2022	20220913

Table EC2. Station identifiers, locations and access type

Station ID	Access Type	Location Description	Latitude	Longitude
AR-1	Shore	Hunting Cr just above GW Parkway Bridge	38.78992	-77.05126
AR-2	Boat	Northern portion of Hunting Cr.	38.78509	-77.04951
AR-3	Boat	Southern portion of Hunting Cr.	38.78181	-77.04890
AR-4	Boat	Potomac River Channel off Hunting Cr.	38.78124	-77.03529
AR-10	Boat	Potomac River North of Wilson Bridge	38.79816	-77.03907
AR-12	Shore	Last Riffle of Cameron Run near Beltway crossing	38.80218	-77.08467
AR-21	Shore	South side of Cameron Run downstream from Lake Cook drain	38.80318	-77.09565
AR-23	Shore	South side of Cameron Run across from AlexRenew outfall	38.79372	-77.05966
AR-24	Shore	Hunting Creek Embayment near shore just west of Royal St CSO outfall	38.79156	-77.04680
AR-25	Shore	Hunting Creek Embayment near shore just east of Royal St CSO outfall	38.79205	-77.04538
AR-30	Shore	Cameron Run upstream near metro rail bridge	38.80545	-77.10745
AR-32	Boat	Potomac Mainstem downstream of Outfall 001	38.80940	-77.03727
AR-33	Shore	Hooffs Run at Linden St	38.81103	-77.05993
AR-34	Shore	Hooffs Run at Alex Renew	38.79918	-77.05997
AR-35	Shore	Timber Branch of Hooffs Run at downstream end of Ivy Hill Cemetery	38.8175	-77.070654
AR-38	Boat	Potomac River at Daingerfield Island; at marker '6'	38.82348	-77.03802

Analytical Methods

Determination of the abundance of *E. coli* was performed following the EPA Method 1603 (*Escherichia coli* in Water by Membrane Filtration Using Modified Membrane-Thermotolerant *Escherichia coli* Agar–Modified mTEC, USEPA 2009). This is an EPA-approved method for determining abundance of *E. coli* in fresh water. It is a one-step modification of the EPA Method 1103.1. It is based on *E. coli* production of β -D-glucuronidase and the consequent metabolism of 5-bromo-6-chloro-3-indolyl- β -D-glucuronide in the medium to glucuronic acid and a red- or magenta-colored product (USEPA 2009).

For this work, mTEC medium (Fisher) was prepared in our laboratory at George Mason University (Potomac Science Center) shortly before each sampling trip. The medium was prepared as per package directions, and ~5 mL of the molten medium was placed aseptically into sterile, 50-mm Petri dishes with tight fitting lids. Prepared medium was stored at 4°C in the dark until use. Phosphate buffered saline (PBS) was prepared as per Method 1603 and autoclave sterilized. PBS was added to smaller samples (1.0 mL and 10 mL) to make volumes up to at least 20 mL before filtration. This aids in distributing bacteria uniformly across the membrane surface. The PBS was also used for blank controls.

Upon return to the laboratory, samples were processed immediately. Sterile, gridded, 0.45 µm membrane filters were aseptically positioned, grid side up, on the base of a sterile, polycarbonate filter holder, and the filter tower was placed in position on a vacuum flask over the filter and base. Samples were shaken vigorously to assure complete mixing and appropriate volumes (1.0 mL, 10.0 mL, and 100.0 mL) of sample were added to each of three replicate filter systems. Before adding the two smaller volume aliquots to the filter funnels, sufficient PBS was added to make the final volume approximately 20 mL. Samples were then filtered with vacuum (approximately 10 in. Hg). Each filter was then removed from the filter holder base aseptically with sterile, blunt-tipped forceps and placed onto the surface of the mTEC agar without trapping any air bubbles beneath the filter. After replacing the Petri dish tops, the plates were incubated in a 35°C incubator for 2 ± 0.5 hours. They were then removed, placed in heat-sealed plastic bags and submerged in a water bath at $44.5^\circ\text{C} \pm 0.2^\circ\text{C}$ for 22 ± 2 hours. Three blank controls, consisting of 3 x 100 mL of PBS, were checked each time samples were processed. Generally, no *E. coli* were detected in these blank controls, although occasionally controls had one or two presumptive *E. coli* colonies. The data were not corrected for this low background as it was generally far less than 1 percent of the abundances on countable plates.

After the water bath incubation, samples were retrieved and observed immediately for typical red or magenta *E. coli* colonies. All Petri dishes (3 volumes x 3 replicates = 9 Petri dishes per sample) were observed. Although only dilutions yielding colony counts between 20 and 80 needed to be enumerated, we generally recorded colonies for each countable dilution. Often, however, when *E. coli* were too abundant, the higher volume samples were not countable due to overgrowth. Calculation of final *E. coli* abundances followed the procedures described in Appendix B of the EPA Method 1603 (USEPA 2009). In brief, *E. coli* abundance were reported as 'colony forming units (CFUs) per 100 mL'. Since there were triplicate analyses of each dilution, the colony count per Petri dish was separately converted to CFUs per 100 mL and then the triplicates were averaged. If no dilution gave individual counts between 20 and 80, the nearest count was selected and used for the final calculation as described in appendix B of the EPA Method 1603. If all counts were too numerous to count (TNTC), the colony count was reported as greater than the highest acceptable count for the lowest dilution: in our case, 'greater than 8,000 CFUs per 100 mL', according to appendix B of the EPA Method 1603. If no samples showed positive counts, which was the cases for most of negative controls, results were reported as 'less than 1 CFU per 100 mL', according to appendix B of the EPA Method 1603.

3. Results & Discussion

In 2022, typical *E. coli* colonies were observed in some dilution(s) of every sample tested. There was then a point estimate of *E. coli* CFUs per 100 mL for each sample. *E. coli* abundances grouped by station are shown in **Figure EC1** and *E. coli* abundances grouped by sampling date are shown in **Figure EC3** (tabular data is in Appendix A, **Table A1**). None of the control plates showed any counts. They were reported as 'less than 1 CFU per 100 mL' (data not presented).

Since there was no situation in which four weekly samples were collected in a single calendar month, the '235 CFUs per 100 mL' (in more than 10% of the samples) criterion is applicable in determining impairment.

Data Grouped by Station

The different stations sampled have been selected with the purpose of capturing the potential contribution of AlexRenew's CSOs to receiving waters. These CSOs include the Cameron Run CSO across station AR-23 on Cameron Run, the Hooffs Run CSO between station AR-13 and

AR-34 on Hooffs Run, the Royal St. CSO between stations AR-24 and AR-25 on the Potomac River, and the Pendleton St. CSO by station AR-32 on the Potomac River.

In 2022, thermotolerant *E. coli* abundances grouped by station exceeded the 126 and 235 CFUs per 100 mL 'impaired water' criterion at all shore stations and five out of the six off-shore stations (AR-2, AR-3, AR-10, AR-32, and AR-38) at some time during the sampling period. Only the off-shore site AR-4 did not show any exceedance during the sampling period (**Figure EC1**). This is well in accordance to observations made in 2015, 2016, 2017, 2018, 2019, and 2021, where all stations showed exceedance for at least one sampling date. Only in 2020, three off-shores stations did not show any exceedance, likely because only five sampling campaigns were conducted versus 10-11 in other years. All shore stations showed exceedance of 126 CFUs per 100 mL on all sampling dates (except AR-33, which showed 4 exceedances, but was sampled only 4 times) and exceedance of the 235 CFUs per 100 mL on at least 8 out of the 10 sampling dates (except AR-33, which showed 4 exceedances, but was sampled only 4 times). As usual, off-shore stations showed less exceedances: 3 or less over all sampling dates (except for AR-32, which showed 6 exceedances of the 126 CFUs per 100 mL).

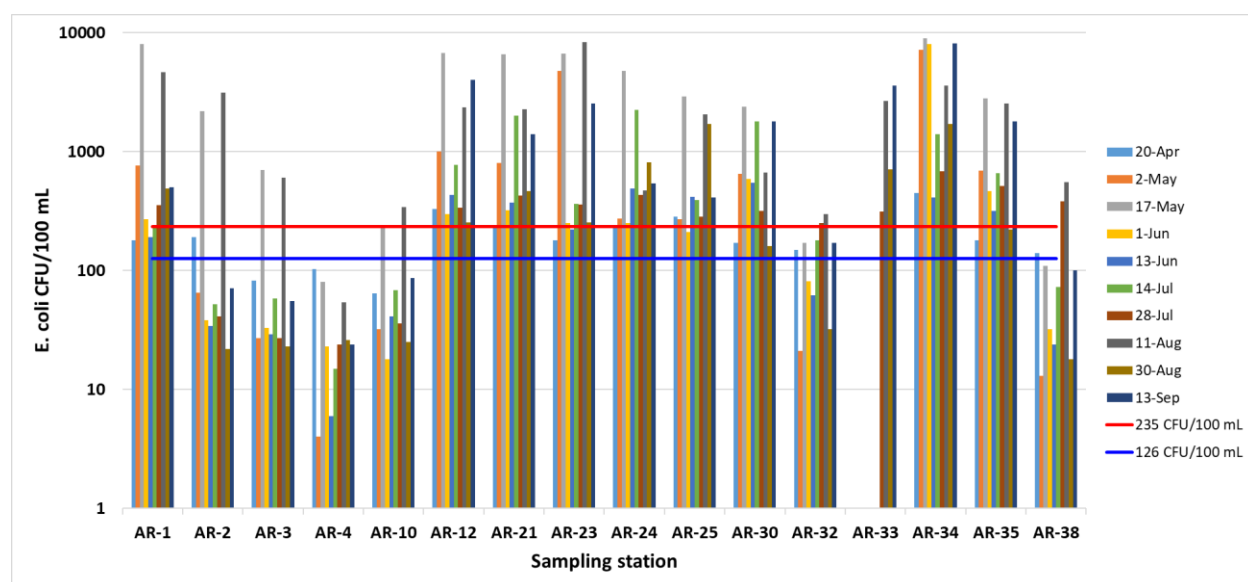


Figure EC1. *E. coli* abundance per 100 mL in Cameron Run, Hunting Creek, and the adjacent Potomac River grouped by stations from April to September 2022. The blue horizontal line represents the *E. coli* criterion for the geometric monthly mean allowable abundance (126 CFUs per 100 mL), and the red line represents the criterion for allowable abundance in the absence of four monthly samples (235 CFUs per 100 mL).

Figure EC2 shows the 'box plots' of *E. coli* numbers per 100 mL as arrayed by site. In this figure, the stations were grouped by streams, including the shore stations on Cameron Run (orange), the shore stations on Hooffs Run (green), the shore stations on the Potomac River near the Royal St. CSO outfall (purple), and the off-shore stations (blue). Five sampling stations are located along Cameron Run and include, from upstream to downstream: AR-30, AR-21, AR-12, AR-23, and AR-1. AR-30 and AR-21 are in flowing Cameron Run, while AR-12, AR-23, and AR-1 are in tidal Cameron Run. Three stations are located along Hooffs Run and include, from upstream to downstream: AR-35, AR-33, and AR-34. Hooffs Run is a tributary of Cameron Run, which is suspected to contribute to the *E. coli* contamination observed in Cameron Run. Two shore stations are located on the Potomac River near the Royal St. CSO: AR-24 and AR-25. Off-shore stations include two stations in the Hunting Creek embayment, near the Hunting

Creek discharge point: AR-2 and AR-3, and four stations in the mainstem Potomac River, from upstream to downstream: AR-38, AR-32, AR-10, and AR-4.

On average, we observed an increase of the detected *E. coli* numbers on Cameron Run when moving downstream from AR-30 (910 CFUs/100 mL) to AR-23 (2,389 CFUs/100 mL). Then the numbers decreased from AR-23 to AR-1 (1,566 CFUs/100 mL) – this is not apparent from EC2, which shows the median counts. Unlike what was seen in 2021, we observed a significant increase of the numbers between AR-12 and AR-23, indicating a potential contribution of the Cameron Run CSO (located at almost the same level as AR-23) to the contamination of Cameron Run.

On average, we also observed a significant increase of the *E. coli* numbers when going downstream along Hooffs Run from AR-35 (1,019 CFUs/100 mL) to AR-34 (4,055 CFUs/100 mL). We did not monitor this year AR-13, but the count increase between AR-33 and AR-34, may again indicate a contribution of Hooffs Run CSO (located between AR-13 and AR-34) to Hooffs Run contamination.

The shore Potomac stations nearby the Royal St. CSO outfall showed average numbers of 1,054 and 892 CFUs/100 mL for AR-24 and AR-25, respectively. These numbers are significantly higher than the nearby off-shore numbers at stations AR-10 (94 CFUs/100 mL) or AR-2 (585 CFUs/100 mL), indicating a possible contribution of the Royal St. CSO outfall to water contamination at these sites. It is noteworthy that other contamination sources are likely to be present on the Potomac River shore.

All off-shore numbers were on average much lower than the shore numbers (36 – 585 versus 892 – 4,055 CFUs/100 mL). Off-shore stations by the Hunting Creek Embayment, AR-2, AR-3, and AR-4, showed a steady decrease of the counts when increasing the distance from Cameron Run discharge: from AR-1 (1,566 CFUs/100 mL) to AR-4 (36 CFUs/100 mL), which suggests that Cameron Run may be a significant source of *E. coli* to the Potomac River. All off-shore stations in the mainstem Potomac River, AR-38, AR-32, AR-10, and AR-4, showed low numbers (36 – 145 CFUs/100 mL). Station AR-32, which is nearby the Pendleton St. CSO in Orinoco Bay shows similar average counts (142 CFUs/100mL) as station AR-38 (142 CFUs/100 mL) upstream the mainstem Potomac River, and higher counts than AR-10 and AR-4 (94 and 36 respectively) downstream the mainstem Potomac river. It is noteworthy that these numbers are low and the differences may not be significant.

In summary, the average *E. coli* counts by stations increased from upstream to downstream, along both Cameron Run and Hooffs Run. These streams also showed the highest counts that we recorded among all stations. Examination of the *E. coli* counts along Cameron Run and Hooffs Run may indicate a contribution of the Cameron Run CSO and Hoof Run CSO to the contamination of these streams. The Potomac River stations near the Royal St. CSO outfall showed numbers higher than nearby off-shore station numbers, also suggesting a contribution of the Royal St. CSO outfall to water contamination at these sites. The off-shore counts were about one or more orders of magnitude lower than the shore counts, which is easily explained by dilution of the stream water.

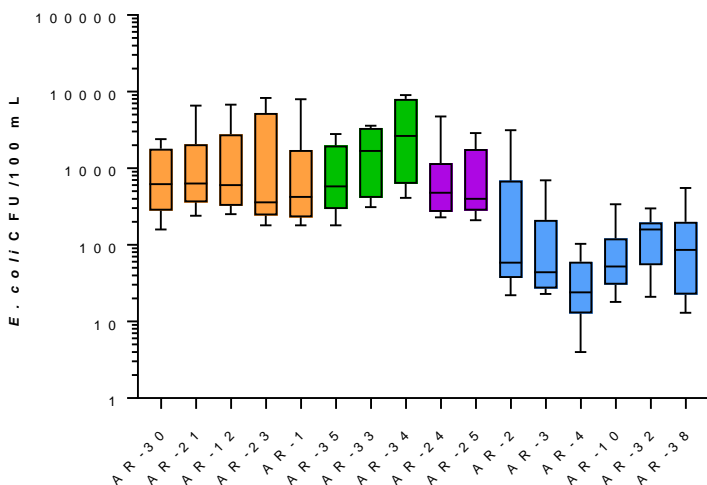


Figure EC2. Box plots of *E. coli* abundance per 100 mL for each site in Cameron Run, Hunting Creek, and the adjacent Potomac River from April to September 2022. The bars show the minimum and maximum counts, the boxes show the 25 and 75-percentile, and the median. Shore stations on Cameron Run are in orange, shore stations on Hooff Run are in green, shore station on the Potomac River are purple, and off-shore stations are blue.

Data Grouped by Date

E. coli abundances grouped by dates are presented in **Figure EC3** and **EC4**. The highest average *E. coli* numbers were observed on May 17, August 11, and September 13 (~3,600, ~2,200, and 1,600 average CFUs/100 mL, respectively). The frequency of exceedances of 235 CFUs/100 mL was the highest on August 11, May 26, and July 27, with 15, 12, and 11 exceedances, respectively, over the 16 sites sampled. As it was observed in prior years, in 2022, we detected a significant correlation between the *E. coli* numbers and the Cameron Run flow (recorded at Wheeler Ave), evaluated as daily flow (Pearson correlation coefficient = 0.75, data not presented).

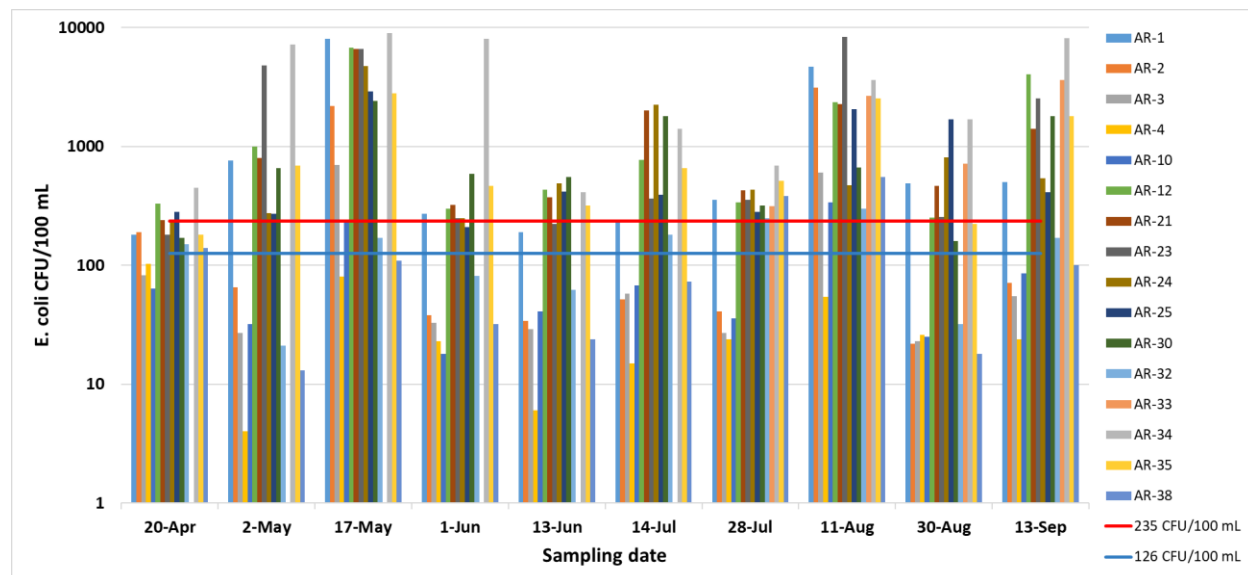


Figure EC3. *E. coli* abundance per 100 mL in Cameron Run, Hunting Creek, and the adjacent Potomac River grouped by sampling dates for all stations. The blue horizontal line represents the *E. coli* criterion

for the geometric monthly mean allowable abundance (126 CFUs per 100 mL), and the red line represents the criterion for allowable abundance in the absence of four monthly samples (235 CFUs per 100 mL).

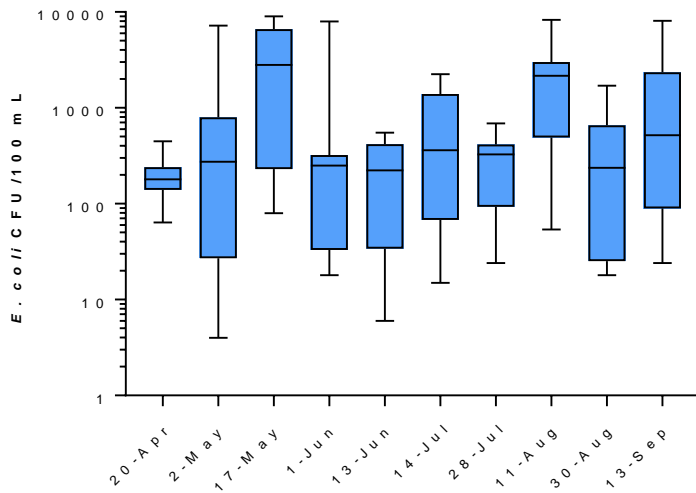


Figure EC4. Box plots of *E. coli* abundance per 100 mL for each sampling dates in Cameron Run, Hunting Creek, and the adjacent Potomac River over all sites. The bars show the minimum and maximum values, the boxes show the 25 and 75-percentile, and the median.

Temporal Trends

The number of stations and sampling events have increased between 2014 and 2022 (i.e., 8 sites and 6 sampling times in 2014 to 16 sites and 10 sampling times in 2022), with the exception of 2020, which was marked by a reduction of the sampling campaigns due to COVID-19 pandemic. We present below a timeline of changes in the percentage of samples that exceeded the 235 CFUs per 100 mL criterion over the 2014 – 2022 period (**Figure EC5**). We also present the average *E. coli* abundances per 100 mL over the 2014 – 2022 period (**Figure EC6**). Even though over the 2014 – 2017 period, both the percent exceedances and average counts globally suggested worsening of the water conditions, these trends were not observed for the 2018 – 2022 period. We observe globally comparable numbers in the years 2018 to 2022.

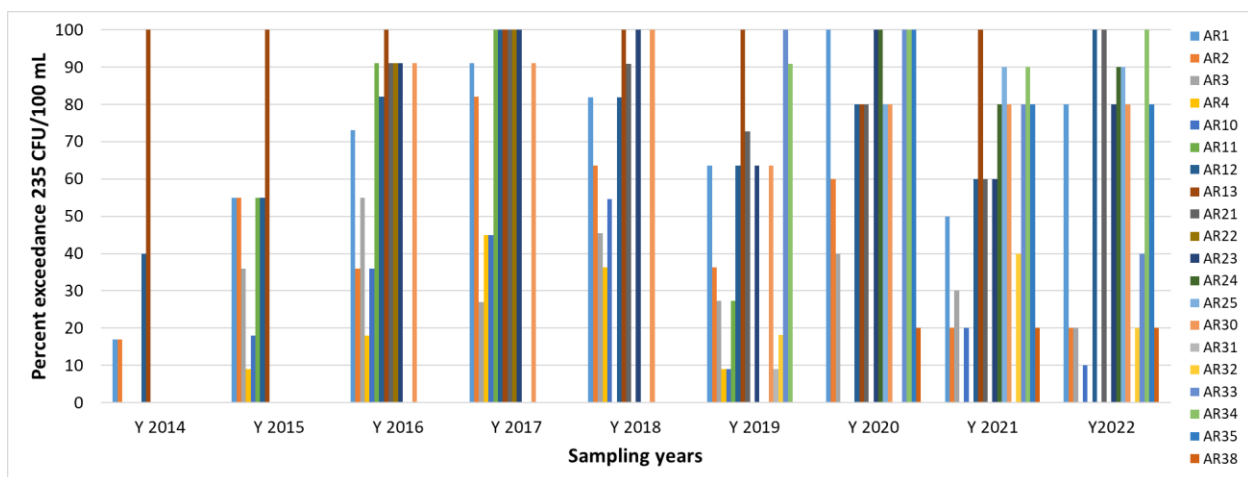


Figure EC5: Percentage of sample events when *E. coli* abundances exceeded 235 per 100 mL in the years 2014 - 2022. Samples were collected 6 times during 2014, whereas in each of the subsequent

years, samples were collected 10 or 11 times.

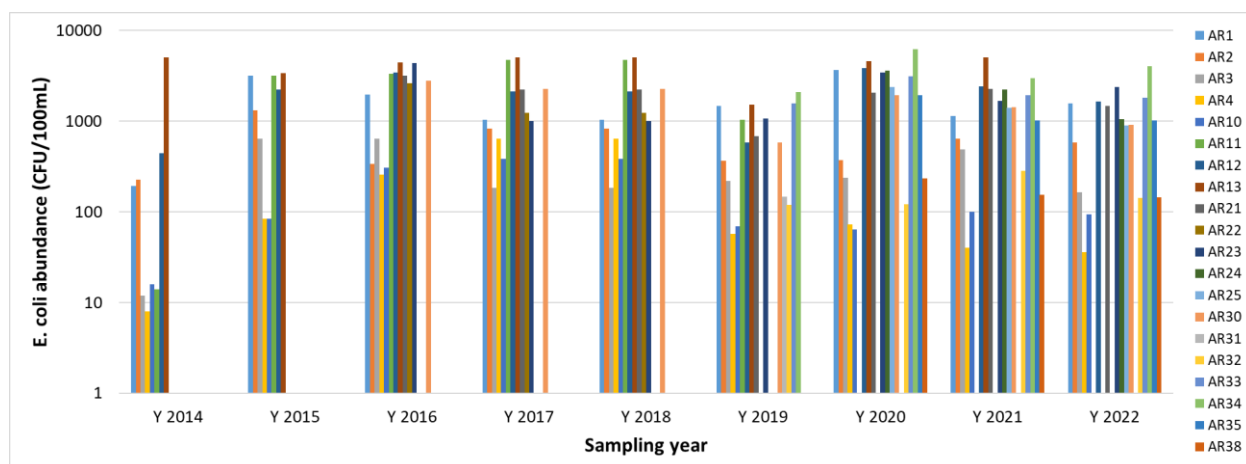


Figure EC6: *E. coli* abundances per 100 mL in the years 2014 – 2022. Samples were collected 6 times during 2014, whereas in each of the subsequent years, samples were collected 10 or 11 times.

4. Conclusions

The data continue to support a conclusion that the entire area sampled, including the mainstem Potomac River, is impaired for the bacteriological water quality criterion (*E. coli*) under Section 9VAC25-260-170 of the Virginia Water Quality Standards that applies to primary contact recreational use surface waters. Although our data showed globally an increase of the *E. coli* abundances and percent exceedances of the 235 CFUs per mL criterion from 2014 to 2017, these numbers seemed to have peaked in 2017-2018 and even seem to show a slight decrease in the subsequent years.

Sampling additional sites in Hooffs Run/Cameron Run and the Potomac River helped to determine the potential contribution of Alex Renew CSOs to receiving waters. The 2022 data may indicate a contribution of the Cameron Run CSO and Hoof Run CSO to the contamination of these streams by *E. coli*. Similarly, the data may indicate a contribution of the Royal St. CSO outfall to the contamination of the Potomac River. The 2022 data does not suggest a significant contribution of the Pendleton St. CSO to the contamination of mainstem Potomac river.

Literature Cited

- U.S. Environmental Protection Agency (USEPA). 2009. Method 1603: *Escherichia coli* (*E. coli*) in Water by Membrane Filtration Using Modified membrane-Thermotolerant *Escherichia coli* Agar (Modified mTEC). Available at: <<http://water.epa.gov/scitech/methods/cwa/bioindicators/>> search Method 1603, December 2009.
- U.S. Environmental Protection Agency (USEPA). 2012. Water: Monitoring & Assessment: 5.11 Fecal Bacteria. Available at: <http://water.epa.gov/type/rs/monitoring/vms511.cfm>
- U.S. Environmental Protection Agency (USEPA). 2014. National Water Quality Assessment Report, water Quality Assessment and Total Maximum Daily Loads Information. Available at: <http://ofmpub.epa.gov/waters10/attains_index.control>

Virginia Department of Environmental Quality (VADEQ). 2010. Bacteria TMDLs for the Hunting Creek, Cameron Run, and Holmes Run Watersheds. Available at: <deq.state.va.us>

Virginia Department of Environmental Quality (VADEQ). 2012. 2012 Impaired Waters: Category 4 & 5 by Basin and Stream Name, Potomac and Shenandoah River Basins, Cause Group Code: A13R-03-BAC - Cameron Run/Hunting Creek. Available at: <<http://www.deq.virginia.gov/Programs/Water/WaterQualityInformationTMDLs/WaterQualityAssessments.aspx>>

Virginia. *State Water Control Board* (VSWCB). 2011. 9 VAC 25-260-10 Designation of uses. Virginia Water Quality Standards. Available at: <<http://lis.virginia.gov/cgi-bin/legp604.exe?000+reg+9VAC25-260-10>>

Virginia. *State Water Control Board* (VSWCB). 2011b. 9 VAC 25-260-170 Bacteria; other recreational waters. Virginia Water Quality Standards. Available at: <<http://lis.virginia.gov/cgi-bin/legp604.exe?000+reg+9VAC25-260-170>>

Appendix A

Figure A1. Map of sampling sites

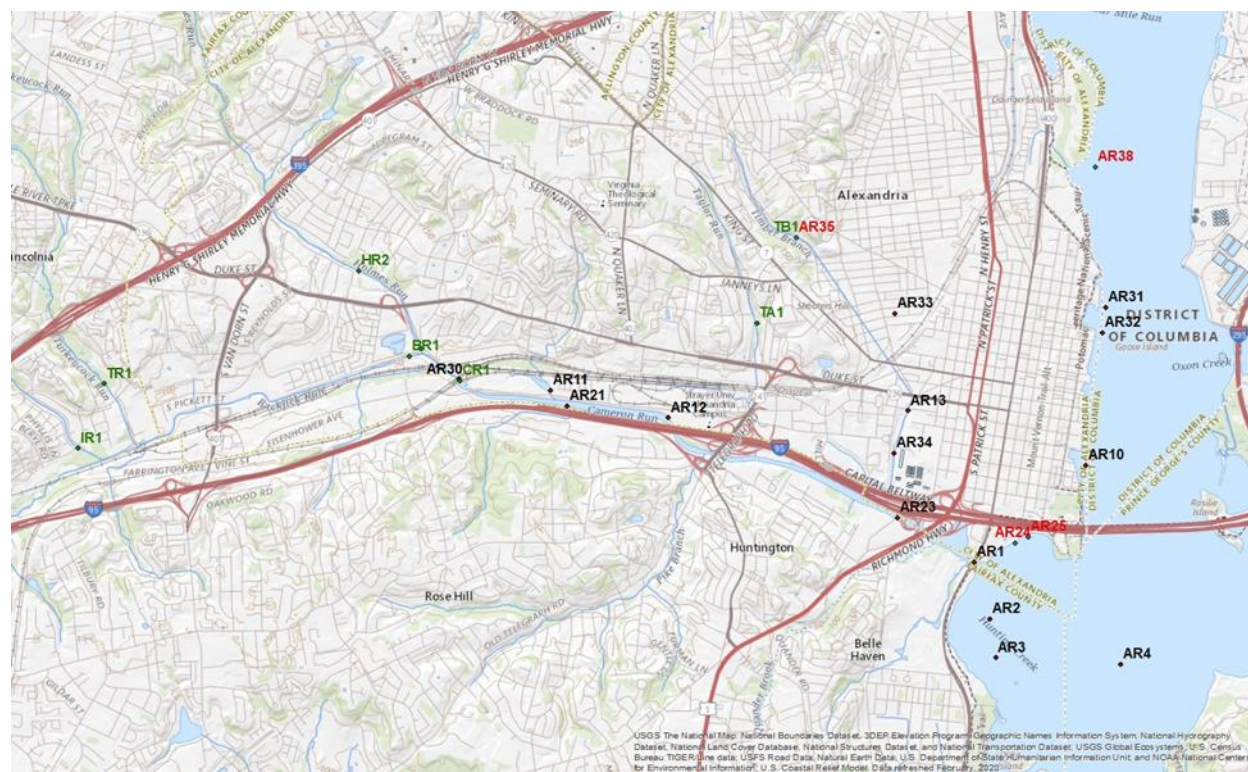


Table A1. 2022 *E. coli* abundances per 100 mL for all station, all sampling dates

Stations	Sampling Dates									
	04/20/22	05/02/22	05/17/22	06/01/22	06/13/22	07/14/22	07/28/22	08/11/22	08/30/22	09/13/22
AR-1	180	760	8000	270	190	243	355	4667	490	503
AR-2	190	65	2200	38	34	52	41	3133	22	71
AR-3	82	27	700	33	29	58	27	605	23	55
AR-4	103	4	80	23	6	15	24	54	26	24
AR-10	64	32	230	18	41	68	36	340	25	86
AR-12	330	1000	6767	300	433	770	337	2367	253	4033
AR-21	240	800	6567	323	373	2000	427	2267	467	1400
AR-23	180	4800	6633	250	223	363	357	8300	255	2533
AR-24	230	275	4767	250	487	2250	430	473	810	537
AR-25	283	270	2900	210	417	390	283	2050	1700	413
AR-30	170	653	2400	586	550	1800	317	665	160	1800
AR-32	150	21	170	81	62	180	250	300	32	170
AR-33							313	2667	713	3600
AR-34	450	7200	9000	8000	410	1400	687	3600	1700	8100
AR-35	180	690	2800	463	317	655	513	2550	223	1800
AR-38	140	13	110	32	24	73	383	553	18	100

Table A2. Mean of *E. coli* abundances per 100 mL, seasonal means and standard deviations and percent exceedances of the 126 and 235 CFUs/100 mL criteria

Station	Seasonal Mean (<i>E. coli</i> /100 mL)	Seasonal St. Dev. (<i>E. coli</i> /100 mL)	Percent Exceedance 126 CFU/100 mL	Percent Exceedance 235 CFU/100 mL
AR-1	1566	2639	100	80
AR-2	585	1120	30	20
AR-3	164	259	20	20
AR-4	36	33	0	0
AR-10	94	106	20	10
AR-12	1659	2168	100	100
AR-21	1486	1929	100	100
AR-23	2389	3086	100	80
AR-24	1051	1435	100	90
AR-25	892	962	100	90
AR-30	910	791	100	80
AR-32	142	92	60	20
AR-33	1823	1569	40	40
AR-34	4055	3601	100	100
AR-35	1019	987	100	80
AR-38	145	180	30	20